ABSTRACT

PITTARD, KARL A. Activation of Carbon-Hydrogen Bonds Mediated by Ru^{II} Complexes. (Under the direction of T. Brent Gunnoe.)

The Ru^{II} complex TpRu(CO)(NCMe)Me (Tp = hydridotris(pyrazolyl)borate) initiates carbon-hydrogen bond activation at the 2-position of furan and thiophene to produce methane and TpRu(CO)(NCMe)Ar (Ar = 2-furyl or 2-thienyl). Solid-state structures have been determined for TpRu(CO)(NCMe)(2-thienyl) and $[TpRu(CO)(\mu\text{-C,S-thienyl})]_2$. The complex TpRu(CO)(NCMe)(2-furyl) serves as a catalyst for the formation of 2-ethylfuran from ethylene and furan. Similar catalytic reactivity was observed with TpRu(CO)(NCMe)(2-thienyl) for the production of 2-ethylthiophene. Density functional theory (DFT) calculations of the C-H activation of furan by {(TAB)Ru(CO)Me} (TAB = tris(azo)borate) indicate that the C-H activation sequence does not proceed through a Ru^{IV} oxidative addition intermediate.

The reaction of TpRu(CO)(NCMe)Me and pyrrole forms $TpRu(CO)\{\kappa^2\text{-}N,N\text{-}(H)N{=}C(Me)(NC_4H_3)\}$. The formation of complex $TpRu(CO)\{\kappa^2\text{-}N,N\text{-}(H)N{=}C(Me)(NC_4H_3)\}$ involves the cleavage of the N-H bond and 2-position C-H bond of pyrrole as well as a C-C bond forming step between pyrrole and the acetonitrile ligand of {TpRu(CO)(NCMe)}. Mechanistic studies indicate that the most likely reaction pathway involves initial metal-mediated N-H activation of pyrrole to produce TpRu(CO)(NCMe)(*N*-pyrrolyl) followed by C-C bond formation and proton transfer. Complex TpRu(CO)(NCMe)(*N*-pyrrolyl) has been independently prepared. At elevated temperatures, TpRu(CO)(NCMe)(*N*-pyrrolyl) converts to $TpRu(CO)\{\kappa^2\text{-}N,N\text{-}(H)N{=}C(Me)(NC_4H_3)\}$. Single crystal X-ray analysis has been achieved for TpRu(CO)(NCMe)(*N*-pyrrolyl), $[TpRu(CO)(NCMe)(\eta^1\text{-}O\text{-}OC_4H_8)$ and $TpRu(CO)\{\kappa^2\text{-}N,N\text{-}(H)N{=}C(Me)(NC_4H_3)\}$. Computational studies support the suggested selectivity for initial N-H bond cleavage in preference to C-H bond activation.

Rational design for a more electron-poor hydroarylation catalyst is discussed. Synthesis of Mp (Mp = tris(pyrazolyl)methane) complexes of the type $[MpRu(PPh_3)(CO)H]BAr'_4$, $[MpRu(PPh_3)(CO)Cl]BAr'_4$, $[MpRu(PPh_3)(PMe_3)Cl]Cl$, $[MpRu(PPh_3)(PMe_3)Cl]BAr'_4$, $[MpRu(PPh_3)_2Cl]BAr'_4$, $[MpRu(PPh_3)\{P(OMe)_3\}Cl]Cl$, $[MpRu(PPh_3)(NCMe)Cl]BAr'_4$, $[MpRu(PPh_3)(NCMe)Cl]BAr'_4$ and $[MpRu(PPh_3)(CO)Cl]BAr'_4$ accomplished. A single-crystal X-ray diffraction study was carried out on the complex $[MpRu(PPh_3)(PMe_3)Cl]Cl$. $[MpRu(PPh_3)_2Me]BAr'_4$ was prepared and examined by Cyclic Voltammetry (CV) where the $E_{1/2}$ = 1.19 V. C-H activation was observed when $[MpRu(PPh_3)_2Me]BAr'_4$ was

heated in neat C_6D_6. Orthometalation appears to dominate reactivity via intramolecular C-H activation of a PPh_3 ligand, however CH_3D was produced at elevated temperatures. A series of Ep (Ep = tris(pyrazolyl)ethane) complexes of the type $MpRu(Cl)_2PR_3$ (R = Ph, OMe, or Me) were also synthesized. The $[EpRu(PPh_3)(NCMe)(Cl)]Cl$ and $[EpRu(PPh_3)(PMe_3)(Cl)]Cl$ complexes were observed spectroscopically as intermediates in these syntheses. Improved synthesis of $[MpRu(PPh_3)_2Cl]Cl$ was also accomplished by **i**mproving the yield by 23%, over the previously reported yield of 53%.

ACTIVATION OF CARBON-HYDROGEN BONDS MEDIATED BY Ru^{II} COMPLEXES

by
KARL A. PITTARD

A dissertation submitted to the Graduate Faculty of
North Carolina State University
in partial fulfillment of the
requirements of the Degree of
Doctor of Philosophy

CHEMISTRY

Raleigh, NC

2007

APPROVED BY:

T. Brent Gunnoe Chair of Advisory Committee	Edmond F. Bowden
James D. Martin	David A. Shultz

DEDICATION

It is with deep gratitude that I dedicate this dissertation to my wife, Wendy Darling Pittard. She has provided me a great gift with her patience, understanding, and encouragement. It is with this dedication that I thank her and promise to her that our future together will be equally as exciting and humorous.

BIOGRAPHY

Karl Ashley Pittard was born in Fayetteville, NC on November 23, 1977, to Dr. Karl F. and Suzan Z. Pittard. Karl graduated with a B.A. in Chemistry from the University of North Carolina at Wilmington, in 2000. He obtained his Master of Science degree in Chemistry from the University of Memphis in 2002. Upon completion of his Ph.D. in Chemistry at North Carolina State University in the spring of 2007, Karl will be joining the BASF Corporation as a research scientist.

ACKNOWLEDGMENTS

There are countless people to whom I owe a great deal of gratitude, who have helped in my attainment of specific goals that culminated in the completion of this research. Without these people and their investments, this work would not have been possible.

Enough cannot be said to my family for their investment in me. Being raised in a Christian home is a far greater gift than any child could ever hope to receive from their parents. Thank you Mom and Dad for teaching me patience, by placing all of the load on Him. Also, I thank you for taking my schooling seriously. How could one forget that you gave me my first desk when I was in the second grade. It was my Christmas present. You made me study at it… every night. Did I mention I was in the second grade. It paid off after all and, seriously, I still prefer to study at a desk. I would also like to thank J. Zeke Pittard for setting the bar high as an older brother (CT State Football Champion, UNCW Student Body President, Miami Law School Graduate, recipient of the Bronze Star in the Iraqi War, and devoted father). He has always encouraged me to succeed. I would also like to thank my wife, Wendy D. Pittard, to whom this dissertation is dedicated. The most giving and sweetest person I know, she kept me laughing and smiling all the way through school. From the late night dorm room chatter of freshman year as friends to these final days at NCSU as my wife, you have always listened to me and encouraged me. For putting up with humor that is only funny to chemists, excess macaroni and cheese, my alarm clock in the middle of the night during kinetic experiments, for going to bed alone on countless nights, and for living like a graduate student for seven years, I thank you.

It is with great honor and pleasure that I thank Dr. T. Brent Gunnoe for his endless guidance and counsel in my quest to become a quali**T**y c**HE**mist. Often unspoken, his leadership and example never failed to inform and motivate. From his enthusi**A**sti**C** le**C**tures to his taking me on as an apprentice, for all of these qualities as a mentor I thank him. I would also like to thank the Gunnoe Group for their teaching me the true spirit of advancing chemical research in a professional and giving environment. It is the professor that sets the tone of group culture but the responsibility falls on the group's graduate students to express these qualities so as to ensure research progress and group tranquility. Never before have I been a part of a research team that is so giving and competitive. It has truly been a pleasure.

It would be nonsensical of me to not mention Dr. James D. Martin and Dr. David A. Shultz, who as professors, have gone beyond the boundaries of scholarly duties to perpetuate my academic advancement. With lengthy discussions, they were a resource for chemical debate and insight. Those committee members, whom I have not yet mentioned, Edmond F. Bowden, Dr. Jeffery L. White, and Dr. Philip L. Sannes, are appreciated for investing time into the review of my accomplishments, as their advice was essential to making me a more complete chemist. Dr. Jeffery L. White and Dr. Sabapathy Sankar must also be acknowledged for their sharing of knowledge and teachings of advanced NMR techniques as it was necessary for advancement of my research.

I would like to also thank North Carolina State University for the use of their facilities as well as Dr. Jeffrey L. Petersen and Dr. Cynthia S. Day at West Virginia University and Wake Forest University, respectively, for their contribution through solving crystal structures. Financial contributions were made by North Carolina State University, through teaching assistantships, and the Department of Energy (Grant # DE-FG02-03ER14811), through providing research assistantships and the necessary materials.

With my last remarks of appreciation, it would be flagrant in nature for me not to recognize those who have built this great science through their life's dedication. From chemistry's earliest beginnings of the alchemists to the world's chemists of the world today, these individuals' great accomplishments have also made this work possible.

TABLE OF CONTENTS

LIST OF FIGURES

LIST OF TABLES

LIST OF SCHEMES

LIST OF SYMBOLS AND ABBREVIATIONS

H	enthalpy
H_f^o	enthalpy of formation at standard conditions
S^o	entropy at standard conditions
cal	calories
mol	moles
K	kelvin
Ac	acetyl
M	metal
UV	ultra-violet
Vis	visible
HOMO	highest occupied molecular orbital
LUMO	lowest occupied molecular orbital
dmpe	dimethylphosphinoethane
$G^{\ddagger}$	Gibbs Free Energy of Activation
TFMS	trifluoromethylsilyl
TCP	tris(cyclohexyl)phosphine
L	dative ligand
X	anionic ligand
K_{eq}	equilibrium constant
py	pyridine
pz	pyrazole
BAr'_4	$[B(3,5\text{-}\{CF_3\}_2C_6H_3)_4]^-$
R	alkyl
Ar	aryl

Cp	cyclopentadienyl
dppe	di(phenyl)phosphinoethane
Mes	mesityl
Tp	hydridotris(pyrazolyl)borate
DFT	density functional theory
Cp*	penta(methyl)cyclopentadienyl
C	Celsius
TFA	trifluoroacetic acid
KIE	kinetic isotope effect
k_{obs}	observed rate
h	hours
psi	pounds per square inch
TON	turnover number
s	seconds
TAB	tris(azo)borate
$H^{\ddagger}$	enthalpy of activation
THF	tetrahydrofuran
D	debye
PES	photoelectron spectroscopy
MeIm	methylimidazole
Het	heteroaromatic
COD	cyclooctadienyl
IR	infrared
CV	cyclic voltammetry
NOE	Nuclear Overhauser Effect
NMR	nuclear magnetic resonance

fw	formula weight
D_{calcd}	calculated density
GOF	goodness of fit
FT	fourier transform
ECP	effective core potentials
VBS	valence basis set
GC	gas chromatography
FID	flame ionization detector
OTf	trifluoromethylsulfonate (triflate)
DMSO	dimethylsulfoxide
Tp*	hydridotris(3,5-dimethylpyrazolyl)borate
Nu^-	nucleophile
BDE	bond dissociation energy
MS	mass spectrometry
Mp	tris(pyrazolyl)methane
Ep	tris(pyrazolyl)ethane
CSD	Cambridge Structural Database
MM	molecular mechanics
Tp^{iPr}	hydridotris(3,5-diisopropylpyrazolyl)borate
Mp^{iPr}	tris(3,5-isopropylpyrazolyl)methane
E_{pa}	oxidation potential
$E_{1/2}$	redox potential

CHAPTER 1:
Introduction

1.1 Catalysis

1.1.1 Introduction

Industrial application of inorganic chemistry substantially focuses on catalytic metal-mediated organic transformations. Through development of highly active, selective, and robust metal catalysts, the generation of commodity and fine chemicals can be obtained at lower cost. This is achieved by the catalyst accessing a low-energy reaction pathway that converts reactants to products thus alleviating the need for harsh reaction conditions, while reducing high levels of waste by increasing chemoselectivity. For example, the production of NH_3 from H_2 and N_2 is thermodynamically favorable (ΔH^o = -22 kcal/mol) but kinetically challenging.[1] To access an alternate route with lower kinetic barriers to NH_3 production, an Fe based catalyst is used in the Haber-Bosch process.[2] Under these catalytic conditions, over one billion turnovers are achieved before catalyst deactivation. The ammonia formation surmounts to 2000 times the worth of the initial Fe catalyst investment.[2]

The earliest reported discovery of catalytic metal-mediated organic transformations occurred in 1836, when J. J. Berzelius took note that substoichiometric traces of certain substances effected overall reactivity of specific reactions.[3] Consequently, Berzelius coined the term “catalysis,” which means “to break down,” in reference to the assumption that the presence of the catalyst was breaking down barriers to chemical transformations thereby rendering them accessible.[3] In 1912, Paul Sabatier shared the Nobel Prize with Victor Grignard for the hydrogenation of organic molecules in the presence of finely divided metallic powders.

Since these early discoveries, interest in catalytic organometallic mediated pathways has heightened. These processes include hydroformylation, olefin polymerization, Grubbs metathesis, Monsanto Acetic Acid Process, and Wacker Process.[4] In all of these examples, transition metal catalysts are employed for the enhancement of chemo-, regio-, and stereoselectivity. Reasons for the use of catalysis in the chemical industry include: a need for novel materials, development of new and existing materials from cheap and readily available feedstocks, the potential reduction of the environmental impact of chemical production and refining, and the ability to provide lower energy pathways for chemical production. In 1992, the National Research Council’s

communication on catalytic science and technology stated that, "Between 1930 and the early 1980s… more than 60% of products and 90% of processes [introduced] were based on catalysis."[2] Though heterogeneous catalysis accounts for approximately 85% of catalytic technologies employed in industry, homogenous catalysis offers greater opportunities for detailed understanding of catalytic features as well as fine tuning of the catalyst for desired outcomes.[5]

1.1.2 Hydroarylation of Olefins

Unsaturated substrates provide a common starting point for many metal-mediated transformations of organic systems that yield new C-C bonds. One potential route to new C-C bond formation is hydroarylation of olefins. Olefin hydroarylation is the net addition of a hydrogen atom (*hydro*arylation) and an aryl functionality (hydro*aryl*ation) across an olefin C=C bond (Figure 1.1). The hydrophenylation of olefins is enthalpically favored and entropically disfavored. For example, Figure 1.1 displays the hydrophenylation of ethylene to yield ethylbenzene with corresponding thermodynamic data. With the potential for hydroarylation to provide efficient routes to produce organic materials, the importance for these chemical transformations cannot be understated. For example, ethylbenzene, which is currently produced using Friedel-Crafts catalysis and related solid state catalysts (see 1.2.1), has been one of the "Top 20 Highest Volume Chemicals" in the U.S. since 1977 with a production of 13.16 billion pounds in 2000.[6]

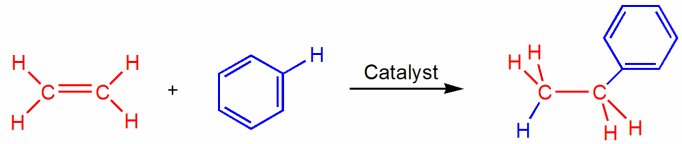

ΔH_f^o	12.5 kcal/mol	19.8 kcal/mol	7.1 kcal/mol
ΔS^o	0.0125 kcal/mol·K	0.0153 kcal/mol K	0.0206 kcal/mol·K

Net ΔH^o = -25.2 kcal/mol

Net ΔS^o = -0.0072 kcal/mol·K

Net ΔG^o = -23.1 kcal/mol (at 298.15 K)

Figure 1.1. Thermodynamics for the hydrophenylation of ethylene to form ethylbenzene.[7]

To outline the potential importance of the research reported herein, several aspects of related chemistry will be discussed. For example, brief synopsis of metal-mediated C_{aryl}-C bond formation reactions, coordination modes of aromatic substrates prior to C-H activation, C-H activation and its mechanisms, and aromatic C-H activation reactivity.

1.2 Metal-mediated C_{aryl}-C Bond Formation

1.2.1 Aromatic Substitution Methods

Reactions that functionalize aromatic molecules are most easily categorized by their mechanism: nucleophilic aromatic substitution and electrophilic aromatic substitution (Scheme 1.1).

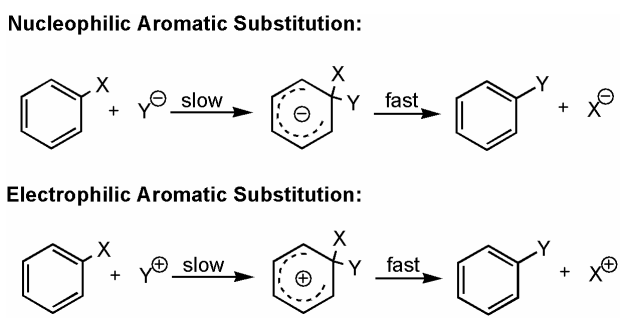

Scheme 1.1. Nucleophilic and electrophilic aromatic substitution reactions.

Stoichiometric nucleophilic aromatic substitution generally requires activation of the aromatic ring by incorporation of electron withdrawing groups ortho to the Ar-X bond (X = halide) (Scheme 1.2).[8] The Wurtz-Fittig reaction couples aryl halides and alkyl halides in the presence of sodium metal.[9] Gilman reagents, $[Li][CuR_2]$ (R = aryl), can be reacted with alkyl halides to form C_{aryl}-C_{alkyl} bonds.[10] The Rosenmund-von Braun reaction can be used to form C-C bonds by adding a cyanide group to the aryl ring.[11] This is done by reacting ArX (X = halide) with CuCN at high temperatures. Cyanation of the arene, alkylation, hydrolysis, and a Clemmensen reduction provide a pathway to alkylarene products. Diazonium salts, ArN_2^+, can also be reacted with oximes, RC(H)=NOH, in the presence of $CuSO_4$ and Na_2SO_3 to yield Ar-C(R)=NOH.[12] Hydrolysis of Ar-

C(R)=NOH followed by Clemmensen reduction, or in the presence of Wilkinson's catalyst ($Rh(PPh_3)_3Cl$), produces the alkylarene. Stephens-Castro coupling involves the reaction of unactivated aryl halides with copper acetylides to give arylacetylenes.[13] These arylacetylenes can be reduced to alkylarenes by hydrogenation in the presence of $[Co(CN)_5]^{3-}$ and H_2. In 1901, Ullmann coupling was introduced as a method for Cu^0 catalyzed coupling of aryl halides.[14] Although these reactions are all of proven utility they present limitations and drawbacks. For example, these reactions at least contain stoichiometric transformations yielding stoichiometric waste. Also, in nearly all cases presented above there is a requirement for halogenation of the aromatic molecule prior to formation of the new C-C bond.

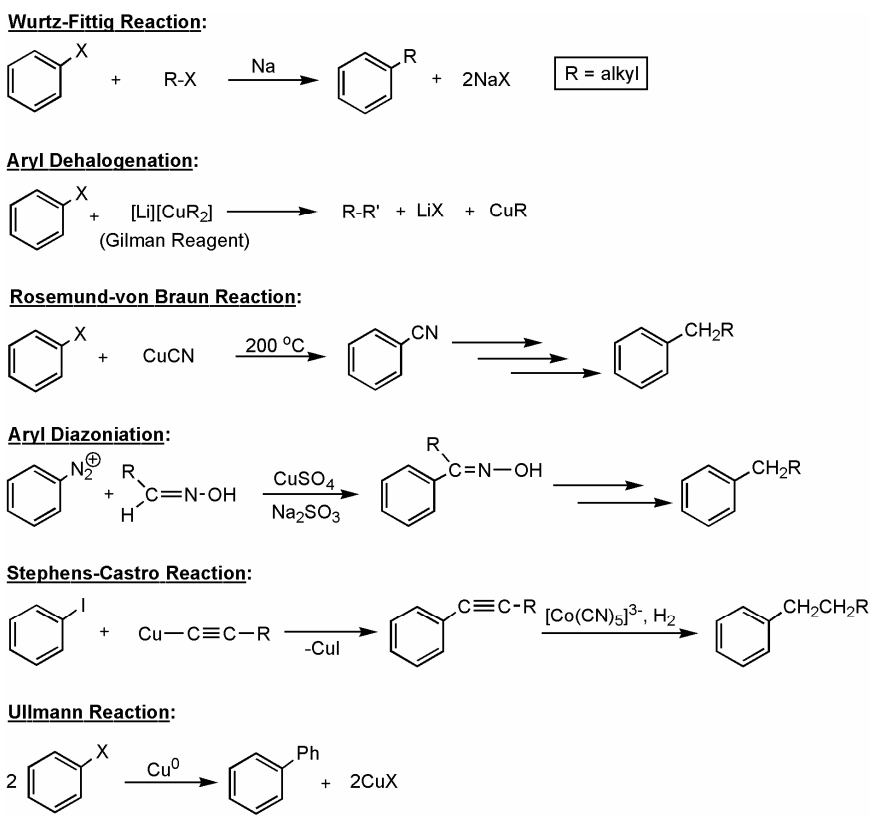

Scheme 1.2. Nucleophilic aromatic substitution reactions resulting in C-C bond formation.

Examples of electrophilic substitution are also prevalent (Scheme 1.4). In 1877, Friedel and Crafts introduced a process by which benzene can be alkylated (Scheme 1.3). This can be carried out by direct

Friedel-Crafts alkylation of arenes or by Friedel-Crafts acylation followed by Clemmensen reduction.[15, 16] Drawbacks to this methods include little control over regioselectivity, polyalkylation, the use of high temperatures, required acid co-catalyst (in many cases), and often stoichiometric use of a Lewis acid.

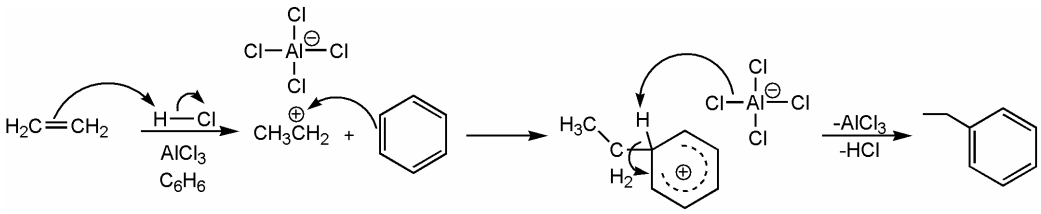

Scheme1.3. Friedel-Crafts catalysis.

Alkylation of arenes can also be achieved by the Hoesch reaction and other reactivity.[8] In this reaction, the arene is reacted with a nitrile in the presence of $ZnCl_2$ and HCl and then undergoes hydrolysis to yield the alkylarene. Alternatively, formylation can be achieved using the Gatterman reaction.[17] Here, benzene is reacted with $Zn(CN)_2$ in water in the presence of a strong acid to yield the benzaldehyde product. The benzaldehyde product can be reduced to the arylalcohol by $NaBH_4$ and then converted to the akylarene upon hydrogenolysis.

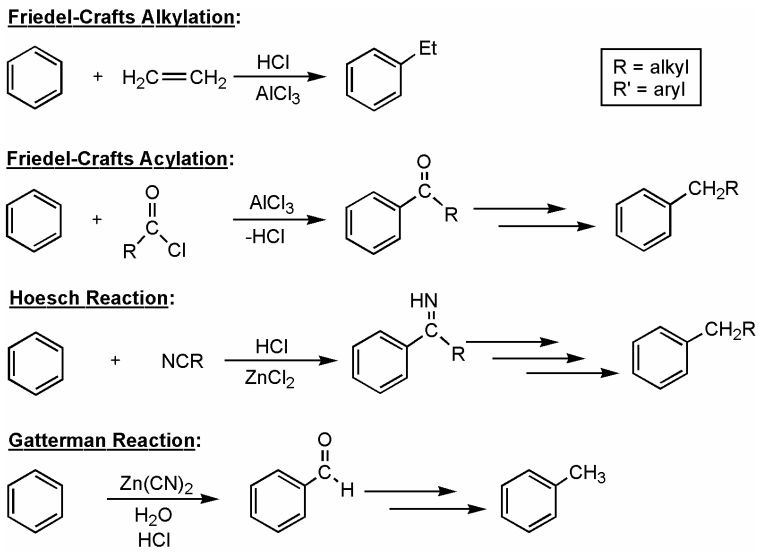

Scheme 1.4. Electrophilic aromatic substitution reactions resulting in C-C bond formation.

1.2.2 Transition Metal Catalyzed C-C Bond Formation with Aromatic Substrates

The development of Fe, Co, Ni, and Cu, and more predominately, Pd and Ni complexes that catalyze C-C bond formation of aromatic compounds with increased selectivity were reported in the late 1960's.[18-21] These methods commonly proceed via oxidative addition and transmetalation. In the 1970's, Kumada developed nickel-phosphine systems that promote Grignard, or Kumada, coupling reactions.[4] In these processes, the active catalyst is a Ni^0 species that initiates oxidative addition of the arylhalide followed by transmetalation with a Grignard reagent to obtain an alkyl-aryl nickel intermediate. Reductive elimination from the alkyl-aryl nickel species yields the new C-C bond. Whereas, Ni catalysts initially offered greater success than Pd catalysts by avoiding undesired β-elimination reactions it was found that Pd catalysts bearing phosphine ligands could avoid β-eliminations and give enhanced coupling activity. The palladium catalyzed coupling reactions have been successfully extended to include Heck,[22] Stille,[23] Suzuki,[24] and Negishi-type[25-27] couplings (Scheme 1.5).

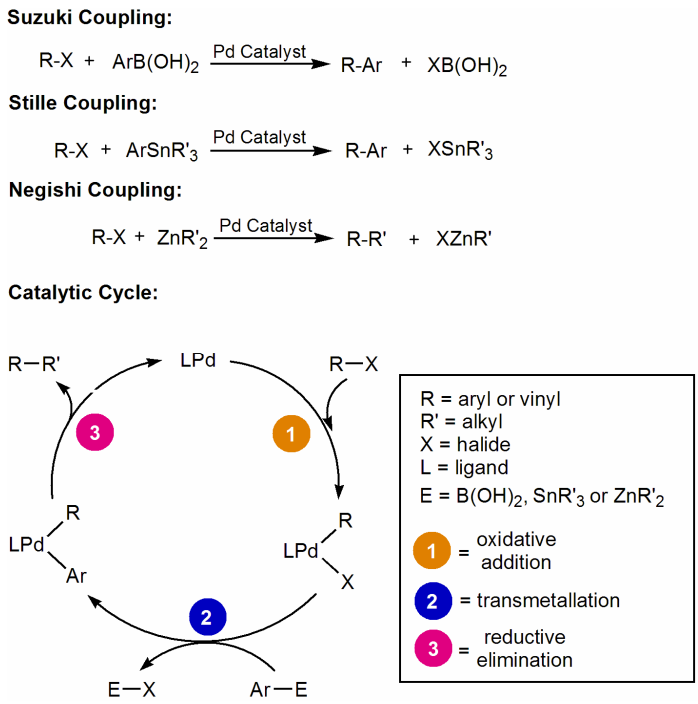

Scheme 1.5. Suzuki, Stille, and Negishi coupling reactions.

The Heck coupling does not involve a transmetalation step. Rather, key steps in the Heck reaction are initial oxidative addition of an arylhalide, insertion of an unsaturated substrate (most commonly an olefin) into the M-C_{aryl} bond, formation of the final organic product by β-hydride elimination, and dissociation with subsequent reductive elimination of a Brönsted acid (Scheme 1.6). The net reaction is conversion of alkene and arene to an alkenylarene. The olefin insertion is often promoted by an electron-withdrawing group on the olefin functionality. Also, a base, usually introduced as NaOAc, is required to facilitate net abstraction of the Brönsted acid from the metal center for the regeneration of the Pd^0 precatalyst. As shown in Scheme 1.4, these reactions are most commonly used in the coupling of aryl and vinyl halides to reduce the propensity for β-hydride elimination. Extension of this C-C bond coupling chemistry has been unsuccessful with internal alkynes; however, Negishi has reported that alkynes can be functionalized with incorporation of a second transmetallation step. First, hydrozirconation of the alkyne is achieved and then a transmetallation reaction of the resulting zirconium-alkene with $ZnCl_2$ can provide an active species to further react with Pd.[28]

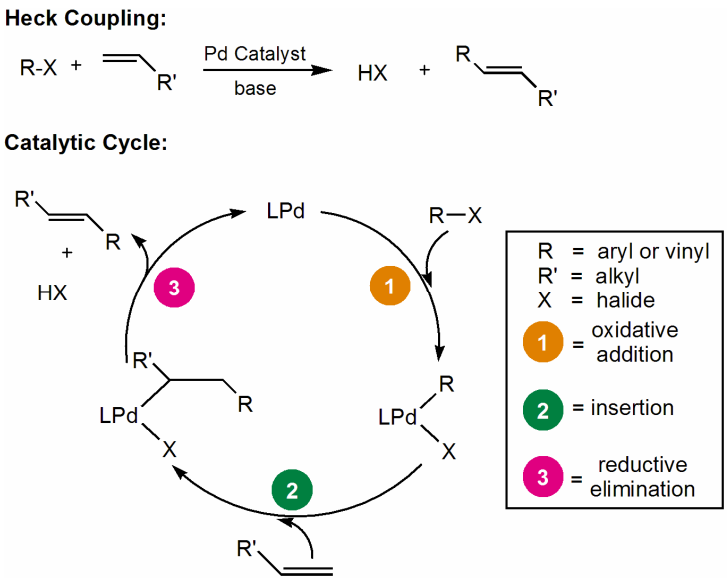

Scheme 1.6. Heck coupling reaction.

Implementation of these technologies into industrial processes has been limited due to "low thermal stabilities" of the catalyst under reaction conditions and the stoichiometric production of salts. However, in some cases the synthetic efficiency overrides these drawbacks. For example, Novartis has implemented the Heck reaction for the production of a synthon for the manufacture of Prosulfuron® (Scheme 1.7).

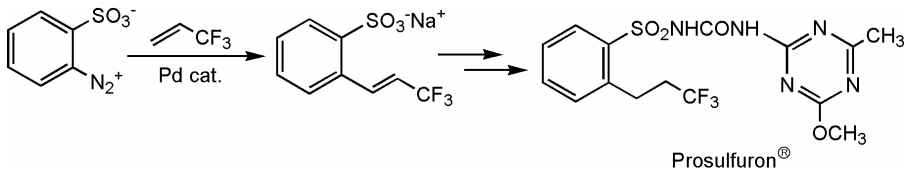

Scheme 1.7. The Heck reaction incorporated into the synthesis of Prosulfuron®.

A recent review by Yamamoto recently discussed organometallic chemistry and its place in the future of chemical research and application.[29] Therein, the importance of moving towards green chemistry by increasing the number of catalytic technologies and increasing the incorporation of halide-free processes is discussed. Yamamoto wrote:

> *If one can cleave bonds other than the carbon-halogen bond, and if one does not need to remove the extra elements in operation, the process will be more favorable from the viewpoint of atom efficiency and environmental aspect.*

An attractive alternative to C-X (X = halide) activation is catalytic methods based on the activation and conversion of C-H bonds to functionalized substrates.

1.3 C-H Bond Activation

1.3.1 Description

C-H bond activation is the cleavage of a C-H bond by way of a metal center interaction.[30-34] A natural inclination to cleave or functionalize C-H bonds is derived from their ubiquity. Their ubiquity also represents a challenge when the selective activation of a single C-H bond is desired. However, C-H activation has remained a challenge largely due to the thermodynamic stability of C-H bonds and their weakly coordinating nature. The thermodynamic stability is indicated by homolytic C-H bond strengths: with sp^3 C-H bond dissociation energies (BDE) of 90-100 kcal/mol and sp^2 bonds with BDEs of 105-120 kcal/mol. Due to the high C-H BDEs these bonds have been termed the "unfunctional group," wherein lies the challenge of their functionalization.[35] Kinetic stability of the C-H connectivity is derived from the relatively high and low energies of the σ^* and σ orbitals, respectively. Further, kinetic reactivity is attenuated by the lack of polarity in the C-H bond, where the C-H bond is nearly 100% covalent.

1.3.2 Role of σ-Complexes in C-H Activation

Hydrocarbons can coordinate to metals through carbon-hydrogen bonds yielding what is described as a σ-complex. In these σ-complexes, the C-H bond serves as a two electron donor to the metal center (Figure 1.2). The electron donation (of σ-symmetry) from the C-H bond to the metal center can be complimented by a reverse electron donation (of π-symmetry) from a filled metal dπ orbital to the empty σ* orbital of the C-H bond (Figure 1.2). Early evidence for direct observation of a σ-interaction with alkanes was reported by Turner and coworkers.[36] In this study, flash photolysis of several $M(CO)_6$ complexes (M = Cr, Mo, and W) yielded $M(CO)_5(CH_4)$ as monitored by IR and UV-Vis spectroscopy. Bergman and coworkers were able to monitor the photolytic C-H activation of hydrocarbons in the presence of $Tp^*Rh(CO)_2$ (Tp* = hydridotris(3,5-

dimethylpyrazolyl)borate), whereby the reaction could be monitored by IR spectroscopy on the femtosecond (10^{-15}) to microsecond (10^{-6}) timescale.[37] Revealed in these studies is the photolytic dissociation of CO from the 18e$^-$ complex Tp*Rh(CO)$_2$ followed by the salvation of the incipient {Tp*Rh(CO)} intermediate yielding Tp*Rh(CO)(alkane). Dechelation of Tp*Rh(CO)(alkane) gives the 16e$^-$ complex {κ^2-TpRh(CO)(alkane)} which is observed to undergo C-H activation of the alkane yielding the product Tp*Rh(CO)(R)(H) (R = alkyl). This study by Bergman reveals further confirmation of the precoordination of hydrocarbons prior to the C-H activation step. Specific bonding modes that have been proposed for alkanes include η^2-*C,H*, κ^2-*H,H*, and κ^3-*H,H,H* interactions (Figure 1.3).[38]

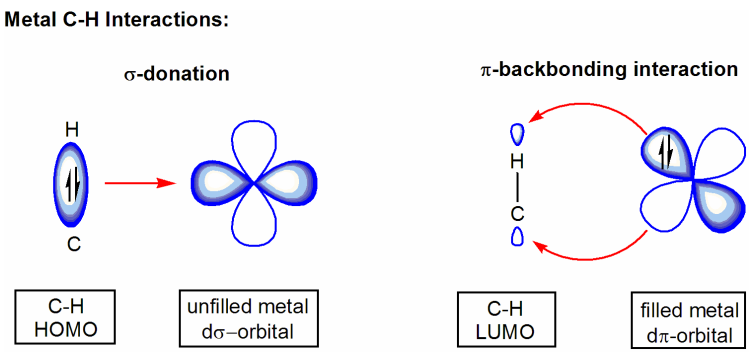

Figure 1.2. Orbital description of the C-H σ and π-interactions with a metal center.

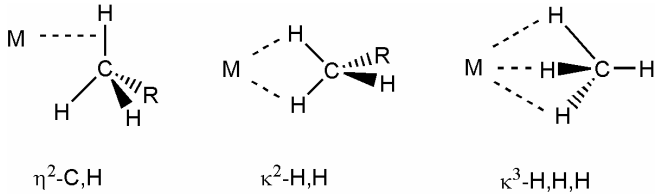

Figure 1.3. Potential precoordination of alkanes to coordinatively unsaturated metal centers.

The bonding interactions of σ-complexes can weaken the C-H bond. It is therefore logical that C-H activation is preceded by an η^2-C-H σ-complex precursor. Furthermore, the C-H σ-interaction is seminal to the C-H bond activation step due to the resulting acidification that occurs in that proximal C-H bond. This explains

the dearth of observed C-H activations when moving from sp^1 to sp^3 hybridized C-H bonds. That is, C-H bonds with enhanced s-character about the carbon (sp hybrid) increases acidity of the C-H bond. The first observed C-H activation by a transition metal was an oxidative addition of a C-H bond of a methyl group of a dmpe (dmpe = dimethylphosphinoethane) ligand on $Ru(dmpe)_2$ resulting in a Ru dimer.[39]

C-H activation mechanisms involving an η^2-C-H interaction with the metal center have been reported. For example, Milstein et. al have observed an intramolecular arene agostic interaction between the 1,3-bis((di-*tert*-butylphosphino)methyl)benzene and the coordinated metal fragment $[Rh(CO)]^+$ in THF.[40] Further evidence for the formation of agostic complexes, prior to intramolecular C-H activation, has been provided by Crabtree and coworkers. Observation of an equilibrium between a C-H agostic interaction of the complex $[Ir(diarpyH)(PR_3)_2H]X$ (diarpyl = 2,6-phenylpyridine, R = Ph, p-$C_6H_4CH_3$, p-C_6H_4F, Me, or ^{n}Bu; X = SbF_6^- or BF_4^-) and the C-H activation and subsequent reductive elimination of a *trans*-C-H fragment yields evidence for C-H σ-complexes in the step proceeding C-H activation (Scheme 1.8).[41] By variation of the phosphine ligands, it is observed that increased σ-donation resulted in the increased rate of C-H activation. The $\Delta G^{\ddagger}$ was calculated to be 12.3 kcal/mol (257 K) for the oxidative addition when $[Ir(diarpyH)(PPh_3)_2H]SbF_6$ was studied.

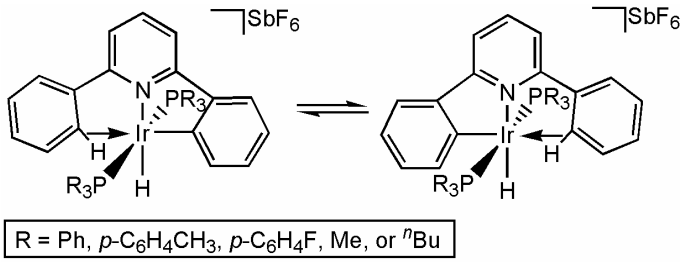

Scheme 1.8. Equilibrium between C-H agostic interaction and *trans* C-H activation of the complex $[Ir(diarpyH)(PR_3)_2H]SbF_6$ (R = Ph, p-$C_6H_4CH_3$, p-C_6H_4F, Me, or ^{n}Bu).

1.3.3 Role of π-Complexes in C-H Activation

The C-H activation of aromatic substrates by transition metals is thought to proceed by precoordination of the aromatic prior to, via either oxidative addition, electrophilic substitution, or σ-bond metathesis, C-H activation. The η^2-binding of an arene (Figure 1.4) is described best by extension of the Dewar-Chatt-

Duncanson Model,[42] in which the π-electrons are stabilized through a σ-interaction with a d-orbital of correct symmetry. Metal-aromatic π-bonding interactions occur through π-back donation into the C=C π* orbital of the aromatic from a filled metal dπ-orbital.

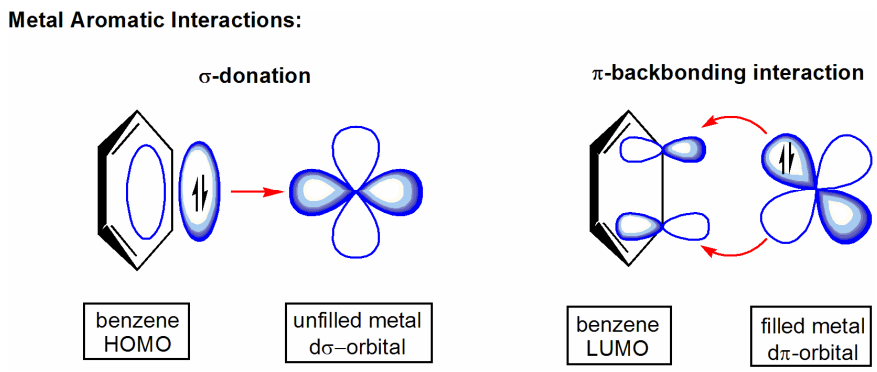

Figure 1.4. Aromatic σ and π-interactions of a metal center and an η^2-coordinated benzene. Benzene HOMO and LUMO are only partially described for simplicity.

Precedence for metal bound η^2-aromatics is well established. Extensive evidence for the existence of these organometallic species has been reported for early *and* late transition metals. For example, in 1966, Amma et al. reported an η^2-C_6H_6·$CuAlCl_4$ complex including solid-state characterization by single-crystal X-ray diffraction study.[43] Wolczanski and coworkers have isolated heteroaromatic, $(silox)_3Ta(\eta^2$-*N,C*-py) (silox = $^tBu_3SiO$; py = pyridine), and carbocyclic $[(silox)_2Ta]_2\{\mu\text{-}\eta^2(1,2):\eta^2(4,5)\text{-}C_6H_6\}$ η^2-coordinated ligands in which the latter serves as a bridging ligand of a dimeric species.[44] Taube and Harman reported monomeric and dimeric Os complexes with dihapto binding of aromatic compounds.[45] For example, Taube and coworkers have synthesized the monomer $[Os(NH_3)_5(\eta^2\text{-}C_6H_6)](OTf)_2$ (OTf = trifluoromethylsulfonate) and the dimer $[Os(NH_3)_5]_2\{\mu\text{-}\eta^2(1,2):\eta^2(4,5)\text{-}C_6H_6\}^{4+}$. Graham and coworkers have reported the formation of $CpRe(NO)(CO)(\eta^2$-*C,C*-$Ph_3CH)$ and propose the dihapto connectivity occurs at the 3,4-position.[46] Evidence for this suggested 3,4-coordination was derived from the observation that both $CpRe(NO)(CO)(meta\text{-}\eta^1\text{-}C_6H_4CHPh_2)$ and $CpRe(NO)(CO)(para\text{-}\eta^1\text{-}C_6H_4CHPh_2)$ are produced when $CpRe(NO)(CO)(\eta^2$-*C,C*-$Ph_3CH)$ is reacted in the presence of a base (i.e., NEt_3). Krüger et al. have synthesized and obtained single-crystal X-ray

analysis on the complex $(TCP)_2Ni(\eta^2\text{-}C,C\text{-}C_{14}H_{10})$ (TCP = triscyclohexylphosphine).[47] Harman et al. have reported advances in the preparation of numerous $\{Os(NH_3)_5(\eta^2\text{-arene})\}^{+2}$ (arene = benzene, naphthalene, furan, thiophene, pyrrole, 2,6-lutidine, etc.) complexes, related dearomatization measurements, structure-property relationships, and reactivity studies.[48, 49] In addition, Harman and coworkers have reported the observed isomerization of dihapto ligands of the complexes of the type $TpRe(CO)(L)(\eta^2\text{-arene})$ (L = ^{t}BuNC, py, PMe_3, or 1-methylimidazole; arene = benzene, anisole, naphthalene, 1-methylpyrrole, furan, or thiophene).[50] Several crystal structures, including $Cp^*Rh(PMe_3)(9,10\text{-}\eta^2\text{-phenanthrene})$ and $Cp^*Rh(PMe_3)(2,3\text{-}\eta^2\text{-perylene})$, were reported by Jones and coworkers providing evidence for the transition metal η^2-aromatic species with species that are known to undergo C-H activation reactivity.[51] These η^2-binding modes provide evidence for the coordination of aromatic systems to transition metals; however, the relation of η^2-precoordination of aromatics to transition metals as it relates to C-H activation was most clearly observed by Jones. Jones and coworkers were the first to report reversible C-H activation of naphthalene from $Cp^*Rh(PMe_3)(\eta^2\text{-naphthalene})$ to form $Cp^*Rh(PMe_3)$(2–naphthyl)H. The K_{eq} = 2.0, favoring the η^2-bound naphthalene complex (Scheme 1.9).[52] As further example of the importance of these dihapto intermediates, Templeton et. al have isolated, characterized, and obtained a crystal structure of the benzene C-H activation intermediate $[(Hpz^*)(\kappa^2\text{-}BHpz^*_2)Pt(H)(\eta^2\text{-}C,C\text{-}C_6H_6)][BAr_4']$ (BAr_4' = $[B(3,5\text{-}\{CF_3\}_2C_6H_3)_4]^-$).[53] A thermally accessible equilibrium for the oxidative addition of benzene from the complex $[(Hpz^*)(\kappa^2\text{-}BHpz^*_2)Pt(H)(C,C\text{-}\eta^2\text{-}C_6H_6)][BAr_4']$ was observed at low temperature by NMR owing reversible nature of these transformations. The $\Delta G^{\ddagger}$ = 12.7 kcal/mol (252 K). Jones et. al calculated the $\Delta H^{\ddagger}$ and $\Delta S^{\ddagger}$ over a range of 25 ^oC for the oxidative addition of benzene to yield $Cp^*Rh(PMe_3)(H)Ph$. At a comparative temperature (252 K) the oxidative addition of coordinated benzene from the complex $Cp^*Rh(PMe_3)(\eta^2\text{-}C,C\text{-}C_6H_6)$ was calculated to be 12.4 kcal/mol.[54]

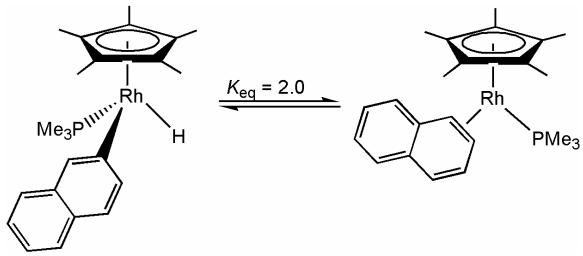

Scheme 1.9. Equilibrium (K_{eq} = 2.0) between Cp*Rh(PMe_3)(η^2-naphthalene) and the C-H activation product Cp*Rh(PMe_3)(H)(2-naphthyl).

Typically, the activation of aromatic C-H bonds is kinetically more facile than alkanes. There are two rationalizations for this trend. Firstly, coordination of aromatic compounds is typically preferred over coordination of alkanes. This is due in part to the higher energy of the arene HOMO (C-C π-bond) relative to the alkane HOMO (C-H σ-bond) and the aromatic's greater ability to act as a π-acceptor ($d\pi \rightarrow \pi^*$) relative to the alkane ($d\pi \rightarrow \sigma^*$). In addition, M-$C_{aryl}$ bonds are typically stronger than M-C_{alkyl} bonds. Jones et al. have demonstrated that stronger incipient M-C bonds can facilitate (kinetically) C-H activation. [55]

It has been reported that relative rates of C-H activation are as follows: sp^2 > sp^3(primary) > sp^3(secondary).[55] This selectivity, addressed by Jones and Feher, is best described by the kinetic competition between arene (benzene) and alkane (propane) C-H activation to rest in the η^2-coordination of arenes vs. C-H activation of alkanes.[56] The rate determining step for benzene C-H activation by the complex {Cp*Rh(PMe_3)} (Cp* = pentamethylcylcopentadienyl) was reported to be the η^2-coordination of benzene, as determined by KIE experiments. Through monitoring the rates of reductive elimination of benzene and propane, at low temperatures, from Cp*Rh(PMe_3)(C_6H_5)H and Cp*Rh(PMe_3)($CH_2CH_2CH_3$)H, respectively, the $\Delta\Delta G^{\ddagger}$ favored the η^2-coordination (benzene) intermediate by 0.6 kcal/mol over the C-H activation product of propane. Though the kinetic barrier is only slightly lower, it is this precoordination that allows arenes to compete with the weaker sp^3 C-H bonds of the aliphatic substrates.

1.3.4 Stoichiometric C-H Bond Activation Mechanisms and Examples

The well developed field of metal-mediated C-H activation is most commonly simplified by the classification of mechanisms.[31, 32, 34, 57-60] Bercaw has presented five synthetic routes for C-H activation including: oxidative addition, σ-bond metathesis, metalloradical activation, 1,2-addition, and electrophilic activation.[61] Radical formation and 1,2-addition are not directly relevant to systems central to this document, therefore these mechanisms will not be discussed in detail.

1.3.4.1 Oxidative Addition

The oxidative addition pathway is common for low oxidation state late transition metals where coordinative unsaturation is accessible. The mechanism for C-H bond oxidative addition involves a net insertion of the metal center (L_nM) into a R-H (R = alkyl or phenyl) bond (eq 1). The two requirements of this pathway are access to a 16 e^- (or fewer) complex and an increase in metal oxidation state of +2.

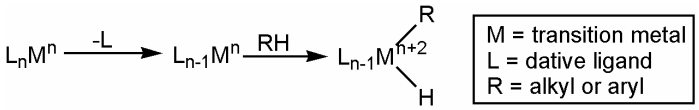

(1)

Examples of C-H activation through the oxidative addition pathway are numerous. For example, Group 9 complexes of the type $Cp^*M(PR_3)(X)_2$ (Cp* = pentamethylcyclopentadienyl; M = Rh or Ir; R = Me or Ph; X = alkyl or hydride) have been used as precursors for C-H activation.[62-69] Either by thermolysis, or more commonly photolysis, the extrusion of X_2 from $CpM(PR_3)(X)_2$ results in a coordinatively unsaturated metal center that can oxidatively add the aromatic substrate by C-H activation. Bergman and Jones have extended this work to include similar Re systems.[70-72] Jones et al. have extended the scope of reactivity to include the first row metal Fe for oxidative addition of C-H bonds.[73] Eisenberg et al. have reported thermally and photolytically promoted reactions that result in oxidative addition of arenes. Despite coordinative unsaturation of the Eisenberg system (dppe)Ir(H)(CO) (dppe = diphenylphosphinoethane), dissociation of one of the dppe arms is necessary to create a reactive intermediate for C-H bond activation (Scheme 1.10).[74] From this 14e^-

species oxidative addition is achieved followed by recoordination of the phosphine arm yielding the octahedral product (dppe)Ir(H)$_2$(CO)Ph.

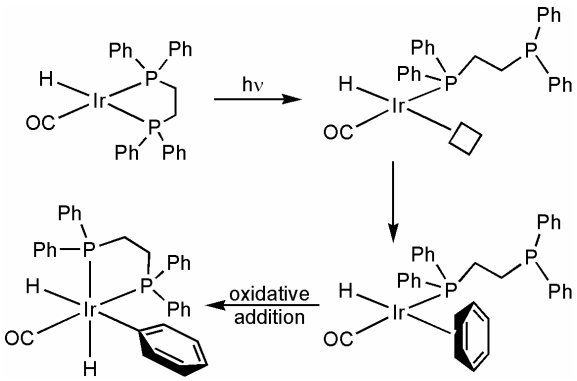

Scheme 1.10. Oxidative addition of benzene to the Ir(H)(CO)(dppe) via dissociation of a phosphine chelate arm.

1.3.4.2 Electrophilic Substitution

For the electrophilic mechanism the metal center acts as an electrophile. This mechanism involves the exchange of a hydrogen atom for a metal center usually occurring through a Wheland-type intermediate (eq 2). In this scenario, the metal coordinates the aromatic using π electrons rather than C-H σ-electrons. Electrophilic substitution is most common with aromatic hydrocarbons; however, this mechanism has been proposed for some alkanes.[61]

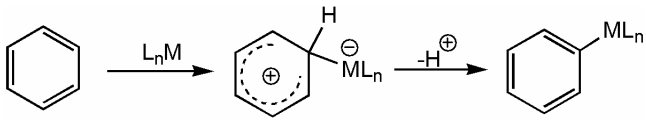

(2)

Yi and coworkers have observed, on the basis of a Hammett study, that C-H activation of arylamines (e.g., aniline) by the complex [Ru(PCy$_3$)$_2$(CO)(NCMe)H]BF$_4$ is consistent with an electrophilic substitution mechanism.[75]

1.3.4.3 Sigma-Bond Metathesis

The metal centers most commonly involved in this type of mechanism possess a d^0 electron configuration, in which a formal oxidation of the metal center is not feasible (eq 3).

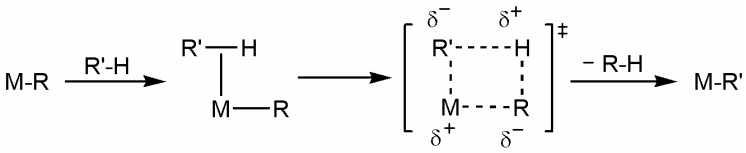

(3)

Tilley et al. have reported σ-bond metathesis reactions involving high oxidation state early transition metals whereby the C-H bonds of benzene and toluene are cleaved in the presence of $Cp_2Hf(Si(H)_2Mes)Me$ and $B(C_6F_5)_3$ (Scheme 1.11).[76] Bercaw and coworkers have observed the production of $(Cp^*\text{-}d_{15})_2Sc(Ph)$ and CH_4 by the reacting $(Cp^*\text{-}d_{15})_2Sc(Me)$ and C_6H_6.[77] Reactivity studies revealed two important characteristics: (1) the reactivity observed with functionalized arenes were inconsistent with an electrophilic mechanism and (2) the C-H activation transition state is likely to undergo η^2-*C,H*-coordination (product of sterics) with the metal center as opposed to η^2-*C,C*-coordination. This chemistry has been extended with alkanes to f-block complexes. For example, Watson has reported the reactivity of $Cp^*_2Lu(^{12}CH_3)$ yields production of $Cp^*_2Lu(^{13}CH_3)$ and $^{12}CH_4$ in the presence of $^{13}CH_4$.[78]

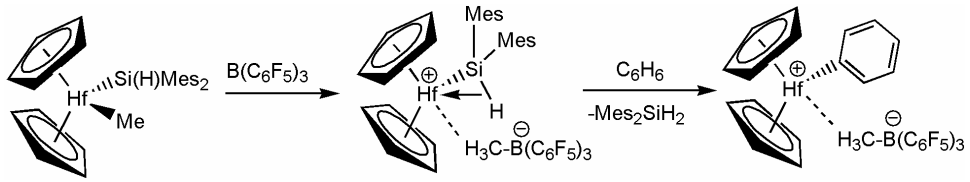

Scheme 1.11. C-H activation of benzene by a σ-bond metathesis pathway using $Cp_2Hf(Si(H)_2Mes)Me$.

While σ-bond metathesis is typically associated with early transition metal complexes, it has been proposed that for late transition metal systems may also initiate C-H activation by this pathway.[79, 80] Eisenstein and coworkers have reported theoretical studies on methane C-H activation by $TpM^{II}(PH_3)H$ (M = Fe, Ru, or

Os) systems.[81] It was shown by density functional theory (DFT) calculations that Fe would be expected to undergo a route that is more comparable to a σ-bond metathesis pathway while the Os derivative is calculated to undergo an oxidative addition mechanism where the potential energy surface predicts stability for the Os^{IV} intermediate. C-H activation by the Ru complex is predicted to go through a pathway intermediate to that of the σ-bond metathesis route and an oxidative addition route. The mechanisms of C-H activation by $[Cp^*Ir(PMe_3)Me]^+$ systems has been closely scrutinized. Hinderling and coworkers published a theoretical study[82] methane activation by $[Cp^*Ir(PMe_3)Me]^+$ supporting a σ-bond metathesis pathway. Hall and coworkers have reevaluated the system with new DFT computational, using a B3LYP functional and the BS1 and BS2 basis sets, and report an oxidative addition pathway as most likely. [83] Bergman et al. have since shown that intramolecular C-H activation of phosphine ligand C-H bonds occurs through an oxidative addition pathway upon incorporation of phosphine ligands of different nature further supporting the likelihood of oxidative addition over σ-bond metathesis.[68] It was calculated that the transition state for the σ-bond metathesis pathway (for the electron deficient Ir^{III} cationic complex) does not exist and therefore should likely be dismissed. Instead, the intramolecular oxidative addition of the phosphine PMe_3 ligand is likely to occur. These conclusions were drawn despite the relatively high oxidative addition kinetic barrier of 26.5 kcal/mol at the BS1 level of theory, reported by Hall et al. DFT calculations are still being reported that assign late-transition metal C-H activation transition states as being consistent for σ-bond metathesis routes. For example, Periana, in conjunction with Oxgaard and Goddard, have proposed that the C-H activation of benzene by the complex $Ir(\kappa^2\text{-}O,O\text{-acac})_2(py)(OMe)$ to yield $Ir(\kappa^2\text{-}O,O\text{-acac})_2(py)Ph$ and MeOH undergoes a transition state consistent to a σ-bond metathesis mechanism.[84] In this study the transannular hydrogen was calculated to be 1.98 Å from the Ir^{III} metal center in the transition state, consistent with a σ-bond metathesis pathway. It is proposed that this pathway might be optimal due to presence of five oxygen atoms coordinated to the Ir metal center in the transition state.

1.3.5 Catalytic Aromatic C-H Bond Activation

Oxidative coupling (Scheme 1.12) of unsaturated substrates and arenes provide potentially valuable pathways for C-C bond forming reactions. This dissertation is not meant to serve as an exhaustive comprehensive review of catalytic C-H activation, nor are oxidative coupling reactions directly pertinent to the mechanisms for catalytic C-H activation reported herein, however, these mechanisms will be discussed in brief for the sake of completeness. Similar to the Heck reaction, the oxidative coupling of an olefin and arene yields an unsaturated product. Metal-mediated oxidative coupling usually involves (1) electrophilic attack of the metal center on an aromatic C-H bond to give a C-H activated product, M-Ar, (2) olefin insertion into the M-Ar bond, (3) β-hydride elimination and olefin dissociation, and (4) reductive regeneration of the active metal catalyst.

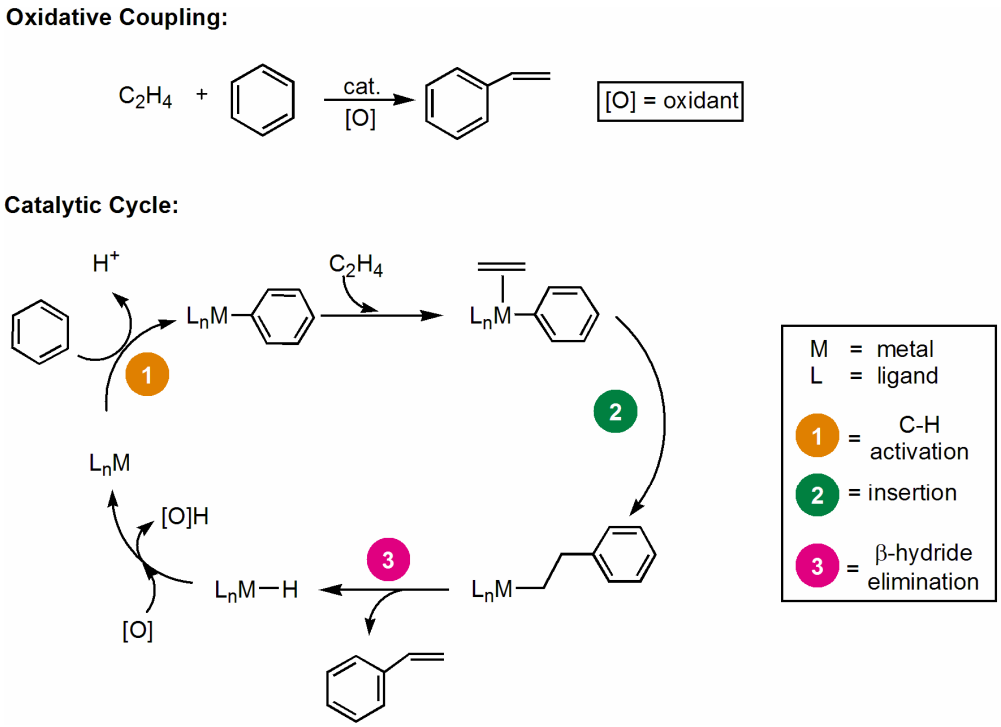

Scheme 1.12. Oxidative hydrophenylation of ethylene to produce styrene.

Milstein and coworkers have observed 88 turnovers for methyl cinnamate production in 48 hours by heating (180 ^{o}C) catalytic amounts of $RuCl_3 \cdot 3H_2O$ in the presence of benzene, methyl acrylate, CO, and O_2.[85] Progress has been made with the C-H activation of unactivated arenes by Tsuji et al. In this work, it was reported that $Pd(OCOPh)_2$ in the presence of (Ph)(H)C=C(H)(OMe), benzene, *tert*-butyl perbenzoate as the oxidant, and acetic acid as the solvent gives catalytic production of $(Ph)_2C=C(H)(OMe)$, at 100 ^{o}C.[86]

Catalytic hydroarylation of olefins (see Figure 1.1) is more common than oxidative coupling. Processes included a range of substrates and arenes. Fujiwara has reported that $Pd(OAc)_2$ initiates hydroarylation of olefins and alkynes.[87, 88] In most cases, an activated olefin is required for successful catalysis. Miura et al. have used the heteroatom functionality of 1-napthols to demonstrate regioselective Ir-catalyzed arene C-H activation that leads to C-C bond addition reactions with alkynes.[89] Yamazaki et al. found that $Ru_4(CO)_{12}$, in the presence of CO gas, benzene, and diphenylacetylene, yields the catalytic formation of triphenylethylene.[90] Based on independently reported Ir-phenylene complexes, it was suggested that oxidative addition, insertion, and reductive elimination are key steps in the triphenylethylene production. Tsukada et al. have demonstrated the ability to form new C-C bonds between benzene and disubstituted alkynes to yield arylated alkenes in the presence of a Pd dimer and trialkylboranes at 100 ^{o}C.[91] Nolan has shown that $(IPr)Pd(O_2CCF_3)_2$ (IPr = 1,3-bis(2,6-diisopropyl-phenyl)imidazol-2-ylidene) catalyzes the insertion of ethyl propiolate into the C-H bond of mesitylene in 78% yield under harsh acidic conditions.[92]

Catalytic intramolecular C-H activation for the annulation of aromatic imines was reported by Bergman et al.[93] For example, benzyl-{3-[2-allyl]-benzylidine}-amine was heated to 125 ^{o}C in the presence of Wilkinson's catalyst $(PPh_3)_3RhCl$ and toluene to produce indan-4-methylketone (indan = 1,2-cyclopentanebenzene) and 3-[(1-methyl)-vinyl]-acetophenone (3:1 ratio) upon acid workup. In addition to indans, Bergman et al. have used these intramolecular cyclizations to produce tetralins, dihydrofurans, and dihydroindoles. These cyclizations are thought to proceed through (1) precoordination of substrate (e.g., allyl substituted ketimines), (2) oxidative addition of the C-H bond ortho to the imine functionality, (3) olefin insertion, and (4) reductive elimination of product (e.g, indan derivative), Scheme 1.13.

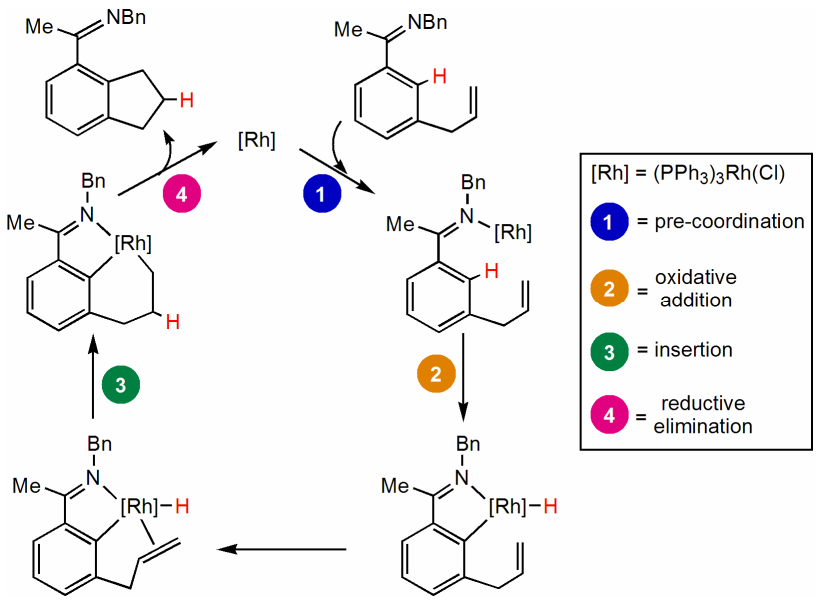

Scheme 1.13. Catalytic annulation of aromatic imines via intramolecular C-H bond activation.

Substituted benzenes also undergo catalytic C-H activation to yield new C-C bonds. For example, Fujiwara et al. have reported intramolecular cyclizations via C-H activation and subsequent C-C bond formation steps in excess of 1000 turnovers using $Pd(OAc)_2$ at room temperature with alkynanilides and alkynoates to yield quinolinones and coumerins, respectively.[94] It is proposed that a highly electrophilic cationic metal, $Pd(O_2C(CF_3))_2$, is generated in trifluoroacetic acid (TFA).

Hydroarylation of olefins for aromatic substrates that posses *O*- or *N*-functionality has been reported. Murai has introduced systems that consistently produce regioselective catalytic C-H activation ortho to aldehyde or ketone functional groups.[95] Initially, Murai discovered that $Ru(H)_2(CO)(PPh_3)_3$ catalyzes the C-H activation of aryl ketones ortho to the acyl functionality and subsequent C-C bond formation with triethoxyvinylsilane through an insertion mechanism to yield the ortho alkylated product (Scheme 1.14).[95] Intermediates, proposed by Murai, have also independently isolated giving further evidence of the precoordination and therefore the directing ability of the heteroatomic functionality. Similarly, Whittlesey and coworkers have achieved isolation and single-crystal X-ray analysis of $Ru(H)(\kappa^2\text{-}O,C\text{-}C_6H_4C(O)CH_3)(CO)(PPh_3)_2$.[96] Brookhart et al. have observed that $[Cp^*Rh(C_2H_3SiMe_2)_2]$ catalyzes the

production of acetophenone and vinyltrimethylsilane at 120 ^{o}C in cyclohexane.[97] This chemistry has been extended to heteroaromatic compounds to yield bond functionalization at less reactive C-H bonds. For example, heteroaromatic ketones such as 3-acetylthiophene undergo functionalization at the 3-position.[98] Similar chemistry has been observed by Mares and coworkers whereby aniline undergoes orthometalation and insertion of ethylene into the insipient M-C bond is achieved for the catalytic production of 2-methylquinoline.[99]

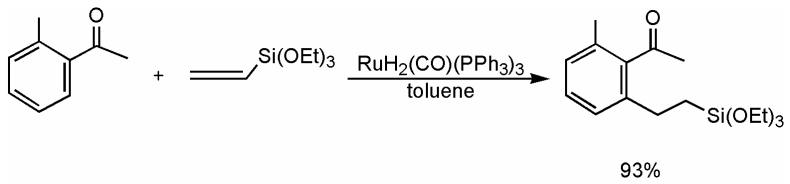

Scheme 1.14. Chelate assisted C-H bond activation ortho to the heteroatomic functionality.

Under photolytic conditions, $CpRe(PPh_3)_2(H)_2$ catalyzes production of ethylbenzene from benzene, ethylene, and dihydrogen.[100] Other products are formed and catalyst decomposition limits catalytic activity to approximately 15 turnovers. Hydrophenylation of terminal acetylenes using $Rh(PMe_3)_2(CO)(Cl)$ has been reported by Goldman et al.[101] In addition, crossover studies revealed the hydrogen and phenyl substituents to be from the same source. Also, a KIE (kinetic isotope effect, K_H/K_D) of 1.4 was measured.

The ability to perform hydroarylation of olefins with unactivated arenes and unactivated olefins remains a challenge. Periana et al. have reported a $(acac)_2Ir(py)Ph$ complex (acac = κ^2-*O,O*-acetonate, py = pyridine) that has been shown to hydroarylate olefins.[84, 102-105] For α-olefins, moderate selectivity for anti-Markovnikov products was observed. These catalytic reactions (e.g., the reaction with ethylene and benzene) occur at high temperatures (180 ^{o}C) and low pressures (284 psi) to achieve 455 turnovers after only 3 hours.

1.4 Chemistry of TpRu(CO)(NCMe)R (R = Me or Ph)

1.4.1 Rationale for Catalyst Design

Dyker recently wrote a review on catalytic coupling reactions involving C-H activation. In this review he discussed the importance of C-H activation. Dyker stated:

> *The activation of C-H bonds is of the same fundamental importance as the formation of C-C bonds for the construction of organic molecules. Particularly in the last ten years, transition metal catalyzed processes have been developed which achieve both these in a single preparative step and hence combine economy, efficiency, and elegance… For instance, ruthenium has proved to be particularly efficient for the C-H activation of arenes…*

Our group has reported that TpRu(CO)(NCMe)Ph catalyzes the hydrophenylation of ethylene and α-olefins (see below), Figure 1.5.[106, 107] In the κ^3 coordination mode, Tp coordinates in a facial fashion and tends to enforce the octahedral environment. The anionic Tp ligand is a relatively strong electron donor and is typically inert. The carbonyl ligand is a strong π-acid, while the acetonitrile ligand is labile and dissociates in CD_3CN at 70 °C with a k_{obs} = 3.2(2) x 10^{-5} s^{-1}. The dissociation of acetonitrile provides a path for coordination of Lewis basic substrates (e.g., ethylene, benzene, etc.). The metal is a Ru^{II} center, which is a relatively low-oxidation state that potentially provides redox flexibility. The catalyst architecture makes available the ability to tune the catalyst for potential enhanced reactivity by varying the steric and electronic nature of ancillary ligands. For example, CO can be substituted for dative ligands (e.g., phosphines) and Tp can be varied at the 3, 4, and/or 5 position of the pyrazolyl rings.

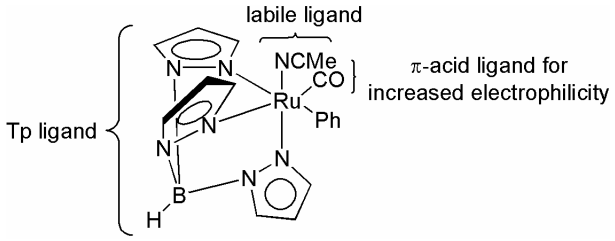

Figure 1.5. TpRu(CO)(NCMe)Ph.

1.4.2 Reactivity of TpRu(CO)(NCMe)R (R = Me or Ph)

Similar to the technology developed by Periana and coworkers, we have synthesized a late transition metal catalyst, TpRu(CO)(NCMe)Ph (Tp = hydridotris(pyrazolyl)borate), for the hydroarylation of olefins.[106, 107] The TpRu(CO)(NCMe)Ph complex is prepared by stoichiometric C-H activation of benzene from the methyl derivative, TpRu(CO)(NCMe)Me, as shown in Scheme 1.15.

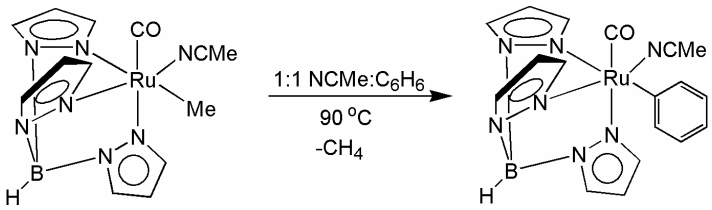

Scheme 1.15. Stoichiometric C-H activation of benzene with TpRu(CO)(NCMe)Me yielding TpRu(CO)(NCMe)Ph and methane.

Catalytic production of alkylbenzenes is achieved upon heating arene and olefin in the presence of TpRu(CO)(NCMe)Ph (Table 1.1). For example, when TpRu(CO)(NCMe)Ph (0.1 mol %) is placed under 25 psi of ethylene in benzene (90 ^{o}C), ethylbenzene is produced (51 turnovers after 4 hours). After a reaction time of 4 hours the reactivity of the catalyst slows. This is most likely due to catalyst degradation.

Table 1.1. Data for the catalytic hydrophenylation of alkenes and alkynes using TpRu(CO)(NCMe)Ph (0.1 mol %; 25 psi of gas), at 90 °C, over a 4 h period (unless otherwise noted).

Arene	Unsaturated Substrate	TON[a]	Products
benzene	ethylene	51 (77)[b]	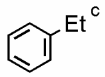
benzene	propene	10	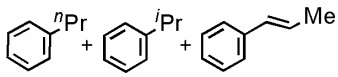 (1.6:1:trace)
benzene	1-hexene[d]	11	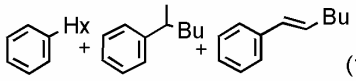 (1.7:1:trace)
benzene[e]	isobutylene	No Reaction	No Organic Products
ethylbenzene	ethylene	11	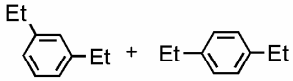
benzene[d]	acetylene[f]	Trace Product	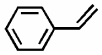

[a] mol $[TpRu(CO)(NCMe)(Ph)]^{-1}s^{-1}$. [b] Turnovers observed after 24 h are given in parentheses. [c] Trace quantities of 1,3- and 1,4-diethylbenzene are also produced. [d] 50 equiv. based on TpRu(CO)(NCMe)(Ph), after 6 h. [e] 24 h. [f] 10 psi.

This chemistry was successfully extended to include catalytic hydroarylation of propene and 1-hexene; however there is decline in total TON (turnover number) of α-olefins vs. ethylene. After 4 hours, the combination of ethylbenzene with ethylene yielded 11 turnovers of 1,3-diethylbenzene and 1,4-diethylbenzene when reacting ethylbenzene with ethylene under similar catalytic conditions. The turnover frequency for the production of ethylbenzenes is approximately 5 times slower for alkylation of ethylbenzene (7.6×10^{-4} turnovers·s^{-1}) than that of benzene (3.5×10^{-3} turnovers·s^{-1}). This is consistent with a metal-mediated single-site catalyst performing the transformation. This is further confirmed by the catalyst's inability to hydroarylate isobutylene, most likely due to steric inhibition. Second, the regioselectivity of alkylation is inconsistent with that of Friedel-Crafts chemistry. Further evidence for this complex not acting as a Lewis acid catalyst for the promotion of Friedel-Crafts chemistry was observed. For example, Friedel-Crafts chemistry for the coupling of propene and benzene would produce the branched product (isopropylbenzene) exclusively. That is, the natural predilection for stabilization of the carbocation intermediate, necessary and common in Friedel-Crafts

chemistry, would provide a route for isopropylbenzene production whereas the TpRu(CO)(NCMe)Ph complexes produce a linear to branched ratio of ~1.6. In addition, no ethylbenzene is produced in the conproportionation reaction of 1,4-diethylbenzene with benzene, as is often witnessed in the presence of Lewis acid catalysts.

Our group has also studied the mechanism for catalytic hydroarylation of olefins by TpRu(CO)(NCMe)R.[106] The proposed catalytic cycle is, outlined in Scheme 1.16. Three key steps in this mechanism include (1) dissociation of the labile ligand (NCMe) to gain access to the coordinatively unsaturated $16e^-$ reactive intermediate {TpRu(CO)Ph}, (2) olefin coordination and insertion into the M-C_{aryl} bond, and (3) the C-H activation of benzene to release the free organic product and regenerate the catalyst. The intermediate from ethylene insertion, {TpRu(CO)(CH_2CH_2Ph)}, was independently synthesized and trapped with NCMe to give TpRu(CO)(NCMe)(CH2CH2Ph) lending evidence that this intermediate is stable. Also, in stoichiometric reactions, the phenethyl intermediate activates benzene to produce ethylbenzene. A kinetic isotope effect (KIE) of 2.1(1) was observed in the catalytic formation of ethylbenzene and ethylbenzene-d_6 when catalysis was carried out in a 1:1 mixture of C_6H_6 and C_6D_6. From these data, it can be proposed that the rate determining step for the catalytic formation of ethylbenzene is C-H activation of benzene. Consistent with these results, the stoichiometric C-H activation of C_6H_6 and C_6D_6 with TpRu(CO)(NCMe)Me yielded a similar KIE of 2.5(5). An inverse dependence of rate of catalysis on [ethylene] lends evidence for the TpRu(CO)(H(R)C=CH_2)(CH_2CH_2Ph) is the resting state of the cycle. Lastly, β-hydride elimination is not likely the source of decomposition due to the lack of styrene formation over a range of ethylene pressures.

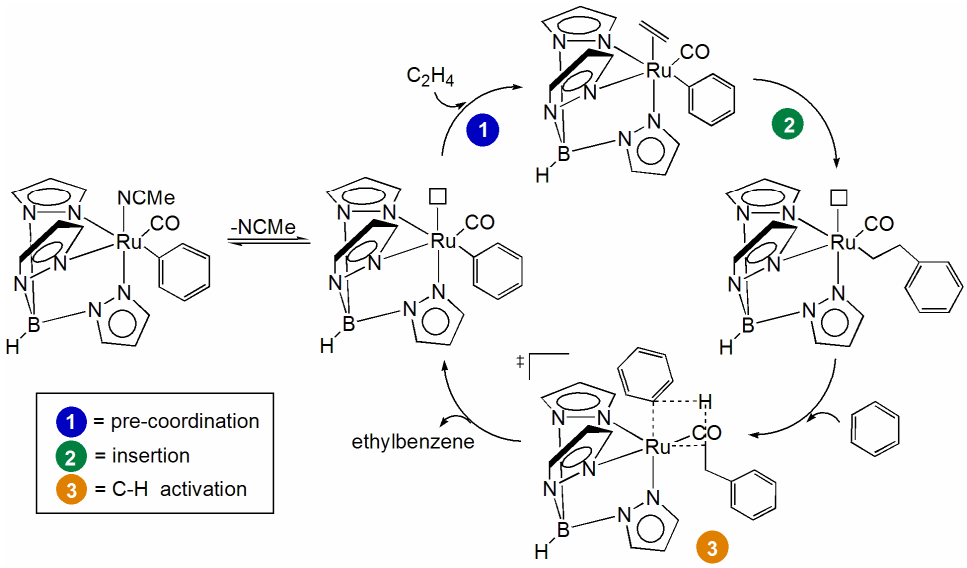

Scheme 1.16. The proposed catalytic cycle for the TpRu(CO)(NCMe)Ph promoted hydroarylation of olefins in the presence benzene.

To further evaluate the mechanism, theoretical work has also been published on this system for insight into parameter and catalyst optimization.[106, 108, 109] Computational studies completed under the direction of Cundari and coworkers in conjunction with Gunnoe et al. utilized a B3LYP/SBK(d) functional and basis set at the DFT level of theory.[106] For the minimization of computational time, the tris(azo)borate (TAB) ligand, $HB(N{=}NH)_3$, was used as a substitute for Tp.[110] In addition, NCMe was replaced with NCH for modeling purposes. The highest kinetic barrier in the catalytic cycle was calculated to be the C-H activation step with a $\Delta H^{\ddagger}$ of 21.2 kcal/mol. In these studies it was reported that the catalytic cycle does not involve the formation of Ru^{IV} intermediates.

For the transition state, it was found that the transannular hydrogen is bent out of the plane of the arene ring with a Ru-H-C bond angle of 50.3°. Cundari et al. report that this is likely either due to the rehybridization of the aryl carbon of hydrogen origin due to an electrophilic aromatic substitution mechanism causing a rehybridization of the carbon of origin or is the product of the proton migration path. In this transition state, a Ru-H distance of 1.72 Å potentially reveals oxidative character.

Independent theoretical studies of TpRu(CO)(NCMe)Ph were carried out by Goddard et al. at the B3LYP/LACVP** level of theory.[108] The authors propose a mechanism for C-H activation termed "oxidative

hydrogen migration" based on similar results. These independent calculations reveal a similar transannular hydrogen-Ru bond distance of 1.61 Å. These studies report that the highest calculated kinetic barrier is the olefin insertion ($\Delta H^{\ddagger}$ = 24.9 kcal/mol) and not the C-H activation step (19.7 kcal/mol). Further evaluation by Goddard et al. provides a direct comparison between Periana's [Ir(μ-acac-*O*)(acac-*O*,*O*)(acac-C^3)]$_2$ system and our TpRu(CO)(NCMe)Ph system.[109] There it is projected, based on empirical data, that the TpRu(CO)(NCMe)Ph precatalyst is approximately 200 times faster than the Ir system. Though it is proposed that at high pressures of ethylene "significant oligomerization" should be obtainable, less than stoichiometric amounts of butylbenzene were achieved.[106] Further discussion based on an in depth computational analysis reveals that π-backbonding interactions with unsaturated substrates and oxidizability of the metal center, necessary for competent C-H activation routes with oxidative character, are the two competing characteristics in these hydroarylation processes.[109] Initial theoretical evaluations reveal that it might not be possible to have independent control of one of these characteristics as they will not have isolated effects.

Further, a mechanistic evaluation has been completed by Gunnoe et al. on the TpRu(CO)(NCMe)Ph system whereby elucidation of the decomposition products was investigated. During catalysis of ethylbenzene at increased ethylene pressures, 250 psi, the TpRu(CO)(η^3-C_4H_7) was observed (Scheme 1.17). In addition, the TpRu(CO)(η^3-C_4H_7) was synthesized almost quantitatively under stoichiometric conditions in THF, at 70 ^{o}C. The intermediate in this reaction, TpRu(CO)(η^2-C_2H_4)(CH_2CH_2Ph), was observed spectroscopically by ^{1}H NMR. From the TpRu(CO)(η^2-C_2H_4)(CH_2CH_2Ph) species, it is proposed that C-H activation of ethylene eliminates ethylbenzene and produces the unobservable vinyl complex intermediate {TpRu(CO)(C(H)CH_2)}. Upon addition of ethylene to this coordinatively unsaturated reactive species, it is further proposed that insertion of ethylene occurs resulting in the isolated allyl product TpRu(CO)(η^3-C_4H_7).

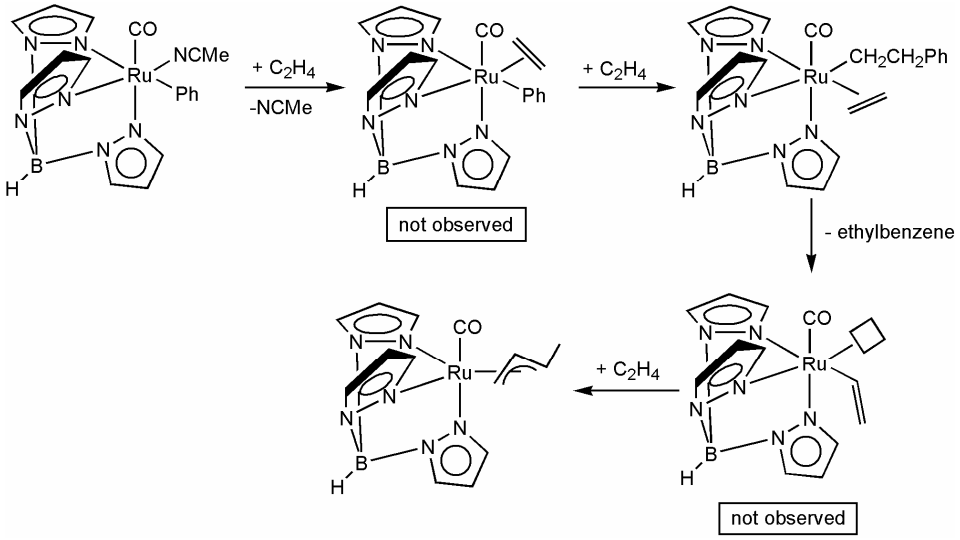

Scheme 1.17. Proposed mechanism for TpRu(CO)(η^3-C_4H_7) formation.

C-H activation has also been observed with electron rich species. Possible hydroarylation of with electron rich olefins has been probed where is was found that TpRu(CO)(NCMe)Ph reacts with 2,3-dihydrofuran to produce TpRu(CO)(NCMe)(C≡C(CH_2)$_2$OH) and C_6H_6 (Scheme 1.18).[111] Initial C-H activation at the 2-position of 2,3-dihydrofuran to yield a TpRu(CO)(NCMe)(2-2,3-dihydrofuryl) intermediate and C_6H_6 was proposed. Subsequent reactivity proceeds through a C-O bond cleavage ring opening step yielding the TpRu(CO)(NCMe)(C≡C(CH_2)$_2$OH) product.

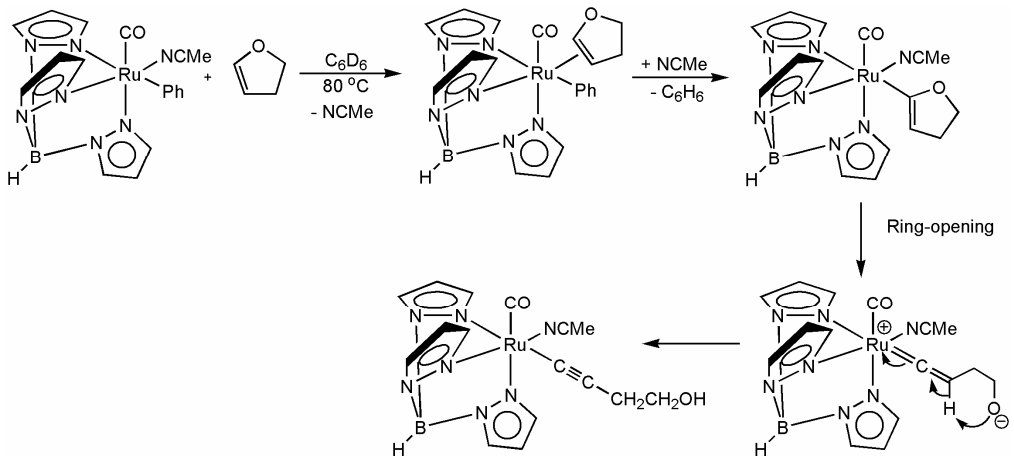

Scheme 1.18. Proposed pathway for the formation of TpRu(CO)(NCMe)(C≡C(CH_2)$_2$OH).

TpRu(CO)(NCMe)Ph has also been shown to activate aldehydic C-H bonds.[112] For example, Gunnoe and coworkers have observed that TpRu(CO)(NCMe)Ph initiates C-H activation and subsequent decarbonylation of benzaldehyde to yield the TpRu(CO)$_2$Ph complex and benzene (Scheme 1.19) at 90 °C. Theoretical analysis, combined with the experimental results, reveal a $\Delta G^{\ddagger}$ value of 18.6 kcal/mol, which is considerably lower than the calculated value for benzene C-H activation (21.2 kcal/mol).

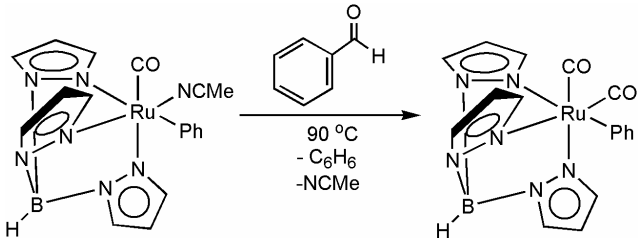

Scheme 1.19. Decarbonylation of benzaldehyde by TpRu(CO)(NCMe)Ph yielding TpRu(CO)$_2$Ph and benzene.

1.5 Summary

Initial success has been met with the C-H activation of arenes and their subsequent C-C bond formation has been realized; however, progress can still be had so the implementation of like technologies is economically feasible for the reasons described above. The marriage of experimental and theoretical analysis has aided in the understanding of the TpRu(CO)(NCMe)Ph catalyst in the hydrophenylation via C-H activation.

While substantial progress has been made in the area of catalytic functionalization of aromatic C-H bonds substantial challenges remain. The goal of this dissertation is to expand upon the known scope of reactivity of TpRu(CO)(NCMe)Ph and the development of its analogs for the purpose of catalytic C-H activation yielding hydroarylation products. Herein, we disclose the progress made in C-H activation and functionalization of heteroaromatics, competition studies where N-H and C-H bonds are present, and the development of cationic analogs through Mp (Mp = tris(pyrazolyl)methane and Ep (Ep = tris(pyrazolyl)ethane) incorporation.

Reference

1. Zumdahl, S. S., *Chemistry*. fourth edition ed.; Houghton Mifflin Co.: Boston, 1997.

2. Technology, N. R. C. B. o. C. S. a., *Catalysis Looks to the Future*. National Academy Press: Washington, D.C., 1992.

3. Bond, G. C., *Metal-Catalysed Reactions of Hydrocarbons*. Springer Science and Business Media, Inc.: New York, 2005.

4. Collman, J. P.; Hegedus, L. S.; Norton, J. R.; Finke, R. G., *Principles and Applications of Organotransition Metal Chemistry*. Second ed.; University Science Books: Sausalito, 1987.

5. Bhaduri, S.; Doble, M., *Homogeneous Catalysis: Mechanism and Industrial Application*. John Wiley and Sons, Inc.: New York, 2000.

6. Wittcoff, H. A.; Reuben, B. G.; Plotkin, J. S., *Industrial Organic Chemicals*. Second ed.; John Wiley and Sons, Inc.: Hoboken, 2004.

7. Weast, R. C.; Selby, S. M., Handbook of Chemistry and Physics. 48th Ed.; The Chemical Rubber Co.: Cleveland, 1966.

8. Smith, M. B.; March, J., *March's Advanced Organic Chemistry: Reactions, Mechanisms, and Structure.* Fifth ed.; John Wiley & Sons, Inc.: New York, 2001.

9. Kwa, T. L.; Boelhouwer, C. *Tetrahedron* **1970**, *25*, 5771.

10. Stemmler, T. L.; Barnhart, T. M.; Penner-Hahn, J. E.; Tucker, C. E.; Knochel, P.; Boehme, M.; Frenking, G. J. *J. Am. Chem. Soc.* **1995**, *117*, 12489.

11. Ellis, G. P.; Romneyalexander, T. M. *Chem. Rev.* **1987**, *87*, 779-794.

12. Beech, W. F. *J. Am. Chem. Soc.* **1954**, 1297-1302.

13. Stephens, R. D.; Castro, C. E. *J. Org. Chem.* **1963**, *28*, 3313-&.

14. Fanta, P. E. *Synthesis-Stuttgart* **1974**, 9-21.

15. Gore, P. H. *Chem. Ind*. **1974**, 727-731.

16. Roberts, R. M.; Khalaf, A. A., *Friedel-Crafts Alkylation Chemistry*. Marcel-Dekker: New York, 1984.

17. Tanaka, M.; Fujiwara, M.; Ando, H. *J. Org. Chem.* **1995**, *60*, 2106-2111.

18. Kumada, M. *Pure Appl. Chem*. **1980**, *52*, 669-679.

19. Kumada, M.; Tamao, K.; Sumitani, K. *Org. Synth*. **1988**, Collect. VI, 407-411.

20. Negishi, E.-I.; Takahashi, T.; King, O. A. *Org. Synth.* **1988**, *66*, 67-74.

21. Sekiya, A.; Ishikawa, N. *J. Organomet. Chem*. **1976**, *118*, 349-354.

22. Crisp, G. *Chem. Soc. Rev*. **1998**, *27*, 2457-2483.

23. Hassan, J.; Sevignon, M.; Gozzi, C.; Schulz, E.; Lemaire, M. *Chem. Rev*. **2002**, *102*, 1359-1469.

24. Miyaura, N.; Suzuki, A. *Chem. Rev*. **1995**, *95*, 2457-2483.

25. Herbert, J. M. *Tetrahedron Lett*. **2004**, *45*, 817-819.

26. Negishi, E.; Vanhorn, D. E. *J. Am. Chem. Soc.* **1977**, *99*, 3168-3170.

27. Peyrat, J. F.; Thomas, E.; L'Hermite, N.; Alami, M.; Brion, J. D. *Tetrahedron Lett*. **2003**, *44*, 6703-6707.

28. Negishi, E.; Okukado, N.; King, A. O.; Vanhorn, D. E.; Spiegel, B. I. *J. Am. Chem. Soc.* 1978, *100*, 2254-2256.

29. Yamamoto, A. *J. Organomet. Chem*. **2000**, *600*, 159-167.

30. Goj, L. A.; Gunnoe, T. B. *Curr. Org. Chem*. **2005**, *9*, 671-685.

31. Guari, Y.; Sabo-Etienne, S.; Chaudret, B. *Eur. J. Inorg. Chem*. **1999**, 1047-1055.

32. Ritleng, V.; Sirlin, C.; Pfeffer, M. *Chem. Rev*. **2002**, *102*, 1731-1769.

33. Rothwell, I. P. *Polyhedron* **1985**, *4*, 177-200.

34. Shilov, A. E.; Shul'pin, G. B. *Chem. Rev.* **1997**, *97*, 2879-2932.

35. Goldberg, K. I.; Goldman, A. S., *Activation and Functionalization of C-H Bonds*. Oxford University Press: Washington, D.C., 2004.

36. Perutz, R. N.; Turner, J. J. *J. Am. Chem. Soc*. **1975**, *97*, 4791-4800.

37. Asplund, M. C.; Snee, P. T.; Yeston, J. S.; Wilkens, M. J.; Payne, C. K.; Yang, H.; Kotz, K. T.; Frei, H.; Bergman, R. G.; Harris, C. B. *J. Am. Chem. Soc*. **2002**, *124*, 10605-10612.

38. Northcutt, T. O.; Wick, D. D.; Vetter, A. J.; Jones, W. D. *J. Am. Chem. Soc*. **2001**, *123*, 7257-7270.

39. Chatt, J.; Davidson, J. M. *J. Am. Chem. Soc.* **1965**, 843-845.

40. Vigalock, A.; Uzan, O.; Shimon, L. J. W.; Ben-David, Y.; Martin, J. M. L.; Milstein, D. *J. Am. Chem. Soc*. **1998**, *120*, 12539-12544.

41. Albeniz, A. C.; Schulte, G.; Crabtree, R. H. *Organometallics* **1992**, *11*, 242-249.

42. Chatt, J.; Duncanson, L. A. *J. Am. Chem. Soc*. **1953**, 2939-2947.

43. Turner, R. W.; Amma, E. L. *J. Am. Chem. Soc*. **1966**, *88*, 1877-1879.

44. Neithamer, D. R.; Parkanyi, L.; Mitchell, J. F.; Wolczanski, P. T. *J. Am. Chem. Soc*. **1988**, *110*, 4421-4423.

45. Harman, W. D.; Taube, H. *J. Am. Chem. Soc*. **1987**, *109*, 1883-1885.

46. Sweet, J. R.; Graham, W. A. G. *Organometallics* **1983**, *2*, 135-140.

47. Brauer, D. J.; Kruger, C. *Inorg. Chem*. **1977**, *16*, 884-891.

48. Brooks, B. C.; Gunnoe, T. B.; Harman, W. D. *Coord. Chem. Rev*. **2000**, *206*, 3-61.

49. Harman, W. D. *Chem. Rev.* **1997**, *97*, 1953-1978.

50. Brooks, B. C.; Meiere, S. H.; Freidman, L. A.; Carrig, E. H.; Gunnoe, T. B.; Harman, W. D. *J. Am. Chem. Soc.* **2001**, *123*, 3541-3550.

51. Chin, R. M.; Dong, L.; Duckett, S. B.; Partridge, M. G.; Jones, W. D.; Perutz, R. N. *J. Am. Chem. Soc*. **1993**, *115*, 7685-7695.

52. Jones, W. D.; Dong, L. Z. *J. Am. Chem. Soc*. **1989**, *111*, 8722-8723.

53. Reinartz, S.; White, P. S.; Brookhart, M.; Templeton, J. L. *J. Am. Chem. Soc*. **2001**, *123*, 12724-12725.

54. Belt, S. T.; Dong, L.; Duckett, S. B.; Jones, W. D.; Partridge, M. G.; Perutz, R. N. J. *Chem. Soc., Chem. Commun.* **1991**, 266-269.

55. Jones, W. D.; Feher, F. J. *J. Am. Chem. Soc.* **1984**, *106*, 1650-1663.

56. Jones, W. D.; Feher, F. *J. Acc. Chem. Res*. **1989**, *22*, 91-100.

57. Bergman, R. G. *Science* **1984**, *223*, 902-908.

58. Crabtree, R. H. *J. Chem. Soc., Dalton Trans*. **2001**, 2437-2450.

59. Dyker, G. *Angew. Chem. Int. Ed.* **1999**, *38*, 1699-1712.

60. Jia, C. G.; Kitamura, T.; Fujiwara, Y. *Acc. Chem. Res*. **2001**, *34*, 633-639.

61. Labinger, J. A.; Bercaw, J. E. *Nature* **2002**, *417*, 507-514.

62. Jones, W. D.; Chandler, V. L.; Feher, F. J. *Organometallics* **1990**, *9*, 164-174.

63. Jones, W. D.; Feher, F. J. *Organometallics* **1983**, *2*, 562-563.

64. Jones, W. D.; Kuykendall, V. L.; Selmeczy, A. D. *Organometallics* **1991**, *10*, 1577-1586.

65. Alaimo, P. J.; Arndtsen, B. A.; Bergman, R. G. *J. Am. Chem. Soc.* **1997**, *119*, 5269-5270.

66. Janowicz, A. H.; Bergman, R. G. *J. Am. Chem. Soc.* **1982**, *104*, 352-354.

67. Klei, S. R.; Tilley, T. D.; Bergman, R. G. *J. Am. Chem. Soc*. **2000**, *122*, 1816-1817.

68. Luecke, H. F.; Bergman, R. G. *J. Am. Chem. Soc.* **1997**, *119*, 11538-11539.

69. Stoutland, P. O.; Bergman, R. G. *J. Am. Chem. Soc.* **1988**, *110*, 5732-5744.

70. Jones, W. D.; Maguire, J. A. *Organometallics* **1986**, *5*, 590-591.

71. Jones, W. D.; Maguire, J. A. *Organometallics* **1987**, *6*, 1728-1737.

72. Wenzel, T. T.; Bergman, R. G. *J. Am. Chem. Soc*. **1986**, *108*, 4856-4867.

73. Jones, W. D.; Foster, G. P.; Putinas, J. M. *J. Am. Chem. Soc*. **1987**, *109*, 5047-5048.

74. Fisher, B. J.; Eisenberg, R. *Organometallics* **1983**, *2*, 764-767.

75. Yi, C. S.; Yun, S. Y. *J. Am. Chem. Soc.* **2005**, *127*, 17000-17006.

76. Sadow, A. D.; Tilley, T. D. *J. Am. Chem. Soc*. **2002**, *124*, 6814-6815.

77. Thompson, M. E.; Baxter, S. M.; Bulls, A. R.; Burger, B. J.; Nolan, M. C.; Santarsiero, B. D.; Schaefer, W. P.; Bercaw, J. E. *J. Am. Chem. Soc*. **1987**, *109*, 203-219.

78. Watson, P. L. *J. Am. Chem. Soc*. **1983**, *105*, 6491-6493.

79. Heiberg, H.; Gropen, O.; Swang, O. *J. Quant. Chem*. **2003**, *92*, 391-399.

80. Milet, A.; Dedieu, A.; Kapteijn, G.; vanKoten, G. *Inorg. Chem*. **1997**, *36*, 3223-3231.

81. Lam, W. H.; Jia, G. C.; Lin, Z. Y.; Lau, C. P.; Eisenstein, O. *Chem. Eur. J.* **2003**, *9*, 2775-2782.

82. Hinderling, C.; Plattner, D. A.; Chen, P. *Angew. Chem. Int. Ed*. **1997**, *36*, 243-244.

83. Niu, S. Q.; Hall, M. B. *J. Am. Chem. Soc*. **1998**, *120*, 6169-6170.

84. Tenn, W. J.; Young, K. J. H.; Bhalla, G.; Oxgaard, J.; Goddard, W. A.; Periana, R. A. *J. Am. Chem. Soc*. **2005**, *127*, 14172-14173.

85. Weissman, H.; Song, X. P.; Milstein, D. *J. Am. Chem. Soc*. **2001**, *123*, 337-338.

86. Tsuji, J.; Nagashima, H. *Tetrahedron* **1984**, *40*, 2699-2702.

87. Lu, W. J.; Jia, C. G.; Kitamura, T.; Fujiwara, Y. *Org. Lett.* **2000**, *2*, 2927-2930.

88. Jia, C. G.; Piao, D. G.; Oyamada, J. Z.; Lu, W. J.; Kitamura, T.; Fujiwara, Y. *Science* **2000**, *287*, 1992-1995.

89. Satoh, T.; Nishinaka, Y.; Miura, M.; Nomura, M. *Chem. Lett.* **1999**, 615-616.

90. Hong, P.; Cho, B. R.; Yamazaki, H. *Chem. Lett.* **1979**, 339-342.

91. Tsukada, N.; Mitsuboshi, T.; Setoguchi, H.; Inoue, Y. *J. Am. Chem. Soc*. **2003**, *125*, 12102-12103.

92. Viciu, M. S.; Stevens, E. D.; Petersen, J. L.; Nolan, S. P. *Organometallics* **2004**, *23*, 3752-3755.

93. Thalji, R. K.; Ahrendt, K. A.; Bergman, R. G.; Ellman, J. A. *J. Org. Chem*. **2005**, *70*, 6775-6781.

94. Jia, C.; Piao, D.; Kitamura, T.; Fujiwara, Y. *J. Org. Chem*. **2000**, *65*, 7516-7522.

95. Kakiuchi, F.; Murai, S. *Acc. Chem. Res.* **2002**, *35*, 826-834.

96. Jazzar, R. F. R.; Mahon, M. F.; Whittlesey, M. K. *Organometallics* **2001**, *20*, 3745-3751.

97. Lenges, C. P.; Brookhart, M. *J. Am. Chem. Soc.* **1999**, *121*, 6616-6623.

98. Murai, S.; Kakiuchi, F.; Sekine, S.; Tanaka, Y.; Kamatani, A.; Sonoda, M.; Chatani, N. *Nature* **1993**, *366*, 529-531.

99. Diamond, S. E.; Szalkiewicz, A.; Mares, F. *J. Am. Chem. Soc*. **1979**, *101*, 490-491.

100. Macguire, J. A. University of Rochester, Rochester, **1986**.

101. Boese, W. T.; Goldman, A. S. *Organometallics* **1991**, *10*, 782-786.

102. Matsumoto, T.; Periana, R. A.; Taube, D. J.; Yoshida, H. *J. Mol. Catal. A: Chem*. **2002**, *180*, 1-18.

103. Wong-Foy, A. G.; Bhalla, G.; Liu, X. Y.; Periana, R. A. *J. Am. Chem. Soc*. **2003**, *125*, 14292-14293.

104. Periana, R. A.; Bhalla, G.; Tenn, W. J.; Young, K. J. H.; Liu, X. Y.; Mironov, O.; Jones, C. J.; Ziatdinov, V. R. *J. Mol. Catal. A: Chem*. **2004**, *220*, 7-25.

105. Matsumoto, T.; Taube, D. J.; Periana, R. A.; Taube, H.; Yoshida, H. *J. Am. Chem. Soc*. **2000**, *122*, 7414-7415.

106. Lail, M.; Bell, C. M.; Conner, D.; Cundari, T. R.; Gunnoe, T. B.; Petersen, J. L. *Organometallics* **2004**, *23*, 5007-5020.

107. Lail, M.; Arrowood, B. N.; Gunnoe, T. B. *J. Am. Chem. Soc*. **2003**, *125*, 7506-7507.

108. Oxgaard, J.; Goddard, W. A. *J. Am. Chem. Soc*. **2004**, *126*, 442-443.

109. Oxgaard, J.; Periana, R. A.; Goddard, W. A. *J. Am. Chem. Soc*. **2004**, *126*, 11658-11665.

110. Bergman, R. G.; Cundari, T. R.; Gillespie, A. M.; Gunnoe, T. B.; Harman, W. D.; Klinckman, T. R.; Temple, M. D.; White, D. P. *Organometallics* **2003**, *22*, 2331-2337.

111. Goj, L. A.; Lail, M.; Pittard, K. A.; Riley, K. C.; Gunnoe, T. B.; Petersen, J. L. *Catal. Commun*. **2006**, 982-984.

112. Lee, J. P.; Pittard, K. A.; DeYonker, N. J.; Cundari, T. R.; Gunnoe, T. B.; Petersen, J. L. *Organometallics* **2006**, *25*, 1500-1510.

CHAPTER 2:
Stoichiometric and Catalytic Ru^{II} Mediated Regioselective C-H Activation of Heteroaromatic Substrates

2.1 Introduction

Heteroaromatic molecules are present in a diverse array of compounds, playing key roles in technological, material, and physiological advances. The agricultural industry is one area of application, where approximately 2.5 billion tons of pesticides are annually produced. A specific example of the prevalence of heteroaromatic scaffolds in the agricultural products can be observed in the production of the naturally occurring plant hormone, Kinetin (Figure 2.1). Heteroaromatic compounds also pervade the pharmaceutical industry in both the areas of antibiotics and the treatment for infectious disease. In particular, the production of antibiotics commonly incorporates heterocyclic functionality. Ranitidine (Figure 2.1) has been a successful drug for the treatment of peptic ulcers, as it is the active ingredient in Zantac™. Dyes are another area of heteroaromatic application. The colors of these compounds are easily varied by structural changes about the ring while solubility and fabric affinity can be varied by changing the heteroatom to vary the charge. Photographic materials, fire-retardant materials, the flavor and aroma industry, fine chemicals, natural products, and the food industry commonly uses, or contains, functionalized heteroaromatics. An example for application in the food industry is with preservatives, where the acrylic acid shown below (Figure 2.1) is a wine preservative. Given their highly variable utility, selective functionalization of core heteroatomic substrates is an important goal.[1]

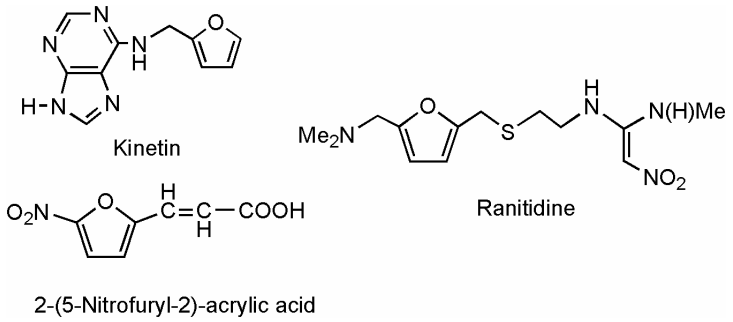

Figure. 2.1. Examples of heteroaromatic compound incorporation in industrial applications.

Not only are heteroaromatic fragments useful in many products, but they are also often used as synthetic precursors. For example, heteroaromatic compounds can be ring opened yielding desired functionality. Scheme 2.1 depicts the method for unmasking a 1,4-dicarbonyl compound from a functionalized furan.[2]

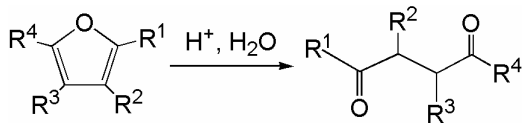

Scheme 2.1. Ring opening of a masked 1,4-dicarbonyl compound.

Before addressing the specific reactivity reported in this chapter, involving heteroaromatic compounds with TpRu(CO)(NCMe)Me, and drawing comparisons between these and previously reported analogous carbocyclic reactivity,[3] it will be necessary and appropriate to first address the chemistry of this heteroaromatic class of molecules. Whereas, isocyclic compounds are ring structures consisting of one type of atom contiguous about the ring, heterocyclic molecules incorporate at least one heteroatom into the ring. Herein, only five-membered heteroaromatic compounds will be discussed. They are defined as [5]-heteroannulene compounds that obey Huckel's rule for aromaticity.

The difference in chemical properties, and hence chemical reactivity, for five-membered heteroaromatic compounds (of particular interest here, furan and thiophene), from their carbocyclic analogs, is derived from two main factors. First, the ring system is π-rich due to six π-electrons being distributed amongst only five sp^2-orbitals of the five contiguous ring atoms. Second, the ring contains a heteroatom that has a more electronegative value and, as a result, polarizes the electron density of the ring as well as distributing a lone pair into the ring π-system with varying degrees of efficiency. Stabilization due to resonance energy is decreased with increased electronegativity of the heteroatom. Empirical evidence for the greater resonance delocalization of thiophene relative to furan is observed in the difference in dipole moment (furan = 0.71 D, thiophene = 0.52 D) and in the calculated Dewar resonance energies (furan = 16.2 kcal/mol, thiophene = 29.1 kcal/mol).[4] As well, the difference in dipole moment between furan (0.71 D) and tetrahydrofuran (THF) (1.75 D) is likely a

function of the oxygen's ability to donate its lone pair into the ring's π-system and can therefore be thought of as evidence for aromaticity.[5] Aromaticity can be qualitatively evaluated by ^{1}H NMR ring current effects, vicinal coupling, bond lengths, UV-Vis absorption bands and PES.[5]

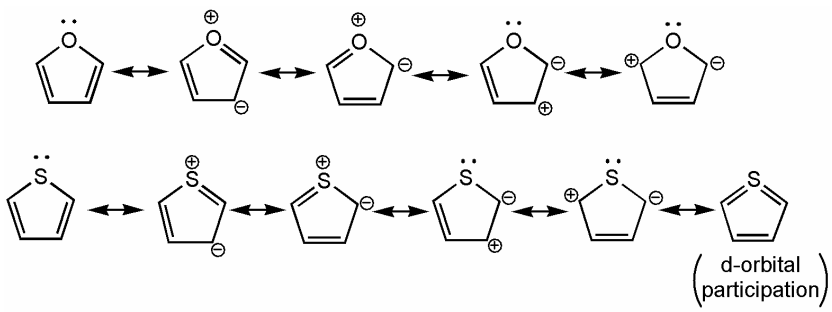

Figure 2.2. Resonance structures for furan and thiophene.

Electronic structure diagrams are a useful tool when predicting reactivity of heteroaromatic components. Below is a qualitative electronic structure diagram (Figure 2.3) representing the molecular orbital construct of furan and thiophene. The electronic structure of heteroaromatic compounds is much different relative to the π-isoelectronic carbocycle derivative. First, the degeneracy has been broken among Ψ_2 and Ψ_3 and Ψ_4^* and Ψ_5^* molecular orbitals due to the drop in symmetry from D_{5h} (e.g., cyclopentadienyl) to C_{2v} (e.g., furan). This break in degeneracy also leads to a smaller HOMO→LUMO gap, but not so small that Huckel's Rule is ignored. This renders heteroaromatic compounds more reactive than their carbocyclic analogs. The destabilization of the HOMO gives an increase in reactivity particularly toward electrophilic aromatic substitution. For example, these lower aromatic resonance energies and π-richness of the ring enable furan to undergo electrophilic attack 10^{11} times more rapidly than benzene, while thiophene is $10^{3\text{-}5}$ times faster.[5] The order of reactivity for electrophilic aromatic substitution is as follows: furan > thiophene > benzene.

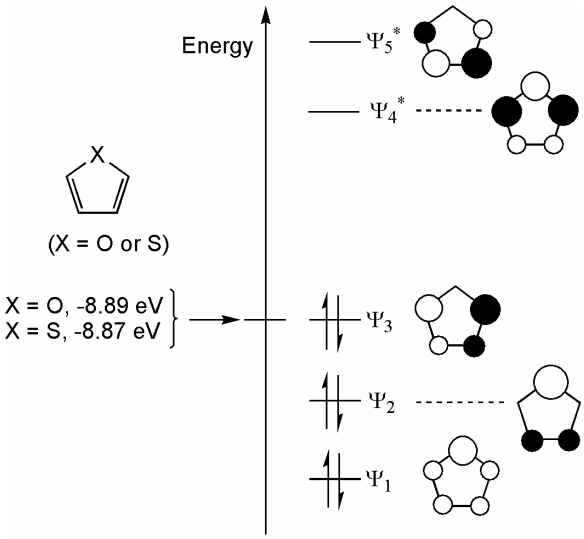

Figure 2.3. Qualitative electronic structure of furan and thiophene.

Preference for reactivity at the 2-position in electrophilic aromatic substitution of 5-membered heteroaromatics can be explained by the large molecular orbital coefficient about the 2-position of the HOMO. Also, regioselective substitutions can be explained by the unequal delocalization of positive charge about the ring whereby the 2-position provides greater stabilization (Figure 2.4). Therefore, selectivity for the 2-position is a function of the molecular orbital coefficient and the delocalization of the positive charge about the ring in the electrophilic addition intermediate. This regioselectivity is to be highly desired as many of the applications of heteroaromatic containing compounds require physiological activity.

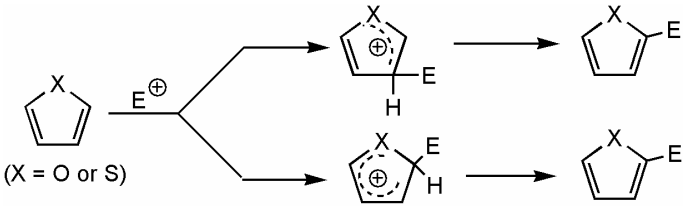

Figure 2.4. Electrophilic aromatic substitution of furan and thiophene.

The HOMO being centered about the 2,3 and 4,5-positions (Figure 2.3) explains the η^2-binding preference for heteroaromatic molecules with electron deficient metal centers (Figure 2.5). There are many examples of this η^2-coordination in the literature for both furan and thiophene with complexes that are isoelectronic to the complexes reported herein.[6-13] Observed to a lesser extent is the η^1-coordination of thiophenes, by way of a sulfur lone pair dative bond (Figure 2.5).[14] Ru^{II} η^1-thiophene complexes[15] as well as isoelectronic complexes.[16-18] are known and have been studied by X-ray diffraction studies. To our knowledge there are no examples of an isolated η^1-furan complex (Figure 2.5) and there are no examples of η^1-coordination of furan to any transition metal in the Cambridge Crystallographic Database.[19] The rarity of η^1-binding of furan and thiophene is most likely explained by the lower energies of the lone pair MO relative to that of the HOMOs. John P. Lee performed PM3 geometry optimizations of furan and thiophene at the SEQM level of theory revealing lone pair MO energies of -13.90 eV and -12.01 eV, respectively.

Harman and coworkers have observed intrafacial and interfacial migrations of η^2-thiophene and η^2-furan with isoelectronic complexes of the type TpRe(CO)(L)(η^2-arene) (L = ^{t}BuNC, PMe_3, py, and MeIm) by spin saturation exchange experiments.[20] In these studies, it is reported that the slowest rates for interfacial and intrafacial linkage isomerization are considerably faster, even at significantly lower temperatures, than the previously reported rates of C-H activation of benzene with the {TpRu(CO)Ph} fragment.[21] With this evidentiary support, it is likely that all of the positions on furan and thiophene can be accessed on a time scale faster than that of C-H activation.

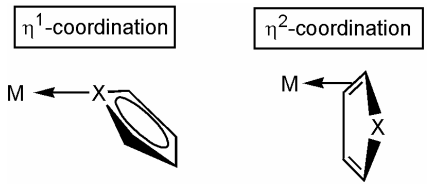

Figure 2.5. Coordination modes of furan and thiophene (M = metal; X = O or S).

Though advances in the area of heteroaromatic functionalization will be summarized, it is important to acknowledge that synthetic routes for the formation of substituted aromatic rings often involve functionalization prior to a final ring-closing reaction step rather than direct functionalization of the aromatic substrate. These methods generally employ the reactivity of noncyclic dicarbonyls or 2-thiol ketones. For example, the *Paal-Knorr* and *Feist –Benary* syntheses can be used to achieve ring closings of 1,4-dicarbonyl compounds and reactions of α-haloketones with 1,3-dicarbonyl compounds, respectively.[2] Also, functionalized thiophenes can be obtained by cyclizations via the Paal, Hinsberg, and Gewald syntheses.[2]

The formation of new C-C bonds in the functionalization of heteroaromatic compounds is an important transformation for the creation of desired organic synthons and products. Reactive fragments can be generated at the 2-position of furan or thiophene by lithiation using alkyl lithium reagents whereby subsequent C-C bond formation can be achieved by carboxylation followed by esterification.[22] Advancements in radical based reactions have also been achieved. For example, carbon radicals from an alkyl halide source can be generated using triethyllborane autooxidation (with air as the oxidant) to achieve homolytic aromatic substitution of furan and thiophene in the presence of $Fe(SO_4)_3 \cdot H_2O$. In these reactions, esters consisting a halogen functionality were reacted for the preparation of 2-substituted ester products.[23] Also, it has been shown that halogenated heteroaromatic compounds can react with two equivalents of alkylidine phosphorane (Wittig reagent) to yield the heterocyclic ylide. From this intermediate net alkylation or alkenylation can be achieved by hydrolysis or by reaction with a carbonyl compound, respectively.[24]

Catalytic methods for C-C bond formation with heteroaromatic compounds have been reported. Arguably the most well-known catalytic transformation yielding sp^2-sp^3 C-C bonds is the Friedel-Crafts class of reactions.[25] Recently, Jorgensen et al. have reported an aza-Friedel-Crafts C-C bond formation between substituted furans and *N*-alkoxycarbonyl α-imino esters using a chiral BINAP-Cu^I Lewis acid. These chemical transformations yield optically active heteroaromatic α-amino acids with moderate to exceptional % ee's.[26] Successful cross-coupling has also been achieved with the Pd and Ni catalyzed systems for heteroaromatics by Grignard and Negishi coupling.[27, 28] As illustrated in the Scheme 2.2, the organometallic fragment can be introduced into the reaction as a heterocyclic halide or as the heteroaromatic Grignard or Zn reagent. These

systems require only mild reaction temperatures and in general produce the coupled products in high yields. In the Pd systems, lower yields were observed for the route in which the heteroaromatic functionality is contained in the Grignard reagent. However, this less productive route offers two advantages. First, it allows for the ability of the heteroaromatic Grignard reagents to be functionalized. Second, although relatively unstable, these heteroarenes can be functionalized by allylsilanes without isomerization. It should also be noted that the Pd catalyzed reactions do, however, produce more desirable results when the functionalization of the 2-position is required.[27, 28]

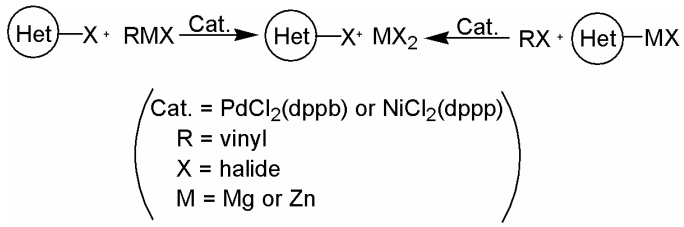

Scheme 2.2. Ni and Pd Grignard and Negishi coupling with heteroaromatic fragments.

More efficient methods for the functionalization of heteroaromatic substrates have been developed whereby a C-H activation step occurs in the catalytic cycle. Whereas a great deal of advancement has been made in the area of C-H activation of arenes,[29-42] less is known about C-H activation of heteroaromatic compounds[24, 43-50]. As discussed in the previous chapter, if a catalytic process can be developed for heteroaromatic compounds, whereby C-H bonds are cleaved and new C-C bonds are formed, it would circumvent many of the drawbacks that exist with currently wed catalyst technologies.

The majority of advancements in the C-H activation of heteroaromatic compounds are stoichiometric reactions involving low oxidation state late transition metal systems that have been shown to undergo oxidative addition pathways.[51, 52] For example, Merola and coworkers have shown that $[Ir(COD)(PMe_3)_3]Cl$ reacts with furan or pyridine to achieve regioselective oxidative addition of a C-H bond yielding the $(PMe_3)_3Ir(Cl)(H)$(2-furyl) or $(PMe_3)_3Ir(Cl)(H)$(2-pyridinyl) complex.[50] Different reactivity was observed with thiophene, whereby instead of C-H activation C-S bond cleavage was observed yielding the $(PMe_3)_3Ir(Cl)(\kappa^2\text{-}C,S\text{-}C_4H_4S)$, Scheme

2.3. {Cp*Rh(PMe_3)} was observed by Jones et al. to undergo oxidative addition of furan C-H bonds selectively at the 2-position.[53] Selectivity for the 2-position was observed. Binuclear complexes have also been observed to C-H activate heteroaromatics. For example, $[(Cp^*Ir)_2(\mu\text{-dmpm})(\mu\text{-H})_2]^{2+}$, in the presence of one equivalent of NaO^tBu, C-H activates of furan to yield the 2-furyl and 3-furyl complexes. The Ir-H and Ir-C connectivities reside on differing Ir atoms of the dimer.[48] The 2-furyl complex was formed exclusively, however, by the reductive elimination of benzene from $[(Cp^*Ir)(H)(\mu\text{-dmpm})(\mu\text{-H})(Cp^*Ir)Ph]^+$ in refluxing furan. Murai and coworkers have demonstrated that heteroatom pendent functionality on heteroaromatic compounds can direct the regioselectivity of C-H activation. For example, 3-acetylthiophene can undergo C-H activation at the 2-position of thiophene when in the presence of $Ru(H)_2(CO)(PPh_3)$.[37] In a similar fashion, Eguillor and coworkers have shown that $Os(H)_3(SnPh_2Cl)(\eta^2\text{-}CH_2{=}C(CH_3)(P^iPr_3)$ reacts with 3-formylfuran where the pendent functionality directs C-H activation at the 2-position yielding the $Os(H)_2(SnPh_2Cl)(C_4(O)H_2C(O)H)(P^iPr_3)$ product.[47]

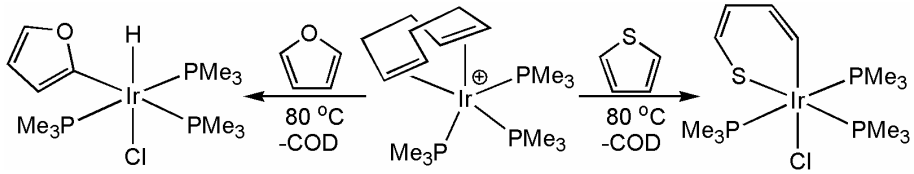

Scheme 2.3. C-H activation of furan and C-S activation of thiophene by $[(COD)Ir(PMe_3)_3]Cl$.

Stoichiometric C-H activations of heteroaromatics that proceed through a σ-bond metathesis route have also been achieved by high oxidation state early transition metal systems. For example, Deelman and coworkers have shown that $[Cp^*_2Y(\mu\text{-H})]_2$ in the presence of furan gives the observable Cp^*_2Y(2-furyl), releasing $H_2(g)$.[45] The $[Cp^*_2Y(\mu\text{-H})]_2$ complex was also shown to activate C-H bonds of thiophene to yield the Cp^*_2Y(2-thienyl)(THF) complex. Similar complexes have been shown to undergo the same reactivity when reacted with furan and thiophene substrates.[43]

Advances have been made in the area of photolytic C-H activation. Whereas this document does not report photolytic activity in the cleavage of C-H bonds, and with less chance for this chemistry to be applicable

in scaled-up industrial process, due to the inherent physical limitations that exist, it is still relevant to the work herein. Bianchini et al. have shown that $(PP_3)Ru(H)_2$ (where $PP_3 = P(CH_2CH_2PPh_2)_3$) initiates C-H activation of thiophene to give the $(PP_3)Ru(H)$(2-thienyl) complex.[44] Also, ethyl 2-thiophenecarboxylate undergoes C-H activation at the 5-position as opposed to the 3-position that might be expected if precoordination via the carboxylate were to direct the regioselectivity. Jones and coworkers have observed C-H activation of thiophene upon photolysis of $Cp^*Rh(PMe_3)(H)_2$ in the presence of thiophene to produce $Cp^*Rh(PMe_3)$(2-thienyl)H.[46] During this photolytic reaction, the C-S insertion product $Cp^*Rh(PMe_3)(\kappa^2\text{-}C,S\text{-}S(CH)_3C(H))$ is also produced. The $Cp^*Rh(PMe_3)$(2-thienyl)D and $Cp^*Rh(PMe_3)$(3-thienyl)D were both independently synthesized and their reactivity observed. The 3-thienyl derivative isomerizes to the 2-thienyl complex and then undergoes transformation to the C-S insertion product with deuterium incorporation into the 3- and 4-position. The 2-thienyl complex was observed to decompose to the C-S insertion product with deuterium incorporation into the 3- and 4-positions.

Several advances have also been made in catalytic C-C bond formation between heteroaromatic compounds and unsaturated substrates that undergo C-H activation as a key intermediary step. For example, Pd^0 tandem cyclizations have been achieved with monohalogenated furan and thiophene compounds.[54] In these reactions, a C-X (X = halogen) *and* C-H bond are cleaved and two new sp^2-sp^3 C-C bonds are formed incorporating the furan or thiophene fragment into the carbon backbone of the newly formed ring. Fujiwara and coworkers have coupled furan and thiophene with electron deficient alkenes (e.g., methyl acrylate, acrylonitrile, or 3-arylpropenoates) using a $Pd(OAc)_2$ or $Cu(OAc)_2$ precatalyst.[55, 56] It is proposed that cleavage of the C-H bonds of these heteroaromatic molecules is achieved by interaction with the Pd^{II} (or Cu^{II}) metal center. Yamazaki et al. has observed the ability of $Rh_4(CO)_{12}$ to catalytically couple substituted or unsubstituted furans to functionalized alkynes yielding new heteroalkenes whereby substitution was achieved at the 2-position of the furan fragment.[49] Probably the most relevant example that could be found for the catalytic C-C bond formation subsequent to a C-H bond activation step is that reported by Ringelberg et al.[57] Reported therein was the catalytic formation of thienyl capped polyethylene using a $[Cp^*LaH]_2$ species.

Our group has recently reported that TpRu(CO)(NCMe)R (Tp = hydridotris(pyrazolyl)borate; R = Me or Ph) catalyzes the addition of arene C-H bonds across C=C bonds of olefins, [3]and the closely related complex $TpRu(PPh_3)(NCMe)H$ has been reported to activate C-H bonds.[58] We have extended studies to reactions of TpRu(CO)(NCMe)Me with heteroaromatic substrates and report herein the initial details of these transformations.

2.2 Results and Discussion

TpRu(CO)(NCMe)Me (**1**) reacts with furan at 90 ^{o}C to yield TpRu(CO)(NCMe)(2-furyl) (**2**) and methane (Scheme 2.4). The formation of methane has been confirmed by GC-MS analysis of the headspace of a reaction in a gastight NMR tube. Full characterization of **2** was achieved by ^{1}H NMR (Figure 2.6), ^{13}C NMR (Figure 2.7), IR, elemental analysis, and CV. Important features in the IR include the ν_{CO}, ν_{CN}, and ν_{BH} at 1949 cm^{-1}, 2286 cm^{-1}, and 2484 cm^{-1}, respectively. Although only isolated in 60% yield after workup, ^{1}H NMR spectroscopy of the crude reaction mixture reveals that complex **2** is produced in nearly quantitative yield. The C-H activation of furan is regioselective, and ^{1}H NMR, ^{13}C NMR, homonuclear decoupling, and NOE experiments are consistent with regioselective attack at the 2-position. For example, the chemical shifts (^{1}H NMR) of complex **2** indicate one downfield resonance and two upfield resonances due to the furyl ligand (7.99, 6.62, and 6.23 ppm) that are consistent with a single α-proton and two β-protons. The ^{13}C NMR spectrum of **2** reveals two resonances at 114.8 and 109.6 ppm that are consistent with *unsubstituted* C-H bonds at the β-position, while the α-carbons resonate at approximately 135 ppm (consistent with an unsubstituted C-H moiety) and 178.8 ppm.

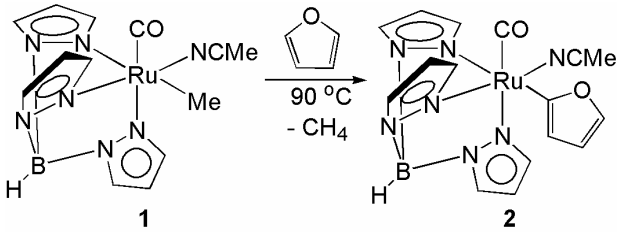

Scheme 2.4. Reaction of TpRu(CO)(NCMe)Me (**1**) with furan yields TpRu(CO)(NCMe)(2-furyl) (**2**).

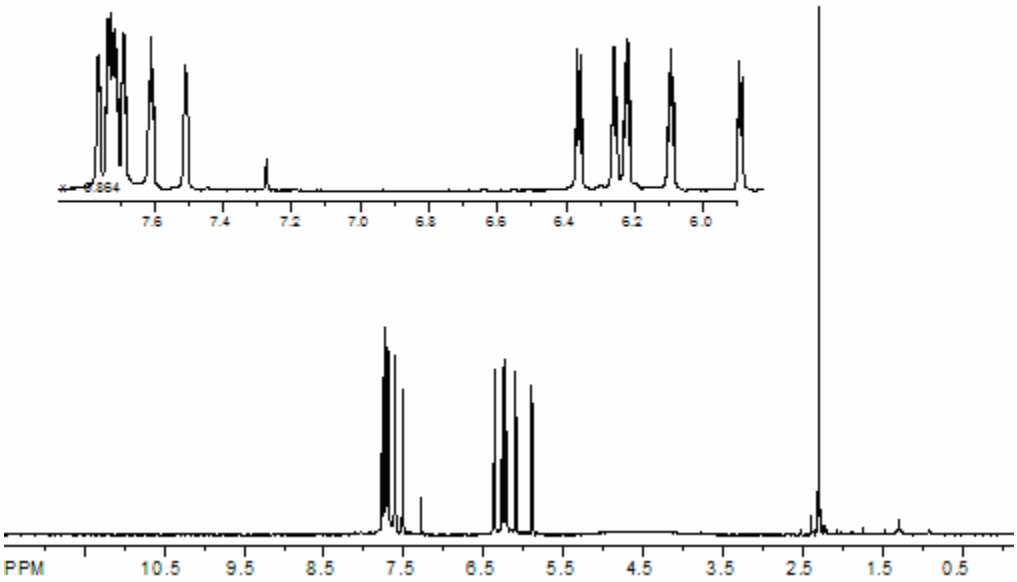

Figure 2.6. ^{1}H NMR spectrum of TpRu(CO)(NCMe)(2-furyl) in $CDCl_3$.

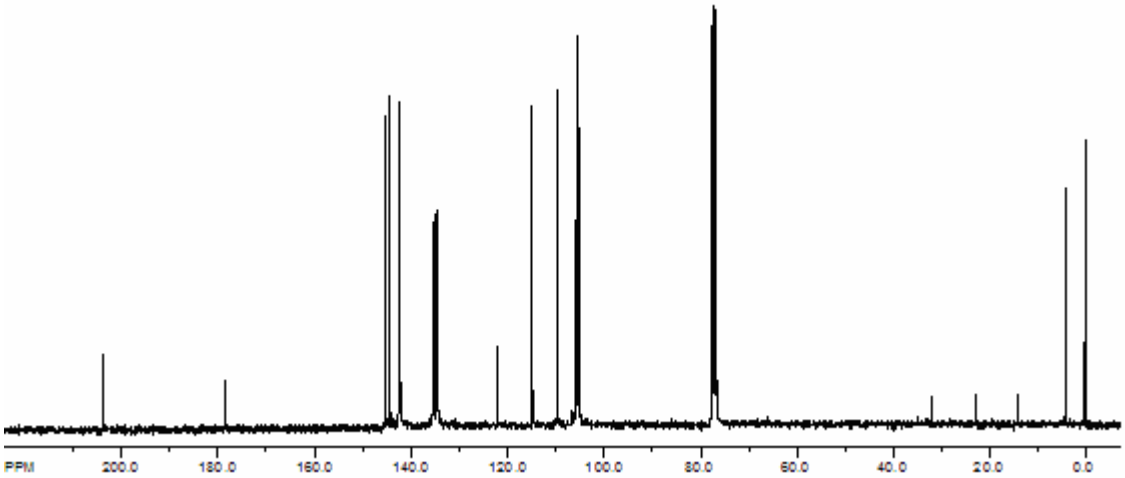

Figure 2.7. ^{13}C NMR spectrum of TpRu(CO)(NCMe)(2-furyl) in $CDCl_3$.

To confirm the regioselectivity of the C-H activation, ^{1}H NMR NOE and homonuclear decoupling experiments were performed (Figure 2.8). Most importantly, the resonance at 6.62 ppm (β-position) shows

NOEs with the other two furyl resonances. In the case of ruthenium substitution at the 3-position, irradiation of the β-proton would be expected to yield a NOE with a single furyl resonance. Likewise, a 3-furyl ligand would produce a resonance for an α-proton that would not be anticipated to exhibit a NOE with either of the remaining two resonances of the furyl ligand. Metal-mediated C-H activations at the 2-position of furan have been reported for Rh and W complexes.[50, 53, 59] In addition, Komiya et al. have reported C-H oxidative addition of furan to an Fe^0 complex in which the regioselectivity was not conclusively determined.[52] A binuclear iridium complex has been reported to activate furan to give a 5:2 mixture of 2-furyl and 3-furyl complexes.[48] Heating (90 °C) complex **2** with excess furan for 144 h does not result in observable isomerization to the 3-furyl complex.

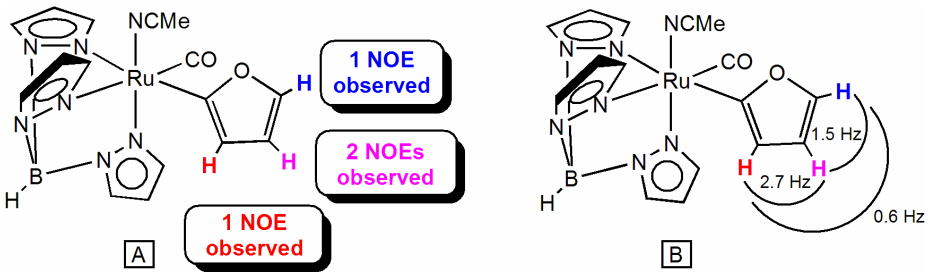

Figure 2.8. NOE (A) and homonuclear decoupling studies (B) for the 2-furyl ligand of TpRu(CO)(NCMe)(2-furyl) (**2**).

We have previously reported that the phenyl complex TpRu(CO)(NCMe)Ph serves as a precatalyst for the hydroarylation of olefins.[30] The combination of furan and 1 mol % of complex **2** (based on furan) in mesitylene at 120 °C under mild ethylene pressure (10-40 psi) results in the catalytic production of 2-ethylfuran (Scheme 2.5), and optimal conditions allow approximately 17 catalytic turnovers after 24 h (after which time the catalyst activity decreases). This transformation demonstrates the feasibility of Ru^{II}-mediated olefin hydroarylation using heteroaromatic substrates. The proposed catalytic cycle is given in Scheme 2.6. Although quantitative rate data have not been acquired, higher ethylene pressures result in an increased production of 2-ethylfuran after 24 h of reaction (Figure 2.9). For example, 9 turnovers are observed after 24 h of reaction at 10 psi of ethylene, 15 turnovers are observed at 30 psi of ethylene, and 17 turnovers are observed using 40 psi of

ethylene. The direct relationship between ethylene pressure and catalyst turnovers is potential evidence for olefin binding or olefin insertion being the rate limiting step of the catalytic cycle under these conditions.

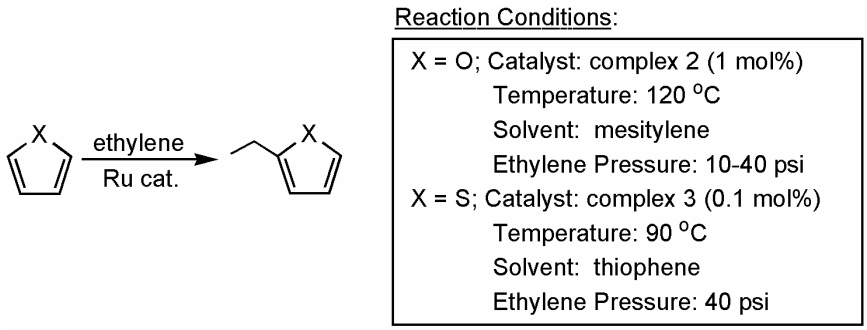

Scheme 2.5. Catalytic production of 2-ethylfuran and 2-ethylthiophene using TpRu(CO)(NCMe)(2-furyl) (**2**) or TpRu(CO)(NCMe)(2-thienyl) (**3**)as the precatalyst.

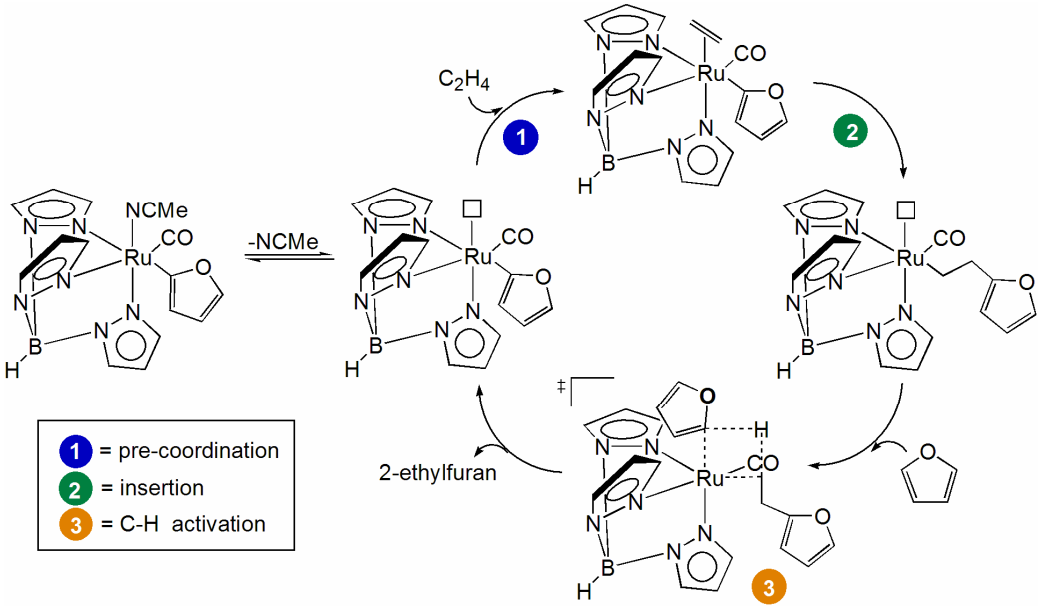

Scheme 2.6. Proposed catalytic cycle for the formation of 2-ethylfuran with TpRu(CO)(NCMe)(2-furyl) (**2**).

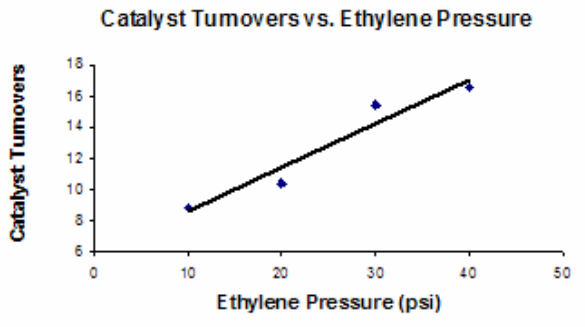

Figure 2.9. A plot displaying the relationship catalyst turnovers (after 24 h at 120 ^{o}C) and ethylene pressure.

The reaction of **1** with thiophene produces TpRu(CO)(NCMe)(2-thienyl) (**3**) and methane after approximately 19 h at 90 ^{o}C (Scheme 2.7). Analyzing the reaction mixture by NMR spectroscopy after 4 h reveals the presence of a reaction intermediate. Although the product of thiophene/NCMe exchange is a likely candidate for a reaction intermediate, we have been unable to separate and characterize this species. The reversible formation of metallacycles that result from Ru insertion into the C-S bond of thiophene is also possible.[60] After extended heating, ^{1}H NMR spectroscopy indicates that all TpRu intermediates cleanly convert to complex **3** (Figure 2.10). The ^{1}H NMR spectrum of complex **3** reveals resonances at 7.25, 6.97, and 6.57 ppm due to the 2-thienyl ligand. Similar to complex **2**, NOE and homonuclear decoupling experiments are consistent with a 2-substituted heterocycle (Figure 2.11). Metal-mediated C-H activation of thiophene has been reported.[44]

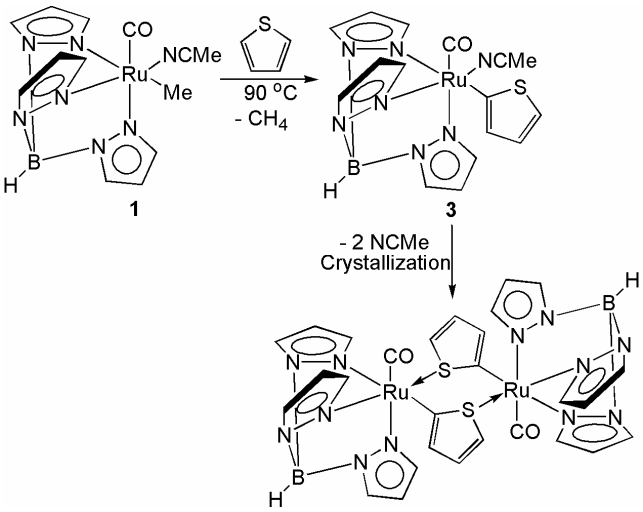

Scheme 2.7. Reaction of TpRu(CO)(NCMe)Me (**1**) with thiophene yields TpRu(CO)(NCMe)(2-thienyl) (**3**) and under crystallization conditions $[TpRu(CO)(2\text{-thienyl})]_2$.

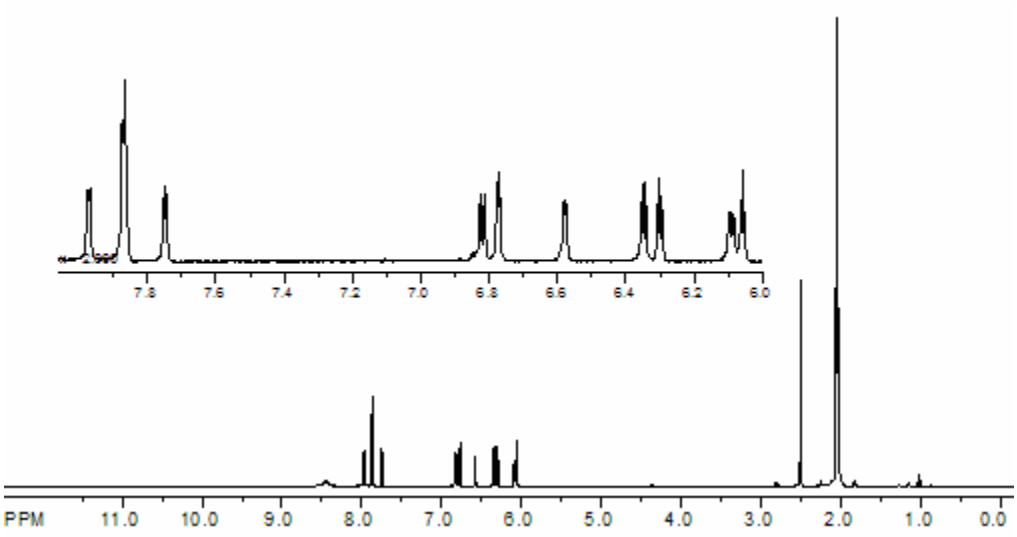

Figure 2.10. ^{1}H NMR spectrum of TpRu(CO)(NCMe)(2-thienyl) in CD_3CN.

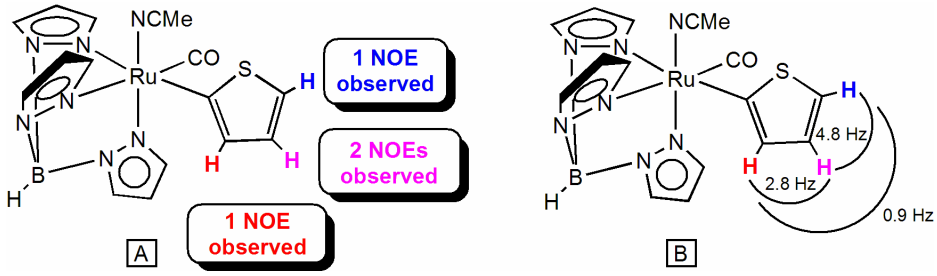

Figure 2.11. NOE (A) and homonuclear decoupling studies (B) for the 2-thienyl ligand of TpRu(CO)(NCMe)(2-thienyl) (**3**).

Similar to the catalytic addition of furan (Scheme 2.6) to ethylene, complex **3** catalyzes the formation of 2-ethylthiophene from a solution of thiophene and ethylene. For example, a thiophene solution of **3** (0.1 mol % versus thiophene) with 40 psi of ethylene pressure at 90 ^{o}C produces 2-ethylthiophene (Scheme 2.5). A total of 3 catalytic turnovers are observed after 12 h of reaction. The formation of additional 2-ethylthiophene is not observed after 12 h of catalysis.

The addition of HCl to complex **3** ultimately results in the production of free thiophene and a single TpRu product whose ^{1}H NMR spectrum is consistent with TpRu(CO)(NCMe)Cl (Scheme 2.8). TpRu(CO)(NCMe)Cl has been independently prepared by reaction of **1** with HCl (Scheme 2.8). Performing the HCl addition to TpRu(CO)(NCMe)(2-thienyl) (**3**) at -65 ^{o}C reveals a kinetic product whose ^{1}H NMR spectrum is consistent with [TpRu(CO)(NCMe)(*S*-thiophene)][Cl]. Warming the CD_2Cl_2 solution to room temperature results in the observation of free thiophene and TpRu(CO)(NCMe)Cl.

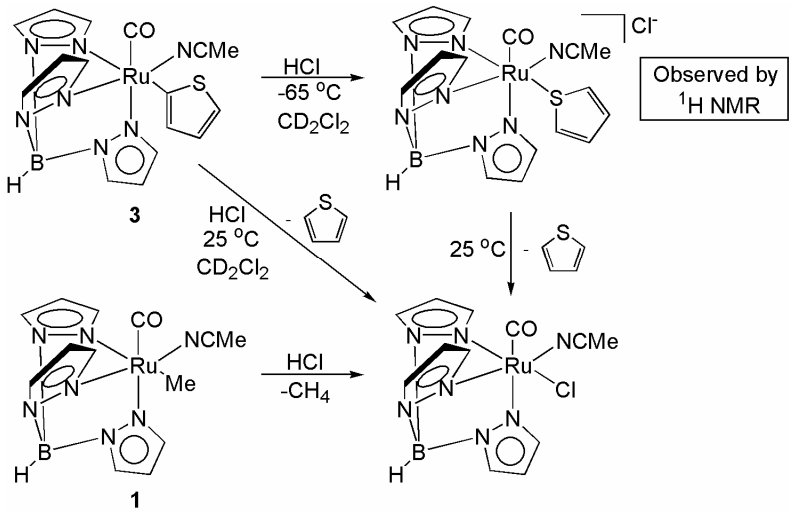

Scheme. 2.8. Reaction of TpRu(CO)(NCMe)(2-thienyl) (**3**) with HCl.

Layering of a methylene chloride solution of **3** with hexane resulted in the growth of crystals, and the structure of complex **3** has been confirmed by a solid-state single-crystal X-ray diffraction study (Figure 2.12). Data collection parameters are listed in Table 2.1. Similar to the solid-state structure of Cp*Rh(PMe_3)(Cl)(2-thienyl),[46] the 2-thienyl ligand exhibits a 70:30 two-site disorder with the two orientations of the ring differing by an approximately 180 ^{o} rotation about the Ru-C(13) bond. For each of the planar five-membered rings, the *S*-C(13) bond distance was refined using a restraint of 1.68 Å, the C(14)-C(15) bond distance using a restraint of 1.45 Å, and the C(13)-C(14) and C(15)-C(16) bond distances with restraints of 1.38 Å. The structure confirms the proposed regioselective C-H activation at the 2-position of thiophene.

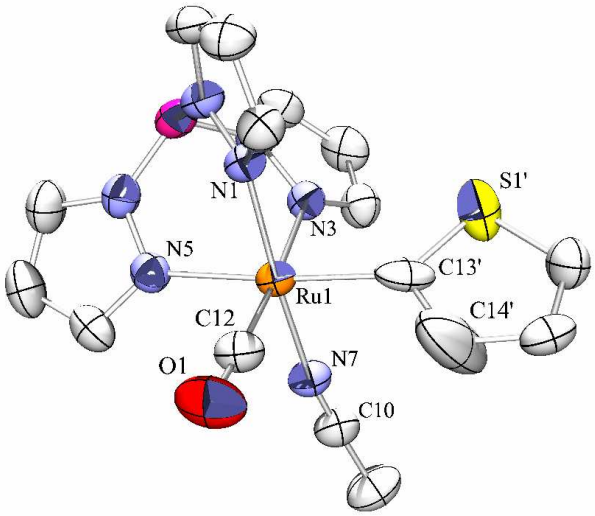

Figure 2.12. ORTEP of TpRu(CO)(NCMe)(2-thienyl) (**3**) (30% probability). Selected bond distances (Å): Ru-N7 2.029(1), Ru-C13 2.072(2), Ru-N1 2.062(1), Ru-N3 2.141(1), Ru-N5 2.151(1), Ru-C12 1.833(1), N7-C10 1.126(2), S1-C13 1.660(2). Selected bond angles (deg): Ru-C13-S1 125.3(1), C14-C13-S1 108.4(2), Ru-C12-O1 176.0(1).

Table 2.1. Selected crystallographic data and collection parameters for TpRu(CO)(NCMe)(2-thienyl) (**3**) and [TpRu(CO)(μ-*C*,*S*-2-thienyl)]$_2$.

	TpRu(CO)(NCMe)(2-thienyl) (**3**)	[TpRu(CO)(μ-*C*,*S*-2-thienyl)]$_2$
empirical formula	$C_{16}H_{16}BN_7ORuS$	$C_{14}H_{13}BN_6ORuS$
fw	466.30	425.24
cryst syst	monoclinic	triclinic
space group	$P2_1/n$	PI
a, Å	10.5469(9)	8.911(1)
b, Å	12.1519(11)	9.790(1)
c, Å	15.5119(13)	10.200(2)
α, deg		73.405(3)
β, deg	104.698(2)	77.475(3)
γ, deg		78.396(3)
V (Å^3)	1923.0(3)	823.1(2)
Z	4	2
D_{calcd}, g cm^{-3}	1.611	1.716
R1, wR2 (I >	0.0321, 0.0827	0.0436, 0.1021
GOF	1.037	1.015

In contrast to crystallization from methylene chloride/hexane, the crystallization of complex **2** from methylene chloride/cyclohexane (over a period of approximately two weeks) yields the binuclear complex [TpRu(CO)(μ-*C*,*S*-thienyl)]$_2$ (Scheme 2.6). Thus, the coordinatively unsaturated species {TpRu(CO)(2-thienyl)} is likely trapped by the sulfur atom of the 2-thienyl ligand of a second Ru complex. [TpRu(CO)(μ-*C*,*S*-thienyl)]$_2$ was only characterized by a single-crystal X-ray diffraction study (Figure 2.13). Data collection parameters are listed in Table 2.1. The two symmetry equivalent Ru fragments are approximately octahedral and are bridged by two μ-*C*,*S*-2-thienyl ligands. The geometry of the thienyl sulfur atom is pyramidal with the bond angles summing to 316.8(2)^{o}. The Ru-S bond distance of 2.365(1) Å is similar to other Ru^{II} thiophene complexes.[16]

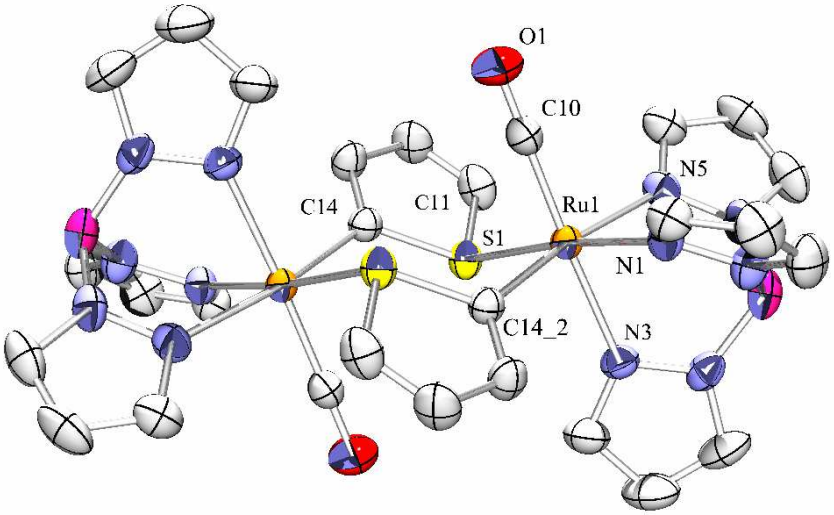

Figure 2.13. ORTEP of [TpRu(CO)(μ -*C*,*S*-thienyl)]$_2$ (30% probability). Selected bond distances (Å): Ru-S1 2.365(1), Ru-C10 1.824(4), Ru-C14' 2.043(4), Ru-N1 2.076(3), Ru-N3 2.139(3), Ru-N5 2.164(3), S1-C14 1.767(4), C10-O1 1.154(5). Selected bond angles (deg): Ru-S1-C14 110.9(1), C14-S1-C11 94.3(2).

The reaction of pyridine with **1** at 90 ^{o}C forms the product from nitrile/pyridine ligand exchange TpRu(CO)(*N*-py)Me (**4**) (py = pyridine; Scheme 2.9). Consistent with this assignment of **4** is the loss of ν_{CN} at

2278 cm^{-1} absorption in the IR of **4**. In addition, no resonances consistent with bound NCMe are observed in the ^{1}H NMR or ^{13}C NMR of **4** (Figure 2.14 and 2.15). The ^{1}H NMR spectrum of **4** reveals three resonances due to the five hydrogen atoms of pyridine. The two ortho and meta hydrogen atoms of the pyridine ligand are likely rendered equivalent on the NMR timescale due to rapid rotation about the Ru-N_{py} bond.

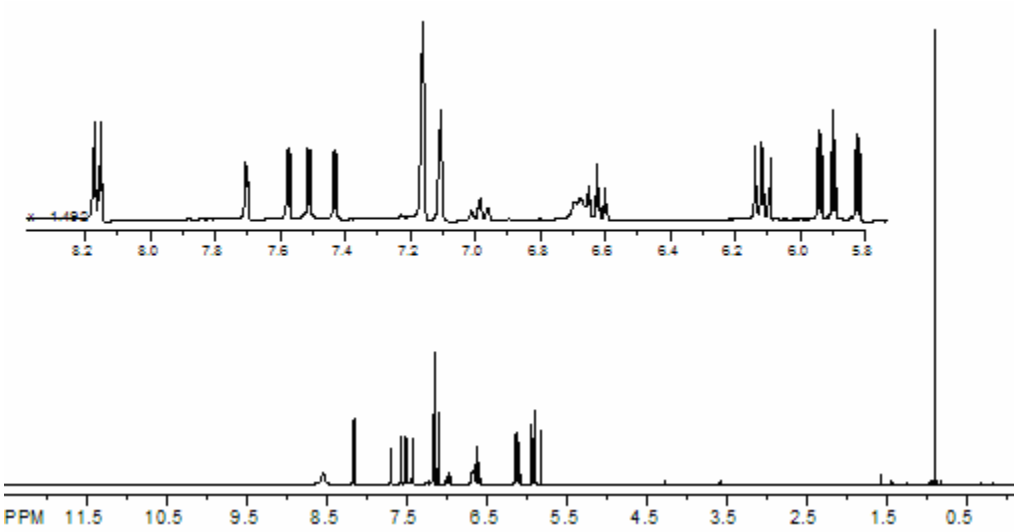

Figure 2.14. ^{1}H NMR spectrum of TpRu(CO)(*N*-py)Me (**4**) in C_6D_6.

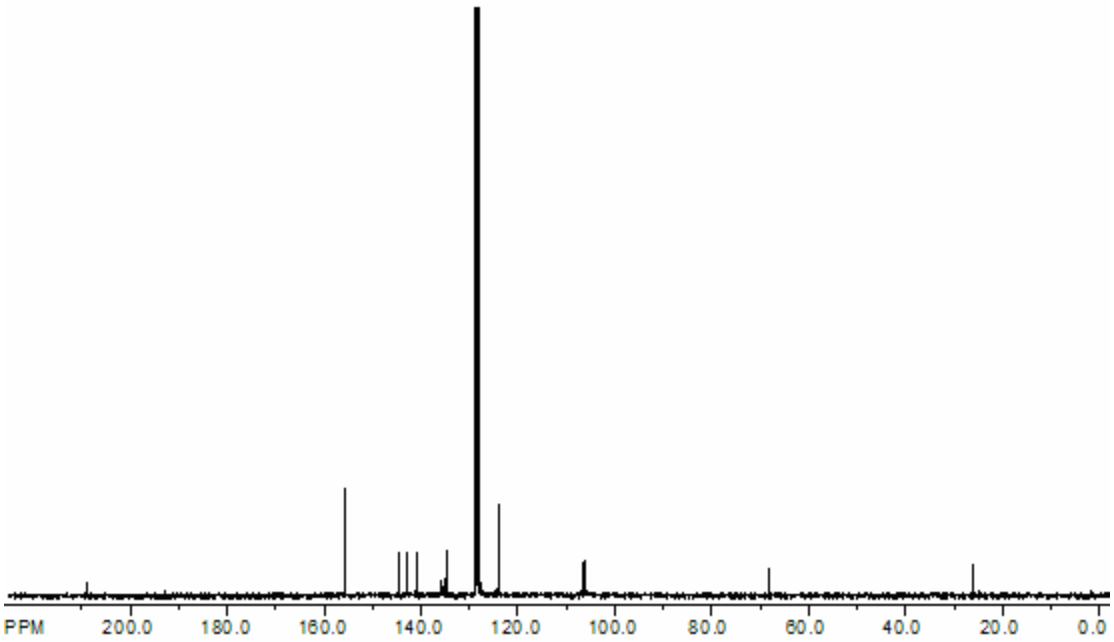

Figure 2.15. ^{13}C NMR spectrum of TpRu(CO)(*N*-py)Me (**4**) in C_6D_6.

Access to a stable coordination mode of pyridine renders subsequent C-H activation more difficult compared with the reaction of **1** with furan; however, at elevated temperature (115 ^{o}C) complex **4** undergoes slow reaction that requires approximately 7 days to reach completion. The final product mixture is complex and contains multiple TpRu systems. Column chromatography allows the isolation of a complex whose ^{1}H NMR and IR spectra are consistent with TpRu(CO)(NCMe)(2-pyridyl) (**5**). The production of **5** in low yield likely indicates that pyridine C-H activation is not regioselective or that **5** is not stable under the forcing conditions required to achieve C-H activation of pyridine.

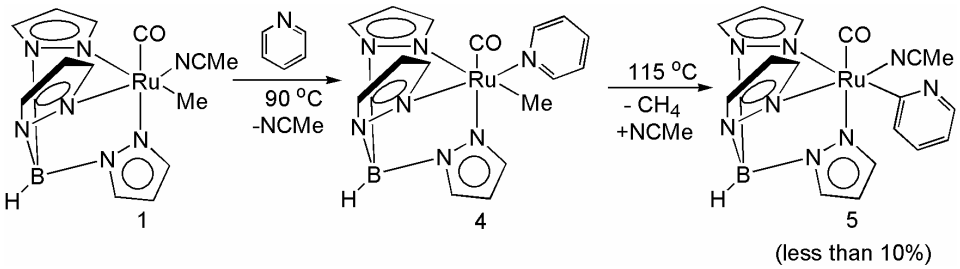

Scheme 2.9. Reaction of TpRu(CO)(NCMe)Me (**1**) with pyridine yields the intermediate TpRu(CO)(NCMe)(*N*-pyridinyl) (**4**) and at elevated temperatures TpRu(CO)(NCMe)(2-pyridinyl) (**5**).

In the proposed catalytic cycle for production of alkylated arenes (Scheme 2.6), the catalytic precursor TpRu(CO)(NCMe)Ar (Ar = 2-furyl (**2**), 2-thienyl (**3**), or phenyl) dissociates the labile NCMe ligand to make the catalytically active species {TpRu(CO)Ar}. To confirm NCMe dissociation, this aspect of the catalytic cycle was studied in greater detail by following degenerate ligand exchange in $NCCD_3$. The rates of NCMe/$NCCD_3$ exchange for the phenyl, 2-furyl (**2**), and 2-thienyl (**3**) complexes (Scheme 2.10) are (Figure 2.16) 3.2(2) x 10^{-5} s^{-1}, 1.8(1) x 10^{-5} s^{-1}, and 1.7(4) x 10^{-5} s^{-1}, respectively. The rates of nitrile exchange for the 2-furyl and 2-thienyl complexes were determined to be statistically identical with the nitrile exchange for TpRu(CO)(NCMe)Ph being approximately 1.8 times more rapid than the 2-furyl/2-thienyl complexes **2** and **3**. By examination of the architecture of TpRu(CO)(NCMe)(2-thienyl), it does not seem that steric influences would promote increased rates of dissociation of the NCMe ligand when moving to a 6-coordinate ring (e.g., phenyl) to the extent observed. Steric influences cannot be ruled out, however, it is more likely that combined σ and π-effects arising from the heteroatom of the coordinated arene is the source of retardation. That is as the electron withdrawing ability of the ligand is enhanced (2-fuyl > 2-thienyl > phenyl) the Lewis acidity of the {TpRu(CO)Ar} is increased. Evidence for this argument can be drawn from the ν_{CO} stretches of the complexes. As the ν_{CO} of the complexes increase, a decrease should be observed in the rate of dissociation of the labile ligand NCMe. With a ν_{CO} being an indication of less electron density about the metal center, it would be assumed that the metal center would perform as a better Lewis acid binding the NCMe more efficiently. This is consistent with the progression of the observed IR stretches. For example, the ν_{CO} stretches for Ar = Ph, 2-thienyl, and 2-furyl are 1935 cm^{-1} 1946 cm^{-1}, and 1949 cm^{-1}, respectively. The importance of this study lies in the labile nature of the

nitrile ligand allowing accessibility to the reactive coordinatively unsaturated 16 e^- complex {TpRu(CO)Ar}. This is further demonstrated by John P. Lee's observation that TpRu(CO)(NCMe)(2-furyl) (**2**) reacts with PMe_3 to produce TpRu(CO)(PMe_3)(2-furyl) (**6**).

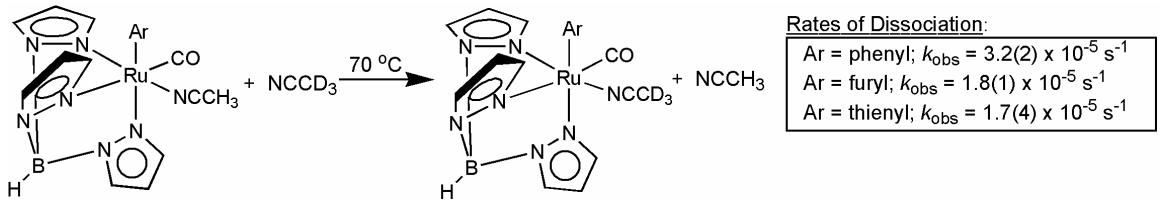

Scheme 2.10. Nitrile exchange is observed for TpRu(CO)(NCMe)Ar {Ar = phenyl, 2-furyl (**2**), or 2-thienyl (**3**)} under pseudo-first-order conditions ([Ru] = 0.072 M).

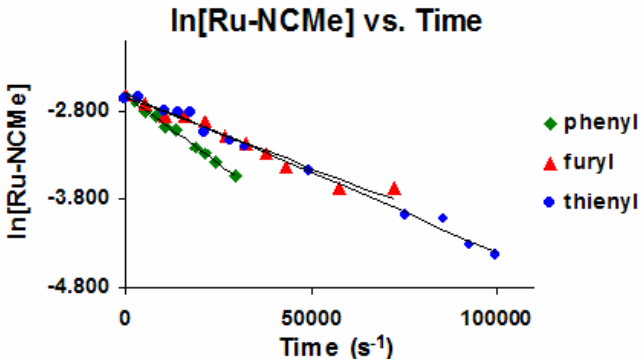

Figure 2.16. First-order rate plot tracking the dissociation of NCMe for TpRu(CO)(NCMe)Ar {Ar = Ph, 2-furyl (**2**), and 2-thienyl (**3**)} in $NCCD_3$.

One aspect of the mechanism that deserved further evaluation was the mechanism of C-H activation. Late transition metal centers in low oxidation states have been demonstrated to cleave C-H bonds via insertion of the metal into the C-H bond with a formal +2 increase in metal oxidation state (i.e., oxidative addition). Of particular relevance here are C-H activations by d^6 metal centers that are isoelectronic to TpRu(CO)(NCMe)R. For example, Bergman et al. have reported that Cp*(PMe_3)Ir^{III}(Me)(OTf) and [Cp*(PMe_3)Ir^{III}(Me)(CH_2Cl_2)][BAr'$_4$], Ar' = 3,5-$(CF_3)_2C_6H_3$, can selectively activate the C-H bonds of a range of substrates below room temperature.[61, 62] In addition, Ir^{III} complexes with oxygen-donor ligands can *catalytically* add arene C-H bonds across unsaturated carbon-carbon bonds as well as initiate alkane C-H

activation.[63-66] Substantial speculation has been focused on the mechanism of the C-H bond breaking step for the Ir(III) systems.[67-71] An oxidative addition mechanism is consistent with known pathways for late transition metal complexes but would involve an atypically high Ir^{V} oxidation state (See Ch. 1). An alternative pathway is σ-bond metathesis (See Ch. 1);[41, 72-74] however, to our knowledge, σ-bond metathesis mechanisms for C-H activation have not been definitively demonstrated for late transition metal systems. Hartwig et al. have demonstrated that Ru^{II} activation of B-H bonds likely occurs through a σ-bond metathesis mechanism.[75]

To help discern the likely mechanism of C-H activation by the fragment {TpRu(CO)Me}, B3LYP/SBK(d) calculations were employed by Prof. Thomas R. Cundari at the University of North Texas. As a model of the full (tris-pyrazolyl)borate (Tp) ligand, the tris(azo)borate (Tab) ligand, $[HB(-N{=}NH)_3]^-$ was used. In previous research, Tab was shown to faithfully reproduce the structure and energetics of the full Tp models for C-H activation potential energy surfaces.[76] Calculations were performed with furan as the representative reactant.

Experimental kinetic studies suggest that C-H activation of benzene by **1** proceeds through initial acetonitrile/benzene ligand exchange,[30] and we considered an analogous initial step for the C-H activation of furan. Two coordination modes were considered for the interaction of ruthenium and furan: σ (η^1-coordination through oxygen) and π (η^2-coordination through C=C bond; Figure 2.5). Both coordination modes were constructed and evaluated. The π-coordination mode is preferred relative to the corresponding σ-isomer by 3.8 kcal/mol. The calculated free energies for π- versus σ-coordination are consistent with experimental observations since η^2-coordinated furan complexes have been isolated, while, to our knowledge, examples of isolable η^1-*O*-bound furan systems are unknown.[10, 77-79] Hence, in the discussion below, (Tab)Ru(Me)(C_4H_4O)(CO) refers exclusively to the more stable π-coordinated isomer.

Studies of the overall process of furan C-H activation and methane release were broken down into three steps: (1) furan coordination, (2) C-H activation of furan, and (3) coordination of the acetonitrile model N≡CH to complete the reaction. The resulting energetic parameters are depicted in Scheme 2.11. The displacement of N≡CH by C_4H_4O is calculated to be *endergonic* by 14.4 kcal/mol. Given a calculated free energy of binding of N≡CH to {(Tab)Ru(CO)Me} of 14.9 kcal/mol, this corresponds to a binding free energy of

furan to (Tab)Ru(Me)(CO) of -0.5 kcal/mol. Weak binding is expected for dihapto-ligation of a π-heteroatomic system to a closed-shell, d^6 ML_5 fragment. The C-H activation step is *exergonic* by 13.4 kcal/mol with a calculated free energy of activation of 17.4 kcal/mol. The overall reaction sequence (Tab)Ru(CO)(NCH)Me + C_4H_4O → (Tab)Ru (CO)(NCH)(2-C_4H_3O) + CH_4 is *exergonic* by 10.3 kcal/mol. Assuming that the change in entropy for the overall C-H activation is negligible, the C-H bond dissociation energies of methane (104 kcal/mol) and furan (118 kcal/mol) indicate that the Ru-2-furyl bond is stronger than the Ru-CH_3 bond by approximately 24 kcal/mol.[80]

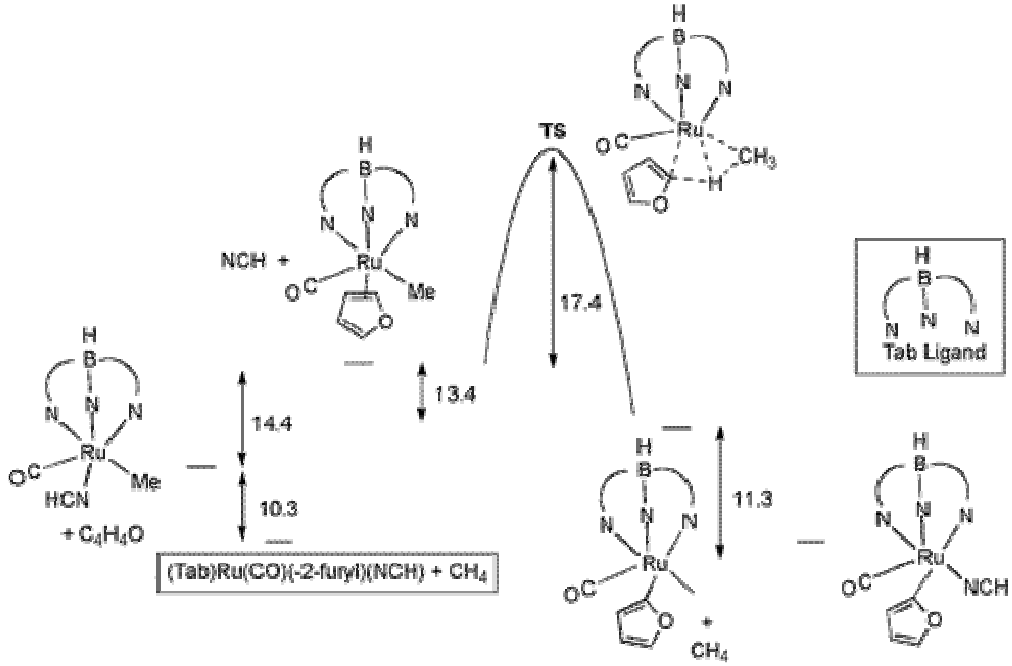

Scheme 2.11. B3LYP/SBK-31G(d) calculated free energies (kcal/mol) for the C-H activation of furan by TabRu(CO)(NCMe)Me.

To explore the C-H activation step, a variety of calculations were performed using furan as a model substrate (Figure 2.17). Several pathways were investigated including oxidative addition of a furan C-H bond to the Ru of {(Tab)Ru(CO)Me} (**A**), oxidative addition of a methane C-H bond to the Ru of {(Tab)Ru(CO)(2-furyl)} (**B**), and nonoxidative addition at the 2-position C-H bond of furan to the Ru-CH_3 bond of

{(Tab)Ru(CO)Me} (**C**). Multiple starting geometries were investigated for each of the proposed transition states. In all cases, the transition states collapsed to **C** (i.e., the non-oxidative addition transition state).

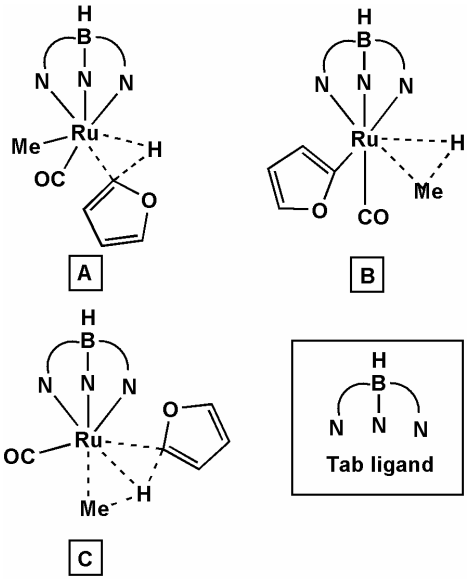

Figure 2.17. Various pathways for furan C-H activation that were studied by DFT calculations.

The calculated transition-state geometry for C-H activation of furan and pertinent metric data are depicted in Figure 2.18. The near equivalent C-H distances between the methyl and furyl ligands and the hydrogen atom undergoing transfer are indicative of a transition state that is roughly intermediate between reactants and products and hence neither early nor late. One interesting factor regarding the transition-state geometry is the close metal-transannular hydrogen distance (1.75 Å). Closely related results have been reported from calculations to probe the mechanism of C-H activation for $TpM(PH_3)Me$ (M = Fe or Ru) complexes in which the authors suggested that the reaction pathways are intermediate between oxidative addition and σ-bond metathesis processes.[81] Computational studies of methane activation by $Pt(H_2O)Cl_2$ indicate a similar four-center transition state with a Pt-H bond distance of 1.99 Å.[82] Calculations on the transition state of benzene C-H activation by $(acac)_2Ir(CH_2CH_2Ph)$ and $TpRu(CO)(CH_2CH_2Ph)$ reveal an Ir-H bond distance of 1.58 Å and a Ru-H bond distance of 1.61 Å, respectively, and Goddard et al. have differentiated this transition state (in which

there is a metal-hydrogen interaction) from a σ-bond metathesis transition state using the label oxidative hydrogen migration.[83, 84]

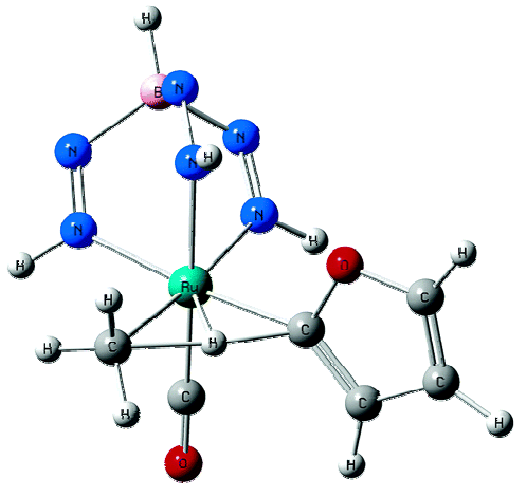

Figure 2.18. Calculated transition-state geometry for furan C-H activation by {(Tab)Ru(CO)Me}. Bond lengths for C-H activation active site: Ru-C_{furyl} = 2.17 Å; C_{furyl}-H_t = 1.44 Å; H_t-C_{methyl} = 1.54 Å; Ru-C_{methyl} = 2.32 Å; Ru-H_t = 1.75 Å.

As previously discussed for early transition metal systems,[85-87] for C-H activation that proceeds without an oxidative addition intermediate, a distinction can be made between σ-bond metathesis and electrophilic aromatic substitution. The calculated transition state for furan C-H activation by {(Tab)Ru(CO)Me} reveals that the hydrogen atom undergoing transfer to the methyl ligand is out of the aromatic plane (Figure 2.18). The calculated Ru-C_{furyl}-H bond angle in the transition state is 53.3°, and the out-of-plane position is consistent with a change in hybridization from sp^2 to sp^3 at the center of C-H activation. The disruption of planarity and hence aromaticity could reflect a pathway for C-H activation that is related to electrophilic substitution in which the electrophilic Ru^{II} center attacks the furan π-system. Alternatively, the out-of-plane hydrogen could reflect progress along the reaction coordinate and incipient Ru-C bond formation.

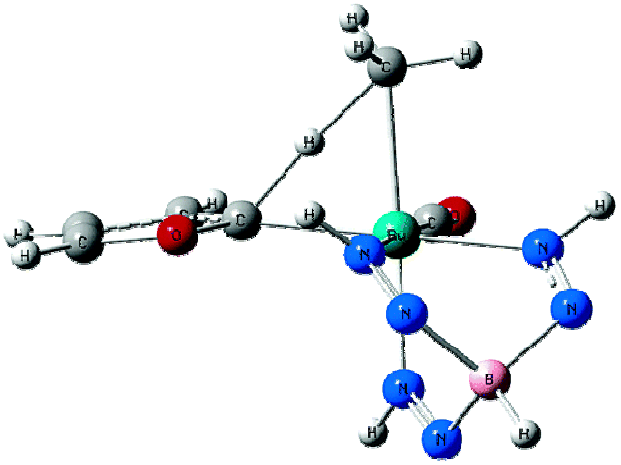

Figure 2.19. View of calculated transition state for C-H activation of furan that illustrates the "out-of-plane" position of the transannular hydrogen.

Given the similar C-H bond dissociation energies at the 2- and 3-position of five-membered heteroaromatic compounds,[80] the regioselective cleavage of the 2-position C-H bonds of thiophene and furan implicates the potential importance of the electrophilic nature of the Ru^{II} center. It is known that electrophilic additions to five-membered heteroaromatic compounds occur selectively at the 2-position due to favorable resonance stabilization,[88] and we propose that an electrophilic attack of Ru on the aromatic substrate likely precedes and/or initiates C-H activation, a supposition supported by the calculated positive charge on the furan fragment in (Tab)Ru(CO)(η^2-C_4H_4O)Me. Electrophilic addition of Ru^{II} would substantially increase the acidity of ring C-H bonds, and subsequent C-H activation through a non-oxidative addition pathway could be viewed as an intramolecular heterolytic process for which the methyl ligand acts as a base to remove a proton from furan or thiophene (Scheme 2.12). The Ru-H interaction in the calculated transition state likely imparts more hydridic (or, perhaps equally accurate, less acidic) character to the transannular hydrogen; however, the bonding orbitals involving the transannular hydrogen are predominantly Ru in character. The proposed model of the Ru^{II}-mediated C-H activation is closely related to that suggested for C-H activation by tungsten and iron boryl complexes.[89] Selnau and Merola have previously noted that the acidity of C-H bonds may play a role in metal-mediated oxidative addition transformations, although the relative acidity of C-H bonds of "free" heteroaromatic substrates may not be as important as that of substrates that result from electrophilic addition.[50]

The regioselectivity of furan and thiophene C-H activation by **1** is not conclusive for a non-oxidative addition pathway since identical regioselectivities have been reported for systems that initiate well-defined oxidative addition,[50, 53] however, not all oxidation addition transformations are regioselective, as illustrated by a binuclear iridium system that initiates oxidative addition of furan to produce a 5:2 ratio of 2-furyl and 3-furyl products.[36] Even though the regioselectivity for oxidative addition of hydrocarbons is often guided by bond dissociation energies,[90-92] the observation of a final oxidative addition product for heteroaromatic substrates neither precludes the intermediacy of an electrophilic addition product that precedes C-H activation nor rules out the importance of the electrophilic character of the metal center in the overall C-H activation. Thus, even in the absence of a "true" electrophilic addition of Ru^{II}, the electrophilic nature of the metal center could still serve to guide the regioselectivity.

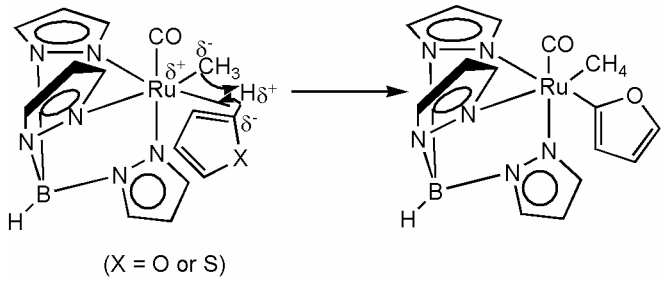

Scheme 2.12. Intramolecular proton transfer is consistent with the regioselectivity of C-H Activation.

2.3 Summary

The presence of the Tp ligand may predispose the Ru^{II} systems {TpRu(CO)R} against oxidative addition intermediates given the well-documented predilection against seven-coordinate complexes for complexes that possess Tp or related ligands.[76] Experimental and computational studies of aromatic C-H activation by the {TpRu(CO)Me} fragment are consistent with a nonoxidative addition pathway in which the electrophilic character of Ru^{II} may dictate regioselectivity. The potential synthetic advantage of this pathway is

the ability to utilize charge localization on aromatic substrates to direct the regioselectivity of C-H activation as demonstrated by the catalytic synthesis of 2-ethylfuran from furan and ethylene.

2.4 Experimental Section

General Methods. Unless otherwise noted, all synthetic procedures were performed under a dinitrogen atmosphere using either standard Schlenk line or glovebox techniques. Glovebox atmosphere was maintained at O_2 (g) < 15 ppm for all reactions. Mesitylene was vacuum distilled prior to use. Furan was distilled prior to use. Acetonitrile was distilled over CaH_2. Hexanes, methylene chloride, and tetrahydrofuran were purchased as OptiDry solvents (<50 ppm H_2O) and passed through columns of activated alumina (under nitrogen pressure) prior to use. Decane and 2-ethylfuran were used as received from commercial sources. Ethylene was purchased from National Welders Supply Co. and used as received. CD_3CN, acetone-d_6, CD_2Cl_2, benzene-d_6, and $CDCl_3$ were degassed with three freeze-pump-thaw cycles and stored under a dinitrogen atmosphere over 4 Å molecular sieves. ^{1}H and ^{13}C NMR spectra were recorded on a Varian Mercury 300 or 400 MHz spectrometer. NOE experiments were conducted on a Varian Mercury 400 MHz spectrometer using 64 scans with a 1 s mixing time. Gas chromatography was carried out on a Hewlett-Packard 5890 GC equipped with a J&W SE-30 or HP5-MS capillary column, split inlet, and FID detector. Chromatographs were produced using an HP3396 Series II integrator or PE Totalchrome software package. IR spectra were acquired by a Mattson Genesis II FT-IR as thin films on KBr plates or as solutions in KBr solvent cells. TpRu(CO)(NCMe)(Me) and TpRu(CO)(NCMe)(Ph) were prepared according to the published procedures.[30]

Calculations. Quantum calculations were carried out using the Gaussian 98 package.[93] The B3LYP hybrid functional was employed for all calculations.[94] Heavy atoms were described with the Stevens relativistic effective core potentials (ECPs) and valence basis sets (VBSs).[95, 96] The valence basis sets of main group elements were augmented with a d polarization function. This ECP/VBS combination, termed SBK(d), has been validated for the calculation of a wide variety of transition metal properties in previous studies.[76, 97, 98] All stationary points were fully optimized without symmetry constraint. Several conformations of the different ligands were investigated by torsion about the appropriate metal-ligand bonds; the lowest energy conformers

found were used in the analyses given in this paper. The energy Hessian was calculated at all stationary points to characterize them as minima (no imaginary frequencies) or transition states (one and only one imaginary frequency). The quoted energies include zero-point, enthalpy, and entropic corrections determined from unscaled vibrational frequencies calculated at the B3LYP/SBK(d) level of theory. All energetic determinations were done at 298.15 K and 1 atm.

TpRu(CO)(NCMe)(2-furyl) (2). TpRu(CO)(NCMe)Me (**1**) (0.227 g, 0.570 mmol) was added to a thick-walled glass pressure vessel containing approximately 25 mL of furan. The vessel was sealed, and the reaction mixture was heated in a 90 ^{o}C oil bath for 36 h. After cooling the solution to room temperature, all volatiles were removed in vacuo. The resulting pale pink-colored solid was taken up in THF (~2 mL) and precipitated with hexanes (~25 mL). The resulting amorphous solid was collected via filtration and washed with hexanes (2 × 10 mL). The isolated product was dried under reduced pressure to yield a pale pink-colored solid (0.155 g, 60%). IR (KBr): ν_{CO} = 1949 cm^{-1}, ν_{CN} = 2286 cm^{-1}, ν_{BH} = 2484 cm^{-1}. ^{1}H NMR (C_6D_6, δ): 7.99 (1H, dd, J_{HH} = 1.5 and 0.6 Hz, α-furyl C*H*), 7.89, 7.60, 7.43, 7.40, 7.29 (6H, 1:2:1:1:1 integration, each a d, Tp C*H* 3- or 5-position), 6.62 (1H, dd, J_{HH} = 2.7 and 1.5 Hz, β-unbound of furyl C*H*), 6.23 (1H, dd, J_{HH} = 2.7 and 0.6 Hz, β-bound of furyl C*H*), 5.96, 5.67 (3H, 2:1 integration, each a t, Tp C*H* 4-position), 0.37 (3H, s, NCCH_3). ^{13}C{^{1}H} NMR ($CDCl_3$, δ): 203.9 (*C*O), 178.8 (ipso-furyl), 145.2, 144.3, 142.4, 142.2 (Tp 3- and 5-position), 135.3, 134.7, 134.5 (α-unbound of furyl and Tp 3- and 5-position), 122.1 (Ru-N*C*CH_3), 114.8, 109.6 (β-position of furyl), 105.5, 105.2 (Tp 4-position, coincidental overlap of two resonances), 4.3 (Ru-NC*C*H_3). Anal. Calcd for $C_{16}H_{16}BN_7O_2Ru$: C, 42.68; H, 3.58; N, 21.78. Found: C, 42.71; H, 3.50; N, 21.57. To determine the composition of the crude reaction product, an aliquot of the homogeneous solution was taken prior to workup. The solvent was removed under reduced pressure, and the resulting film was dissolved in C_6D_6. The entire solid was dissolved to give a homogeneous solution. Complex **1** was the only observable species using ^{1}H NMR spectroscopy. The NOE data were acquired using a Varian Mercury 400 MHz instrument in C_6D_6 with a mixing time of 1 s and delay time of 25 s.

TpRu(CO)(NCMe)(2-thienyl) (3). A thick-walled glass reaction vessel was charged with TpRu(CO)(NCMe)Me (**1**) (0.243 g, 0.609 mmol) and thiophene (~5 mL). The reaction vessel was heated to 90

^{o}C for 19 h. The reaction solution was then cooled to room temperature, and the volatiles were removed under reduced pressure. The residuals were taken up in methylene chloride, and upon addition of hexanes, a precipitate formed. The resulting beige solid was collected via vacuum filtration and dried under reduced pressure to yield 0.242 g (88%) of product. IR (KBr): ν_{CO} = 1946 cm^{-1}, ν_{CN} = 2284 cm^{-1}, ν_{BH} = 2484 cm^{-1}. ^{1}H NMR (CD_3CN, δ): 7.86 (1H, d, Tp C*H*, 3- or 5-position), 7.81 (2H, m, Tp C*H*, 3- or 5-position), 7.79 (1H, dd, Tp C*H* 3- or 5-position), 7.47 (1H, d, Tp C*H*, 3- or 5-position), 7.25 (1H, dd, *J* = 5, 1 Hz, thienyl 2-position C*H*), 6.97 (1H, dd, *J* = 5, 3 Hz, thienyl 3-position unbound C*H*), 6.57 (1H, dd, *J* = 3, 1 Hz, thienyl 2-position bound C*H*), 6.31, 6.25, 6.18 (each 1H, each a t, Tp C*H* 4-position), 2.33 (3H, s, NCCH_3). ^{13}C{^{1}H} NMR (CD_3CN, δ): 204.0 (*C*O), 158.9 (ipso thienyl), 145.7, 142.8, 142.6, 135.6, 135.1, 134.7, 132.5, 127.2, 125.9 (Tp 3- and 5-position *or* thienyl), 122.5 (Ru-N*C*CH_3), 105.7, 105.3 (Tp 4-position with overlap of two resonances), 4.4 (Ru-NC*C*H_3). Anal. Calcd for $C_{16}H_{16}BN_7O_1RuS$: C, 41.21; H, 3.46; N, 21.03. Found: C, 40.77; H, 3.52; N, 20.32.

Reaction of TpRu(CO)(NCMe)(2-thienyl) (3) with HCl: Observation of [TpRu(CO)(NCMe)(*S*-thiophene)][Cl]. Under an atmosphere of dinitrogen, a screw-cap NMR tube was charged with TpRu(CO)(NCMe)(2-thienyl) (**3**) (0.020 g) and CD_2Cl_2 (0.6 mL). The solution was cooled to -65 ^{o}C, and 1 equiv of HCl (44 μL, 1 M in Et_2O) was added. Upon addition of HCl, a color change from pink to yellow was noted. A ^{1}H NMR spectrum was acquired of the reaction solution at -65 ^{o}C. As detailed below, the spectrum was consistent with the formation of [TpRu(CO)(NCMe)(*S*-thiophene)][Cl]. Upon warming to room temperature, ^{1}H NMR spectroscopy revealed the formation of TpRu(CO)(NCMe)(Cl) and free thiophene. The addition of thiophene to the reaction sample confirmed the presence of free thiophene.

[TpRu(CO)(NCMe)(*S*-thiophene)][Cl]. ^{1}H NMR (CD_2Cl_2, δ): 7.93, 7.85 (each 1H, br s, Tp C*H* 3- and 5-position), 7.72 (3H, m, Tp C*H* 3- and 5-position) 7.61 (2H, br s, α-thiophene), 7.36 (2H, br s, β-thiophene), 7.05 (1H, br s, Tp C*H*, 3- and 5-position), 6.39, 6.27, 6.18 (each 1H, br s, Tp C*H*, 4-position), 2.09 (3H, s, NCCH_3).

TpRu(CO)(*N*-pyridine)Me (4). In a thick-walled glass pressure vessel, TpRu(CO)(NCMe)Me (**1**) (0.101 g, 0.256 mmol) was dissolved in pyridine (5 mL). The mixture was heated to 90 ^{o}C for 5 h. The reaction

solution was then cooled to room temperature and purged into a glovebox, and the volatiles were removed under reduced pressure. The resulting product was precipitated from methylene chloride upon addition of hexanes, and the precipitate was collected by vacuum filtration through a fine-porosity frit. The resulting solid was dried under vacuum to yield a bright yellow product (0.063 g, 56%). IR (KBr): ν_{CO} = 1902 cm^{-1}, ν_{BH} = 2478 cm^{-1}. ^{1}H NMR (C_6D_6, δ): 8.16 (2H, m, pyridine ortho C*H*), 7.70 (1H, dd, Tp C*H*, 3- or 5-position) 7.57 (1H, dd, Tp C*H* 3- and 5-position), 7.51 (1H, dd, Tp C*H*, 3- and 5-position), 7.43 (1H, dd, Tp C*H*, 3- and 5-position), 7.12 {2H, s (overlapping doublets), Tp C*H*, 3- or 5-position}, 6.62 (1H, tt, J_{HH} = 7.7, 1.8 Hz, pyridine para-C*H*), 6.12 (2H, m, pyridine meta-C*H*), 5.94 (1H, t, Tp C*H* 4-position), 5.90 (1H, t, Tp C*H* 4-position), 5.82 (1H, t, Tp C*H*, 4-position), 0.89 (3H, s, NCCH_3). ^{13}C{^{1}H} NMR (C_6D_6, δ): 209.0 (*C*O), 155.7, 144.7, 142.7, 140.8, 135.6, 135.1, 135.0, 134.6, 124.0 (Tp 3- and 5-position, pyridine and Ru-N*C*Me) 106.5, 106.3, 106.2 (Tp 4-position), -4.1 (Ru-*C*H_3). Anal. Calcd for $C_{16}H_{18}BN_7ORu$: C, 44.05; H, 4.16; N, 22.47. Found: C, 44.12; H, 4.22, N, 22.16.

TpRu(CO)(NCMe)(2-pyridinyl) (5). Method 1. To a pyridine (20 mL) solution of TpRu(CO)(NCMe)Me (**1**) (0.1030 g, 0.2606 mmol) was added a slight excess of acetonitrile (0.02 mL, 0.3827). The solution was allowed to reflux for seven days. The dried product was purified by column chromatography on silica gel using a methylene chloride mobile phase. After the precipitated removal of volatile from the eluent, the solid was dissolved in methylene chloride and precipitated upon addition of hexanes. The solid was isolated by vacuum filtration through a fine porosity frit to yield yellow/green solid.

Method 2. Pyridine (25 mL) and TpRu(CO)(*N*-pyridine)Me (**5**) (0.1050 g, 0.2406 mmol) were placed into a 100 mL flask equipped with a vigeroux column and heated to reflux for five days. The volatiles were removed under vacuum. The solid was dissolved in methylene chloride and precipitated upon addition of hexanes. The yellow/green solid was collected on a fine porosity frit by vacuum filtration. IR (KBr): ν_{CO} = 1935 cm^{-1}, ν_{CN} = 2278 cm^{-1}, ν_{BH} = 2482 cm^{-1}. ^{1}H NMR (CD_3CN, δ): 8.14 (1H, t, β-pyridinyl CH), 7.84 (2H, m, overlapping α,β-pyridinyl), 7.80, 7.46, 7.44, 7.22, 7.19 (1H, d, Tp 3 and 5 position), 6.28 (1H, t, γ-pyridinyl), 6.21 (2H, m, overlapping Tp CH 4 position), 5.45 (1H, d, Tp CH 3 or 5 position), 0.36 (3H, s, $NCCH_3$).

TpRu(CO)(PMe$_3$)(2-furyl) (6). A thick-walled pressure tube was charged with TpRu(NCMe)(CO)(2-furyl) (**2**) (0.228 g, 0.051 mmol) and THF (~8 mL). To the orange-yellow solution was added PMe$_3$ (80 μL, 0.08 mmol), and the mixture was heated at 90 ^{o}C for 20 h. The solvent was removed in vacuo, and the resulting solid was stirred in hexanes. The pale yellow solid was collected after vacuum filtration and dried (0.099 g, 38%). IR (KBr): ν_{CO} = 1943 cm^{-1}. ^{1}H NMR (CDCl$_3$, δ): 7.74 (1H, α-furyl CH, d, $^{3}J_{HH}$ = 1.5 Hz), 7.69, 7.65, 7.58, 7.55, 7.42 (6H, 2:1:1:1:1 integration, each a d, Tp C*H* 3- or 5-position), 6.26 (1H, β-furyl CH unbound, dd, $^{3}J_{HH}$ = 3.0 and 1.5 Hz), 6.21, 6.06 (3H total, 2:1 integration, overlapping t's and t, Tp 4-position), 5.63 (1H, β-furyl CH bound, d, $^{3}J_{HH}$ = 3 Hz), 1.30 (9H, PMe$_3$, d, $^{3}J_{HP}$ = 9 Hz). ^{13}C{^{1}H} NMR (CDCl$_3$, δ): 205.2 (CO, d, $^{2}J_{CP}$ = 19 Hz), 180.1 (1C, ipso-furyl, d, $^{2}J_{CP}$ = 16 Hz), 143.7, 143.6, 143.3, 135.4, 135.2, 134.4 (each a s, Tp 3- and 5-position), 115.2 (α-furyl, s), 110.0 (β-furyl, s), 105.6 (β-furyl, s), 105.3, 105.2, 105.1 (each a s, Tp 4-position), 17.5 (PMe$_3$, d,$^{2}J_{CP}$ = 31 Hz). ^{31}P{^{1}H} NMR (CDCl$_3$, δ): 14.3 (PMe$_3$, s). Anal. Calcd for $C_{17}H_{22}BN_6O_2PRu(C_4H_8O)_{0.2}$ (Note: ^{1}H NMR spectroscopy of the analysis sample revealed 1/5 equivalents of THF per equivalent of complex **6**): C, 42.79; H, 4.76; N, 16.81. Found: C, 42.34; H, 4.75; N, 16.59.

Catalytic Reactions of Furan with Ethylene Using TpRu(CO)(NCMe)(2-furyl) (2). The procedures for all catalytic reactions were analogous. A representative example is given: Under an atmosphere of dinitrogen, TpRu(CO)(NCMe)(2-furyl) (**2**) (0.073 g, 0.162 mmol) was added to a high-pressure reaction tube containing furan (1.2 mL, 16.2 mmol), decane (0.31 mL, 1.62 mmol), and mesitylene (5 mL). The reaction vessel was sealed, removed from the glovebox, and placed under 20 psi of ethylene pressure. The resulting solution was submersed in an oil bath (120 ^{o}C) equipped with digital temperature regulation. Product formation was monitored periodically using analysis with a GC FID (and compared to an authentic sample 2-ethylfuran purchased from a commercial vendor). Prior to analysis using GC FID, the reaction mixture was cooled in an ice water bath for 15 min. Aliquots were removed using a syringe under a light purge of dinitrogen. Product quantities were determined using integrated ratios of the peaks due to 2-ethylfuran and the internal standard decane. A series of five known standards were prepared consisting of 3:1, 2:1, 1:1, 1:2, and 1:3 molar ratios of decane:2-ethyl furan. A plot of the peak area ratios versus molar ratios gave a regression line. The slope is 2.5 (R^2 = 0.96).

Catalytic Reactions of Thiophene with Ethylene Using TpRu(CO)(NCMe)(2-thienyl) (3). Under an atmosphere of dinitrogen, a thick-walled high-pressure reaction tube was charged with TpRu(CO)(NCMe)(2-thienyl) (**3**) (0.040 g, 0.087 mmol), thiophene (6.9 mL, 87 mmol), and decane (0.17 mL, 0.87 mmol) as an internal standard. The reaction vessel was placed under 40 psi of ethylene pressure and submersed in a hot oil bath (90 ^{o}C) equipped with digital temperature regulation. The formation of 2-ethylthiophene was monitored by GC-FID analysis. Prior to analysis using GC FID, the reaction mixture was cooled in an ice water bath for 15 min. Aliquots were removed using a syringe under a light purge of dinitrogen. Product yields were determined using integrated areas of 2-ethylthiophene versus the internal standard decane. A series of five known standards were prepared consisting of 3:1, 2:1, 1:1, 1:2, and 1:3 molar ratios of decane:2-ethylthiophene. A plot of the peak area ratios versus molar ratios gave a regression line. The slope is 1.6 with R^2 = 0.99.

Kinetic Study of Acetonitrile Ligand Exchange for TpRu(CO)(NCMe)(Ph). TpRu(CO)(NCMe)Ph (0.020 g, 0.043 mmol) was placed in a screw-cap NMR tube and taken up in CD_3CN (0.6 mL). A ^{1}H NMR spectrum of the solution was acquired. The tube was placed into a hot oil bath (70 ^{o}C), and the ligand exchange reaction was monitored versus time. Every 45 min, the solution was removed from the oil bath and cooled in a solution of ice water, and a ^{1}H NMR spectrum was acquired. The disappearance of the resonance for bound acetonitrile was monitored relative to the peak area of Tp resonances. The decreased intensity of the resonance due to coordinated acetonitrile and increased intensity of the resonance due to free acetonitrile were the only observed changes in the NMR spectra.

Kinetic Study of Acetonitrile Ligand Exchange for TpRu(NCMe)(CO)(2-furyl) (2). TpRu(CO)(NCMe)(2-furyl) (**2**) (0.019, 0.043 mmol) was placed in a screw-cap NMR tube and taken up in CD_3CN (0.6 mL). A ^{1}H NMR spectrum was acquired. The tube was placed into a hot oil bath (70 ^{o}C), and the progress of acetonitrile exchange was monitored versus time. Every 90 min, the solution was cooled in an ice bath, and a ^{1}H NMR spectrum was acquired. The disappearance of the resonance for bound acetonitrile was monitored relative to the peak area of Tp resonances. The decreased intensity of the resonance due to coordinated acetonitrile and increased intensity of the resonance due to free acetonitrile were the only observed changes in the NMR spectra.

Kinetic Study of Acetonitrile Ligand Exchange for TpRu(CO)(NCMe)(2-thienyl) (3). TpRu(CO)(NCMe)(2-thienyl) (**3**) (0.020, 0.042 mmol) was placed in a screw-cap NMR tube and taken up in acetonitrile-d_3 (0.6 mL). The solution was heated to 70 ^{o}C for approximately 28 h. A ^{1}H NMR spectrum was periodically acquired. Prior to data acquisition, the reaction solution tube was cooled in an ice bath. The disappearance of the resonance for bound acetonitrile was monitored relative to the peak area of Tp resonances. The decreased intensity of the resonance due to coordinated acetonitrile and increased intensity of the resonance due to free acetonitrile were the only observed changes in the NMR spectra.

Attempted Isomerization of TpRu(CO)(NCMe)(2-furyl) (2). Representative experiment: In a glovebox under dinitrogen atmosphere, a reaction tube was prepared with TpRu(CO)(NCMe)(2-furyl) (**2**) (0.201 g, 0.045 mmol), furan (0.10 mL, 1.3 mmol), and 5 mL of THF. This vessel was removed from the glovebox and placed into a hot oil bath (90-100 ^{o}C) for 144 h. The reaction solution was cooled to room temperature, and volatiles were removed under reduced pressure. A ^{1}H NMR spectrum of the resulting solid revealed the quantitative recovery of TpRu(CO)(NCMe)(2-furyl) (**2**).

X-ray Diffraction Study of TpRu(CO)(NCMe)(2-thienyl) (**2**) and [TpRu(CO)(μ-*C*,*S*-2-thienyl)]$_2$. The same general procedures were used to perform the X-ray crystallographic analyses of complexes 2 and 4. A suitable crystal was covered in perfluoropolyether (PFO-XR75, Lancaster) and sealed under nitrogen in a glass capillary. The crystal was optically aligned on the four-circle of a Siemens P4 diffractometer equipped with a graphite monochromatic crystal, a Mo Kα radiation source (λ = 0.71073 Å), and a SMART CCD detector held at 5.084 cm from the crystal. Four sets of 20 frames each were collected using the ω scan method and with a 10 s exposure time. Integration of these frames followed by reflection indexing and least-squares refinement produced a crystal orientation matrix and a lattice. Data collection consisted of the measurement of a total of 1650 frames in five different runs covering a hemisphere of data. The program SMART (version 5.6) was used for diffractometer control, frame scans, indexing, orientation matrix calculations, least-squares refinement of cell parameters, and the data collection.[99] All 1650 crystallographic raw data frames were read by the program SAINT (version 5/6.0) and integrated using 3D profiling algorithms. The resulting data were reduced to produce a total of 12 921 reflections (complex 2) or 5678 reflections (complex 4) and their intensities and

estimated standard deviations. An absorption correction was applied using the SADABS routine available in SAINT. The data were corrected for Lorentz and polarization effects as well as any crystal decay. Data preparation was carried out by using the program XPREP, which gave 4367 unique reflections (R_{int} = 3.83%) with indices $-12 \leq h \leq 13$, $-15 \leq k \leq 15$, $-19 < l \leq 20$ for complex 2 and gave 3607 unique reflections (R_{int} = 0.0391) with indices $-10 \leq h \leq 11$, $-12 \leq k \leq 11$, $-11 \leq l \leq 13$ for complex 4. The monoclinic space group was determined to be $P2_1/n$, which is a nonstandard setting of the space group $P2_1/c$ (No. 14). The structure was solved by a combination of direct methods and Fourier methods with the use of SHELXTL6.1.[100] Idealized positions for the hydrogen atoms were included as fixed contributions using a riding model with isotropic temperature factors set at 1.2 (aromatic protons) or 1.5 (methyl protons) times that of the adjacent carbon. The position of the B-H proton was refined with a fixed isotropic temperature factor set at 1.2 times that of the boron atom. The positions of the methyl hydrogen atoms were optimized by a rigid rotating group refinement with idealized tetrahedral angles. For complex 2, the 2-thienyl ligand suffered from a 70:30 two-site disorder, with the two orientations of the planar five-membered ring differing by a nearly 180° rotation around the Ru-C(13) bond axis. The five non-hydrogen atoms within each of these ring orientations were refined anisotropically with the S(1)-C(13) and S(1)-C(16) bonds restrained to 1.68 ± 0.04 Å, the C(14)-C(15) bond restrained to 1.45 ± 0.04 Å, and the C(13)-C(14) and C(15)-(16) bonds restrained to 1.38 ± 0.04 Å. For complex 4, the dimeric structure is constrained by a crystallographic center of inversion. Full-matrix least-squares refinement, based upon the minimization of $\Sigma w_i|F_o^2 - F_c^2|^2$, with $w_i^{-1} = [\sigma^2(F_o^2) + (aP)^2 + bP]$, where a = 0.0436, b = 0.3172 for complex 2; a = 0.0473, b = 0.0 for complex 4; $P = (\mathrm{Max}(F_o^2, 0) + 2F_c^2)/3$, converged to give the final discrepancy indices. A correction for secondary extinction was not applied. The maximum and minimum residual electron density peaks in the final difference Fourier map were 0.462 and -0.403 e/Å^3 for complex 2 and 0.680 and -0.479 e/Å^3 for complex 4, respectively. The linear absorption coefficient, atomic scattering factors, and anomalous dispersion corrections were calculated from values from the International Tables for X-ray Crystallography.[101]

References

1. Pozharskhii, A. F.; Soldatenkov, A. T.; Katritzky, A. R., *Heterocycles in Life and Society*. Wiley: New York, 1997.

2. Gilchrist, T. L., *Heterocyclic Chemistry*. 3rd ed.; Longman: Essex, 1997.

3. Lail, M.; Arrowood, B. N.; Gunnoe, T. B. *J. Am. Chem. Soc.* **2003,** *125*, 7506-7507.

4. Klages, F. *Chem. Ber. Recl.* **1949,** *82*, 358-375.

5. Eicher, T.; Hauptmann, S., *The Chemistry of Heterocycles*. 1st ed.; Thieme: New York, 1995.

6. Friedman, L. A.; Sabat, M.; Harman, W. D. *J. Am. Chem. Soc.* **2002,** *124*, 7395-7404.

7. Gunnoe, T. B.; Sabat, M.; Harman, W. D. *Organometallics* **2000,** *19*, 728-740.

8. Chen, H. Y.; Liu, R. G.; Myers, W. H.; Harman, W. D. *J. Am. Chem. Soc.* **1998,** *120*, 509-520.

9. Brooks, B. C.; Gunnoe, T. B.; Harman, W. D. *Coord. Chem. Rev.* **2000,** *206*, 3-61.

10. Harman, W. D. *Chem. Rev.* **1997,** *97*, 1953-1978.

11. Harman, W. D. *Coord. Chem. Rev.* **2004,** *248*, 853-866.

12. Keane, J. M.; Harman, W. D. *Organometallics* **2005,** *24*, 1786-1798.

13. Harman, W. D. *Top. Organomet. Chem.* **2004,** *7*, 95-127.

14. Amari, C.; Ianelli, S.; Pelizzi, C.; Pelizzi, G.; Predieri, G. *Inorg. Chim. Acta* **1993,** *211*, 89-94.

15. Draganjac, M.; Ruffing, C. J.; Rauchfuss, T. B. *Organometallics* **1985,** *4*, 1909-1911.

16. Benson, J. W.; Angelici, R. J. *Organometallics* **1992,** *11*, 922-927.

17. Goodrich, J. D.; Nickias, P. N.; Selegue, J. P. *Inorg. Chem.* **1987,** *26*, 3424-3426.

18. Weinberger, D. A.; Higgins, T. B.; Mirkin, C. A.; Stern, C. L.; Liable-Sands, L. M.; Rheingold, A. L. *J. Am. Chem. Soc.* **2001,** *123*, 2503-2516.

19. Lane, T. G.; Paul, B.; Wippler, J.; Schwaller, T.; Adler, M. *Conquest*, 1.2; Cambridge Crystallographic Data Centre: Cambridge, 1998.

20. Brooks, B. C.; Meiere, S. H.; Freidman, L. A.; Carrig, E. H.; Gunnoe, T. B.; Harman, W. D. *J. Am. Chem. Soc.* **2001,** *123*, 3541-3550.

21. Lail, M.; Bell, C. M.; Conner, D.; Cundari, T. R.; Gunnoe, T. B.; Petersen, J. L. *Organometallics* **2004,** *23*, 5007-5020.

22. Chadwick, D. J.; Willbe, C. *J. Chem. Soc., Perkin Trans. 1* **1977**, 887-893.

23. Baciocchi, E.; Muraglia, E. *Tetrahedron Lett.* **1993,** *34*, 5015-5018.

24. Taylor, E. C.; Martin, S. F. *J. Am. Chem. Soc.* **1974,** *96*, 8095-8102.

25. Smith, M. B.; March, J., *March's Advanced Organic Chemistry: Reactions, Mechanisms, and Structure*. Fifth ed.; John Wiley & Sons, Inc.: New York, 2001.

26. Saaby, S.; Bayon, P.; Aburel, P. S.; Jorgensen, K. A. *J. Org. Chem.* **2002,** *67*, 4352-4361.

27. Minato, A.; Suzuki, K.; Tamao, K.; Kumada, M. *Tetrahedron Lett.* **1984,** *25*, 83-86.

28. Tamao, K.; Kodama, S.; Nakajima, I.; Kumada, M.; Minato, A.; Suzuki, K. *Tetrahedron* **1982,** *38*, 3347-3354.

29. Belt, S. T.; Dong, L.; Duckett, S. B.; Jones, W. D.; Partridge, M. G.; Perutz, R. N. *J. Chem. Soc., Chem. Commun.* **1991**, 266-269.

30. Boese, W. T.; Goldman, A. S. *Organometallics* **1991,** *10*, 782-786.

31. Fisher, B. J.; Eisenberg, R. *Organometallics* **1983,** *2*, 764-767.

32. Goj, L. A.; Gunnoe, T. B. *Curr. Org. Chem.* **2005,** *9*, 671-685.

33. Guari, Y.; Sabo-Etienne, S.; Chaudret, B. *Eur. J. Inorg. Chem.* **1999**, 1047-1055.

34. Jazzar, R. F. R.; Mahon, M. F.; Whittlesey, M. K. *Organometallics* **2001,** *20*, 3745-3751.

35. Jia, C.; Piao, D.; Kitamura, T.; Fujiwara, Y. *J. Org. Chem.* **2000,** *65*, 7516-7522.

36. Jones, W. D.; Dong, L. Z. *J. Am. Chem. Soc.* **1989,** *111*, 8722-8723.

37. Kakiuchi, F.; Murai, S. *Acc. Chem. Res.* **2002,** *35*, 826-834.

38. Luecke, H. F.; Bergman, R. G. *J. Am. Chem. Soc.* **1997,** *119*, 11538-11539.

39. Reinartz, S.; White, P. S.; Brookhart, M.; Templeton, J. L. *J. Am. Chem. Soc.* **2001,** *123*, 12724-12725.

40. Ritleng, V.; Sirlin, C.; Pfeffer, M. *Chem. Rev.* **2002,** *102*, 1731-1769.

41. Rothwell, I. P. *Polyhedron* **1985,** *4*, 177-200.

42. Shilov, A. E.; Shul'pin, G. B. *Chem. Rev.* **1997,** *97*, 2879-2932.

43. Arndt, S.; Spaniol, T. P.; Okuda, J. *Eur. J. Inorg. Chem.* **2001**, 73-75.

44. Bianchini, C.; Casares, J. A.; Osman, R.; Pattison, D. I.; Peruzzini, M.; Perutz, R. N.; Zanobini, F. *Organometallics* **1997,** *16*, 4611-4619.

45. Deelman, B. J.; Booij, M.; Meetsma, A.; Teuben, J. H.; Kooijman, H.; Spek, A. L. *Organometallics* **1995,** *14*, 2306-2317.

46. Dong, L. Z.; Duckett, S. B.; Ohman, K. F.; Jones, W. D. *J. Am. Chem. Soc.* **1992,** *114*, 151-160.

47. Eguillor, B.; Esteruelas, M. A.; Olivan, M.; Onate, E. *Organometallics* **2004,** *23*, 6015-6024.

48. Fujita, K.; Nakaguma, H.; Hamada, T.; Yamaguchi, R. *J. Am. Chem. Soc.* **2003,** *125*, 12368-12369.

49. Hong, P.; Cho, B. R.; Yamazaki, H. *Chem. Lett.* **1980**, 507-510.

50. Selnau, H. E.; Merola, J. S. *Organometallics* **1993,** *12*, 1583-1591.

51. Chantson, J. T.; Lotz, S. *J. Organomet. Chem.* **2004,** *689*, 1315-1324.

52. Morikita, T.; Hirano, M.; Sasaki, A.; Komiya, S. *Inorg. Chim. Acta* **1999,** *291*, 341-354.

53. Jones, W. D.; Dong, L. Z.; Myers, A. W. *Organometallics* **1995,** *14*, 855-861.

54. Ohno, H.; Miyamura, K.; Mizutani, T.; Kadoh, Y.; Takeoka, Y.; Hamaguchi, H.; Tanaka, T. *Chem. Eur. J.* **2005,** *11*, 3728-3741.

55. Lu, W. J.; Jia, C. G.; Kitamura, T.; Fujiwara, Y. *Org. Lett.* **2000,** *2*, 2927-2930.

56. Maruyama, O.; Yoshidomi, M.; Fujiwara, Y.; Taniguchi, H. *Chem. Lett.* **1979**, 1229-1230.

57. Ringelberg, S. N.; Mettsma, A.; Hessen, B.; Teuben, J. H. *J. Am. Chem. Soc.* **1999,** *121*, 6082-6083.

58. Ng, S. M.; Lam, W. H.; Mak, C. C.; Tsang, C. W.; Jia, G. C.; Lin, Z. Y.; Lau, C. P. *Organometallics* **2003,** *22*, 641-651.

59. Samat, A.; Salapala, J.; Guglielmetti, R.; Guerchais, J. *New J. Chem.* **1978,** *2*, 13-14.

60. Myers, A. W.; Jones, W. D. *Organometallics* **1996,** *15*, 2905-2917.

61. Arndtsen, B. A.; Bergman, R. G. *Science* **1995,** *270*, 1970-1973.

62. Burger, P.; Bergman, R. G. *J. Am. Chem. Soc.* **1993,** *115*, 10462-10463.

63. Matsumoto, T.; Periana, R. A.; Taube, D. J.; Yoshida, H. *J. Mol. Catal. A: Chem.* **2002,** *180*, 1-18.

64. Matsumoto, T.; Taube, D. J.; Periana, R. A.; Taube, H.; Yoshida, H. *J. Am. Chem. Soc.* **2000,** *122*, 7414-7415.

65. Periana, R. A.; Mirinov, O.; Taube, D. J.; Gamble, S. *Catal. Commun.* **2002**, 2376-2377.

66. Wong-Foy, A. G.; Bhalla, G.; Liu, X. Y.; Periana, R. A. *J. Am. Chem. Soc.* **2003,** *125*, 14292-14293.

67. Alaimo, P. J.; Bergman, R. G. *Organometallics* **1999,** *18*, 2707-2717.

68. Hinderling, C.; Feichtinger, D.; Plattner, D. A.; Chen, P. *J. Am. Chem. Soc.* **1997,** *119*, 10793-10804.

69. Strout, D. L.; Zaric, S.; Niu, S. Q.; Hall, M. B. *J. Am. Chem. Soc.* **1996,** *118*, 6068-6069.

70. Su, M. D.; Chu, S. Y. *J. Am. Chem. Soc.* **1997,** *119*, 5373-5383.

71. Tellers, D. M.; Yung, C. M.; Arndtsen, B. A.; Adamson, D. R.; Bergman, R. G. *J. Am. Chem. Soc.* **2002,**

124, 1400-1410.

72. Rothwell, I. P., *Selective Hydrocarbon Activation: Principles and Progress*. VCH Publishers: New York, 1990.

73. Thompson, J. S.; Harlow, R. L.; Whitney, J. F. *J. Am. Chem. Soc.* **1983,** *105*, 3522-3527.

74. Watson, P. L., *Selective Hydrocarbon Activation: Principles and Progress*. VCH Publishers: New York, 1990.

75. Hartwig, J. F.; Bhandari, S.; Rablen, P. R. *J. Am. Chem. Soc.* **1994,** *116*, 1839-1844.

76. Bergman, R. G.; Cundari, T. R.; Gillespie, A. M.; Gunnoe, T. B.; Harman, W. D.; Klinckman, T. R.; Temple, M. D.; White, D. P. *Organometallics* **2003,** *22*, 2331-2337.

77. Brooks, B. C.; Chin, R. M.; Harman, W. D. *Organometallics* **1998,** *17*, 4716-4723.

78. Friedman, L. A.; Harman, W. D. *J. Am. Chem. Soc.* **2001,** *123*, 8967-8973.

79. Gunnoe, T. B.; Sabat, M.; Harman, W. D. *J. Am. Chem. Soc.* **1998,** *120*, 8747-8754.

80. Barckholtz, C.; Barckholtz, T. A.; Hadad, C. M. *J. Am. Chem. Soc.* **1999,** *121*, 491-500.

81. Lam, W. H.; Jia, G. C.; Lin, Z. Y.; Lau, C. P.; Eisenstein, O. *Chem. Eur. J.* **2003,** *9*, 2775-2782.

82. Siegbahn, P. E. M.; Crabtree, R. H. *J. Am. Chem. Soc.* **1996,** *118*, 4442-4450.

83. Oxgaard, J.; Goddard, W. A. *J. Am. Chem. Soc.* **2004,** *126*, 442-443.

84. Oxgaard, J.; Muller, R. P.; Goddard, W. A.; Periana, R. A. *J. Am. Chem. Soc.* **2004,** *126*, 352-363.

85. Bulls, A. R.; Schaefer, W. P.; Serfas, M.; Bercaw, J. E. *Organometallics* **1987,** *6*, 1219-1226.

86. Chesnut, R. W.; Jacob, G. G.; Yu, J. S.; Fanwick, P. E.; Rothwell, I. P. *Organometallics* **1991,** *10*, 321-328.

87. Thompson, M. E.; Baxter, S. M.; Bulls, A. R.; Burger, B. J.; Nolan, M. C.; Santarsiero, B. D.; Schaefer, W. P.; Bercaw, J. E. *J. Am. Chem. Soc.* **1987,** *109*, 203-219.

88. Gupta, R. R.; Kumar, M.; Gupta, V., *Heterocyclic Chemistry: II: Five-Membered Heterocycles*. Springer: Berlin, 1999; Vol. 2.

89. Webster, C. E.; Fan, Y. B.; Hall, M. B.; Kunz, D.; Hartwig, J. F. *J. Am. Chem. Soc.* **2003,** *125*, 858-859.

90. Flood, T. C.; Janak, K. E.; Iimura, H.; Zhen, H. *J. Am. Chem. Soc.* **2000,** *122*, 6783-6784.

91. Jones, W. D.; Feher, F. J. *Acc. Chem. Res.* **1989,** *22*, 91-100.

92. Northcutt, T. O.; Wick, D. D.; Vetter, A. J.; Jones, W. D. *J. Am. Chem. Soc.* **2001,** *123*, 7257-7270.

93. Frisch, M. J.; Trucks, G. W.; Schlegel, H. B.; Scuseria, G. E.; Robb, M. A.; Cheeseman, J. R.; Zakrzewski, V. G.; Montgomery, J. A.; Stratmann, R. E.; Burant, J. C.; Dapprich, S.; Millam, J. M.; Daniels, A. D.; Kudin, K. N.; Strain, M. C.; Farkas, O.; Tomasi, J.; Barone, V.; Cossi, M.; Cammi, R.; Mennucci, B.; Pomelli, C.;

Adamo, C.; Clifford, S.; Ochterski, J.; Petersson, G. A.; Ayala, P. Y.; Cui, Q.; Morokuma, K.; Malick, D. K.; Rabuck, A. D.; Raghavachari, K.; Foresman, J. B.; Cioslowski, J.; Ortiz, J. V.; Baboul, A. G.; Stefanov, B. B.; Liu, G.; Liashenko, A.; Piskorz, P.; Komaromi, I.; Gomperts, R.; Martin, R. L.; Fox, D. J.; Keith, T.; Al-Laham, M. A.; Peng, C. Y.; Nanayakkara, A.; Challacombe, M.; Gill, P. M. W.; Johnson, B.; Chen, W.; Wong, M. W.; Andres, J. L.; Gonzalez, C.; Head-Gordon, M.; Replogle, E. S.; Pople, J. A. *Gaussian 98*, A.9; Gaussian Inc.: Pittsburgh, PA, 1998.

94. Becke, A. D. *J. Chem. Phys.* **1993,** *98*, 5648-5652.

95. Stevens, W. J.; Konowalow, D. D.; Ratcliff, L. B. *J. Chem. Phys.* **1984,** *80*, 1215-1224.

96. Stevens, W. J.; Krauss, M.; Basch, H.; Jasien, P. G. *Can. J. Chem./Rev. Can. Chim.* **1992,** *70*, 612-630.

97. Cundari, T. R.; Klinckman, T. R.; Wolczanski, P. T. *J. Am. Chem. Soc.* **2002,** *124*, 1481-1487.

98. Holland, P. L.; Cundari, T. R.; Perez, L. L.; Eckert, N. A.; Lachicotte, R. J. *J. Am. Chem. Soc.* **2002,** *124*, 14416-14424.

99. SMART, SAINT, and XPREP programs are part of Bruker AXS crystallographic software package for single-crystal data collection, reduction, and preparation. In.

100. Sheldrick, G. M. *SHELTXTL6.1, Crystallographic software package*, Bruker AXS, Inc.: Madison, WI, 2000.

101. *International Tables for X-ray Crystallography*. Kynoch Press: Birmingham, 1974; Vol. 4.

CHAPTER 3:
Ru^{II}-Mediated Carbon-Carbon Bond Formation between Acetonitrile and Pyrrole

3.1 Introduction

Pyrrole, first extracted from bone oil in 1857, is found incorporated into the architectures of porphyrins, chlorophylls, polymers, and naturally occurring antibiotics. The pyrrole subunit is incorporated into the structure of the only naturally occurring organometallic complex, Vitamin B_{12}.[1] Similar to that of furan and thiophene (discussed in Ch. 2), pyrrole is a 5-membered heteroaromatic molecule consisting of an N-H fragment incorporated into one of the ring positions (Figure 3.1). The ionization potential of pyrrole, -8.20 eV, is derived from the HOMO, Ψ_3.[2] Pyrrole has an intermediary resonance energy, 24 kcal/mol, relative to that of other 5-membered heteroaromatic molecules. This value lies directly between the value of furan (19 kcal/mol) and thiophene (29 kcal/mol) resonance energy values.[2]

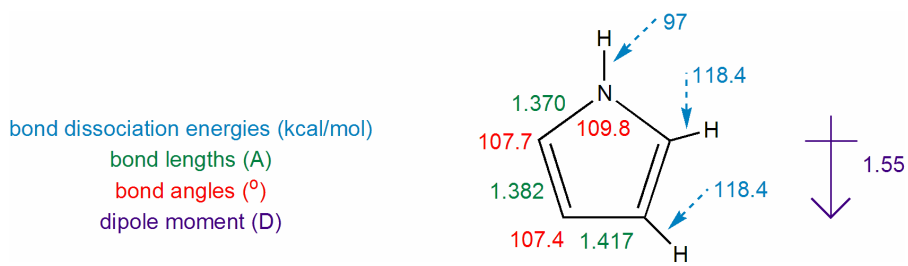

Figure 3.1. Bond dissociation energies[3], bond lengths[4], bond angles[4], and the dipole moment[1] of pyrrole.

The reactivity of pyrrole in electrophilic aromatic substitution is ~10^5 times faster than that of furan. This is counter-intuitive since the resonance energy of pyrrole is 5 kcal/mol higher than that of furan (19 kcal/mol).[2] This is likely due to the increased stabilization contributed by the carbenium-imminium mesomer (Figure 3.2). The unusual stabilization of this mesomer (Wheland intermediate) likely lowers the kinetic barrier (resulting from a lower $\Delta H^{\ddagger}$) thereby providing a more easily accessible kinetic pathway for these transformations. This lowering of the $\Delta H^{\ddagger}$ is likely due to the trivalent nature of the heteroatom. This increases the ability of the heteroatom to mesomerically distribute its electron density, relative to divalent furan or thiophene, into the 2 and 5-position. Evidence for this further stabilization can be explained by the additional

strength of π-donation from the nitrogen lone pair into the ring, with an overall dipole moment (1.55 D) that is opposite in direction from that of furan or thiophene (Figure 3.1).[1]

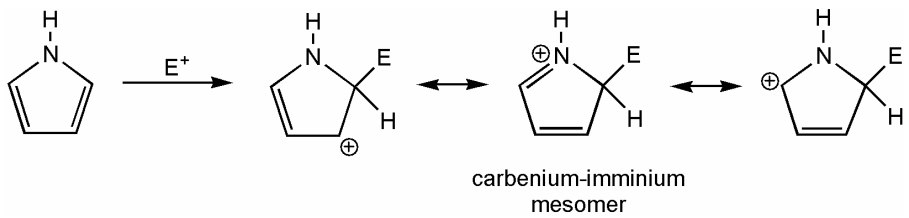

Figure 3.2. Resonance stabilization favors electrophilic attack at the 2-position.

There are two common binding modes for pyrrole with transition metals (Figure 3.3). The η^2-olefinic binding mode ($2e^-$ donor) of pyrrole is observed with electron rich Os^{II} systems.[5-8] For example, Taube et al. have shown that $(NH_3)_5Os(OTf)_3$ reacts with pyrrole in the presence of Mg metal to yield the complex $[(NH_3)_5Os(\eta^2\text{-2,3-pyrrolyl})](OTf)_2$.[5] This complex was also observed, at low temperatures, to undergo isomerization to the $[(NH_3)_5Os(\eta^2\text{-3,4-pyrrolyl})](OTf)_2$ tautomer. In this coordination mode, the pyrrole donates $2e^-$ to the metal center. There is also precedent for η^5-binding of pyrrole. For example, Dotzauer and coworkers have isolated $(\eta^5\text{-}C_5H_5N)Cr(CO)_3$.[9]

Net removal of a proton from pyrrole yields pyrrolyl, which can coordinate to metal centers in several different modes (Figure 3.3). For example, η^1, η^3, and η^5-pyrrolyl complexes have been observed. Heenan and coworkers have shown that photo-induced linkage isomerism occurs upon binding of CO to $(\eta^5\text{-}C_5H_5)Fe(\eta^5\text{-}C_4H_4N)$ yielding the intermediate mode $\eta^3\text{-}C_\alpha,C_\beta,C_\beta\text{-}C_4H_4N$ *or* $\eta^3\text{-}N,C_\alpha,C_\beta\text{-}C_4H_4N$ before binding a second equivalent of CO to generate the $(\eta^5\text{-}C_5H_5)Fe(CO)_2(\eta^1\text{-}N\text{-}C_4H_4N)$ product.[10] DFT calculations have also been pursued to understand the potential role of pyrrolyl coordinative isomerization in catalyzed processes.[11] The 2-pyrrolyl species has been isolated as well but it should be mentioned that these systems are very rare.[12, 13]

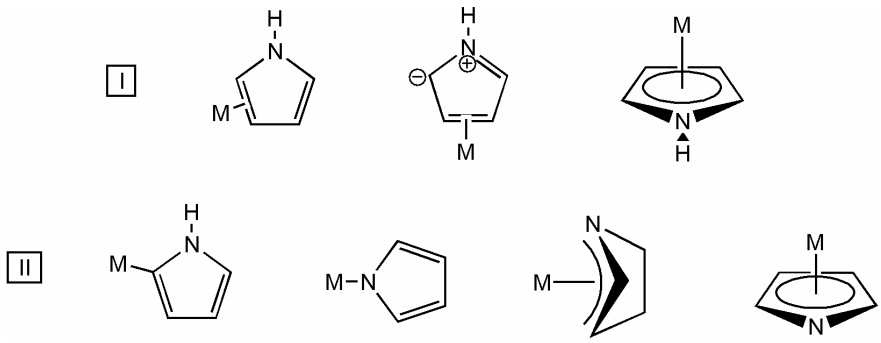

Figure. 3.3. Binding modes of pyrrole (I) and pyrrolyl (II).

Due to our group's recent progress on C-H activation of five-membered heteroaromatic compounds (i.e., furan and thiophene), we sought to extend this chemistry to pyrrole. Reactivity is expected to be more complex due to the existence of a heteroatom-hydrogen bond. With the incorporation of this weaker and more acidic bond (Figure 3.1), it was of interest to discern regioselectivity of aryl bond activation.

Late transition metal complexes have been demonstrated to activate pyrrole via C-H or N-H bond cleavage. Regioselective C-H activation rarely competes w/ N-H activation. In general, pyrrole activation reactions are most common for late transition metal complexes that initiate oxidative addition. For example, Ir^{I} dimers, $[(COD)Ir(X)]_2$ (X = Cl or OMe), have been proposed to be the precursors for the monomeric Ir^{III} species Ir^{III}(trisboryl) that forms upon reaction of the Ir^{I} dimer with pin_2B_2 (pin_2B_2, pin = $Me_4C_2O_2$). This enables the cleavage of C_α-H bonds of pyrrole and form C_α-B bonds.[14, 15] It is hypothesized that this reactivity involves an oxidative addition of a pyrrole C-H bond by the Ir^{III} intermediate resulting in the (trisboryl)Ir^{V}(2-pyrrolyl)(H) intermediate.[14] More well-defined examples have been observed by Komiya et al. whereby the oxidative addition products have been fully characterized showing preference for the N-H activated product $L_nM(H)$(*N*-pyrrolyl) (M = Ru or Fe).[16, 17] Photolysis has also been shown to drive the oxidative addition of C-H bonds of pyrrole across late transition metal center.[18] Oxidative addition of C-H and N-H bonds have also been observed by reacting pyrrole with the trimer $Os_3(CO)_{12}$. Several products were formed from these thermolytic reactions whereby C-H bond cleavage was achieved at the 2- and 3-position as well as the N-H position.[19, 20] High oxidation state early transition metal systems have been observed to cleave the N-H bond of pyrrole via a σ-bond metathesis mechanism.[21] Lastly, our own group has recently reported the reaction of (IPr)CuMe {IPr =

1,3-bis(2,6-diisopropylphenyl)imidizol-2-ylidene} with pyrrole to give the products (IPr)Cu(*N*-pyrrolyl) and methane.[22]

N-H activation can be preferred over C-H activation at the 2-position of pyrrole when the 2,5-positions are blocked by alkyl substituents.[23] Similarly, the methyl appendage of *N*-methylpyrrole directs C-H activation to the 2-position of *N*-methylpyrrole.[23] Dimers have also been shown to C-H activate *N*-methylpyrrole at the 2-position forming the product $[Cp^*Ir(H)(2\text{-}N(Me)C_4H_3)](\mu\text{-}H)_2[Cp^*Ir]$ where the $2\text{-}N(Me)C_4H_3$ fragment is η^2-coordinated through the 2,3-positions to the distal Ir center.[24] Hung and coworkers have observed the C-H activation at the 3-position of pyrrole, the most rare form of bond activation in pyrrole, by Mn porphyrins $(NCPP)Mn^{II}Br$ (NCPP = *N*-confused phenyl porphyrins).[25]

In rare examples of catalytic C-H bond activation of pyrrole, Fujiwara et al. have demonstrated that pyrrole and phenylpropiolate convert to ethyl (2Z)-3-(2-pyrryl)-phenylpropenoate in the presence of $Pd(OAc)_2$.[26]

Our group has reported the utilization of Ru^{II} complexes for the catalytic hydroarylation of olefins.[27-29] For example, TpRu(CO)(NCMe)Ph (Tp = hydridotris(pyrazolyl)borate) catalyzes the addition of arene C-H bonds across the carbon-carbon bonds of ethylene and α-olefins, and heteroaryl systems of the type TpRu(CO)(NCMe)Ar {Ar = 2-furyl (**2**) or 2-thienyl (**3**)} catalyze the regioselective addition of furan or thiophene 2-position C-H bonds across the carbon-carbon bond of ethylene. Mechanistic studies of these Ru^{II}-catalyzed olefin hydroarylation transformations provide evidence for catalytic cycles that proceed through olefin coordination and insertion into metal-aryl bonds, followed by a metal-mediated C-H bond activation to release organic product and reintroduce a metal-aryl bond.[28]

Herein, we report on the stoichiometric reaction of TpRu(CO)(NCMe)Me (**1**) with pyrrole to form a product that contains an *N*-pyrrolyl ligand with a pendant imine group that is chelated to Ru. The overall reaction involves cleavage of pyrrole N-H and C-H bonds and C-C bond formation with the acetonitrile ligand of **1**. Combined experimental and computational studies reported herein indicate that the transformation likely occurs through initial metal-mediated N-H activation.

3.2 Results and Discussion

Upon heating the Ru^{II} methyl complex TpRu(CO)(NCMe)Me (**1**) to 90 ^{o}C in neat pyrrole the metallacycle TpRu(CO){κ^2-*N*,*N*-(H)N=C(CH_3)(NC_4H_3)} (**7**) is produced after 2 h (Scheme 3.1). Analysis of the crude reaction mixture by ^{1}H NMR spectroscopy reveals that complex **7** is the only observable TpRu species produced. Complex **7** was isolated in 45% yield after workup and IR spectroscopy reveals ν_{CO} = 1948 cm^{-1}. Resonances due to three pyrrolyl hydrogen atoms (6.82, 6.77, and 6.09 ppm) and a broad singlet due to the Ru-coordinated imine NH group at 8.45 ppm are observed in the ^{1}H NMR spectrum (Figure 3.4). The complex was also examined by ^{13}C NMR (Figure 3.5). Furthermore, a single-crystal X-ray diffraction study has confirmed the identity of **7** (Figure 3.6 and Table 3.1). The structure reveals a five-membered metallacycle that incorporates the former pyrrole and acetonitrile substrates. The Ru1-N2 bond distance of the imine group is statistically identical to the Ru1-N1 bond distance to the *N*-pyrrolyl moiety {2.070(2) versus 2.073(2) Å}. A closely related $CpRu^{II}$ (Cp = cyclopentadienyl) complex has a Ru-$N_{pyrrolyl}$ bond distance of 2.056(11) Å and a Ru-N_{imine} bond distance of 2.127(11) Å, while an analogous (η^6-C_6H_6)Ru^{II} system has Ru-$N_{pyrrolyl}$ and Ru-N_{imine} bond distances of 2.037(6) and 2.101(5) Å, respectively.[30, 31]

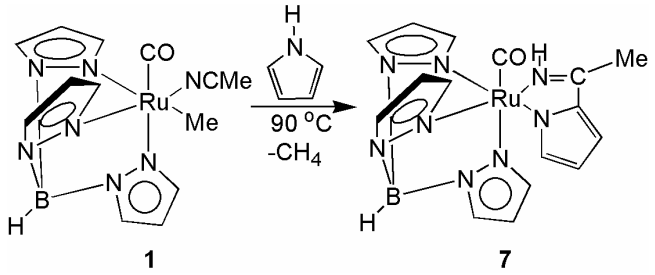

Scheme 3.1. Reaction of TpRu(CO)(NCMe)(Me) (**1**) with pyrrole yields TpRu(CO){κ^2-*N*,*N*-(H)N=C(CH_3)(NC_4H_3)} (**7**).

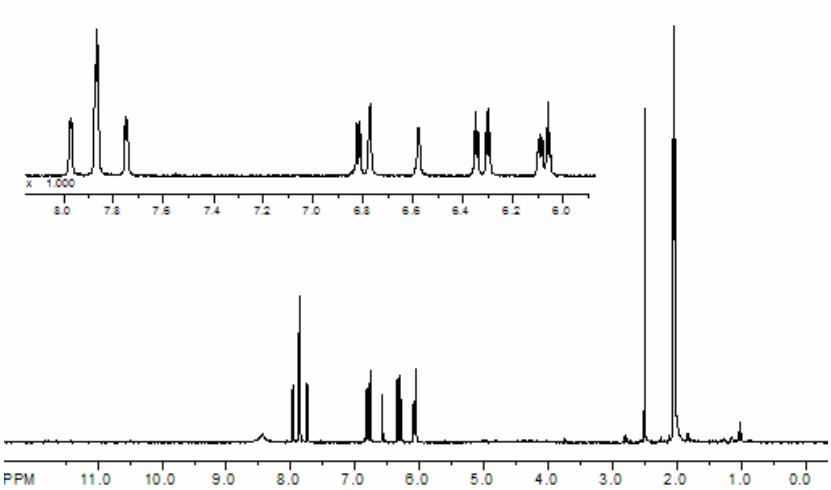

Figure 3.4. ^{1}H NMR spectrum of TpRu(CO){κ^{2}-*N*,*N*-(H)N=C(CH_3)(NC_4H_3)} (**7**) in acetone-d_6.

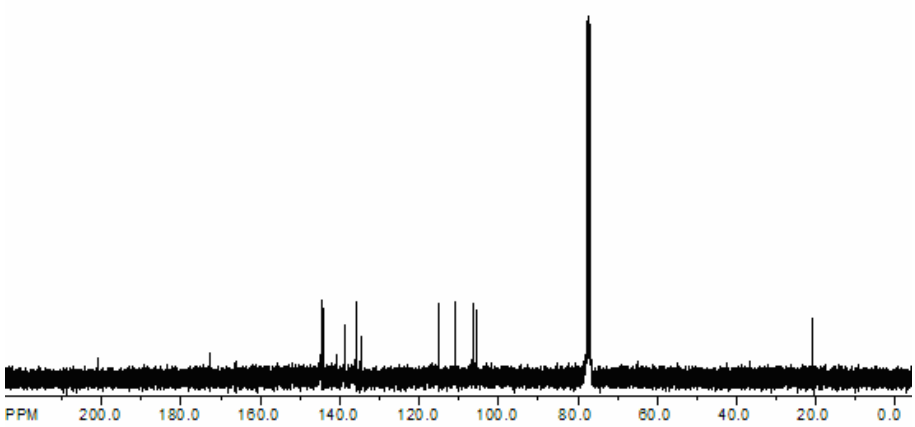

Figure 3.5. ^{13}C NMR spectrum of TpRu(CO){κ^{2}-*N*,*N*-(H)N=C(CH_3)(NC_4H_3)} (**7**) in $CDCl_3$.

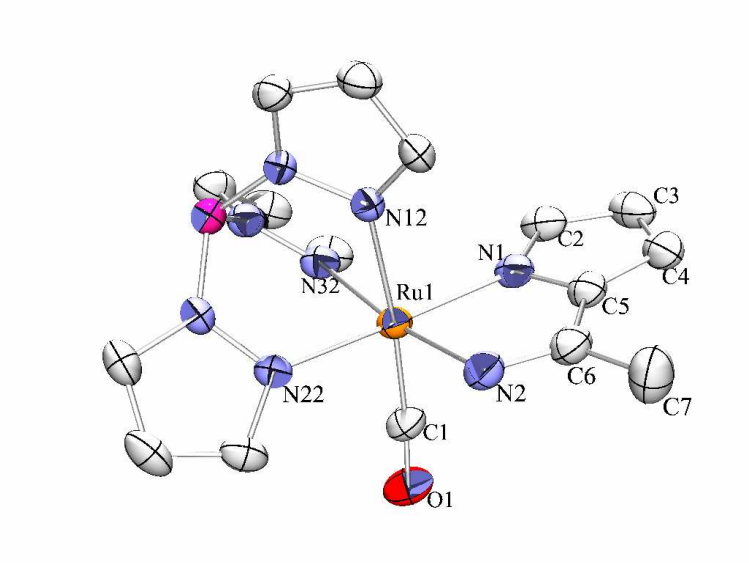

Figure 3.6. ORTEP of TpRu(CO){κ^2-*N*,*N*-(H)N=C(CH_3)(NC_4H_3)} (**7**) (30% probability). Selected bond distances (Å): Ru1-C1 1.831(3), Ru1-N1 2.073(2), Ru1-N2 2.070(2), N1-C5 1.377(3), N1-C2 1.348(3), N2-C6 1.297(3), C5-C6 1.435(4), C4-C5 1.403(4), C2-C3 1.399(4), C3-C4 1.375(4). Selected bond angles (deg): Ru1-N2-C6 117.6(2), Ru1-N1-C5 113.8(2), Ru1-N1-C2 139.4(2), N1-C5-C6 116.0(2), N2-C6-C7 123.6(3), N2-C6-C5 115.2(2), Ru1-C1-O1 174.3(2), N2-Ru1-N1 77.44(9), N22-Ru1-N32 87.38(8), N12-Ru1-N22 83.47(7), N32-Ru1-N12 86.36(8), N32-Ru1-N2 171.91(8), N22-Ru1-N1 172.54(8), N12-Ru1-C1 174.06(9).

Table 3.1. Selected crystallographic data and collection parameters for TpRu(CO){κ^2-*N*,*N*-(H)N=C(CH_3)(NC_4H_3)} (**7**) and TpRu(CO)(NCMe)(*N*-pyrrolyl) (**8**).

	TpRu(CO){κ^2-*N*,*N*-(H)N=C(CH_3)(NC_4H_3)} (**7**)	TpRu(CO)(NCMe)(*N*-pyrrolyl) (**8**)
emperical formula	$C_{16}H_{17}BNORu$	$C_{16}H_{17}BN_8ORu$
fw	449.26	449.26
cryst syst	monoclinic	monoclinic
space group	$P2_1/c$	$P2_1/n$
a, Å	7.8719(6)	10.413(2)
b, Å	17.595(1)	12.170(2)
c, Å	13.497(1)	15.495(3)
α, deg	90	90
β, deg	96.007(1)	106.195(3)
γ, deg	90	90
V (Å)	1859.1(3)	1885.7(6)
Z	4	4
D_{calcd}, g cm^{-3}	1.605	1.582
R1, wR2 (I > 2σ(I))	0.0404, 0.0842	0.0478, 0.0998
GOF	0.963	1.022

Regardless of the specific mechanism, the production of **7** occurs through C-C bond formation between pyrrole and the nitrile ligand of **1** and is accompanied by release of CH_4. Methane production has been detected by ^{1}H NMR spectroscopy in sealed tubes as well as by analysis of the reaction headspace using GC-MS. We have previously demonstrated that complex **1** reacts with benzene, furan, or thiophene to produce methane and TpRu(CO)(NCMe)Ph, TpRu(CO)(NCMe)(2-furyl) (**2**), or TpRu(CO)(NCMe)(2-thienyl) (**3**), respectively, and these reactions likely occur through metal-mediated C-H activation.[27-29] For the transformation of **1** and pyrrole to produce complex **7**, we have considered two possible reaction pathways that are differentiated by initial metal-mediated N-H versus C-H activation (Scheme 3.2). In the top pathway of Scheme 3.2, initial N-H activation of pyrrole produces methane and the *N*-pyrrolyl complex TpRu(CO)(NCMe)(*N*-pyrrolyl) (**8**). Subsequent intramolecular C-C bond formation followed by proton transfer would produce complex **7**. Alternatively, initial C-H bond activation at the 2-position of pyrrole would produce the 2-pyrrolyl complex TpRu(CO)(NCMe)(2-pyrrolyl) (the lower pathway of Scheme 3.2). For the latter reaction pathway, insertion of the acetonitrile ligand into the Ru-2-pyrrolyl bond followed by proton transfer would complete the formation of complex **7**. The insertion of coordinated NCMe into a M-$C_{alkyl/aryl}$ (M = d-block metal) bond is not common; however, there is precedence for this reactivity.[32-38] This insertion is most common for early transition metal systems. For example, the first example of this type of insertion was observed for the [Cp*$_2$ScMe] reacting with free N≡CR (R = Me, ^{t}Bu, or C(H)=CH_2) to yield the products [Cp*$_2$Sc{N=C(Me)R}].[33]

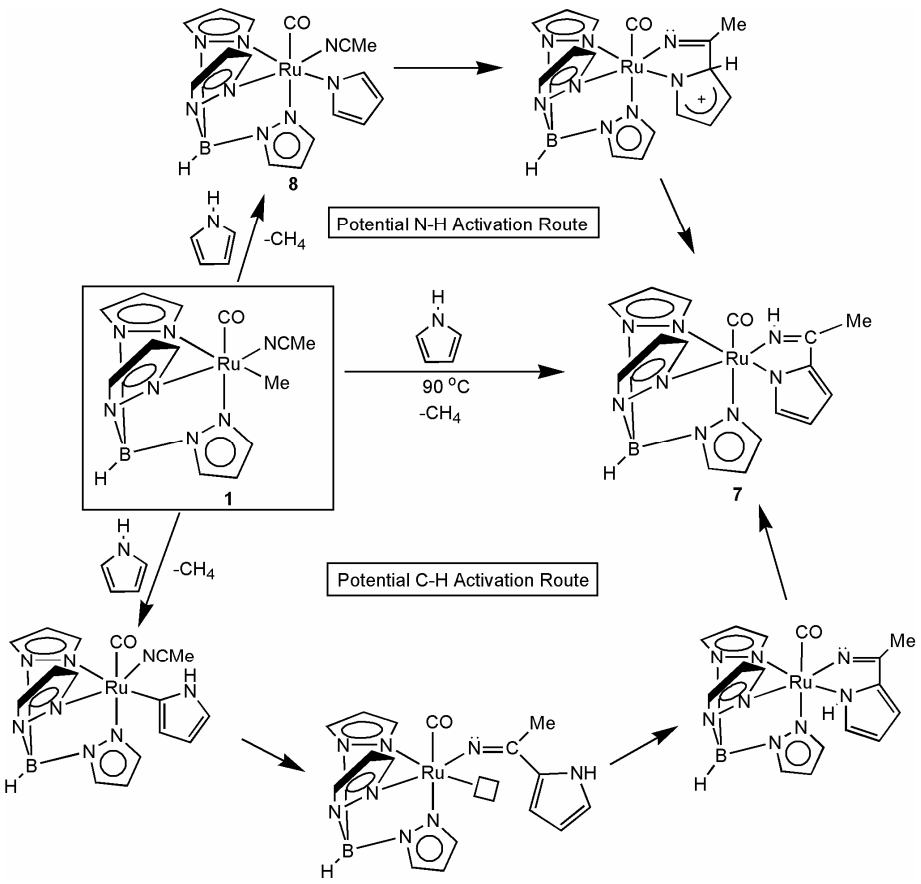

Scheme 3.2. Two possible pathways for the conversion of TpRu(CO)(NCMe)Me (**1**) and pyrrole to TpRu(CO){κ^2-*N*,*N*-(H)N=C(CH_3)(NC_4H_3)} (**7**).

We attempted to use isotopic labeling of pyrrole to probe the likely reaction pathway. In a control experiment, the reaction of **1** with pyrrole-d_5 leads to the production of CH_3D, confirmed through analysis of the reaction headspace using GC-MS as well as ^{1}H NMR spectroscopy (Scheme 3.3). In addition, the ^{1}H NMR spectrum of the product from this reaction revealed deuterium incorporation into the *N*-pyrrolyl ligand (Figure 3.7) and at the imine position to produce **7**-d_4. The treatment of **7**-d_4 with H_2O at 70 ^{o}C results in H/D exchange to produce complex **7**-d_3 with hydrogen incorporated at the imine position, as determined by ^{1}H NMR spectroscopy. This process is reversible, as indicated by the disappearance of the resonance due to the imine hydrogen (^{1}H NMR spectroscopy) upon heating **7**-d_3 in CD_3CN with added D_2O (Scheme 3.3).

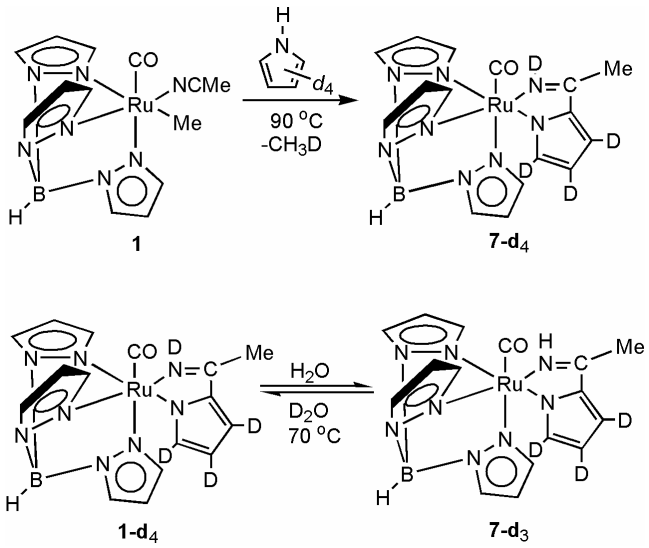

Scheme 3.3. Reactivity of TpRu(CO)(NCMe)Me (**1**) with d_5-pyrrole yields TpRu(CO){κ^2-*N*,*N*-(D)N=C(CH_3)(NC_4D_3)} (**7**-d_4) and the observed isotopic exchange between TpRu(CO){κ^2-*N*,*N*-(D)N=C(CH_3)(NC_4D_3)} (**7**-d_4) and TpRu(CO){κ^2-*N*,*N*-(H)N=C(CH_3)(NC_4D_3)} (**7**-d_3) with water and heavy water.

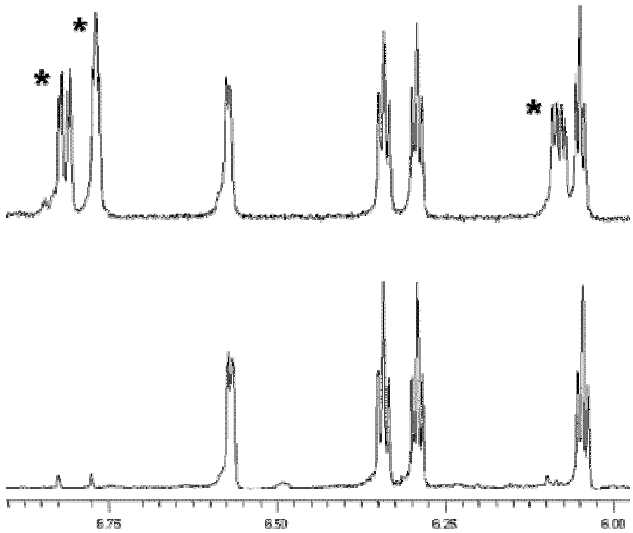

Figure 3.7. (Top) ^{1}H NMR spectrum of complex **7** in the aromatic region that includes resonances due to the *N*-pyrrolyl ligand (resonances due to *N*-pyrrolyl ligand are labeled with *). (Bottom) ^{1}H NMR spectrum of complex **7**-d_4, produced by reaction of **1** with pyrrole-d_5, that demonstrates a decrease in intensity for the resonances due to the *N*-pyrrolyl ligand.

In contrast to the reaction with pyrrole-d_5, the reaction of **1** with *N*-d_1-pyrrole (DNC_4H_4, > 90% deuterium incorporation) results in the production of complex **7** and CH_4 without observation of substantial

quantities of CH_3D (Scheme 3.4). This result is consistent with a reaction mechanism that involves initial metal-mediated C-H bond activation at the 2-position of pyrrole to produce an intermediate Ru^{II} 2-pyrrolyl complex; however, GC-MS of the *N*-d_1-pyrrole solution before and after reaction indicates at least 30% H/D scrambling occurs during the course of the reaction. In addition, ^{1}H NMR spectroscopy of the reaction products indicates the incorporation of hydrogen at the imine position, and this observation is inconsistent with initial metal-mediated C-H activation at the 2-position of pyrrole (determination of the extent of H incorporation is complicated by line broadening due to the quadrapolar N). Thus, due to isotopic scrambling, reliable conclusions about the mechanism are impossible based on these experiments.

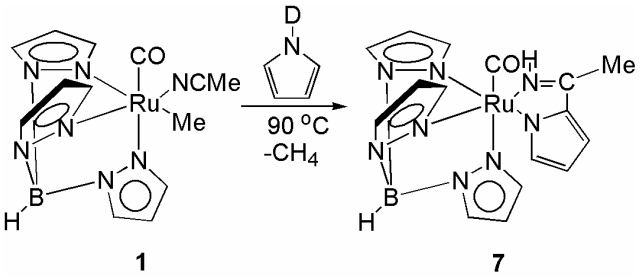

Scheme 3.4. Reaction of *N*-d_1-pyrrole with TpRu(CO)(NCMe)Me (**1**) yields TpRu(CO){κ^2-*N*,*N*-(H)N=C(CH_3)(NC_4H_3)} (**7**).

The triflate complex TpRu(CO)(NCMe)(OTf) (**9**) (OTf = trifluoromethanesulfonate) is prepared upon reaction of the previously reported complex TpRu(CO)(NCMe)Cl with AgOTf,[39] and the reaction of **9** with [Li][NC_4H_4] produces TpRu(CO)(NCMe)(*N*-pyrrolyl) (**8**) (Scheme 3.5). The *N*-pyrrolyl complex **8** has been characterized by IR (ν_{CO} = 1961 cm^{-1}), ^{1}H and ^{13}C NMR spectroscopy (Figures 3.8 and 3.9), and a single-crystal X-ray diffraction study. ^{1}H NMR spectroscopy reveals multiplets integrating for 2H each at 6.36 and 6.16 ppm due to the 2- and 3-position hydrogen atoms of the *N*-pyrrolyl ligand, respectively. Additional evidence of the identity of **3** is derived from its reaction with HCl at -78 ^{o}C to produce free pyrrole and the previously reported complex TpRu(CO)(NCMe)Cl (Scheme 3.6).[28] An X-ray diffraction study of a single crystal of **8** reveals its structure as a monomeric Ru^{II} *N*-pyrrolyl complex (Table 3.1 and Figure 3.10). The Ru-$N_{pyrrolyl}$ bond distance of 2.083(4) Å is shorter than the corresponding bond distance {2.153(6) Å} of Ru(1,5-η^5-C_8H_{11})(*N*-pyrrolyl)(PEt_3)$_2$.[16]

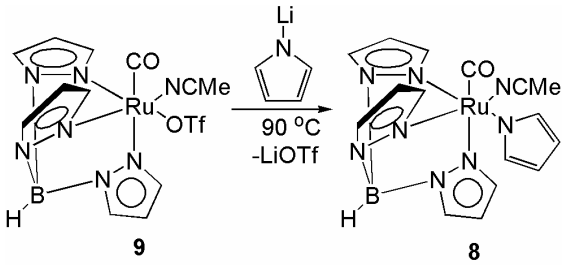

Scheme 3.5. Reaction of *N*-lithiumpyrrolyl with TpRu(CO)(NCMe)(OTf) (**9**) yields TpRu(CO)(NCMe)(*N*-pyrrolyl) (**8**).

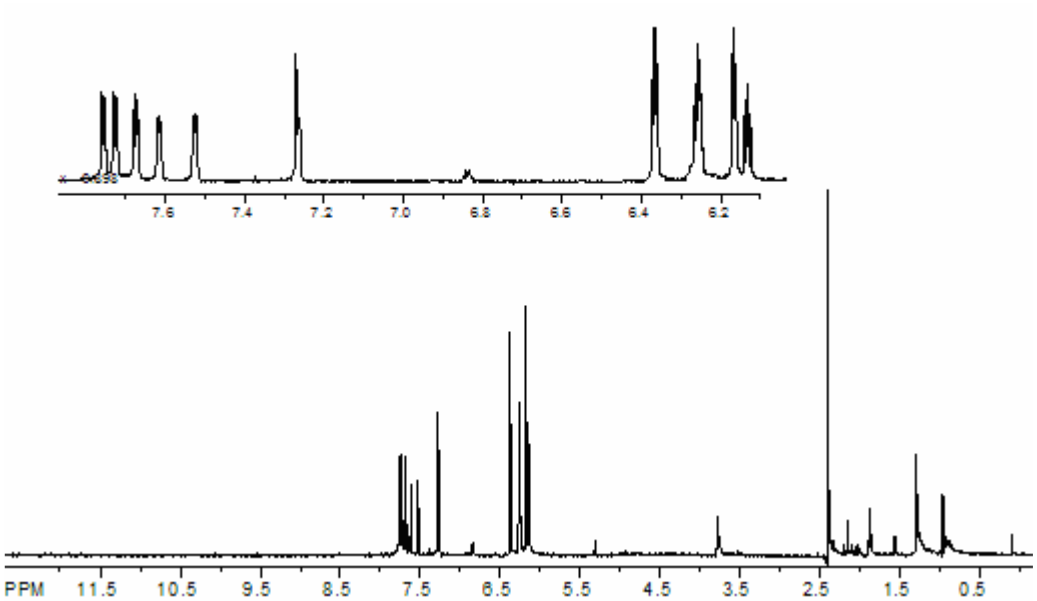

Figure 3.8. ^{1}H NMR spectrum of TpRu(CO)(NCMe)(*N*-pyrrolyl) (**8**) in $CDCl_3$.

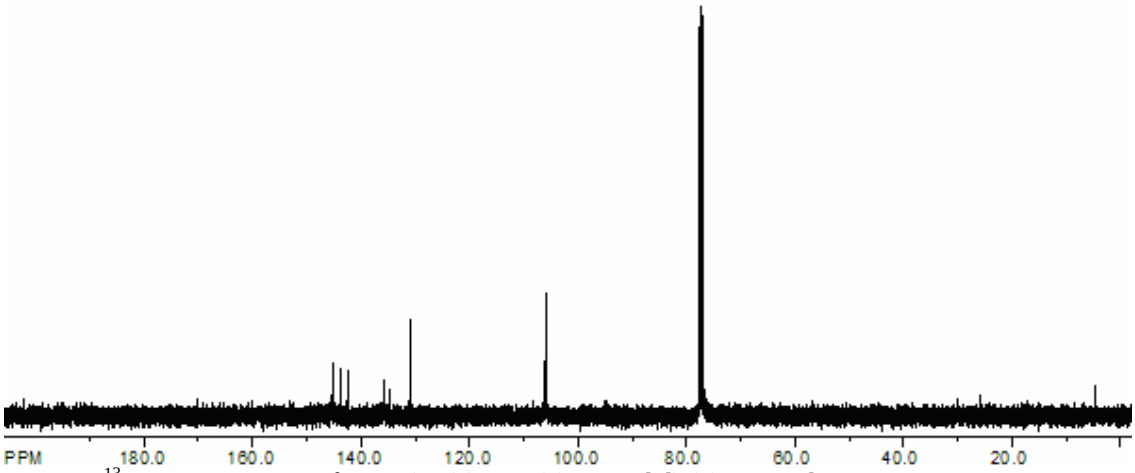

Figure 3.9. ^{13}C NMR spectrum of TpRu(CO)(NCMe)(*N*-pyrrolyl) (**8**) in $CDCl_3$.

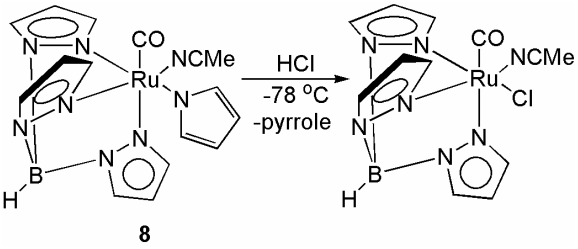

Scheme 3.6. Reaction of HCl with TpRu(CO)(NCMe)(*N*-pyrrolyl) (**8**) yields TpRu(CO)(NCMe)Cl.

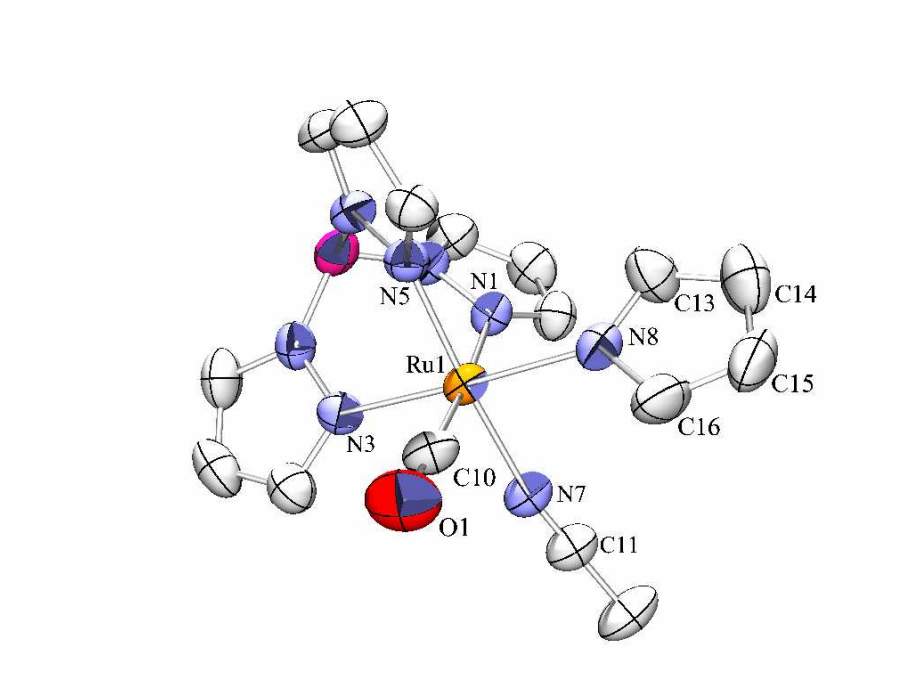

Figure 3.10. ORTEP of TpRu(CO)(NCMe)(*N*-pyrrolyl) (**8**) (30% probability). Selected bond distances (Å): Ru1-N8 2.083(4), N8-C16 1.357(7), N8-C13 1.361(7), C13-C14 1.364(8), C14-C15 1.379(8), C15-C16 1.362(8), Ru1-C10 1.836(6), C10-O1 1.140(6), Ru1-N7 2.038(4), N7-C11 1.127(6). Selected bond angles (deg): C10-Ru1-N8 94.5(2), N7-Ru1-N8 86.6(2), N5-Ru1-N8 91.8(2), N8-Ru1-N1 90.6(2), C16-N8-Ru1 127.5(4), C16-N8-C13 104.4(5), C13-N8-Ru1 127.2(4).

Reports of 2-pyrrolyl complexes are rare,[13, 40] and efforts to synthesize and isolate the 2-pyrrolyl complex TpRu(CO)(NCMe)(2-pyrrolyl) did not yield clean, isolable products. For example, heating solutions of TpRu(CO)(NCMe)Cl or **9** with Hg(2-pyrrolyl)Cl did not yield new products. Considering the possibility that the coordinating ability of chloride or OTf might be problematic, we converted **9** to

[TpRu(CO)(NCMe)(THF)][BAr'$_4$] (**10**) upon reaction with NaBAr'$_4$ (Ar' = 2,6-$(CF_3)_2C_6H_3$) in THF (Scheme 3.7); however, the reaction of complex **10** with Hg(2-pyrrolyl)Cl under various conditions did not yield clean and isolable products (complex **8** was not observed in these reactions). A single crystal X-ray diffraction study was achieved to further characterize **10** (Figure 3.11 and Table 3.2). There was ambiguity in the crystal structure in that both the [TpRu(CO)(NCMe)(THF)][BAr'$_4$] and [TpRu(CO)$(NCMe)_2$][BAr'$_4$] were observed.

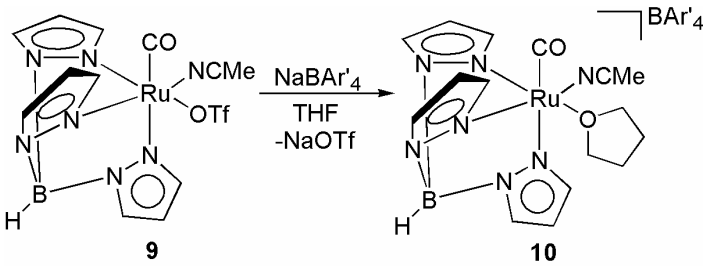

Scheme 3.7. Reaction of TpRu(CO)(NCMe)(OTf) (**9**) with NaBAr′$_4$ in THF yields [TpRu(CO)(NCMe)(THF)]BAr′$_4$ (**10**).

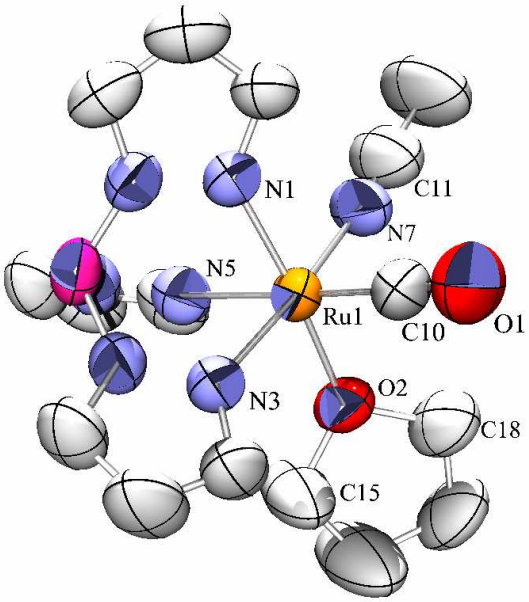

Figure 3.12. ORTEP of TpRu(CO)(NCMe)(THF)]BAr′$_4$ (**10**) (30% probability). Selected bond distances (Å): Ru1-C10 1.849(3), C10-O1 1.146(4), Ru1-N7 2.048(2), N7-C11 1.364(8), Ru1-O2 2.164(4), O2-C15 1.467(7), O2-C18 1.482(7). Selected bond angles (deg): C10-Ru1-O2 99.5(2), C10-Ru1-N7 92.4(1), N7-Ru1-O2 86.8(1), O2-Ru1-N3 94.7(1), O2-Ru1-N5 83.9(1), C15-O2-C18 106.7(5).

Table 3.2. Selected crystallographic data and collection parameters for [TpRu(CO)(NCMe)L]BAr′$_4$ (L = THF or NCMe) (**10**).

	[TpRu(CO)(NCMe)L]BAr'$_4$ (L = THF or NCMe) (**10**)
emperical formula	$C_{46.88}H_{30.25}B_2F_{24}N_{7.50}O_{1.50}Ru$
fw	1301.23
cryst syst	orthorhombic
space group	Pbca
a, Å	24.0840(1)
b, Å	18.3730(1)
c, Å	25.4220(1)
α, deg	90
β, deg	90
γ, deg	90
V (Å)	11249(1)
Z	8
D_{calcd}, g cm^{-3}	1.537
R1, wR2 (I > 2σ(I))	0.0544, 0.1230
GOF	0.995

TpRu(CO)(*N*-pyrrolyl)(NCMe) (**8**) is the species that would result from metal-mediated N-H activation of pyrrole by complex **1** (see the upper portion of Scheme 3.2). Thus, if the formation of **7** from the reaction of **1** and pyrrole proceeds through initial metal-mediated N-H activation, it is anticipated that upon heating to 90 ^{o}C complex **8** should convert to complex **7**. Heating **8** (90 ^{o}C) in neat CD_3CN results in the formation of **7**, with the rate of the transformation of **8** to **7** increasing upon addition of free pyrrole. For example, a plot of k_{obs} versus equivalents of pyrrole (based on **8**) using 0, 6, 10, and 22 equiv of pyrrole reveals a linear relationship (Figure 3.13). The kinetic experiments were performed at 90 ^{o}C in CD_3CN. These data suggest that free pyrrole potentially serves as a catalyst for the transformation of **8** to **7**. Suspecting that free pyrrole may function as a base to promote proton transfer from the 2-position C-H bond of the *N*-pyrrolyl ligand to the acetonitrile nitrogen, we studied the effect of adding the non-coordinating base 2,6-lutidine. In the absence of 2,6-lutidine, the conversion of **8** to **7** (90 ^{o}C in CD_3CN) occurs with $k_{obs} = 9.7 \times 10^{-7}$ s^{-1}, while the addition of 6 equiv (based on **8**) of 2,6-lutidine increases k_{obs} by a factor of approximately 2.5 ($k_{obs} = 2.5 \times 10^{-6}$ s^{-1}). Pyrrole is a weak base (pK_a = -3.80, in DMSO; 2*H*-pyrrolium cation) but can be protonated at all positions (Scheme 3.8).[4] Protio exchange occurs at the highest rates at the 1-position (at the nitrogen) but is most

thermodynamically stable at the 2-position.[4] It might be expected that to complete the pyrrole promoted shuttling of the proton to the imine position of product **7**, pyrrole is protonated at the 2-position.

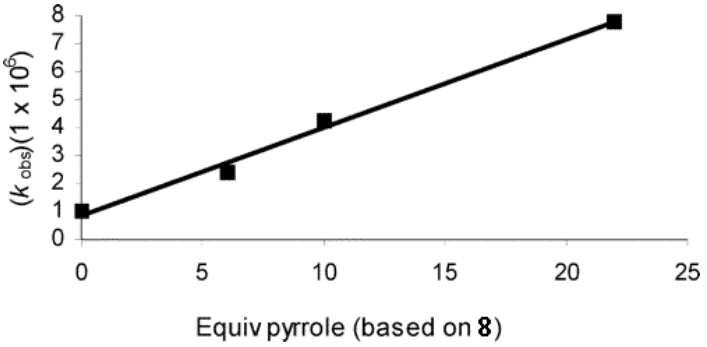

Figure 3.13. Plot of k_{obs} versus equivalents of pyrrole (based on **8**) for the conversion of complex **8** to complex **7**. Reactions were monitored in CD_3CN at 90 °C.

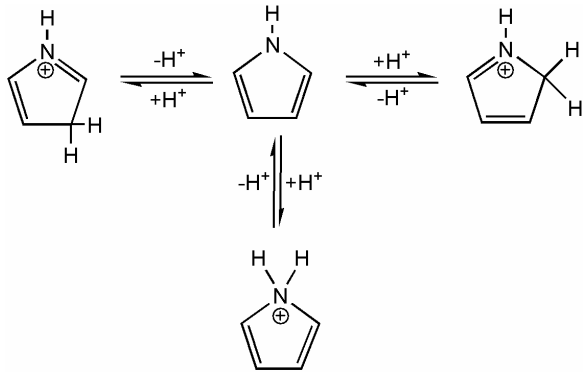

Scheme 3.8. Protonation of pyrrole at the 1-, 2-, and 3-position.

We have previously reported that the rate of conversion of complex **1** and benzene to methane and TpRu(CO)(NCMe)R is suppressed by the presence of free acetonitrile,[29] and these results have been interpreted to indicate a reaction pathway that involves the formation of the five-coordinate system {TpRu(CO)R}, which initiates benzene C-H activation. Kinetic experiments were performed to determine if a similar reaction pathway (i.e., metal-mediated N-H or C-H bond activation by a five-coordinate Ru^{II} system) is likely for the conversion of **1** and pyrrole to complex **7**. These experiments revealed that the addition of acetonitrile does suppress the rate of disappearance of **1**. For example, for the formation of **7** at 75 °C, the rate of disappearance

of **1** (first-order process, see Figure 3.14) in the absence of added acetonitrile proceeds with a half-life of approximately 340 min {k_{obs} = 4.0(8) × 10^{-5} s^{-1}}, while the addition of 30 equiv of acetonitrile increases the half-life to approximately 502 min {k_{obs} = 2.2(1) × 10^{-5} s^{-1}}. The rate equation for the nucleophilic addition of free pyrrole to the NCMe ligand of complex **1** (Scheme 3.9) reveals that this transformation would not be dependent on the concentration of free NCMe. Nucleophilic additions to coordinated nitriles leading to the formation of azavinylidines have been reported.[41] For example, Templeton et al. have reported the formation of several azavinylidine complexes from the reaction of Tp*W(CO)$_2$(NCR) (Tp* = (3,5-dimethyl)hydridotris(pyrazolyl)borate; R = Me or Ph) with various nucleophiles (Nu = H, Et, or MeO).[42] Alternatively, if the mechanism for formation of **7** involves a dissociative mechanism, whereby a reactive {TpRu(CO)Me} species is formed, applying the steady-state approximation the rate law (Scheme 3.9) reveals an inverse first-order dependence on [NCMe]. With an observed inverse first-order dependence on concentration of free NCMe, it was concluded that NCMe dissociation is likely required for the formation of **7**.

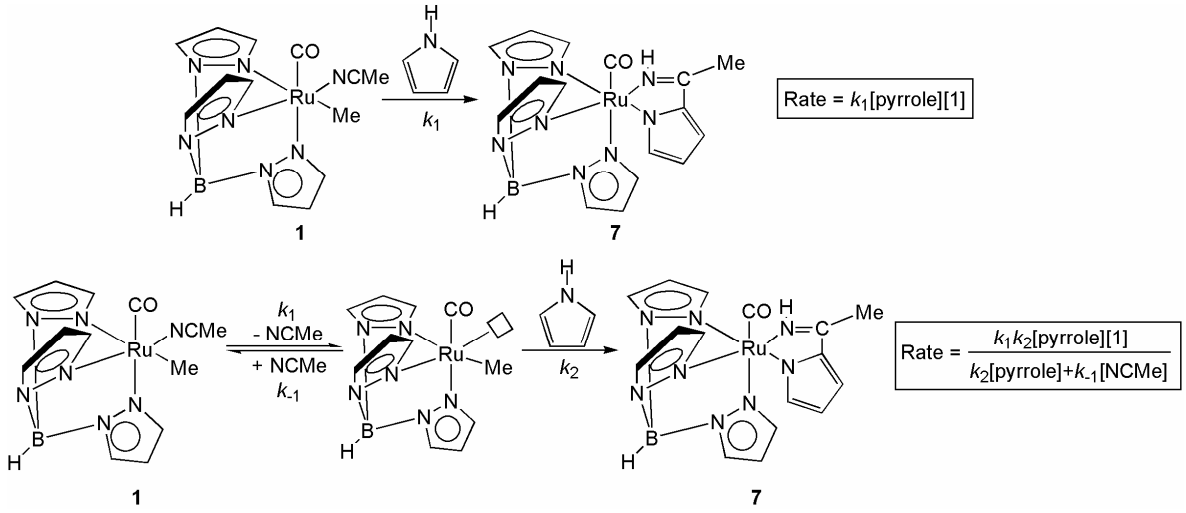

Scheme 3.9. Rate laws for nucleophilic addition of pyrrole and dissociative mechanisms.

*Importantly, monitoring the transformation of **1** and pyrrole to **7** by ^{1}H NMR spectroscopy reveals that the N-pyrrolyl complex **8** is an intermediate in this transformation* (Figure 3.15). Resonances due to **8** are clearly observed by ^{1}H NMR spectroscopy during the conversion of **1** and pyrrole to complex **7**.

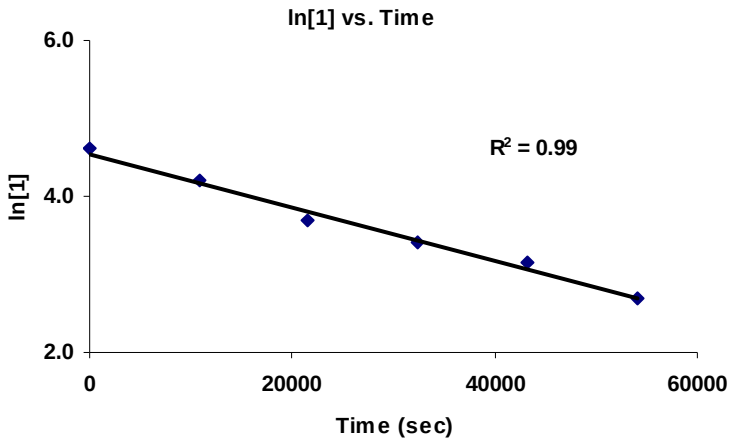

Figure 3.14. First-order plot (R^2 = 0.99) for the disappearance of TpRu(CO)(NCMe)Me (**1**) for the conversion of **1** and pyrrole to complex **7** (75 ^{o}C, complex **1** in pyrrole, 0 equiv of NCMe).

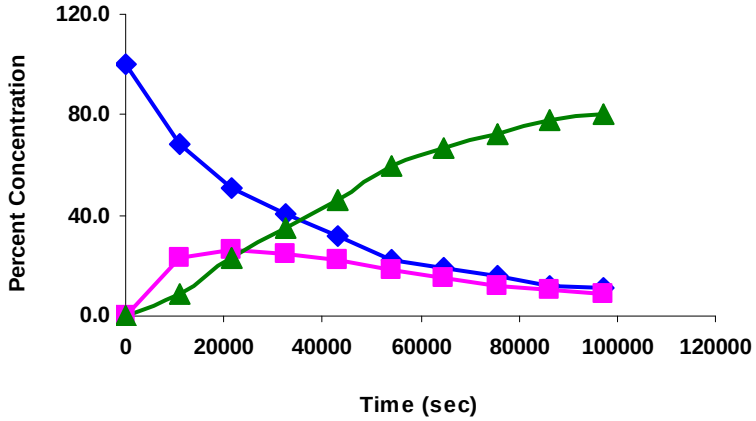

Figure 3.15. Plot of percent composition of the reaction solution versus time for the conversion of complex **1** and pyrrole to complex **7**: ♦/red line = complex **1**; ■/black line = complex **8**; ▲/purple line = complex **7**.

Observation of complex **8** as an intermediate in the transformation of **1** and pyrrole to complex **7** suggests that **1** likely initiates N-H activation of pyrrole followed by C-C bond formation with the acetonitrile ligand; however, it is also possible that metal-mediated C-H activation at the 2-position of pyrrole to produce methane and TpRu(CO)(NCMe)(2-pyrrolyl) occurs followed by rapid isomerization of the Ru-2-pyrrolyl complex to the *N*-pyrrolyl complex **8**. Initial activation of the 2-position C-H bond would be consistent with

previously reported regioselective C-H activation at the 2-position of furan and thiophene by **1**;[27] however, the majority of well-defined examples (i.e., products isolated and fully characterized) of metal-mediated activation of pyrrole indicate selectivity for activation of the N-H bond in preference to C-H bond cleavage.[16, 17, 21, 23, 43-48] A possible exception is the reported photolysis of $[Cp_2Re(NCMe)]^+$ (Cp = cyclopentadienyl) in pyrrole to produce $[Cp_2Re(2\text{-pyrrolyl})H]^+$.[18]

The source of the commonly observed selectivity for the pyrrole N-H bond over C-H bond activation could be the lower N-H bond dissociation enthalpy (BDE) of pyrrole (~97 kcal/mol) versus the C-H BDEs at the 2-position or 3-position (~118 kcal/mol) (Figure 3.1).[3] Thus, transformations that result in bond activation of pyrrole by transition metal centers may be directed to the weaker N-H bond; however, control over such transformations could be subtler. For example, it has been demonstrated that oxidative addition reactions of C-H bonds by Rh^I systems are selective for stronger C-H bonds, and such selectivity appears to be kinetic in origin.[49, 50] That is, for alkanes with terminal methyl groups and internal methylene groups, the metal center has access to all C-H bonds on the time scale of the C-H activation event and breaks the stronger terminal C-H bonds more rapidly than the weaker internal C-H bonds. Thus, the relative rates of C-H bond activation by systems that initiate *oxidative* addition are potentially controlled to a significant degree by the metal-carbon bond strengths of the incipient products, and the commonly observed selectivity of oxidative addition reactions of pyrrole could be dictated by the *combination* of weak N-H (relative to C-H BDEs) and relatively strong M-$N_{pyrrolyl}$ bonds (although M-$N_{pyrrolyl}$ bonds may be weaker than M-$C_{pyrrolyl}$ bonds, the difference in BDE may not make up for the approximately 20 kcal/mol difference in N-H versus C-H BDEs of pyrrole).[51-53] Given these considerations, computational studies were performed to assist our efforts to propose the most reasonable pathway for the formation of **7** from complex **1** and pyrrole.

To further examine the initial interactions of pyrrole with the metal center, computational analysis was conducted by Prof. Thomas R. Cundari from the University of North Texas. The "TAB" ligand {tris(azo)borate} and NCH were used to model Tp and NCMe, respectively. In previous research, TAB was shown to reproduce the structure and energetics of the full Tp models for C-H activation potential energy surfaces to within ≤2% and approximately 2 kcal/mol, respectively.[54] Three modes of interaction between the Ru^{II} complex and pyrrole were investigated. One pathway involves metal-mediated N-H activation of pyrrole,

while a second pathway proceeds through C-H bond activation (Scheme 3.2). A third mode of interaction, the potential for nucleophilic addition of free pyrrole to coordinated nitrile, has been studied and disregarded as a likely reaction pathway on the basis of experimental and computational results.

Schemes 3.10 and 3.11 provide calculated free energies for the conversion of (TAB)Ru(CO)(NCH)Me (**1'**) to the cyclometalated product **7'** for both N-H and C-H activation pathways, respectively. The binding of the nitrile is calculated to be quite weak with a ΔG of 14.9 kcal/mol for dissociation of HCN from **1'** (Scheme 3.10). Several different coordination modes of pyrrole to the 16-electron fragment {(TAB)Ru(CO)Me} were investigated (each with several distinct conformational isomers evaluated) including a dihapto-coordinated π-complex and ligation through the pyrrole nitrogen. On the basis of the calculations, the most stable (TAB)Ru(CO)(η^2-pyrrolyl)Me adduct is the π-complex (η^2-coordinated through the 2,3-C=C bond). This complex is calculated to be 4.1 kcal/mol more stable (ΔG) than the *N*-ligated pyrrole complex. The structure of the most stable conformer of (TAB)Ru(CO)(η^2-pyrrole)Me is shown in Figure 3.16.

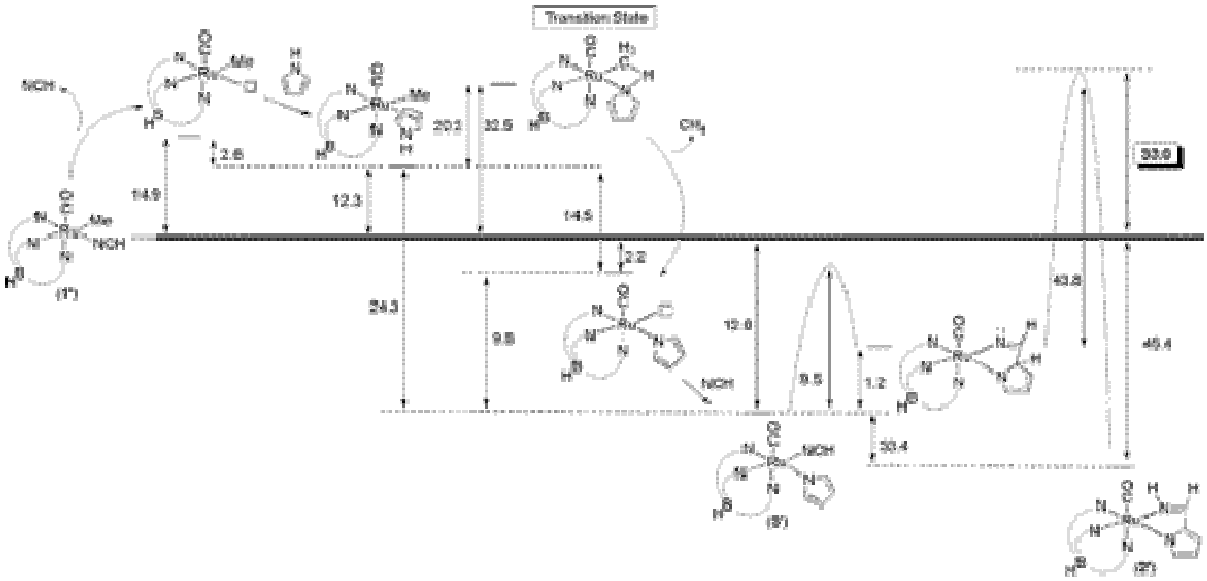

Scheme 3.10. Calculated free energies (kcal/mol) for the conversion of (TAB)Ru(CO)(Me)(NCH) (**1'**) to **7'** that proceeds through initial cleavage of the N-H bond.

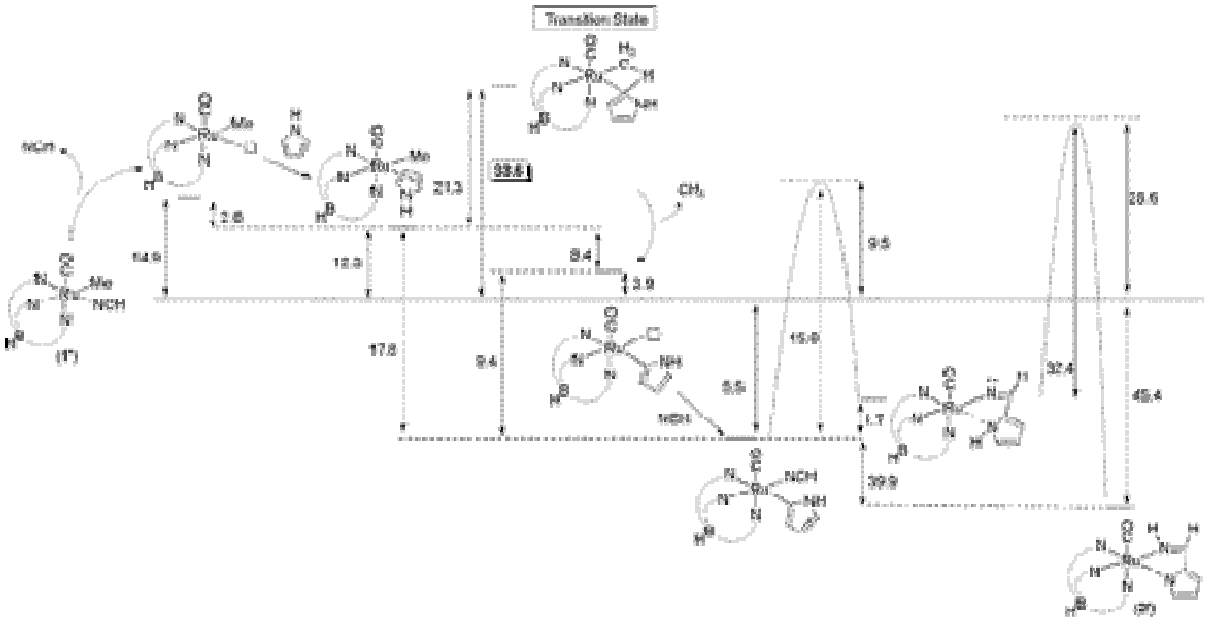

Scheme 3.11. Calculated free energies (kcal/mol) for the conversion of (TAB)Ru(CO)(NCH)Me (**1'**) to **7'** that proceeds through initial cleavage of the C2-H bond.

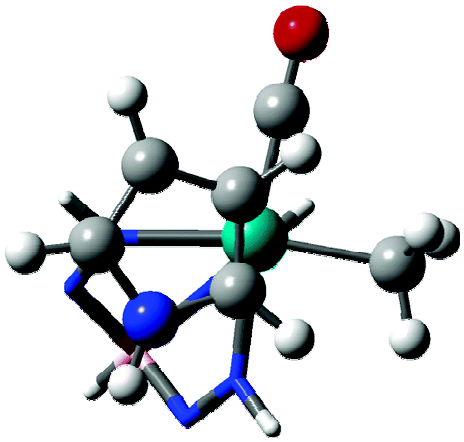

Figure 3.16. Calculated structure of (TAB)Ru(CO)(η^2-pyrrole)Me. The atoms of the Tab ligand in this and all subsequent figures are shown as colored tubes for clarity.

The binding free energy of pyrrole through its π-ring in (TAB)Ru(CO)(η^2-pyrrole)Me is small, only -2.6 kcal/mol, as expected for coordination to a neutral d^6 ML_5 fragment. Hence, the exchange of NCH with pyrrole is calculated to be endergonic by 12.3 kcal/mol.

Computational models were also employed to evaluate the transition states for the C-H and N-H activation pathways. In a previous study on C-H activation of benzene by **1'**, a variety of transition states were

investigated including those derived from oxidative addition and σ-bond metathesis pathways.[28] In all cases, transition state searches converged to four-centered transition states reminiscent of σ-bond metathesis processes that are the hallmark of C-H activation by d^0 metal systems.[55-58] A similar transition state was found by Oxgaard and Goddard for the $TpRu^{II}$ system as well as a related Ir^{III} complex, and the term oxidative hydrogen migration was used to label the transition state due to the close contact between the transition metal and the hydrogen atom undergoing transfer.[59, 60]

The isomeric transition states for activation of the C2-H, C3-H, and N-H bonds of pyrrole were compared (Scheme 3.12). The calculated free energy ordering of the three transition states is (relative energies in parentheses) as follows: N-H (0 kcal/mol) < C2-H (1.1 kcal/mol) < C3-H (3.0 kcal/mol). The geometries of the two lower energy transition states (i.e., C2-H and N-H bond activation) are shown in Figure 3.17. Calculations with full Tp models yield the same $\Delta\Delta G^{\ddagger}$ (1.1 kcal/mol) for C2-H and N-H activation as seen with the more compact TAB models. An obvious structural difference in the N-H and C2-H activation transition states is the distance between the ruthenium and the transannular hydrogen (H_t); it is considerably shorter in the C-H activation transition state (Ru-H = 1.77 Å) compared to the corresponding N-H stationary point (Ru-H_t = 1.90 Å). Thus, the calculated transition state for C2-H bond activation might be considered to possess more oxidative character as compared to the transition state for N-H bond activation.

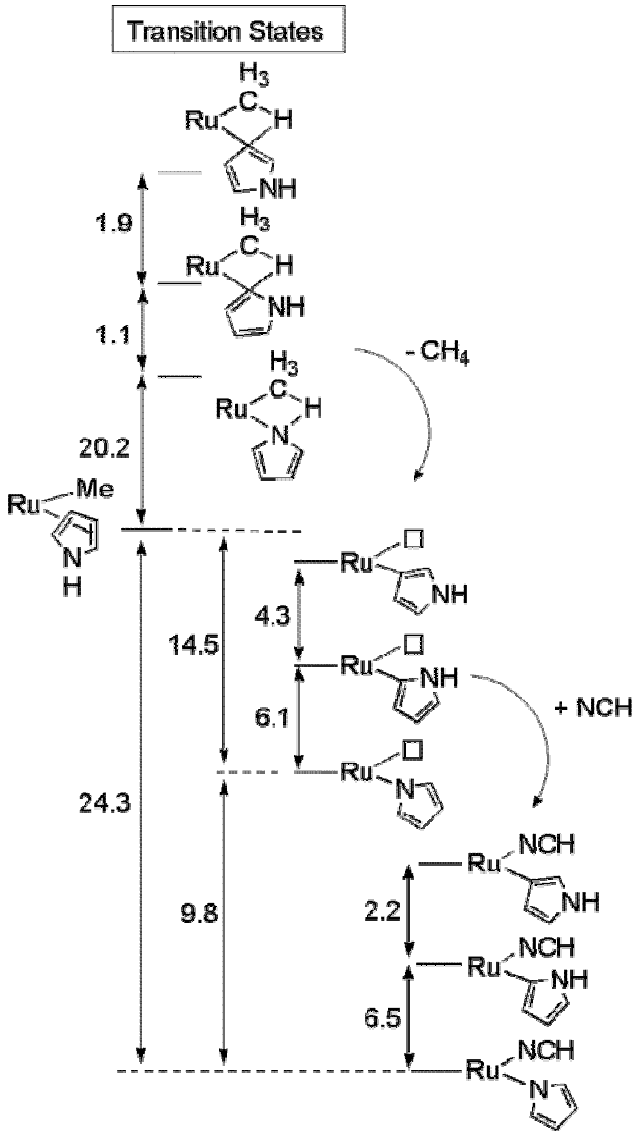

Scheme 3.12. Calculated free energies (kcal/mol) for activation of pyrrole at the N-H, C2-H and C3-H positions by (TAB)Ru(CO)(NCH)Me (**1'**) {Ru = (TAB)Ru(CO)}

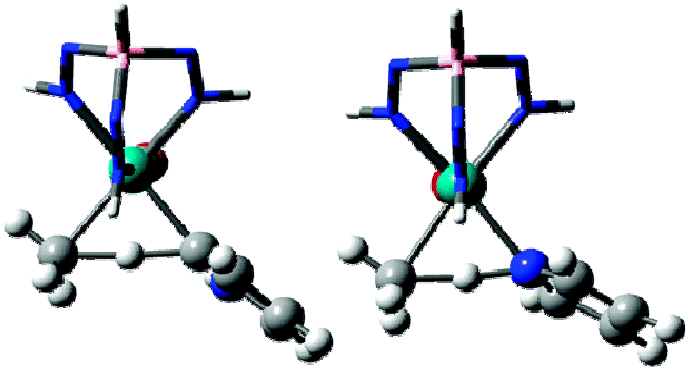

Figure 3.17. Calculated transition states for C2-H (left) and N-H activation (right) of pyrrole by {(TAB)Ru(CO)Me}.

The product of N-H activation of pyrrole by {(TAB)Ru(CO)Me} to release methane, {(TAB)Ru(CO)(*N*-pyrrolyl)}, is calculated to be 6.1 kcal/mol more stable than the corresponding 2-pyrrolyl isomer, {(TAB)Ru(CO)(2-pyrrolyl)}, which results from C2-H activation and methane production (Scheme 3.10). The 2-pyrrolyl system is calculated to be another 4.3 kcal/mol more stable than the 3-pyrrolyl isomer, {(TAB)Ru(CO)(3-pyrrolyl)}, which results from C3-H activation. The coordination of HCN to the various 16-electron pyrrolyl intermediates yields 18-electron, pseudo-octahedral (TAB)Ru(CO)(NCH)(X-pyrrolyl) (X = *N*, 2, or 3) systems. The energy ordering for these six-coordinate species is the same as that seen for the five-coordinate intermediates (relative energies in parentheses): (TAB)Ru(CO)(NCH)(*N*-pyrrolyl) (0 kcal/mol) < (TAB)Ru(CO)(NCH)(2-pyrrolyl) (6.5 kcal/mol) < (TAB)Ru(CO)(NCH)(3-pyrrolyl) (8.7 kcal/mol). The calculated energy differences for each set of 16- and 18-electron product isomers are substantial and outside the error limits expected for the computational and chemical models employed when applied to highly similar species. Hence, the thermodynamic preferences for the various pyrrolyl products mimic the kinetic preferences calculated for the isomeric transition states of N-H, C2-H, and C3-H bond activation with the energetic differences being much more pronounced in the ground states.

The reaction pathway for the production of complex **7** upon reaction of **1** and pyrrole that proceeds through C-H bond activation at the 2-position invokes the insertion of acetonitrile into a Ru-2-pyrrolyl bond. This process was also studied computationally, with the results depicted in Scheme 3.12. The initial insertion step is calculated to be endergonic by 1.7 kcal/mol, with an activation barrier of 15.0 kcal/mol. Subsequent proton transfer produces the *N*-pyrrolyl complex with a chelated imine fragment (**7'**), with the overall process of

insertion and proton transfer calculated to be favorable by 39.9 kcal/mol. The calculated barrier for the final reaction step (i.e., proton transfer) is 32.4 kcal/mol. Thus, according to calculations, the conversion of (TAB)Ru(CO)(NCMe)(2-pyrrolyl) to **7'** is a thermodynamically feasible process with a substantial activation barrier for the proton transfer step in the absence of an external reagent that can assist the proton transfer.

The pathway for formation of metallacycle **7** that involves initial N-H activation of pyrrole would produce the *N*-pyrrolyl complex **8** followed by C-C bond formation and proton transfer. For the model complex (TAB)Ru(CO)(NCH)(*N*-pyrrolyl) (**3'**), the initial step, C-C bond formation, is calculated to be unfavorable by 1.2 kcal/mol, with an activation barrier of 9.5 kcal/mol (Scheme 3.10). The calculated transition state structure for this reaction step is shown in Figure 3.18. The C-C bond formation starting from complex **8'** is calculated to have an activation barrier that is 5.5 kcal/mol less than the C-C bond formation step from the (TAB)Ru(CO)(NCMe)(2-pyrrolyl) system (Schemes 3.10 and Scheme 3.11). The subsequent proton transfer to form complex **7**' is calculated to be favorable relative to **8'** by 33.4 kcal/mol; however, the final reaction step (direct proton transfer between the ligated nitrogen atoms) is calculated to possess a substantial barrier of 43.8 kcal/mol. This calculation is consistent with the *experimental* observation that the conversion of TpRu(CO)(NCMe)(*N*-pyrrolyl) (**8**) to complex **7** in neat CD_3CN or C_6D_6 is a slow reaction (see above). For example, the k_{obs} for the conversion of **8** to **7** in CD_3CN is 9.7×10^{-7} s^{-1}, which yields a $\Delta G^{\ddagger} = 31.4$ kcal/mol (at 90 ^{o}C). According to experimental observations, the rate of conversion increases upon addition of base (e.g., pyrrole or 2,6-lutidine) and likely accounts for the more rapid conversion of **1** and pyrrole to **7** in neat pyrrole. The base provides a catalytic pathway for the transfer of a proton from the 2-position of the pyrrolium intermediate to the azavinylidene nitrogen to yield **7**.

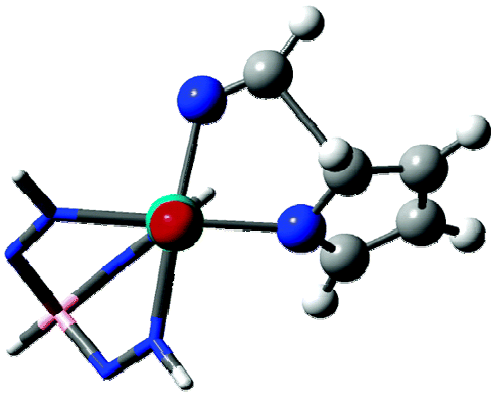

Figure 3.18. Calculated transition state for C-C bond formation from the *N*-pyrrolyl complex **8'**.

3.3 Summary

Experimental studies provide evidence that the conversion of **1** and pyrrole to **7** occurs through initial activation of the N-H bond of pyrrole to produce the *N*-pyrrolyl complex **8**. Although it is possible that initial C-H activation of pyrrole at the 2-position produces TpRu(CO)(NCMe)(2-pyrrolyl) followed by rapid isomerization to the *N*-pyrrolyl complex **8**, computational studies indicate that metal-mediated N-H activation of pyrrole by {(TAB)Ru(CO)Me} is kinetically preferred over C2-H activation by 1.1 kcal/mol. In addition, the formation of (TAB)Ru(CO)(NCH)(*N*-pyrrolyl) (**8'**) is calculated to be thermally favored relative to (TAB)Ru(CO)(NCH)(2-pyrrolyl) by 6.5 kcal/mol. The same kinetic preference is seen for full Tp models of the respective bond activation transition states. For the formation of **7'**, the calculated free energies for the N-H activation pathway" indicate that the highest energy species lies 33.0 kcal/mol above **1'** and corresponds to the transition state for the final proton transfer step. Importantly, experimental results suggest that excess pyrrole increases the rate of this proton transfer step and thus increases the rate of conversion of **8** to **7**. The calculated free energies for the C2-H activation pathway indicate that the highest energy species is 33.6 kcal/mol above **1'** and corresponds to the C2-H activation step. The combination of experimental and computational results leads us to suggest that the pathway involving initial N-H activation (shown on the left side of Scheme 3.2) is the most likely pathway for the formation of complex **7**. The observation of this reaction pathway provides the opportunity to explore C-C bond formation at the 2-position of pyrrole with other unsaturated substrates that

possess C-X (X = N or O) multiple bonds and could ultimately provide a foundation for catalytic C-C bond forming reactions of pyrroles.

3.4 Experimental Section

General Methods. Unless otherwise noted, all synthetic procedures were performed under anaerobic conditions in a nitrogen-filled glovebox or by using standard Schlenk techniques. Glovebox purity was maintained by periodic nitrogen purges and was monitored by an oxygen analyzer (O_2 < 15 ppm for all reactions). Diethyl ether was dried by distillation from sodium/benzophenone. Acetonitrile and methanol were dried by distillation from CaH_2. Hexanes, methylene chloride, and tetrahydrofuran were purified by passage through a column of activated alumina. Pyrrole was distilled from Na_2SO_4 or CaH_2. Acetone-d_6, benzene-d_6, acetonitrile-d_3, and chloroform-d_1 were degassed with three freeze-pump-thaw cycles and stored under a N_2 atmosphere over 4 Å molecular sieves. ^{1}H and ^{13}C NMR spectra were recorded on a Varian Mercury 300 or 400 MHz spectrometer. All ^{1}H and ^{13}C NMR spectra were referenced against tetramethylsilane using residual proton signals (^{1}H NMR) or the ^{13}C resonances of the deuterated solvent (^{13}C NMR). ^{19}F NMR spectra were obtained on a Varian 300 MHz spectrometer and referenced against an external standard of hexafluorobenzene. Resonances due to the Tp ligand are listed by chemical shift and multiplicity only (all coupling constants for the Tp ligand are 2 Hz). IR spectra were acquired using a Mattson Genesis II FT-IR as thin films on KBr plates or in solution using KBr solvent cells. GC-MS was performed using a HP GCD system with a 30 m × 0.25 mm HP-5 column with 0.25 μm film thickness. Complexes **1**, TpRu(CO)(NCMe)Cl, and **9** have been previously reported.[28, 29, 39] All other reagents were used as purchased from commercial sources.

TpRu(CO){κ^2-*N,N*-(H)N=C(Me)(NC$_4$H$_3$)} (7). Method 1. TpRu(CO)(NCMe)Me (**1**) (0.099 g, 0.25 mmol) was dissolved in approximately 5 mL of pyrrole. The reaction mixture was removed from the glovebox and placed in an oil bath at 90 ^{o}C for 12 h. After cooling the solution to room temperature, the volatiles were removed in vacuo. Analysis of the reaction mixture by ^{1}H NMR spectroscopy revealed the presence of a single TpRu complex. The yellow oil was taken up in methylene chloride (~5 mL) and passed through a column of silica gel. After the column was washed with approximately 50 mL of methylene chloride, the eluent was reduced to dryness under vacuum, leaving an off-white solid. The solid was dissolved in methylene chloride (~2

mL) and precipitated upon addition of hexanes (~25 mL). The resulting amorphous solid was collected by vacuum filtration and washed with hexanes. The solid was dried in vacuo to yield an off-white product (0.051 g, 45%).

Method 2. A screw cap NMR tube was charged with **8** (0.017 g, 0.038 mmol) in 0.6 mL of acetonitrile-d_3. The reaction tube was placed in a temperature-regulated oil bath at 90 ^{o}C. The conversion of complex **8** to complex **7** under these conditions (as monitored by ^{1}H NMR) required several days. IR (KBr): ν_{CO} = 1948 cm^{-1}, ν_{BH} = 2489 cm^{-1}. ^{1}H NMR (acetone-d_6, δ): 8.45 (1H, s, imine N*H*), 7.97, 7.75, 6.58 (each 1H, each a d, Tp C*H* 3 or 5 position), 7.87 (3H, m, overlapping Tp C*H* 3 and 5 position), 6.82 (1H, dd, J_{HH} = 3.6 and 1.2 Hz, 3-position C*H* of pyrrolyl), 6.77 (1H, t, J_{HH} = 1.2 Hz, 2-position C*H* of pyrrolyl), 6.35, 6.30, 6.05 (each 1H, each a t, Tp C*H* 4 position), 6.09 (1H, dd, J_{HH} = 3.6 and 1.2 Hz, 3-position C*H* of pyrrolyl), 2.50 (3H, s, NCCH_3). ^{13}C{^{1}H} NMR ($CDCl_3$, δ): 200.7 (*C*O), 172.5 (Ru-N(H)=*C*(Me)), 144.6, 144.1, 140.7, 138.7, 135.9, 135.7, 134.5 (Tp 3 and 5 position and pyrrolyl 2-position with one overlap), 115.0, 110.8 (3-position of pyrrolyl), 106.3, 105.5 (Tp 4 position, one overlap), 21.1 (Ru-N(H)=C*C*H_3). Anal. Calcd for $C_{16}H_{16}BN_7O_2Ru$: C, 42.77; H, 3.81; N, 24.94. Found: C, 43.28; H, 3.92; N, 24.50.

TpRu(CO)(NCMe)(*N*-pyrrolyl) (8). A THF solution of TpRu(CO)(NCMe)(OTf) (**9**) (0.394 g, 0.714 mmol) was cooled to -78 ^{o}C. A cooled (-78 ^{o}C) solution of lithium *N*-pyrrolyl (0.522 g, 0.714 mmol) in THF was slowly transferred by cannula into the solution containing **4**. The resulting mixture was allowed to warm to room temperature, and the solvent was removed under reduced pressure. The residuals were dissolved in minimal methylene chloride and were passed through a column of silica gel. A brown band was collected and reduced to 2 mL under vacuum. The addition of approximately 50 mL of hexanes resulted in the formation of a precipitate. The tan solid was collected via vacuum filtration and dried (0.147 g, 46%). IR (KBr): ν_{CO} = 1961 cm^{-1}, ν_{CN} = 2216 cm^{-1}, ν_{BH} = 2490 cm^{-1}. ^{1}H NMR ($CDCl_3$, δ): 7.75, 7.72, 7.67, 7.61, 7.52, 7.26 (each 1H, each a d, Tp C*H* 3 or 5 position), 6.36 (2H, t, J_{HH} = 2.0 Hz, 2-position pyrrolyl C*H*), 6.25 (2H, m (overlapping triplets), Tp C*H* 4 position), 6.16 (2H, t, J_{HH} = 2.0 Hz, 3-position pyrrolyl C*H*), 6.13 (1H, t, Tp C*H* 4 position), 2.39 (3H, s, NCCH_3). Homonuclear decoupling study of **8**: A screw cap NMR tube was charged with **8** (0.026 g, 0.059 mmol) and 0.7 mL of $CDCl_3$. The irradiation of the resonance at 6.36 ppm produced a singlet at 6.16 ppm. Changes in coupling to other resonances (e.g., doublets due to the Tp ligand 3 and 5 positions) were not

observed. These results confirm that the resonances at 6.36 and 6.16 ppm are due to the *N*-pyrrolyl ligand. $^{13}C\{^1H\}$ NMR ($CDCl_3$, δ): 202.1 (*C*O), 145.2, 143.5, 142.2, 135.6, 135.5, 134.6 (Tp 3 or 5 position), 130.9 (2-position of pyrrolyl), 122.4 (N*C*Me), 106.2, 106.1, 105.7, 105.6 (Tp 4 position and 3-position of pyrrolyl), 4.5 ($NCCH_3$).

Reaction of TpRu(CO)(NCMe)(*N*-pyrrolyl) (8) with HCl. A screw cap NMR tube was charged with **8** (0.017 g, 0.037 mmol) and approximately 0.7 mL of $CDCl_3$. A ^1H NMR spectrum was acquired. The solution was cooled to -78 ^oC, and 0.05 mL (0.2 mmol) of HCl (in dioxane) was added. The solution was allowed to slowly warm to room temperature. A ^1H NMR spectrum revealed new resonances consistent with formation of free pyrrole (6.06 and 6.65 ppm) and TpRu(CO)(NCMe)Cl.

TpRu(CO)(NCMe)(OTf) (9). The preparation of **9** by an alternative method and details of characterization have been previously reported.[43] Two new methods for the preparation of **9** are disclosed. **Method 1.** TpRu(CO)(NCMe)Cl (0.240 g, 0.573 mmol) and AgOTf (0.147 g, 0.573 mmol) were placed in a 50 mL round-bottom flask and dissolved in THF. The solution was heated to reflux for 30 min with the observation of a white precipitate. Upon confirmation of reaction completion by IR, the volatiles were removed under reduced pressure. The residual material was taken up in CH_2Cl_2 and passed through a plug of Celite. Upon addition of hexanes to the filtrate, a yellow solid precipitated. The solid was collected by vacuum filtration and dried (0.286 g, 90%).

Method 2. TpRu(CO)(NCMe)Me (**1**) (2.929 g, 7.35 mmol) was taken up in 50 mL of CH_2Cl_2 and cooled to -78 ^oC. Triflic acid (0.65 mL, 7.3 mmol) was added dropwise to the solution of **1**, yielding observable CH_4 evolution and a dark yellow appearance. After evacuation of all volatiles the residual yellow solid was taken up in minimal CH_2Cl_2 and passed through a column of silica. The yellow eluent was collected and isolated by addition of hexanes and vacuum filtration. The yellow solid (3.240 g, 80%) was dried overnight under vacuum.

[TpRu(CO)(NCMe)(η^1-OC_4H_8)][BAr'$_4$] (10). TpRu(CO)(NCMe)Cl (0.095 g, 0.18 mmol) and NaBAr'$_4$ (0.150 g, 0.179 mmol) were dissolved in 5 mL of THF and placed in a 50 mL reaction flask. The solution was heated to reflux for approximately 5 min. The solution was cooled to room temperature, and the volatiles were removed under vacuum. The residuals were dissolved in 2 mL of methylene chloride and passed

through a plug of Celite. The solvent was removed from the yellow filtrate under reduced pressure to leave an off-white solid. The product was washed with pentane and collected by vacuum filtration. The off-white product was dried in vacuo to yield 0.164 g (60%). IR (KBr): ν_{CO} = 2004 cm^{-1}, ν_{BH} = 2502 cm^{-1}. ^{1}H NMR ($CDCl_3$, δ): 7.87, 7.79, 7.76, 7.32 (each 1H, each a d, Tp C*H* 3 or 5 position), 7.69 (9H, m, overlap of BAr'_4 ortho position and Tp 3 or 5 position), 7.54 (5H, m, overlap of BAr'_4 para position and Tp C*H* 3 or 5 position), 6.41, 6.33, 6.21 (each 1H, each a t, Tp C*H* 4 position), 3.56 (4H, m, THF CH_2 2-position), 2.34 (3H, s, $NCCH_3$), 1.81 (4H, m, THF CH_2 3-position. ^{19}F NMR ($CDCl_3$, δ): -62.7 (BAr'_4). $^{13}C\{^1H\}$ NMR ($CDCl_3$, δ): $^{13}C\{^1H\}$ NMR ($CDCl_3$, δ): 198.6 (*C*O), 161.8 (BAr'_4, *ipso*-carbon), 145.6, 144.9, 141.3, 137.8, 137.7, 136.6 (Tp 3,5 position), 134.9 (BAr'_4, *ortho*), 129.1, (BAr'_4, *meta*-carbon), 126.5 (*N*-pyrrolyl, α-position), 122.9 (*N*-pyrrolyl, β-position), 117.7 (BAr'_4, *para*-carbon), 108.0 ($NCCH_3$), 107.6, 107.5, 107.2 (Tp 4 position), 76.0 (Bound THF, 1 and 2 position), 25.6 (bound THF, 3 and 4 position), 3.6 ($NCCH_3$). Anal. Calcd for $C_{16}H_{17}BN_8ORu$: C, 43.92; H, 4.16; N, 22.42. Found: C, 43.58; H, 3.98; N, 21.82.

Kinetic Studies: Formation of TpRu(CO){κ^2-*N*,*N*-(H)N=C(CH_3)(NC_4H_3)} (7) from TpRu(CO)(NCMe)Me (1) and Pyrrole. Two reaction vessels were each charged with TpRu(CO)(NCMe)Me (**1**) (0.321 g, 0.806 mmol, 0.161 M) and pyrrole (5.0 mL, 0.072 mol) to give homogeneous solutions. To one vessel, 30 equiv of NCMe (based on **1**) was added. Both vessels were heated to 75 ^oC in an oil bath regulated by an IKA-Werke ETC1 temperature probe. Every 3 h the reaction solution was cooled for 15 min in an ice bath and an aliquot of 0.30 mL was taken. The aliquots were dried under vacuum, the residuals were taken up in 0.7 mL of $CDCl_3$, and the resulting solutions were analyzed by ^{1}H NMR spectroscopy. This analysis was performed in triplicate to ensure reproducibility. Sample kinetic plots are given in the Supporting Information.

Kinetic Studies: Formation of TpRu(CO){κ^2-*N*,*N*-(H)N=C(CH_3)(NC_4H_3)} (7) from TpRu(CO)(NCMe)(*N*-pyrrolyl) (8). A representative kinetic study is described. TpRu(CO)(NCMe)(*N*-pyrrolyl) (**8**) (0.019 g, 0.042 mmol) was dissolved in 0.7 mL of acetonitrile-d_3. The resulting yellow solution (0.06 M) was placed in a screw cap NMR tube, and 15.4 μL of pyrrole was added (0.226 mmol). The solution was heated to 90 ^oC in an oil bath. Periodically, the reaction vessel was removed from the oil bath and placed in an ice water bath for 15 min prior to analysis by ^{1}H NMR spectroscopy.

Preparation of *N*-d_1-Pyrrole. Pyrrole (5 mL) was combined with approximately 80 mL of diethyl ether in a round-bottom flask. The solution was cooled to -78 ^{o}C, and MeLi (71.5 mmol) was added dropwise by syringe. The solution was allowed to warm to room temperature and the formation of a white precipitate was noted. The mixture was vacuum filtered, and the resulting solid was washed with diethyl ether. The solid was collected and combined with approximately 80 mL of diethyl ether. The slurry was cooled to -78 ^{o}C, and D_2O (D, 99.9%) (1.5 mL, 83 mmol) was added. The reaction was allowed to warm to room temperature to produce a yellow solution. The solution was vacuum filtered, and the volume of the filtrate was reduced to approximately 15 mL. The organic layer was removed and stirred over Na_2SO_4 for 12 h. The diethyl ether was removed by vacuum distillation. The product was collected by further vacuum distillation and analyzed by mass spectrometry and ^{1}H NMR spectroscopy for purity. Mass spectral data indicated a peak at 68 *m*/*z*, and the ^{1}H NMR spectrum lacked the resonance due to the N-H of pyrrole.

Reactions Using *N*-Deuteriopyrrole and Perdeuteriopyrrole. The following procedures were used for all reactions involving deuterated pyrroles. A screw cap NMR tube was charged with TpRu(CO)(NCMe)Me (**1**) and the respective pyrrole. The tube was removed from the glovebox and heated in an oil bath at 90 ^{o}C for 6 h. Before and after heating the reaction, the solution and headspace were analyzed using GC-MS.

Computational Methods. Quantum calculations were carried out using the Gaussian 98 package.[61] The B3LYP hybrid functional was employed for all calculations.[62] Heavy atoms were described with the Stevens relativistic effective core potentials (ECPs) and valence basis sets (VBSs).[63] The valence basis sets of main group elements were augmented with a d polarization function. This ECP/VBS combination, termed SBK(d), has been validated for the calculation of a wide variety of transition metal properties in previous studies.[39,40] As a model of the full (tris-pyrazolyl)borate (Tp) ligand, the tris(azo)borate (Tab) ligand, $[HB(-N{=}NH)_3]^-$, was used. In previous research, Tab was shown to faithfully reproduce the structure and energetics of the full Tp models for C-H activation potential energy surfaces.[28, 54]

All stationary points were fully optimized without symmetry constraint. Several conformations of the different ligands were investigated by torsion about the appropriate metal-ligand bond lengths; the lowest energy conformers found were used in the analyses given below. The energy Hessian was calculated at all stationary points to characterize them as minima (no imaginary frequencies) or transition states (one and only

one imaginary frequency). The quoted energies include zero-point, enthalpy, and entropic corrections determined from unscaled vibrational frequencies calculated at the B3LYP/SBK(d) level of theory. All energetic determinations were done at 298.15 K and 1 atm.

References

1. Jones, R. A., *Pyrroles*. Wiley: New York, 1990; Vol. 48.

2. Eicher, T.; Hauptmann, S., *The Chemistry of Heterocycles*. 1st ed.; Thieme: New York, 1995.

3. Luo, Y.-R., *Handbook of Bond Dissociation Energies in Organic Compounds*. CRC Press: Boca Raton, 2003.

4. Gupta, R. R.; Kumar, M.; Gupta, V., *Heterocyclic Chemistry: II: Five-Membered Heterocycles*. Springer: Berlin, 1999; Vol. 2.

5. Cordone, R.; Harman, W. D.; Taube, H. *J. Am. Chem. Soc.* **1989,** *111*, 5969-5970.

6. Hodges, L. M.; Gonzalez, J.; Koontz, J. I.; Myers, W. H.; Harman, W. D. *J. Org. Chem.* **1995,** *60*, 2125-2146.

7. Hodges, L. M.; Moody, M. W.; Harman, W. D. *J. Am. Chem. Soc.* **1994,** *116*, 7931-7932.

8. Myers, W. H.; Sabat, M.; Harman, W. D. *J. Am. Chem. Soc.* **1991,** *113*, 6682-6683.

9. Ofele, K.; Dotzauer, E. *J. Organomet. Chem.* **1971,** *30*, 211-213.

10. Heenan, D. P.; Long, C.; Montiel-Palma, V.; Perutz, R. N.; Pryce, M. T. *Organometallics* **2000,** *19*, 3867-3873.

11. van Rensburg, W. J.; Grove, C.; Steynberg, J. P.; Stark, K. B.; Huyser, J. J.; Steynberg, P. J. *Organometallics* **2004,** *23*, 1207-1222.

12. Johnson, T. J.; Arif, A. M.; Gladysz, J. A. *Organometallics* **1993,** *12*, 4728-4730.

13. Ng, M. M. P.; Roper, W. R.; Wright, L. J. *Organometallics* **1994,** *13*, 2563-2565.

14. Ishiyama, T.; Takagi, J.; Yonekawa, Y.; Hartwig, J. F.; Miyaura, N. *Adv. Synth. Catal.* **2003,** *345*, 1103-1106.

15. Mertins, K.; Zapf, A.; Beller, M. *J. Mol. Catal. A: Chem.* **2004,** *207*, 21-25.

16. Hirano, M.; Onuki, K.; Kimura, Y.; Komiya, S. *Inorg. Chim. Acta* **2003,** *352*, 160-170.

17. Morikita, T.; Hirano, M.; Sasaki, A.; Komiya, S. *Inorg. Chim. Acta* **1999,** *291*, 341-354.

18. Ogino, H.; Tobita, H.; Endo, K.; Hashidzume, K. *Int. J. Photoenergy* **1999,** *1*, 157-160.

19. Arce, A. J.; Desanctis, Y.; Deeming, A. J. *J. Organomet. Chem.* **1986,** *311*, 371-378.

20. Hardcastle, K. I.; Minassian, H.; Arce, A. J.; Desanctis, Y.; Deeming, A. J. *J. Organomet. Chem.* **1989,** *368*, 119-130.

21. Arndt, S.; Spaniol, T. P.; Okuda, J. *Eur. J. Inorg. Chem.* **2001**, 73-75.

22. Goj, L. A.; Blue, E. D.; Munro-Leighton, C.; Gunnoe, T. B.; Petersen, J. L. *Inorg. Chem.* **2005,** *44*, 8647-8649.

23. Jones, W. D.; Dong, L. Z.; Myers, A. W. *Organometallics* **1995,** *14*, 855-861.

24. Vicic, D. A.; Jones, W. D. *Organometallics* **1999,** *18*, 134-138.

25. Bohle, D. S.; Chen, W. C.; Hung, C. H. *Inorg. Chem.* **2002,** *41*, 3334-3336.

26. Lu, W. J.; Jia, C. G.; Kitamura, T.; Fujiwara, Y. *Org. Lett.* **2000,** *2*, 2927-2930.

27. Pittard, K. A.; Lee, J. P.; Cundari, T. R.; Gunnoe, T. B.; Petersen, J. L. *Organometallics* **2004,** *23*, 5514-5523.

28. Lail, M.; Bell, C. M.; Conner, D.; Cundari, T. R.; Gunnoe, T. B.; Petersen, J. L. *Organometallics* **2004,** *23*, 5007-5020.

29. Lail, M.; Arrowood, B. N.; Gunnoe, T. B. *J. Am. Chem. Soc.* **2003,** *125*, 7506-7507.

30. Brunner, H.; Neuhierl, T.; Nuber, B. *J. Organomet. Chem.* **1998,** *563*, 173-178.

31. Brunner, H.; Oeschey, R.; Nuber, B. *Organometallics* **1996,** *15*, 3616-3624.

32. Alelyunas, Y. W.; Jordan, R. F.; Echols, S. F.; Borkowsky, S. L.; Bradley, P. K. *Organometallics* **1991,** *10*, 1406-1416.

33. Bercaw, J. E.; Davies, D. L.; Wolczanski, P. T. *Organometallics* **1986,** *5*, 443-450.

34. Bochmann, M.; Wilson, L. M. *J. Chem. Soc., Chem. Commun.* **1986**, 1610-1611.

35. Bochmann, M.; Wilson, L. M.; Hursthouse, M. B.; Motevalli, M. *Organometallics* **1988,** *7*, 1148-1154.

36. Denhaan, K. H.; Luinstra, G. A.; Meetsma, A.; Teuben, J. H. *Organometallics* **1987,** *6*, 1509-1515.

37. Jordan, R. F.; Bajgur, C. S.; Dasher, W. E.; Rheingold, A. L. *Organometallics* **1987,** *6*, 1041-1051.

38. Richeson, D. S.; Mitchell, J. F.; Theopold, K. H. *Organometallics* **1989,** *8*, 2570-2577.

39. Lail, M.; Gunnoe, T. B.; Barakat, K. A.; Cundari, T. R. *Organometallics* **2005,** *24*, 1301-1305.

40. Clark, G. R.; Ng, M. M. P.; Roper, W. R.; Wright, L. J. *J. Organomet. Chem.* **1995,** *491*, 219-229.

41. Storhoff, B. N.; Lewis, H. C. *Coord. Chem. Rev.* **1977,** *23*, 1-29.

42. Feng, S. G.; White, P. S.; Templeton, J. L. *J. Am. Chem. Soc.* **1994,** *116*, 8613-8620.

43. Fornies, J.; Green, M.; Spencer, J. L.; Stone, F. G. A. *J. Chem. Soc., Dalton Trans.* **1977**, 1006-1009.

44. Hsu, G. C.; Kosar, W. P.; Jones, W. D. *Organometallics* **1994,** *13*, 385-396.

45. Iverson, C. N.; Carter, C. A. G.; Baker, R. T.; Scollard, J. D.; Labinger, J. A.; Bercaw, J. E. *J. Am. Chem. Soc.* **2003,** *125*, 12674-12675.

46. Ladipo, F. T.; Merola, J. S. *Inorg. Chem.* **1990,** *29*, 4172-4173.

47. Lopez, C. B., G.; Arevalo, A.; Munoz-Hernandez, M. A.; Garcia, J. J. *J. Organomet. Chem.* **2002,** *664*, 170-175.

48. Samat, A.; Salapala, J.; Guglielmetti, R.; Guerchais, J. *New J. Chem.* **1978,** *2*, 13-14.

49. Flood, T. C.; Janak, K. E.; Iimura, H.; Zhen, H. *J. Am. Chem. Soc.* **2000,** *122*, 6783-6784.

50. Northcutt, T. O.; Wick, D. D.; Vetter, A. J.; Jones, W. D. *J. Am. Chem. Soc.* **2001,** *123*, 7257-7270.

51. Bryndza, H. E.; Domaille, P. J.; Tam, W.; Fong, L. K.; Paciello, R. A.; Bercaw, J. E. *Polyhedron* **1988,** *7*, 1441-1452.

52. Bryndza, H. E.; Fong, L. K.; Paciello, R. A.; Tam, W.; Bercaw, J. E. *J. Am. Chem. Soc.* **1987,** *109*, 1444-1456.

53. Kanzelberger, M.; Zhang, X. W.; Emge, T. J.; Goldman, A. S.; Zhao, J.; Incarvito, C.; Hartwig, J. F. *J. Am. Chem. Soc.* **2003,** *125*, 13644-13645.

54. Bergman, R. G.; Cundari, T. R.; Gillespie, A. M.; Gunnoe, T. B.; Harman, W. D.; Klinckman, T. R.; Temple, M. D.; White, D. P. *Organometallics* **2003,** *22*, 2331-2337.

55. Goldman, A. S.; Goldberg, K. I., *In Activation and Functionalization of C-H Bonds*. American Chemical Society: Washington, D.C., 2004; Vol. 885, p 1-43.

56. Labinger, J. A.; Bercaw, J. E. *Nature* **2002,** *417*, 507-514.

57. Rothwell, I. P. *Polyhedron* **1985,** *4*, 177-200.

58. Watson, P. L., *Selective Hydrocarbon Activation: Principles and Progress*. VCH Publishers: New York, 1990.

59. Oxgaard, J.; Goddard, W. A. *J. Am. Chem. Soc.* **2004,** *126*, 442-443.

60. Oxgaard, J.; Muller, R. P.; Goddard, W. A.; Periana, R. A. *J. Am. Chem. Soc.* **2004,** *126*, 352-363.

61. Frisch, M. J.; Trucks, G. W.; Schlegel, H. B.; Scuseria, G. E.; Robb, M. A.; Cheeseman, J. R.; Zakrzewski, V. G.; Montgomery, J. A.; Stratmann, R. E.; Burant, J. C.; Dapprich, S.; Millam, J. M.; Daniels, A. D.; Kudin, K. N.; Strain, M. C.; Farkas, O.; Tomasi, J.; Barone, V.; Cossi, M.; Cammi, R.; Mennucci, B.; Pomelli, C.; Adamo, C.; Clifford, S.; Ochterski, J.; Petersson, G. A.; Ayala, P. Y.; Cui, Q.; Morokuma, K.; Malick, D. K.; Rabuck, A. D.; Raghavachari, K.; Foresman, J. B.; Cioslowski, J.; Ortiz, J. V.; Baboul, A. G.; Stefanov, B. B.; Liu, G.; Liashenko, A.; Piskorz, P.; Komaromi, I.; Gomperts, R.; Martin, R. L.; Fox, D. J.; Keith, T.; Al-Laham, M. A.; Peng, C. Y.; Nanayakkara, A.; Challacombe, M.; Gill, P. M. W.; Johnson, B.; Chen, W.; Wong, M. W.; Andres, J. L.; Gonzalez, C.; Head-Gordon, M.; Replogle, E. S.; Pople, J. A. *Gaussian 98*, A.9; Gaussian Inc.: Pittsburgh, PA, 1998.

62. Becke, A. D. *J. Chem. Phys.* **1993,** *98*, 5648-5652.

63. Stevens, W. J.; Krauss, M.; Basch, H.; Jasien, P. G. *Can. J. Chem./Rev. Can. Chim.* **1992,** *70*, 612-630.

CHAPTER 4:
Development of Next Generation Hydroarylation Catalysts Through Incorporation of Neutral Scorpionate Ligands

4.1 Introduction

In an effect to probe the influence of charge of the metal hydrophenylation catalyst, on catalytic activity we have attempted to prepare cationic analogs of TpRu(CO)(NCMe)Ph (Tp = hydridotris(pyrazolyl)borate). An isoelectronic cationic system can be obtained upon substitution of the Tp ligand with a tris(pyrazolyl)alkane ligand. The proposed target complexes of this study are $[MpRu(L)(PPh_3)Ph]BAr'_4$ (L = PPh_3, PMe_3, $P(OMe)_3$, NCMe, or CO) and $[EpRu(L)(Cl)Ph]BAr'_4$ (Ep = tris(pyrazolyl)ethane; L = PPh_3 or PMe_3). Chloride removal from EpRu(L)(Cl)Ph (L = PPh_3 or PMe_3), upon reaction with $NaBAr'_4$, would yield a coordinatively unsaturated 16 electron species $\{[EpRu(L)Ph]BAr'_4\}$ potentially capable of catalyzing the hydrophenylation of olefins (Scheme 4.1).

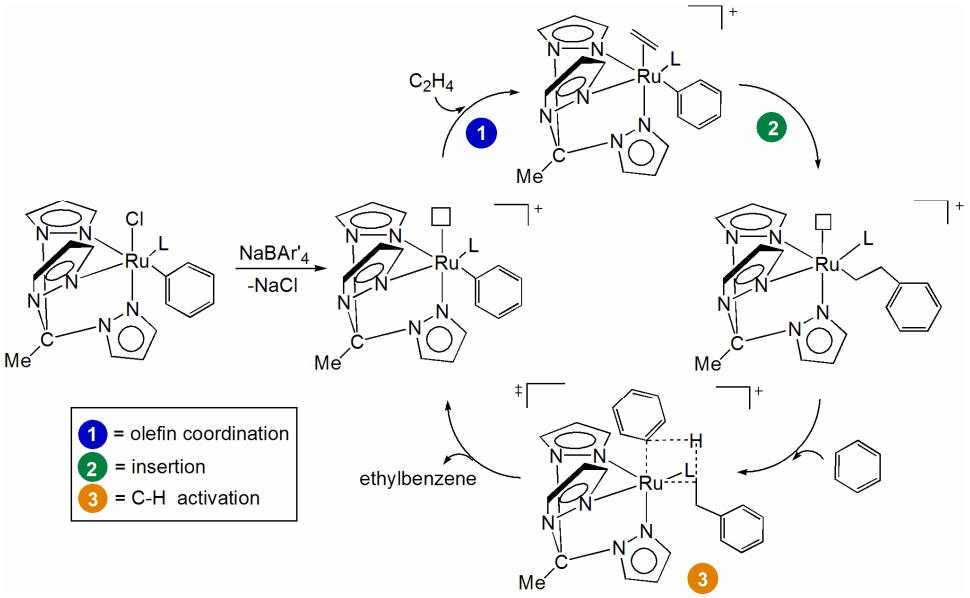

Scheme 4.1. Proposed catalytic cycle for hydrophenylation of ethylene using EpRu(L)(Cl)Ph (L = PPh_3 or PMe_3) as the precatalyst. Counterions have been excluded for clarity.

Calculations by Goddard et al. have been performed on TpRu(CO)(NCMe)Ph at the DFT level of theory using the B3LYP functional and the LACVP** basis set.[1] In contrast to experimental studies that

suggest C-H activation is the rate determining step,[2] Goddard's computational investigation on the hydrophenylation of ethylene to form ethylbenzene using the TpRu(CO)(NCMe)Ph system reveals insertion to be the rate determining step with an activation energy barrier 5.2 kcal/mol greater than that of C-H activation. The Mulliken charges for TpRu(CO)(NCMe)Ph and Periana's system, [Ir-μ-acac-*O*)(acac-*O,O*)(acac-C^3)]$_2$, were calculated to be 0.07e and 0.45e, respectively. Despite the relatively lower electron density, the rate determining step of the Ir system was also calculated to be the insertion step. It was proposed that the electron richness of the system, and therefore the metal's ability to back-donate electron density to the η^2-bound olefin would increase the barrier to olefin insertion. This is consistent with the calculation that the Ru system is ~200 times faster than the Ir system at 90 ^{o}C.[3] Thus, more electron deficient systems might enhance catalytic reactivity might be realized.

As attempts are made to expand olefin hydroarylation chemistry to cationic systems, there are issues that need to be considered. For example, due to the oxidative character of the transition state of C-H activation (Ch. 1), reducing the electron density at the metal center might raise this activation energy barrier. Further complicating matters is the potential for off-loop reactivity. For example, if olefin insertion is too facile, additional insertions of olefin would result in olefin oligomerization or polymerization. However, oligomerization or polymerization might be avoided at lower olefin pressures.

4.2 Scorpionate Comparison

The architectural similarities of the neutral Mp and Ep ligands results in an approximately isosteric and isoelectronic environment to that of the Tp ligand.[4] When the boron atom of Tp is replaced with a carbon atom a neutral species results (Figure 4.1). The apical C-H bond of Mp can be substituted with varying alkyl or aryl groups thereby allowing some structural flexibility. Compared to tris(pyrazolyl)alkanes, Tp ligands dominate in the literature. For example, there is a relatively low population of Mp scorpionate analogs in the Cambridge Structural Database (CSD) relative to that of the borate analogs (Table 4.1).[5]

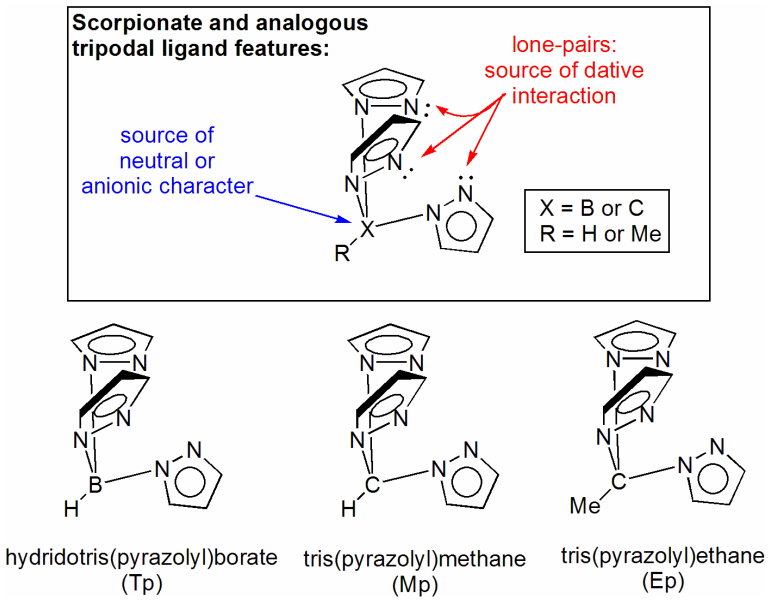

Figure 4.1. Scorpionate and analogous tripodal ligands features: tris(pyrazolyl)borate (Tp), tris(pyrazolyl)methane (Mp), and tris(pyrazolyl)ethane (Ep).

Table 4.1. Populations of complexes of scorpionates and scorpionate analogs in the CSD.[5]

substitution	$RC(pz)_3$	$RB(pz)_3$
unsubstituted	49	436
substituted	89	1624

In attempting to understand structure-property relationships when comparing Tp and Mp ligands, it is imperative that flexibility of the κ^3 tridentate binding modes for these classes of ligands be discussed. Whereas cone angles define the degree of steric hindrance about the surface of a metal center caused by a specific ligand, the bite size refers to the flexibility of a polydentate ligand coordination. For these scorpionate ligands, bite size is defined as the average N-N distance at the points of attachment to the metal center as displayed in Figure 4.2. Zimmer found that as M-N bond distance increases, the bite size also increases, and the tris(pyrazolyl)ligands are flexible as confirmed by CSD analysis through data mining.[5] The Tp ligands were found to have longer apical atom-to-plane bond distances but similar conformational flexibilities.

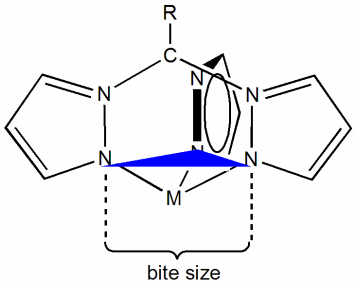

Figure 4.2. Diagram defining bite size as the N-N distance upon coordination to some metal (M = metal).

Zimmer and coworkers have evaluated differences in the structure of κ^3-coordinated Mp analogs by performing molecular mechanics (MM) calculations and evaluating trends in the CSD.[5] It was found that the steric strain of Ep is enhanced relative to Mp due to Me/H substitution. For example, the difference in calculated steric strain is 7.9 kcal/mol between Mp and Ep when the M-N was set at 2.60 Å (longest expected M-N bond distance based on the CSD). These trends have been further substantiated by empirical observations. Sánchez-Méndez et al. have observed that $Me_3SiOCH_2C(pz)_3$ coordinates to Mo, Ti, and Pd yielding the complexes $[Mo(CO)_3\{Me_3SiOCH_2C(pz)_3\}]$, $[Ti(Cl)_2(N^tBu)\{Me_3SiOCH_2C(pz)_3\}]$, and $[Pd(Cl)_2\{Me_3SiOCH_2C(pz)_3\}]$, respectively.[6] Conversely, $Me_3SiC(pz)_3$ does not bind to Mo, Ti, or Pd under similar conditions. These results were interpreted by the authors to be directly related to the "steric pressure" of the carbon substituent.[6]

In addition to the architectural flexibility, electronic differences imparted on the metal center by Mp and Tp have been evaluated by Fujisawa and coworkers.[7] They found that cationic complexes that contain Mp ligands are electron-deficient relative to Tp systems. For example, $Tp^{iPr}Cu(CO)$ (Tp^{iPr} = hydridotris(3,5-isopropylpyrazolyl)borate) and $[Mp^{iPr}Cu(CO)]X$ (Mp^{iPr} = tris(3,5-isopropylpyrazolyl)methane; X = PF_6 or ClO_4) display ν_{CO} of 2056 cm^{-1} and 2107 cm^{-1}, respectively. In addition, cyclic voltammetry was used to measure the oxidation potential (E_{pa}) of $Tp^{iPr}Cu(NCMe)$ and $[Mp^{iPr}Cu(NCMe)]PF_6$ giving values of 0.17 V and 0.58 V (vs. NHE), respectively.

Direct comparisons have also been conducted between Mp and Ep. Gibson et al. have synthesized $[MpRe(CO)_3]Br$ and $[EpRe(CO)_3]I$ and performed single-crystal X-ray diffraction studies to compare the structures.[8] It was found that the methyl group of Ep does not generate significant structural differences from

that of Mp. For example, Re-N bond lengths differ by an average of only 0.013 Å. The average N-Re-N bond angles differ by only 0.9^{o}. The observation by Zimmer that M-N bond length increases with increase in bite size is consistent with the Mp/Ep comparisons where Mp is observed to be of greater, though minor, flexibility.

4.3 Results and Discussion

4.3.1 Mp Complexes

4.3.1.1 Cationic CO Complexes

Synthesis of [MpRu(PPh$_3$)(CO)H]BAr'$_4$ (**11**) was accomplished via counter-ion exchange upon reaction of [MpRu(PPh$_3$)(CO)H]Cl with NaBAr'$_4$ in THF (Scheme 4.2). Complete counter-ion exchange was confirmed by the integration of BAr'$_4$ *ortho*- and *para*-positions in the ^{1}H NMR spectrum relative to the integration of other resonances. The complex is asymmetric, consistent with the observation of 9 resonances due to aromatic Mp positions in the ^{1}H NMR spectrum. The hydride resonates as a doublet at -12.25 ppm. The salient feature in the ^{19}F NMR spectrum is a singlet at -65.5 ppm. Photolysis and heating (120 ^{o}C) of **11** in the presence of C_6D_6 gives multiple products and no reaction, respectively.

The complex [MpRu(PPh$_3$)(CO)H]BAr'$_4$ was refluxed in chloroform to yield [MpRu(PPh$_3$)(CO)Cl]BAr'$_4$ (**12**) (Scheme 4.2). The reaction progress was monitored by IR spectroscopy using the spectroscopic handle ν_{CO}. A shift in ν_{CO} from 1947 cm^{-1} {[MpRu(PPh$_3$)(CO)H]BAr'$_4$ (**11**)} to 2000 cm^{-1} for **12** was observed. The shift to higher ν_{CO} is consistent with reduced electron donating ability of Cl relative to that of the hydride ligand. Furthermore, upon reaction completion, disappearance of the hydride ligand was observed by ^{1}H NMR spectroscopy. Complex **12** was heated to 100 ^{o}C in NCCD$_3$ with the intent to synthesize [MpRu(CO)(NCMe)(Cl)]BAr'$_4$, however, the reaction went to multiple products. Attempted alkylation of **12** with MeLi, MeMgCl, and Me$_2$Mg each failed to give desired results. The reaction of **12** with PhMgCl and PhLi gave no reaction.

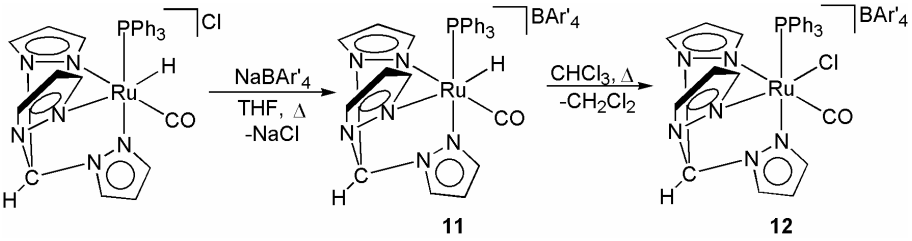

Scheme 4.2. Synthesis of $[MpRu(PPh_3)(CO)H]BAr'_4$ (**11**)and $[MpRu(PPh_3)(CO)Cl]BAr'_4$ (**12**).

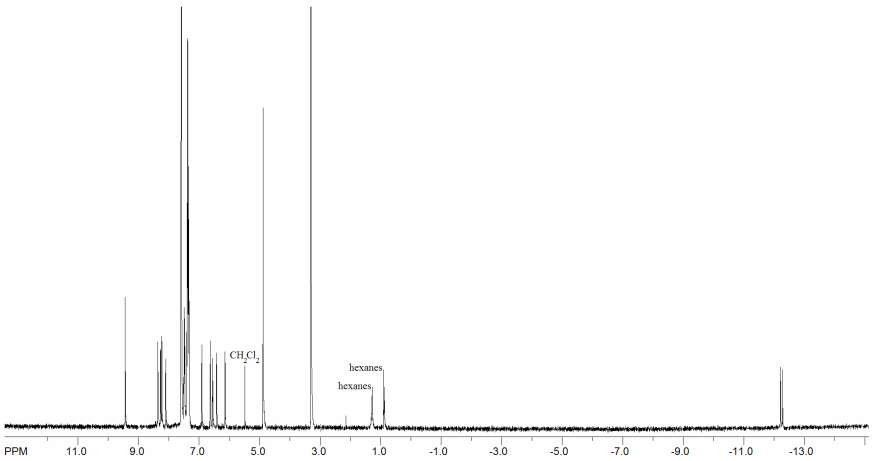

Figure 4.3. ^1H NMR spectrum of $[MpRu(PPh_3)(CO)H]BAr'_4$ (**11**) in CD_3OD.

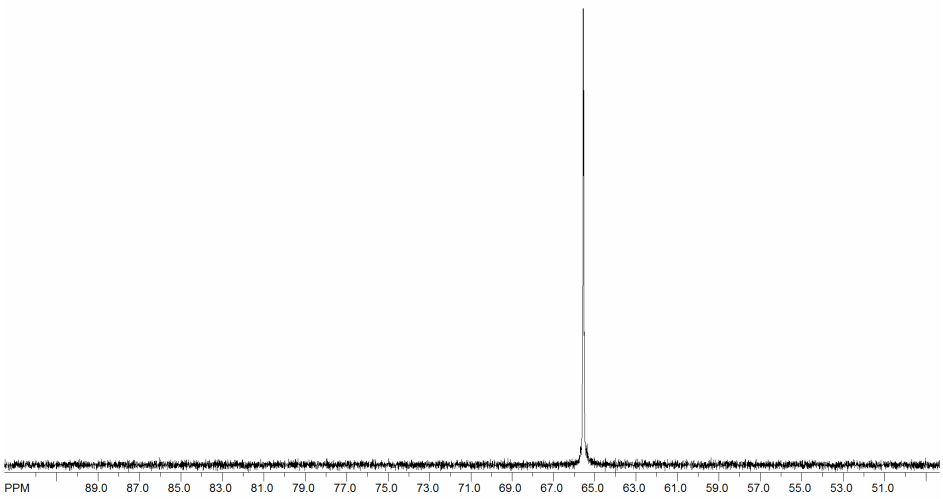

Figure 4.4. ^{31}P NMR spectrum of [MpRu(PPh$_3$)(CO)H]BAr'$_4$ (**11**) in CD$_3$OD.

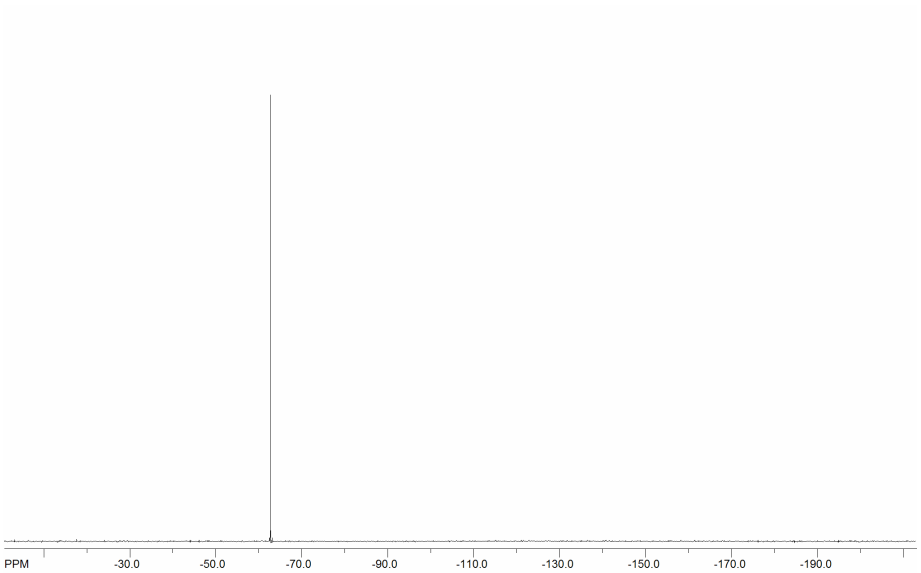

Figure 4.5. ^{19}F NMR spectrum of [MpRu(PPh$_3$)(CO)H]BAr'$_4$ (**11**) in CD$_3$OD.

4.3.1.2 Cationic Phosphine Complexes

Mixed phosphine systems were also prepared. For example, [MpRu(PPh_3)(PMe_3)Cl]Cl (**13**) was synthesized by stirring [MpRu(PPh_3)$_2$Cl]Cl in the presence of PMe_3 in THF at ambient conditions (Scheme 4.3). The loss of symmetry in going from reactants to products ($C_s \rightarrow C_1$) is consistent with the observation of inequivelant resonances due to 3, 4, and 5 pyrazolyl positions in both the ^{1}H and ^{13}C NMR spectra. Integration of PPh_3 peaks in the ^{1}H NMR spectrum of **13** is consistent with the loss of one equivalent of PPh_3. Two doublets are observed in the ^{31}P NMR spectrum. The coupling observed in the ^{31}P NMR ($^2J_{PP}$ = 37 Hz) is consistent with a *cis*-arrangement of phosphine ligands. In addition, a single-crystal X-ray diffraction study was performed on [MpRu(PPh_3)(PMe_3)Cl]Cl (Figure 4.6). Data parameters are listed in Table 4.2. In a separate reaction, [MpRu(PPh_3)(PMe_3)Cl]BAr'$_4$ (**14**) was synthesized by reacting [MpRu(PPh_3)(PMe_3)Cl]Cl with NaBAr'$_4$ in MeOH at reflux conditions (Scheme 4.3). A singlet in the ^{19}F NMR spectrum of **14** confirmed displacement of the chloride counter-ion by the BAr'$_4$ anion. The changes in chemical shift in the ^{1}H NMR spectrum upon conversion of [MpRu(PPh_3)(PMe_3)Cl]Cl to [MpRu(PPh_3)(PMe_3)Cl]BAr'$_4$ are small (≤ 0.6 ppm).

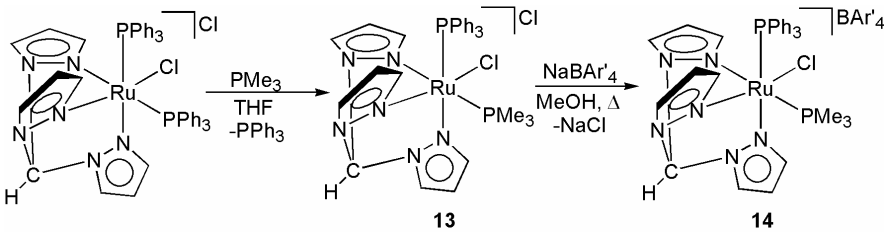

Scheme 4.3. Synthesis of [MpRu(PPh_3)(PMe_3)Cl]Cl (**13**) and [MpRu(PPh_3)(PMe_3)Cl]BAr'$_4$ (**14**).

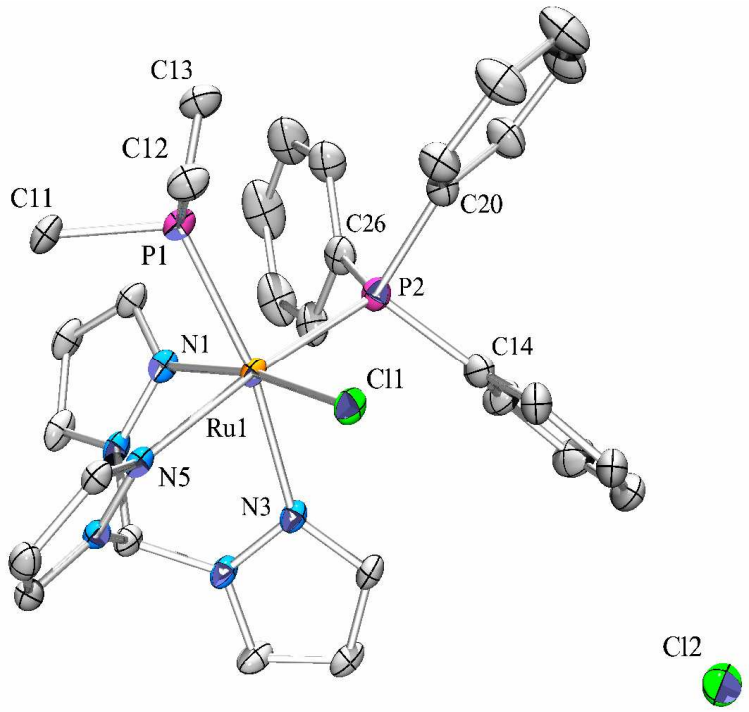

Figure 4.6. ORTEP of [MpRu(PPh$_3$)(PMe$_3$)Cl]Cl (**13**) (30% Probability). Selected bond distances (Å): Ru-N1 2.080(2), Ru-N3 2.132(2), Ru-N(5) 2.173(2), Ru-P1 2.3091(8), Ru-P2 2.3072(9), Ru-Cl 2.4164(7). Selected bond angles (deg.): P1-Ru-P2 96.86(3), Cl1-Ru-P1 94.00(3), Cl1-Ru-P2 93.24(3), N1-Ru-N3 84.94(8), N5-Ru-N3 82.83(8), N1-Ru-N5 84.54(8).

Table 4.2. Selected crystallographic data and collection parameters for [MpRu(PPh$_3$)(PMe$_3$)Cl]Cl (**13**).

	[MpRu(PPh$_3$)(PMe$_3$)Cl]Cl (**13**)
emperical formula	$C_{34}H_{40}Cl_2N_6P_2Ru$
Fw	766.63
cryst syst	triclinic
space group	P1
a, Å	10.262(1)
b, Å	10.920(1)
c, Å	17.114(1)
α, deg	108.246(2)
β, deg	92.637(2)
γ, deg	102.270(2)
V (Å)	1859.1(3)
Z	1766.6(3)
D_{calcd}, g cm^{-3}	1.441
R1, wR2 (I > 2σ(I))	0.0491, 0.1088
GOF	1.000

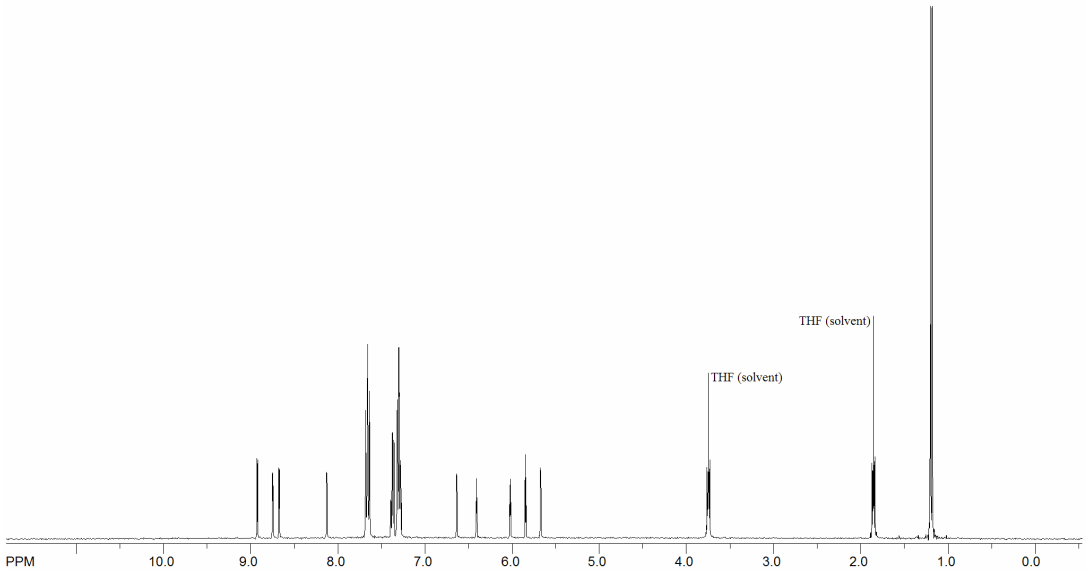

Figure 4.7. ^{1}H NMR spectrum of [MpRu(PPh$_3$)(PMe$_3$)Cl]Cl (**13**) in CDCl$_3$.

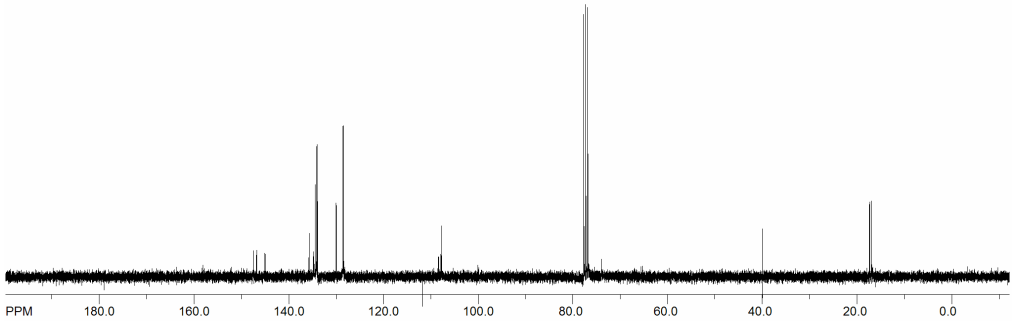

Figure 4.8. ^{13}C NMR spectrum of $[MpRu(PPh_3)(PMe_3)Cl]Cl$ (**13**) in $CDCl_3$.

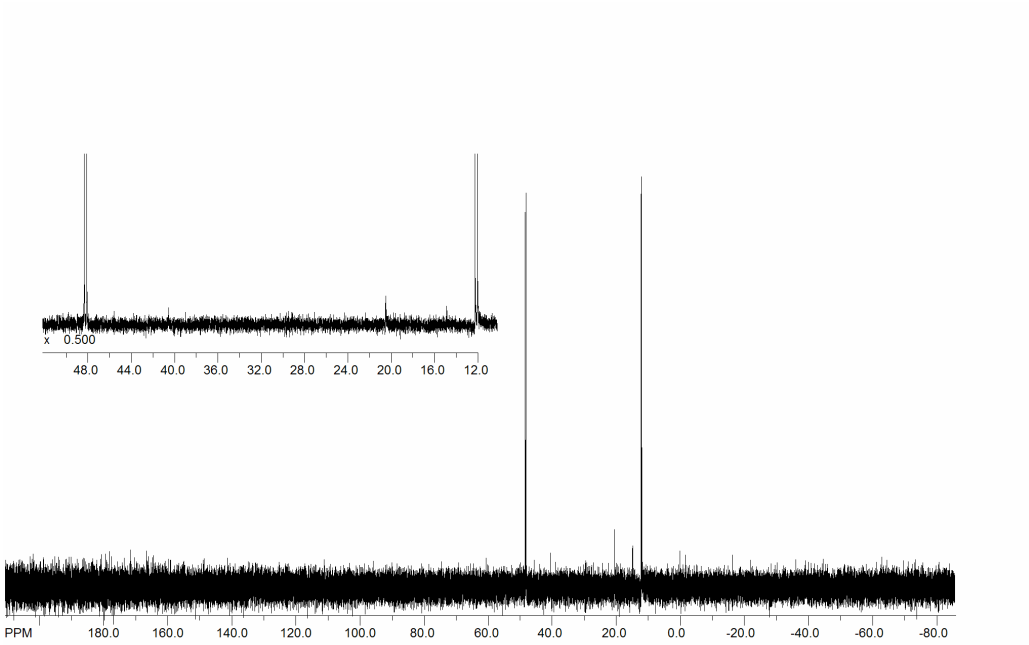

Figure 4.9. ^{31}P NMR spectrum of $[MpRu(PPh_3)(PMe_3)Cl]Cl$ (**13**) in $CDCl_3$.

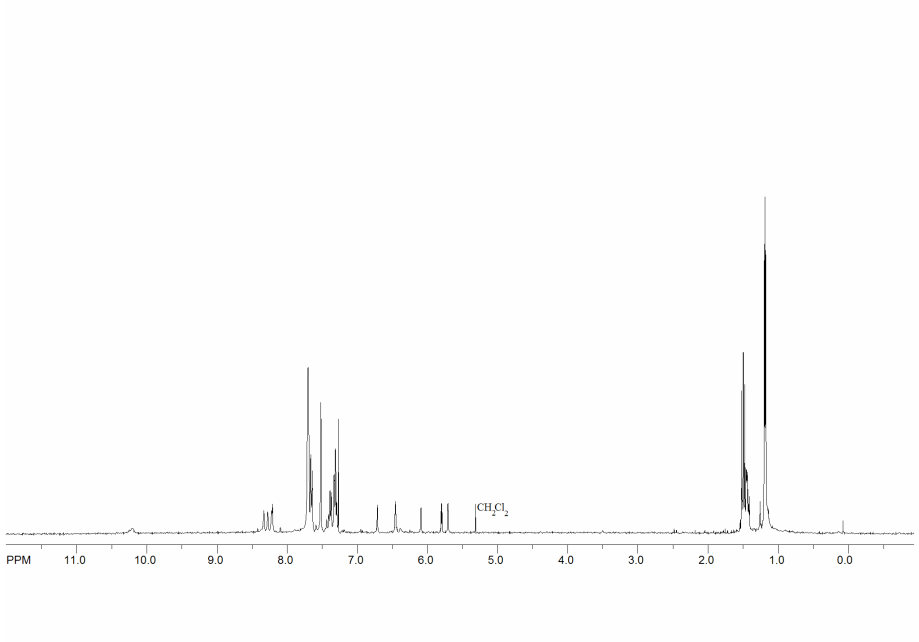

Figure 4.10. ^{1}H NMR spectrum of [MpRu(PPh$_3$)(PMe$_3$)Cl]BAr'$_4$ (**14**) in CDCl$_3$.

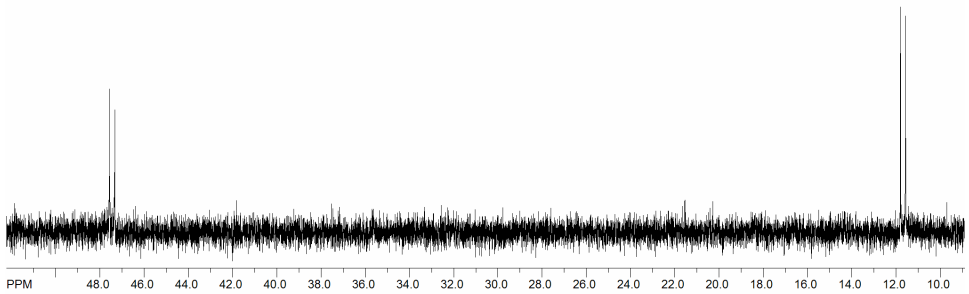

Figure 4.11. ^{31}P NMR spectrum of [MpRu(PPh$_3$)(PMe$_3$)Cl]BAr'$_4$ (**14**) in CDCl$_3$.

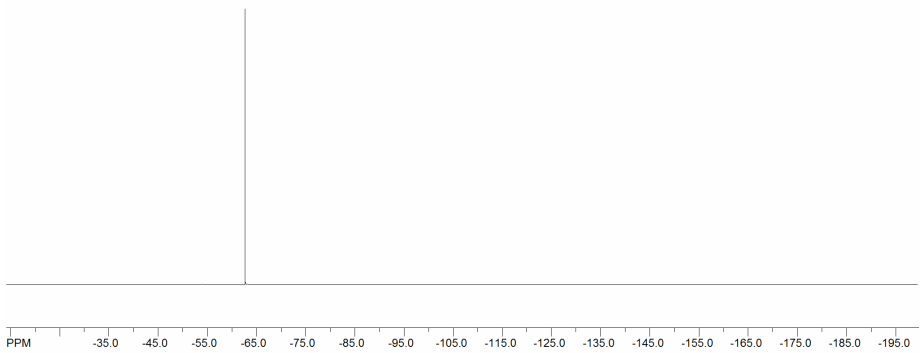

Figure 4.12. ^{19}F NMR spectrum of [MpRu(PPh$_3$)(PMe$_3$)Cl]BAr'$_4$ (**14**) in CDCl$_3$.

The complex [MpRu(PPh$_3$)$_2$Cl]BAr'$_4$ (**15**) was prepared by reacting the previously reported [MpRu(PPh$_3$)$_2$Cl]Cl with NaBAr'$_4$ (Scheme 4.4). ^{1}H and ^{13}C NMR spectroscopy reveal resonances originating due to the Mp 3-, 4-, and 5-positions in a ratio of 2:1. Also consistent with C_s symmetry is the single peak in the ^{31}P NMR spectrum resulting from the equivalent PPh$_3$ ligands. A single peak in the ^{19}F NMR spectrum is observed at -62.6 ppm. From [MpRu(PPh$_3$)$_2$Cl]BAr'$_4$ the complex [MpRu(PPh$_3$)$_2$Me]BAr'$_4$ (**16**) was prepared by reaction with Me$_2$Mg in benzene (Scheme 4.4). A shift in the ^{31}P NMR resonance was observed to occur from 39.3 ppm to 52.1 ppm. A new triplet resonance that integrates for 3H is observed at 0.06 ppm in the ^{1}H NMR spectrum. Cyclic Voltammetry (CV) of **16** reveals the Ru$^{II/III}$ potential at 1.2 V (vs. NHE). No direct electronic comparison can be made between the cationic Mp complex and the Tp analog since TpRu(PPh$_3$)$_2$Me has not been isolated. However, despite the Tp complex containing such a highly efficient π-acid, CO, complex 16 is more electron deficient as indicated by the Ru$^{II/III}$ potential ($E_{1/2}$ = 0.95 V) of the Tp system (TpRu(CO)(NCMe)Me).[9]

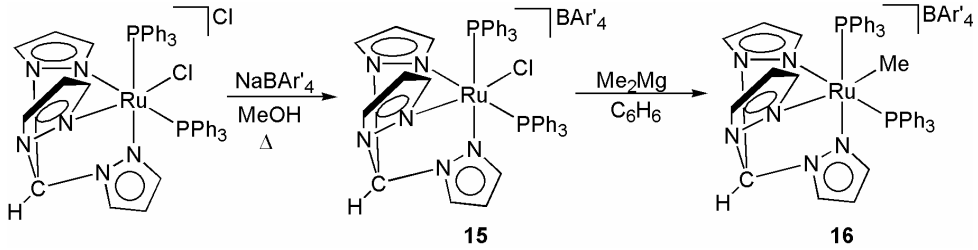

Scheme 4.4. Synthesis of $[MpRu(PPh_3)_2Cl]BAr'_4$ (**15**) and $[MpRu(PPh_3)_2Me]BAr'_4$ (**16**).

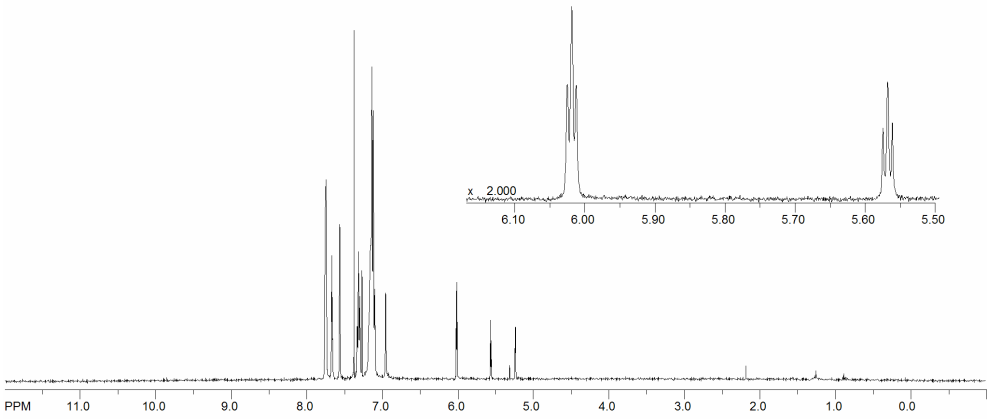

Figure 4.13. ^1H NMR spectrum of $[MpRu(PPh_3)_2Cl]BAr'_4$ (**15**) in $CDCl_3$.

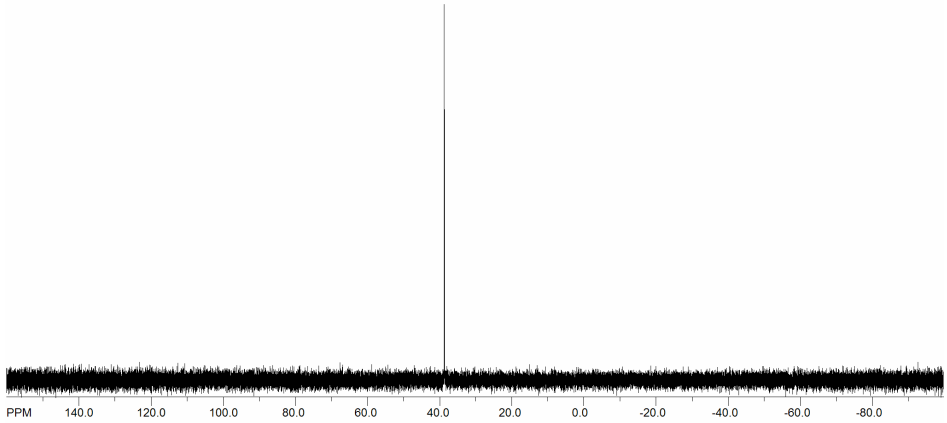

Figure 4.14. ^{31}P NMR spectrum of $[MpRu(PPh_3)_2Cl]BAr'_4$ (**15**) in $CDCl_3$.

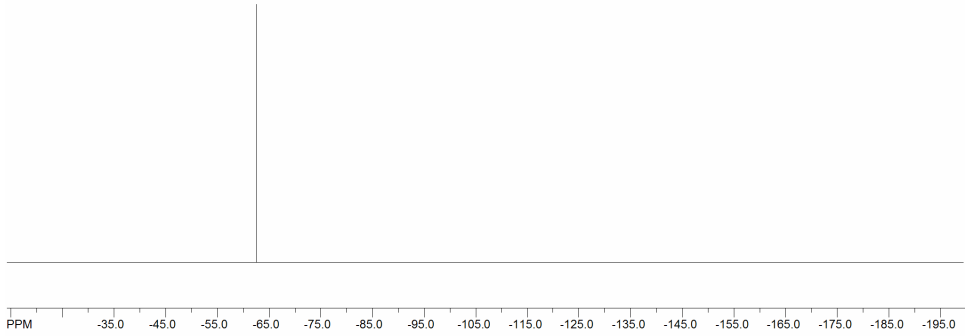

Figure 4.15. ^{19}F NMR spectrum of $[MpRu(PPh_3)_2Cl]BAr'_4$ (**15**) in $CDCl_3$.

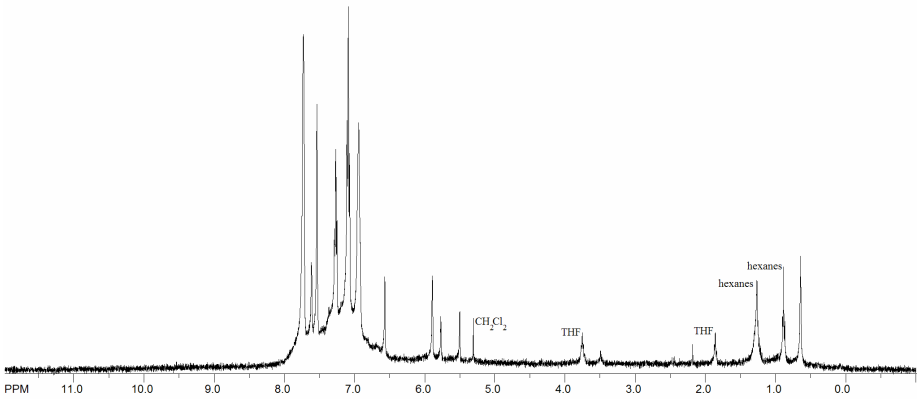

Figure 4.16. ^{1}H NMR spectrum of [MpRu(PPh$_3$)$_2$Me]BAr'$_4$ (**16**) in CDCl$_3$.

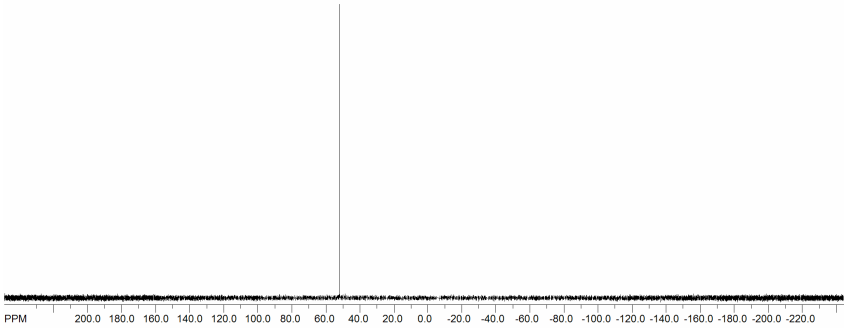

Figure 4.17. ^{31}P NMR spectrum of [MpRu(PPh$_3$)$_2$Me]BAr'$_4$ (**16**) in CDCl$_3$.

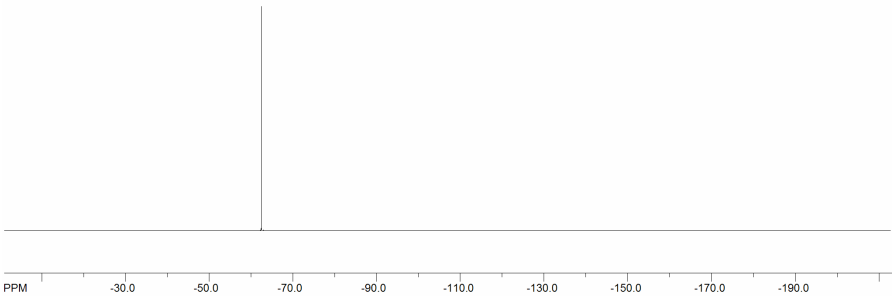

Figure 4.18. ^{19}F NMR spectrum of [MpRu(PPh$_3$)$_2$Me]BAr'$_4$ (**16**) in CDCl$_3$.

Intramolecular C-H activation of a PPh$_3$ ligand is observed when [MpRu(PPh$_3$)$_2$Me]BAr'$_4$ (**16**) was heated (70 ^{o}C) in neat C$_6$D$_6$ (Scheme 4.5). The orthometalated product exhibits two doublets (60 ppm and 40 ppm) with a coupling constant of 40.0 Hz in the ^{31}PNMR spectrum. Interestingly, only CH$_4$ (by ^{1}H NMR spectroscopy) is produced at 70 ^{o}C, however, at 90 ^{o}C both CH$_4$ and CH$_3$D is produced, Figure 4.18, as outlined in Scheme 4.5. Likely, at higher temperatures, C-D activation of benzene is more accessible and therefore also observed.

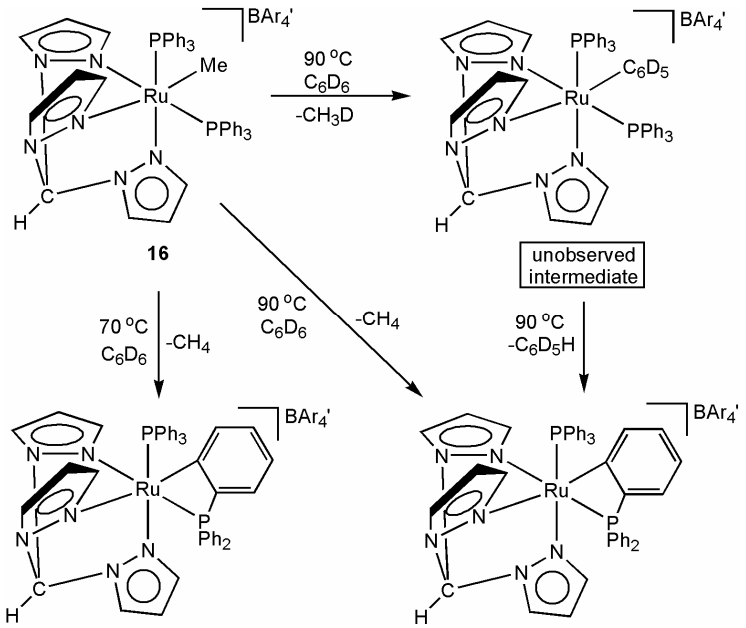

Scheme 4.5. Accessible intramolecular C-H activation and intermolecular C-D activation by $[MpRu(PPh_3)_2Me]BAr'_4$ (**16**) accessed under varying thermolytic conditions.

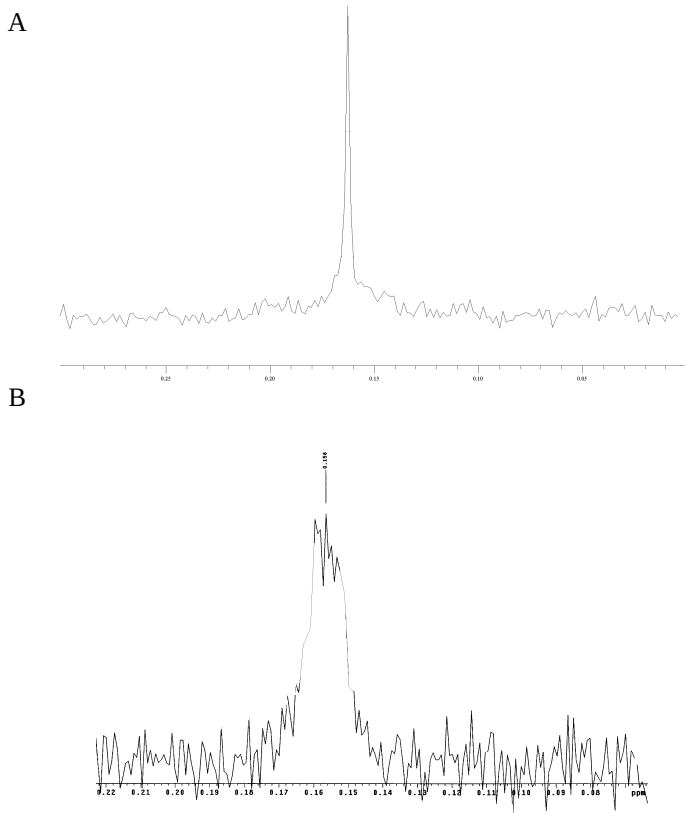

Figure 4.19. (A) CH_4 produced by intramolecular C-H activation of a PPh_3 C-H bond. (B) CH_3D and CH_4 produced by intermolecular C-D activation of C_6D_6 and intramolecular C-H activation of PPh_3 C-H bond.

Preparation of mixed phosphine complexes was also extended to include phosphites. For example, heating (80 ^{o}C) $[MpRu(PPh_3)_2Cl]Cl$ in THF in the presence of $P(OMe)_3$ yields the product $[MpRu(PPh_3)\{P(OMe)_3\}Cl]Cl$ (**17**) and free PPh_3 (Scheme 4.6). Notable upon the coordination of $P(OMe)_3$ is the $^2J_{PP}$ coupling observed in the ^{31}P NMR spectrum. Resonances in the ^{31}P NMR spectrum occur at 138.4 ppm $\{P(OMe)_3\}$ and 142.0 (PPh_3) with a $^2J_{PP}$ = 142 Hz.

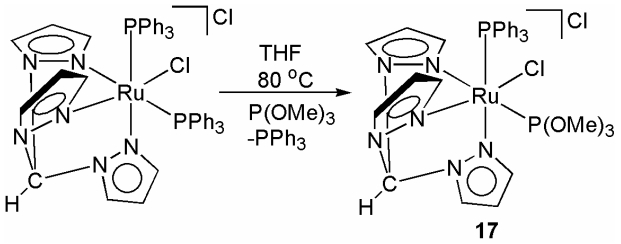

Scheme 4.6. Synthesis of [MpRu(PPh_3){P($OMe)_3$}Cl]Cl (**17**) from [MpRu(PPh_3)$_2$Cl]Cl and P($OMe)_3$.

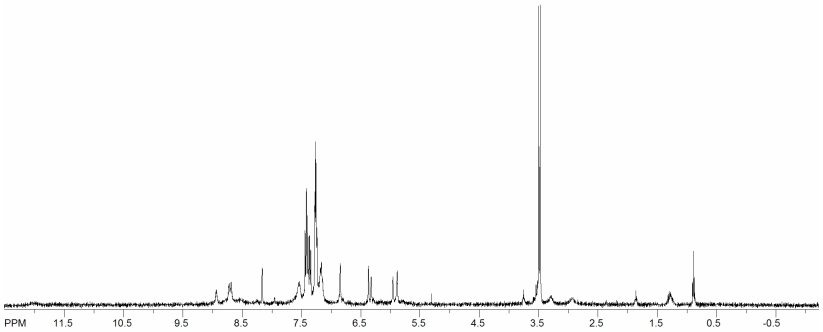

Figure 4.20. ^{1}H NMR spectrum of [MpRu(PPh_3){P($OMe)_3$}Cl]Cl (**17**) in $CDCl_3$.

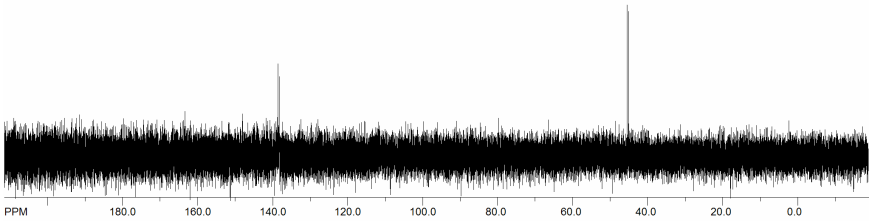

Figure 4.21. ^{31}P NMR spectrum of [MpRu(PPh$_3$){P(OMe)$_3$}Cl]Cl (**17**) in CDCl$_3$.

Photolysis of [MpRu(PPh$_3$)(CO)Cl]BAr'$_4$ (**12**) in the presence of NCMe yields [MpRu(PPh$_3$)(NCMe)Cl]BAr'$_4$ (**18**) (Scheme 4.7). ^{1}H NMR spectroscopy revealed bound NCMe ligand gives a NCC*H*$_3$ resonance at 2.95 ppm.

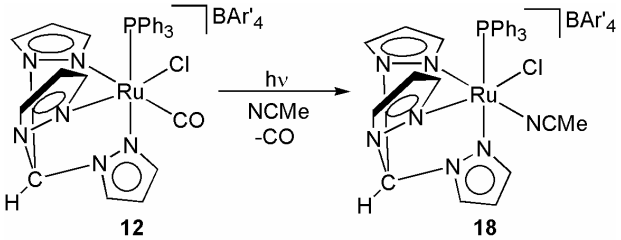

Scheme 4.7. Photolysis of [MpRu(PPh$_3$)(CO)Cl]BAr'$_4$ (**12**) in the presence of NCMe yields [MpRu(PPh$_3$)(NCMe)Cl]BAr'$_4$ (**18**).

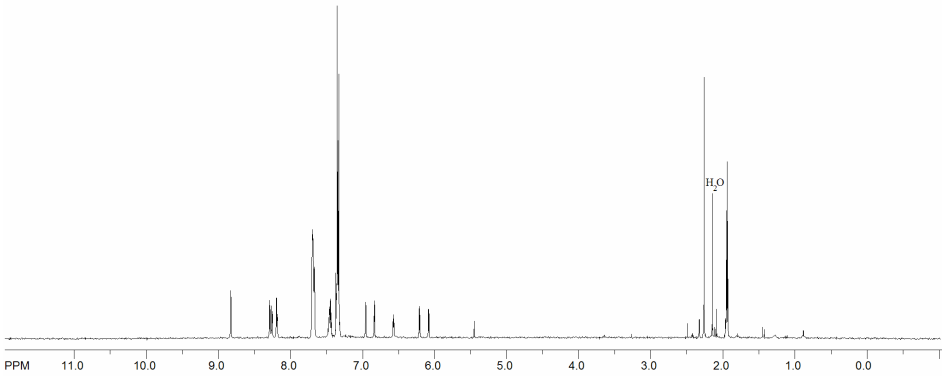

Figure 4.22. ^{1}H NMR spectrum of [MpRu(PPh$_3$)(NCMe)Cl]BAr'$_4$ (**18**) in NCMe-d_3.

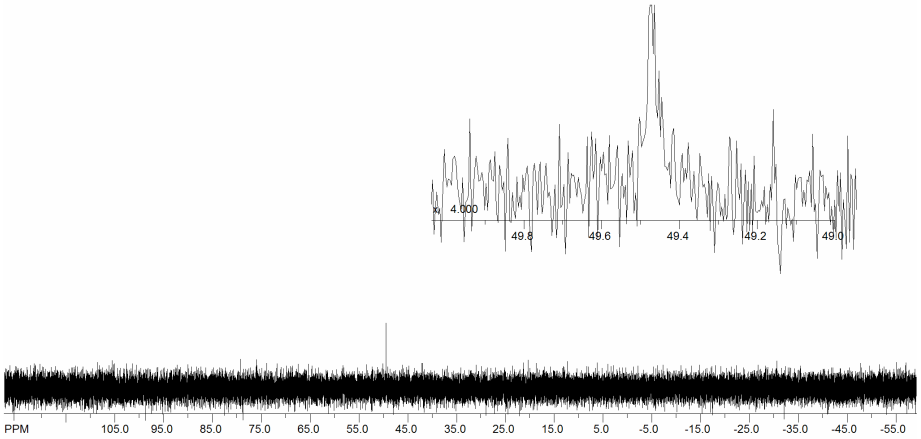

Figure 4.23. ^{31}P NMR spectrum of [MpRu(PPh$_3$)(NCMe)Cl]BAr'$_4$ (**18**) in NCMe-d_3.

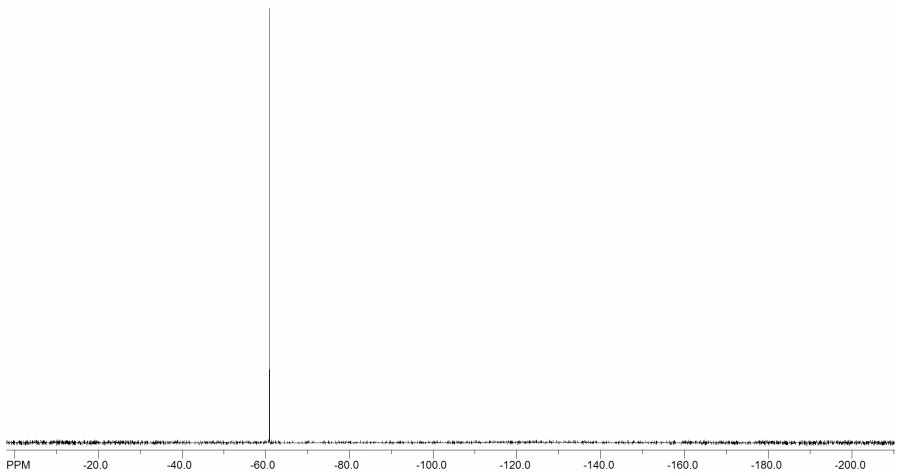

Figure 4.24. ^{19}F NMR spectrum of [MpRu(PPh$_3$)(NCMe)Cl]BAr'$_4$ (**18**) in NCMe-*d*$_3$.

4.3.1.3 Neutral Phosphine Complexes

A series of complexes of the type MpRu(Cl)$_2$PR$_3$ (R = Ph, OMe, or Me) was synthesized. MpRu(PPh$_3$)(Cl)$_2$ (**19**) was prepared by heating [MpRu(PPh$_3$)$_2$Cl]Cl to 130 ^{o}C in THF thereby dissociating one ligand of PPh$_3$ and coordinating the chloride counter-ion (Scheme 4.7). Similarly, the MpRu{P(OMe)$_3$}(Cl)$_2$ (**20**) was prepared by heating [MpRu(PPh$_3$){P(OMe)$_3$}Cl]Cl in THF to 130 ^{o}C (Scheme 4.8). MpRu(PMe$_3$)(Cl)$_2$ (**21**) has been prepared by two different methods (Scheme 4.8). Photolytic scission of the Ru-PPh$_3$ bond of the complex [MpRu(PPh$_3$)(PMe$_3$)Cl]Cl gives MpRu(PMe$_3$)(Cl)$_2$ in 61% isolated yield. Alternatively, thermolysis can also be applied as in the production of MpRu(PR$_3$)(Cl)$_2$ (R = Ph or OMe). For example, heating [MpRu(PPh$_3$)(PMe$_3$)Cl]Cl in THF to 130 ^{o}C gives MpRu(PMe$_3$)(Cl)$_2$ in 79% isolated yield. The MpRu(PR$_3$)(Cl)$_2$ (R = Ph, OMe, or Me) complexes are insoluble in most solvents. This lack of solubility hinders the ability to prepare methyl and phenyl complexes (see below).

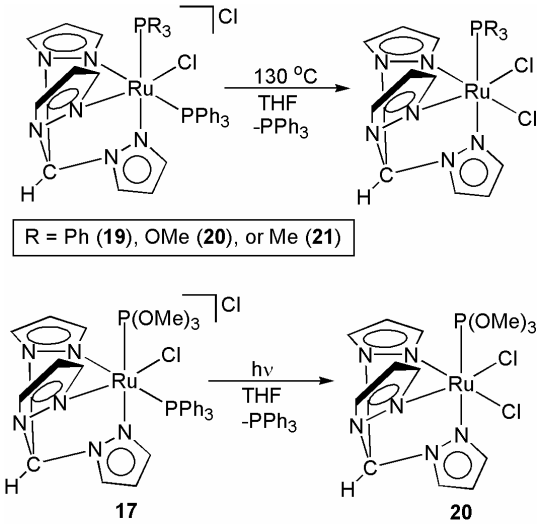

Scheme 4.8. Preparation of complexes of the type $MpRu(PR_3)(Cl)_2$ {R = Ph (**19**), OMe (**20**), or Me (**21**)}.

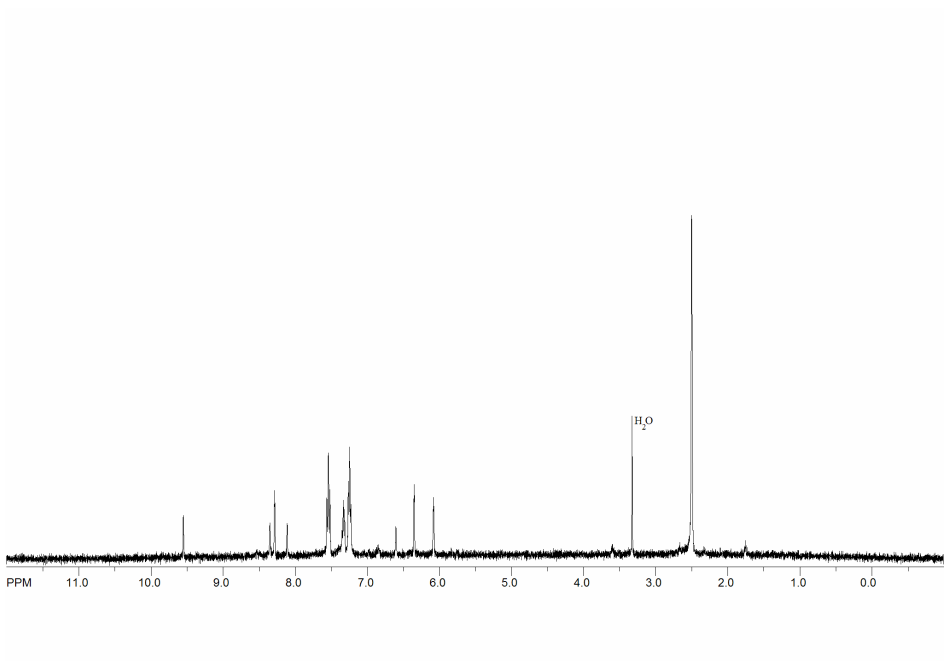

Figure 4.25. ^{1}H NMR spectrum of $MpRu(PPh_3)(Cl)_2$ (**19**) in DMSO-d_6.

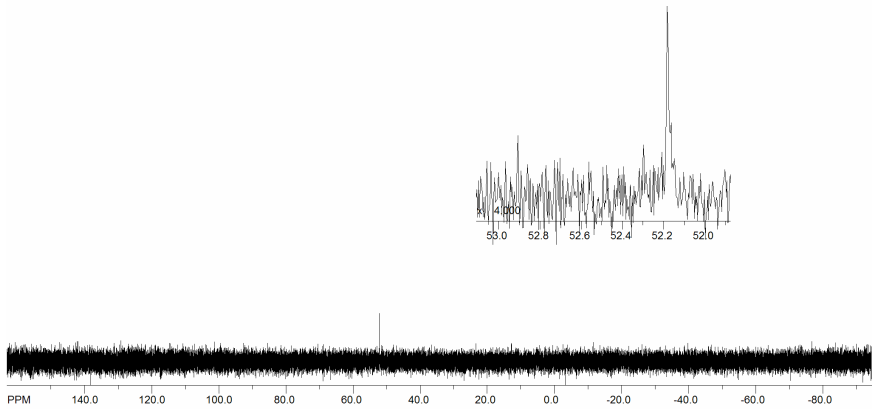

Figure 4.26. ^{31}P NMR spectrum of MpRu(PPh$_3$)(Cl)$_2$ (**19**) in DMSO-d_6.

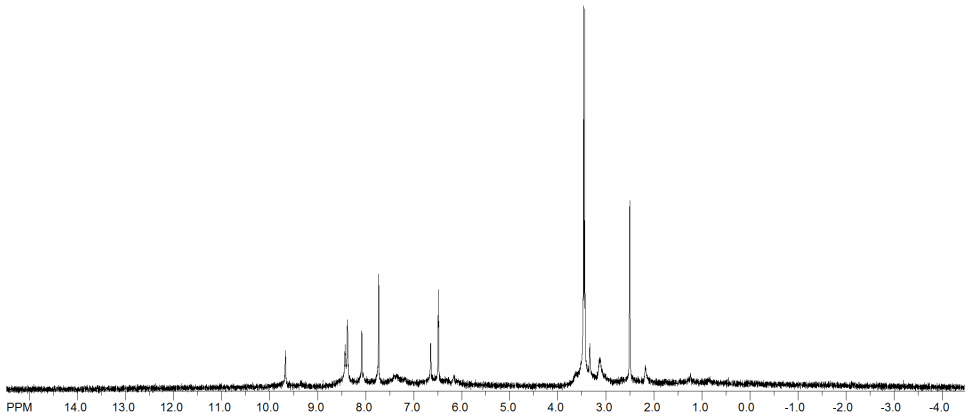

Figure 4.27. ^{1}H NMR spectrum of MpRu{P(OMe)$_3$}(Cl)$_2$ (**20**) in DMSO-d_6.

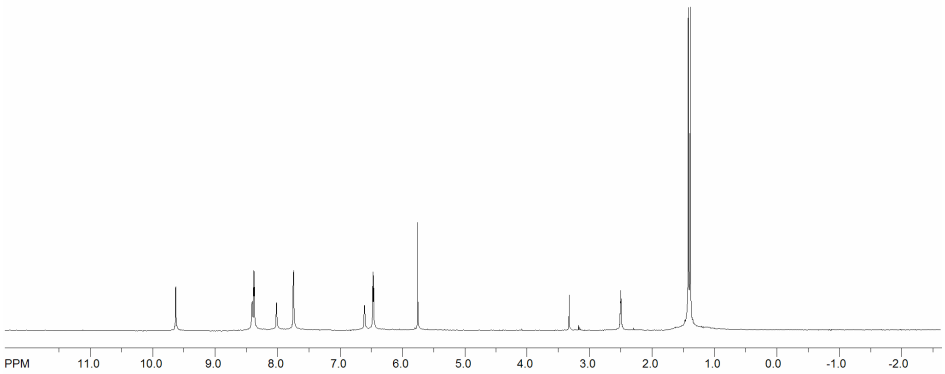

Figure 4.28. ^{1}H NMR spectrum of MpRu(PMe$_3$)(Cl)$_2$ (**21**) in DMSO-d_6.

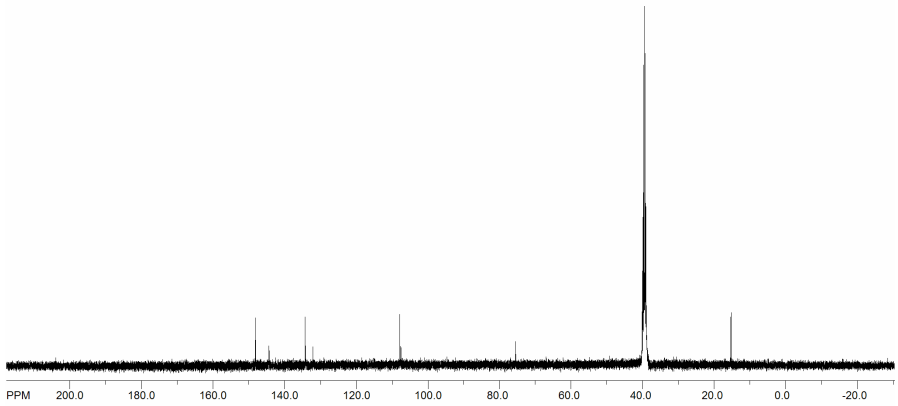

Figure 4.29. ^{13}C NMR spectrum of MpRu(PMe$_3$)(Cl)$_2$ (**21**) in DMSO-d_6.

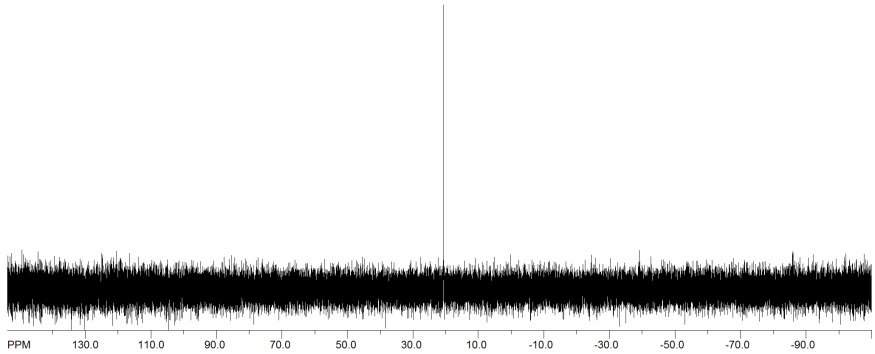

Figure 4.30. ^{31}P NMR spectrum of MpRu(PMe$_3$)(Cl)$_2$ (**21**) in DMSO-d_6.

4.3.2 Ep Complexes

In order to potentially enhance solubility and for protection of the acidic Mp C-H bond, several EpRu(PR$_3$) (R = Ph or Me) were prepared. The Ep ligand was introduced to the metal center by reacting Ep with Ru(PPh$_3$)$_3$(Cl)$_2$ in toluene under reflux conditions to produce EpRu(PPh$_3$)(Cl)$_2$ (**22**) (Scheme 4.9).

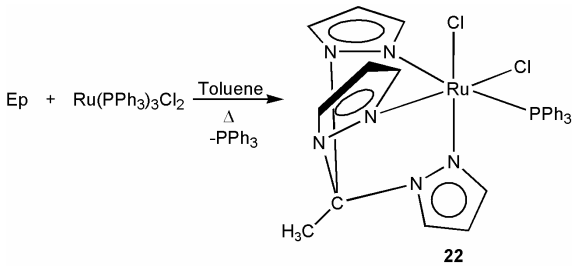

Scheme 4.9. Synthesis of EpRu(PPh$_3$)(Cl)$_2$.

Heating (80 ^{o}C) EpRu(PPh$_3$)(Cl)$_2$ in NCMe in the presence of excess PMe$_3$ produces [EpRu(PPh$_3$)(PMe$_3$)(Cl)]Cl species. During this reaction, spectroscopic observations by ^{31}P NMR spectroscopy are consistent with the formation of the intermediate [EpRu(PPh$_3$)(NCMe)(Cl)]Cl (singlet at 48.2 ppm)

(Scheme 4.10). [EpRu(PPh_3)(NCMe)(Cl)]Cl then reacts with PMe_3 to ultimately convert to [EpRu(PPh_3)(PMe_3)(Cl)]Cl (Scheme 4.10). Formation of a mixed phosphine complex [EpRu(PPh_3)(PMe_3)(Cl)]Cl is indicated by ^{31}P NMR spectroscopy with resonances at 47.8 and 11.2 ppm with 37 Hz coupling (consistent with a *cis*-phosphine arrangement). Due to the inability to cleanly synthesize and isolate the complex [EpRu(PPh_3)(PMe_3)(Cl)]Cl, [EpRu(PPh_3)(PMe_3)(Cl)]Cl was used as an intermediate to produce (THF, 120 ^{o}C) EpRu(PMe_3)$(Cl)_2$ (**23**). Free PPh_3 was observed in the filtrate. Upon reaction between **23** and MeLi, MeMgBr, and Me_2Mg no reaction was observed at ambient or elevated temperatures.

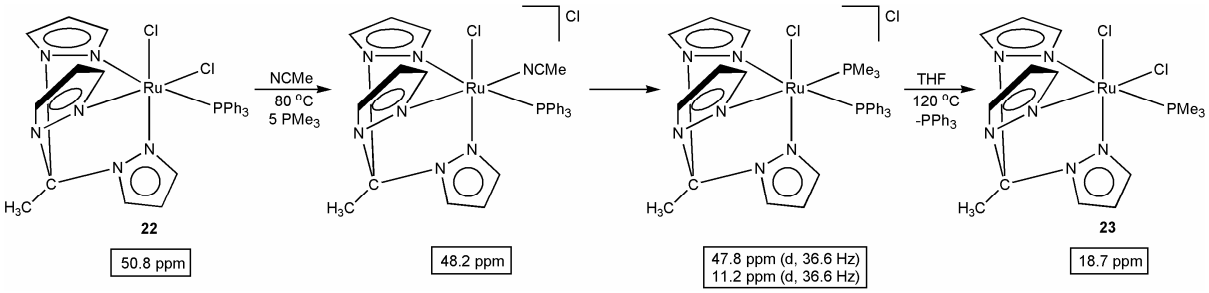

Scheme 4.10. Preparation of EpRu(PMe_3)$(Cl)_2$ (**23**) from EpRu(PPh_3)$(Cl)_2$ (**22**) and PMe_3 with spectroscopic observation of intermediates [EpRu(PPh_3)(NCMe)(Cl)]Cl and [EpRu(PPh_3)(PMe_3)(Cl)]Cl. All resonances listed above are from ^{31}P {^{1}H} NMR spectra in DMSO-d_6.

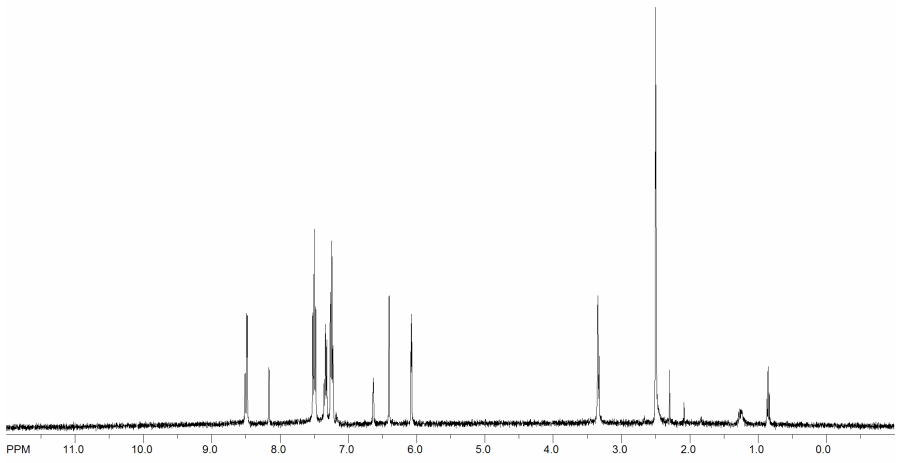

Figure 4.31. ^{1}H NMR spectrum of EpRu(PPh_3)$(Cl)_2$ (**22**) in DMSO-d_6.

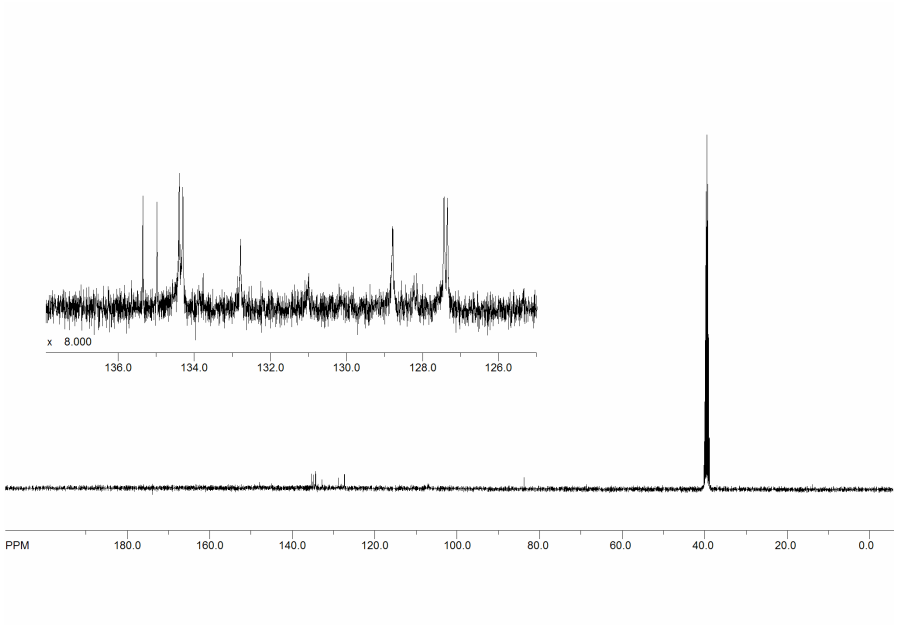

Figure 4.32. ^{13}C NMR spectrum of EpRu(PPh$_3$)(Cl)$_2$ (**22**) in DMSO-d_6.

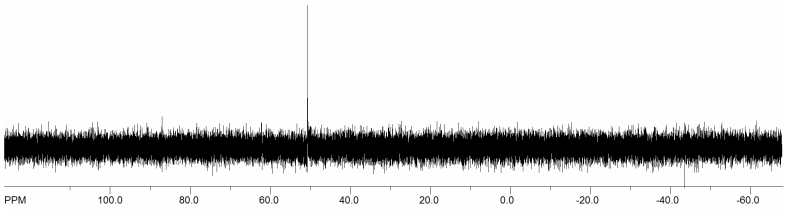

Figure 4.33. ^{31}P NMR spectrum of EpRu(PPh$_3$)(Cl)$_2$ (**22**) in DMSO-d_6.

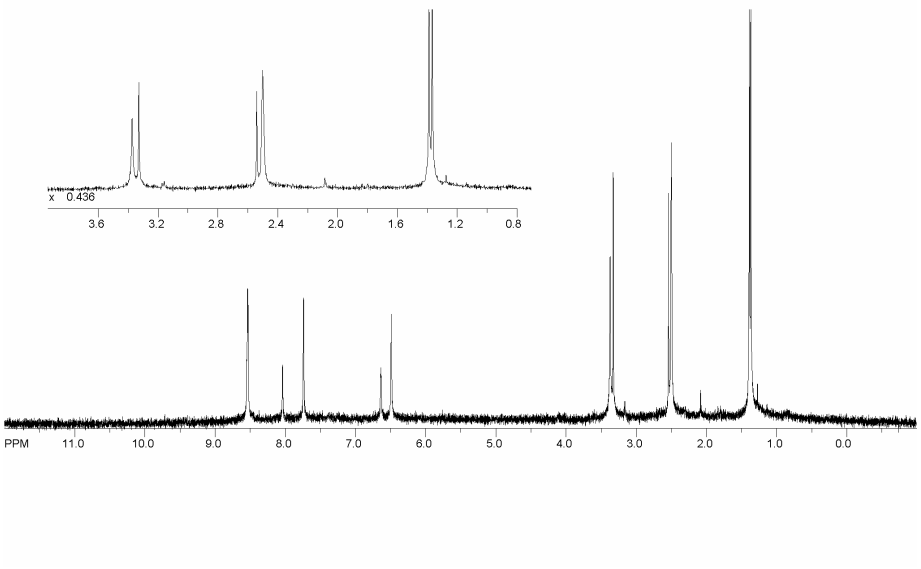

Figure 4.34. ^{1}H NMR spectrum of EpRu(PMe$_3$)(Cl)$_2$ (**23**) in DMSO-d_6.

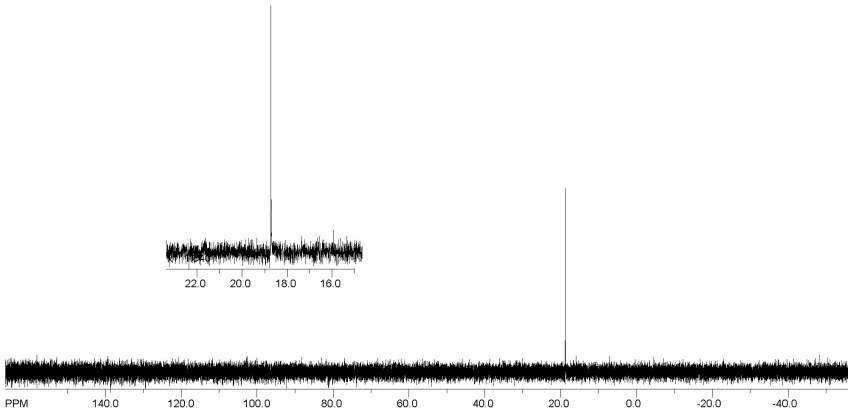

Figure 4.35. ^{31}P NMR spectrum of EpRu(PMe$_3$)(Cl)$_2$ (**23**) in DMSO-d_6.

4.4 Summary

Several new cationic and neutral Ru^{II} complexes containing the Mp or Ep ligand have been synthesized where incorporation of phosphines and other dative ligands has been achieved. These synthetic schemes lay the groundwork for the synthesis of new systems that are potentially active in C-H activation.

4.5 Experimental Section

General Methods. Unless otherwise noted, all synthetic procedures were performed under anaerobic conditions in a nitrogen-filled glovebox or by using standard Schlenk techniques. Glovebox purity was maintained by periodic nitrogen purges and was monitored by an oxygen analyzer (O_2 < 15 ppm for all reactions). Diethyl ether was dried by distillation from sodium/benzophenone. Acetonitrile and methanol were dried by distillation from CaH_2. Hexanes, methylene chloride, and tetrahydrofuran were purified by passage through a column of activated alumina. Acetone-d_6, benzene-d_6, acetonitrile-d_3, dimethylsulfoxide-d_6, and chloroform-d_1 were degassed with three freeze-pump-thaw cycles and stored under a N_2 atmosphere over 4 Å molecular sieves. ^{1}H and ^{13}C NMR spectra were recorded on a Varian Mercury 300 or 400 MHz spectrometer. All ^{1}H and ^{13}C NMR spectra were referenced against tetramethylsilane using residual proton signals (^{1}H NMR) or the ^{13}C resonances of the deuterated solvent (^{13}C NMR). ^{19}F NMR and ^{31}P NMR spectra were obtained on a Varian 400 MHz spectrometer and referenced against an external standard of hexafluorobenzene and phosphoric acid, respectively. IR spectra were acquired using a Mattson Genesis II FT-IR as thin films on KBr plates or in solution using KBr solvent cells. GC-MS was performed using a HP GCD system with a 30 m × 0.25 mm HP-5 column with 0.25 μm film thickness. Complexes $[MpRu(PPh_3)(CO)H]Cl$, $[MpRu(PPh_3)_2Cl]Cl$, $Ru(PPh_3)_3(Cl)_2$, Mp, Ep, and $NaBAr'_4$ have been previously reported.[10-14] All other reagents were used as purchased from commercial sources.

Improved Synthesis of $[MpRu(PPh_3)_2Cl]Cl$. Improved yield by 23%, over the previously reported yield of 53%.[11] A 250 mL round bottom flask was charged with tris(pyrazolyl)methane (0.950 g, 4.44 mmol), $Ru(PPh_3)_3(Cl)_2$ (4.252 g, 4.44 mmol), and THF (150 mL) where the reaction was allowed to stir at room temperature for 5 hrs. The reaction was then filtered on a fine frit. The filtrate was vacuumed to dryness. The

product was precipitated by minimal CH_2Cl_2 and excess hexanes. The yellow solid was collected on a fine frit, washed with pentane, and dried under vacuum overnight yielding 3.0875 g (76%).

[MpRu(PPh$_3$)(CO)H]BAr'$_4$ (11). [MpRu(PPh$_3$)(CO)H]Cl (0.377 g, 0.537 mmol) and NaBAr'$_4$ (0.476 g, 0.537 mmol) were placed in a 100 mL round bottom flask and taken up in 80 mL of THF. The reaction flask, equipped with a Vigreaux column, was heated to reflux in a glovebox, under N_2, for 3 h. During reflux the reaction solution became homogeneous. After heating, the solution was allowed to cool to room temperature. The reaction flask was evacuated of all volatiles under vacuum. The dried product was taken up in 5 mL of CH_2Cl_2 and passed through a plug of Celite by gravity filtration. The filtrate was transferred to a round bottom flask where the volatiles were removed under vacuum. The dried product was then taken up in MeOH and passed through a second plug of Celite. The filtrate was evacuated of all volatiles and the product scraped out and dried for 3 h under vacuum. IR (KBr): ν_{CO} = 1947 cm^{-1}. ^{1}H NMR (CD$_3$OD, δ): 9.44 (1H, s, Mp apical position), 8.36, 8.28, 8.24, 8.10 (1H, d, J_{HH} = 2.8 Hz, Mp C*H* 3 or 5 position), 7.59 (8H, s, BAr'$_4$), 7.47 (7H, m, PPh$_3$ *para*-position and BAr'$_4$), 7.35 (12H, m, PPh$_3$ *meta- and ortho*-position), 6.91, 6.63 (1H, d, J_{HH} = 2.8 Hz, Mp C*H* 3 or 5 position), 6.56, 6.42, 6.15 (1H, t, J_{HH} = 2.4 Hz, Mp C*H* 4 position), -12.25 (1H, d, J_{HP} = 26.4, Ru-*H*). ^{31}P{^{1}H} NMR (CD$_3$OD, δ): 65.6 (s, PPh$_3$). ^{19}F{^{1}H} NMR (CD$_3$OD, δ): 65.5 (s, BAr'$_4$).

[MpRu(PPh$_3$)(CO)Cl]BAr'$_4$ (12). [MpRu(PPh$_3$)(CO)H]BAr'$_4$ (0.015 g, 0.10 mmol) was taken up in $CHCl_3$ (6 mL) (0.310g, 1.36 mmol) and placed in a 100 mL round bottom flask. The reaction flask was equipped with a Vigreaux column and heated to reflux in a glovebox, under N_2, for 2 days. After heating, the solution was allowed to cool to room temperature. The mixture was then evacuated of all volatiles and scraped from the flask. The product was dried overnight in under vacuum leaving a yellow solid. IR (KBr): ν_{CO} = 2000 cm^{-1}. ^{1}H NMR (CDCl$_3$, δ): 8.20, 7.79, 7.78 (1H, s, Mp C*H* 3 or 5 position), 7.72 (8H, s, BAr'$_4$), 7.63 (1H, d, Ep C*H* 3 or 5 position), 7.50 (13H, m, PPh$_3$ and BAr'$_4$), 7.39 (6H, m, PPh$_3$), 6.81 (1H, s, Mp C*H* 3 or 5 position), 6.50, 6.18 (1H, t, Mp C*H* 4 position), 6.13 (1H, s, Mp C*H* 3 or 5 position), 5.93 (1H, t, Mp C*H* 4 position).

[MpRu(PPh$_3$)(PMe$_3$)Cl]Cl (13). [MpRu(PPh$_3$)$_2$Cl]Cl (0.504 g, 0.553 mmol) was taken up in 30 mL of THF in a 50 mL thick-walled glass vessel. Upon addition of PMe$_3$ (0.098 mL, 1.11 mmol) immediate attenuation of color intensity was observed. The heterogeneous solution was stirred overnight in a 50 mL

thick-walled glass vessel and stirred at ambient conditions 12 hours. The solution was purged into the glovebox where all volatiles were removed by vacuum. The product was crashed out with CH_2Cl_2 and hexanes, collected on a fine frit, and washed with pentane. The yellow product was dried overnight under dynamic vacuum (0.384 g, 95.8%). ^{1}H NMR ($CDCl_3$, δ): 8.92, 8.75, 8.67, 8.13, (1H, d, J_{HH} = 2.4 Hz, Mp C*H* 3 or 5 position), 7.66 (6H, d, J_{HH} = 9.2 Hz, PPh_3 *ortho*-position), 7.38 (3H, td, J_{HH} = 2.0 Hz and 7.6 Hz, PPh_3 *para*-position), 7.30 (6H, td, J_{HH} = 2.0 Hz and 8.0 Hz, PPh_3 *meta*-position), 6.64 (1H, d, J_{HH} = 2.4 Hz, Mp 3 or 5 position), 6.46, 6.02, 5.85 (1H, t, J_{HH} = 2.6 Hz, Mp C*H* 4-position), 5.68 (1H, d, J_{HH} = 2.4 Hz, Mp C*H* 3 or 5 position), 1.19 (9H, d, J_{PH} = 8.4 Hz, PMe_3). ^{13}C NMR ($CDCl_3$): 147.5, 146.8, 145.0, 135.7, 134.8, 134.5 (1C, s, Mp 3 or 5 position), 134.1 (6C, d, J_{CP} = 37.3 Hz, PPh_3 *ortho*-position), 133.9 (3C, s, *para*-position), 130.0 (3C, d, J_{CP} = 12.4 Hz, PPh_3 *ipso*-position), 128.5 (6C, d, J_{CP} = 9.2 Hz, PPh_3 *meta*-position), 108.4, 107.9, 107.7 (1C, s, Mp 4 position), 74.2 (1C, s, Mp apical position), 17.1 (3C, d, PMe_3 *C*H_3). ^{31}P{^{1}H} NMR ($CDCl_3$, δ): 48.2 (d, PPh_3), 12.2 (d, PMe_3).

[MpRu(PPh$_3$)(PMe$_3$)Cl]BAr'$_4$ (14). [MpRu(PPh_3)(PMe_3)Cl]Cl (0.857 g, 1.09 mmol) and NaBAr'$_4$ (0.843 g, 1.20 mmol) were placed in a 250 mL round bottom flask and taken up in 150 mL of MeOH. The reaction flask equipped with a Vigreaux column and heated to reflux in a glovebox, under N_2, for 30 minutes. After heating, the solution was allowed to cool to room temperature and then evacuated of all volatiles by vacuum. The product was then taken up in CH_2Cl_2 and passed through a plug of Celite. The filtrate was then filtered on a fine frit by gravity filtration. The Celite plug was then rinsed with 50 mL of CH_2Cl_2. The filtrate was dried in a 100 mL round bottom flask under vacuum and product was scraped out and dried overnight. ^{1}H NMR ($CDCl_3$, δ): 10.20 (1H, s, Mp apical C*H*), 8.33, 8.28, 8.23, 8.21 (1H, d, J_{HH} = 2.4 Hz, Mp C*H* 3 or 5 position), 7.70 (8H, s, BAr'$_4$ *ortho*-position), 7.65 (6H, d, J_{HH} = 9.2 Hz, PPh_3 *ortho*-position), 7.52 (4H, s, BAr'$_4$ *para*-position), 7.38 (3H, dd, J_{HH} = 1.6 Hz and 7.2 Hz, PPh_3 *para*-position), 7.31 (6H, td, J_{HH} = 2.0 Hz and 8.0 Hz, PPh_3 *meta*-position), 6.71 (1H, d, J_{HH} = 2.4 Hz, Mp 3 or 5 position), 6.46, 6.09, 5.80 (1H, t, J_{HH} = 2.4 Hz, Mp C*H* 4-position), 5.71 (1H, d, J_{HH} = 2.4 Hz, Mp C*H* 3 or 5 position), 1.19 (9H, t, J_{PH} = 4.0 Hz, PMe_3). ^{31}P{^{1}H} NMR ($CDCl_3$, δ): 47.4 (d, J_{PP} = 37.3 Hz, PPh_3), 11.7 (d, J_{PP} = 37.3 Hz, PMe_3). ^{19}F{^{1}H} NMR ($CDCl_3$, δ): -62.7 (s, BAr'$_4$ C*F*$_3$).

[MpRu(PPh$_3$)$_2$Cl]BAr'$_4$ (15). [MpRu(PPh_3)$_2$Cl]Cl (1.438 g, 1.58 mmol) and NaBAr'$_4$ (1.220 g, 1.74 mmol) were placed in a 250 mL round bottom flask and taken up in 150 mL of methanol. The reaction flask

was equipped with a Vigreaux column and heated to reflux in a glovebox, under N_2, for 1 h. The volatiles were removed by vacuum. The solid was taken up in CH_2Cl_2 and passed through Celite. The filtrate was then vacuumed to dryness and taken up in C_6H_6 where a brown oil formed on the glass walls. The yellow solution was decanted into a clean round bottom flask where the product was precipitated out with hexanes and collected on a fine frit. The product was rinsed with pentane and dried overnight (0.710 g, 79%). ^{1}H NMR (CD_2Cl_2, δ): 8.01 (1H, s, Mp apical C*H*), 7.98 (1H, d, J_{HH} = 2.4 Hz, Mp C*H* 3 or 5 position), 7.87 (2H, d, J_{HH} = 2.8 Hz, Mp C*H* 3 or 5 position), 7.73 (8H, s, BAr'$_4$ *ortho*-position), 7.56 (4H, s, BAr'$_4$ *para*-position), 7.56 (6H, t, J_{HH} = 7.2 Hz, PPh_3 *para*-position), 7.14 (24H, multiplet, PPh_3 *ortho*- and *meta*-position), 6.95 (2H, d, J_{HH} = 2.4 Hz, Mp C*H* 3 or 5 position), 6.07 (2H, t, J_{HH} = 2.4 Hz, Mp C*H* 4 position), 5.70 (1H, t, J_{HH} = 2.4 Hz, Mp C*H* 4 position), 5.28 (1H, d, J_{HH} = 2.4 Hz, Mp C*H* 3 or 5 position). ^{13}C NMR ($CDCl_3$): 161.7 (4C, q, $^1J_{CB}$ = 49.5 Hz, BAr'$_4$ *ipso*-position), 150.9 (1C, s, Mp 3 or 5 position), 148.7 (2C, s, Mp 3 or 5 position), 134.9 (2C, s, BAr'$_4$ *ortho*-position), 134.2 (12C, t, J_{CP} = 4.1 Hz, PPh_3 *ortho*-position), 133.2 (6C, multiplet, PPh_3 *ipso*-position), 130.1 (6C, s, PPh_3 *para*-position), 129.2, 128.8 (8C, q, $^1J_{CP}$ = 2.8 Hz, BAr'$_4$ *meta*-position), 128.2 (12C, t, J_{CP} = 4.1 Hz, PPh_3 *meta*-position), 122.9 (2C, s, Mp 3 or 5 position), 119.3 (1C, s, Mp 3 or 5 position), 117.6 (4C, t, $^3J_{CF}$ = 4.2 Hz, PPh_3 *para*-position), 109.1 (2C, s, Mp 4 position), 108.4 (1C, s, Mp 4 position), 76.1 (1C, s, Mp apical position). ^{31}P{^{1}H} NMR ($CDCl_3$, δ): 39.31 (s, PPh_3). ^{19}F{^{1}H} NMR ($CDCl_3$, δ): -62.59 (s, BAr'$_4$). Anal. Calcd. For $C_{78}H_{52}N_6P_2Cl_1F_{24}B_1Ru_1$: C, 53.89; H, 3.02; N, 4.83. Found: C, 54.47; H, 3.02; N, 5.22.

[MpRu(PPh$_3$)$_2$Me]BAr'$_4$ (16). [MpRu(PPh_3)$_2$Cl]BAr'$_4$ (0.2168 g, .125 mmol) and Me_2Mg (0.007 g, 0.125 mmol) were placed in a 100 mL round bottom flask and taken up in 50 mL of benzene. After 3 days of stirring the reaction, the solution became homogeneous. The reaction was purged into the box and evacuated of all volatiles by vacuum. The brown product was then taken up in CH_2Cl_2 and passed through a plug of Celite. The yellow filtrate was precipitated by CH_2Cl_2 and hexanes and collected on a fine frit by vacuum filtration.

^{1}H NMR ($CDCl_3$, δ): 7.73 (8H, s, BAr'$_4$ *ortho*-position), 7.62 (2H, Mp C*H* 3 or 5 position), 7.54 (4H, s, BAr'$_4$ *para*-position), 7.27 (6H, t, J_{HH} = 7.2 Hz, PPh_3 *para*-position), 7.26 (1H, s, Mp C*H* 3 or 5 position), 7.09 (12H, t, J_{HH} = 7.6 Hz, PPh_3 *meta*-position), 6.94 (12H, s, PPh_3 *ortho*-position), 6.57 (2H, s, J_{HH} = 2.4 Hz, Mp 3 or 5 position), 5.89 (2H, t, Mp C*H* 4-position), 5.77 (1H, t, Mp C*H* 4-position), 5.50 (1H, d, J_{HH} = 2.0 Hz, Mp C*H*

3 or 5 position), 0.06 (3H, t, Ru-C*H*$_3$). ^{31}P{^{1}H} NMR (CDCl$_3$, δ): 52.1 (s, PPh$_3$). ^{19}F{^{1}H} NMR (CDCl$_3$, δ): -62.4 (s, BAr'$_4$ C*F*$_3$). CV: $E_{1/2}$ = 1.19 V.

[MpRu(PPh$_3$){P(OMe)$_3$}Cl]Cl (17). [MpRu(PPh$_3$)$_2$Cl]Cl (0.500 g, 0.550 mmol) was taken up in 30 mL of THF in a 50 mL thick-walled glass vessel. Upon addition of P(OMe)$_3$ (0.065 mL, 0.550 mmol) the solution was heated in an 80 ^{o}C oil bath for 6 hours. Upon heating, the solution became homogeneous. The solution was filtered under N$_2$ and the filtrate was evacuated of all volatiles. The product was precipitated by CH$_2$Cl$_2$ and collected on a fine frit by vacuum filtration. The product was washed with pentane (50 mL). The yellow product was dried overnight under dynamic vacuum. ^{1}H NMR (CDCl$_3$, δ): 8.94, 8.72, 8.69, 8.16, (1H, s, Mp C*H* 3 or 5 position), 7.42 (6H, t, J_{HH} = 9.2 Hz, PPh$_3$ *ortho*-position), 7.36 (3H, t, J_{HH} = 7.2 Hz, PPh$_3$ *para*-position), 7.26 (6H, t, J_{HH} = 7.2 Hz, PPh$_3$ *meta*-position), 6.85, 6.37 (1H, s, Mp 3 or 5 position), 6.33, 5.96, 5.89 (1H, t, Mp C*H* 4-position), 3.48 (9H, d, J_{PH} = 10.4 Hz, P(OMe)$_3$). ^{31}P{^{1}H} NMR (CDCl$_3$, δ): 138.4 (d, J_{PP} = 142.0 Hz, P(OMe)$_3$), 45.2 (d, J_{PP} = 142.0 Hz PPh$_3$).

[MpRu(PPh$_3$)(NCMe)Cl]BAr'$_4$ (18). [MpRu(PPh$_3$)(CO)Cl]BAr'$_4$ (0.256 g, 0.180 mmol) was placed in a 100 mL thick-walled glass vessel and taken up in NCMe (50 mL) stirred in the presence of a photolysis lamp for 3 days. The reaction was brought back into the glovebox and evacuated of all volatiles. The product was taken up in minimal CH$_2$Cl$_2$ and precipitated with hexanes. The yellow product was dried in the desiccator overnight. IR (KBr): ν_{CN} = 2940 cm^{-1}. ^{1}H NMR (CD$_3$CN, δ): 8.83 (1H, s, Mp apical position), 8.29, 8.26, 8.19, 8.18 (1H, d, J_{HH} = 2.8 Hz, Mp C*H* 3 or 5 position), 7.70 (8H, m, BAr'$_4$ *ortho*-position), 7.67 (4H, s, BAr'$_4$ *para*-position), 7.45 (3H, m, PPh$_3$ *para*-position), 7.34 (12H, m, PPh$_3$ *para*- and *meta*-position), 6.96, 6.84 (1H, d, Mp C*H* 3 or 5 position), 6.57 (1H, m, Mp C*H* 4-position), 6.21, 6.08 (1H, t, J_{HH} = 2.8 Hz, Mp C*H* 4 position), 2.26 (3H, s, NCC*H*$_3$). ^{31}P{^{1}H} NMR (CD$_3$CN, δ): 49.47 (s, PPh$_3$). ^{19}F{^{1}H} NMR (CD$_3$CN, δ): 60.8 (s, BAr'$_4$). Anal. Calcd. For [MpRu(NCMe)(PPh$_3$)(Cl)]BAr$^F_4$: C, 49.08; H, 2.66; N, 6.46. Found: C, 48.25; H, 2.66; N, 6.39.

MpRu(PPh$_3$)(Cl)$_2$ (19). [MpRu(PPh$_3$)$_2$Cl]Cl (0.489 g, 0.592 mmol) and THF (35 mL) were deposited into a 50 mL thick walled glass reaction vessel forming a heterogeneous solution. Upon 2 minutes of heating the reaction vessel in a 130 ^{o}C oil bath the reaction became homogeneous. Upon 5 minutes of heating, a yellow solid began precipitating from solution. After 20 minutes of heating, the product was recovered on a fine frit,

under N_2, by vacuum filtration. The amorphous solid (0.2646 g, 79%) collected was rinsed with 50 mL of pentane and allowed to dry under vacuum overnight. ^{1}H NMR (DMSO-d_6, δ): 9.55 (1H, s, Mp apical position), 8.35 (1H, d, Mp C*H* 3 or 5 position), 8.29 (2H, d, Mp C*H* 3 or 5 position), 8.11 (1H, d, Mp 3 or 5 position), 7.54 (6H, t, J_{HH} = 8.8 Hz, PPh_3 *ortho*- or *meta*-position), 7.34 (6H, t, J_{HH} = 7.2 Hz, PPh_3 *para*-position), 7.25 (6H, t, J_{HH} = 7.2 Hz, PPh_3 *ortho*- or *meta*-position), 6.61 (1H, m, Mp C*H* 4-position), 6.35 (2H, d, Mp C*H* 3 or 5 position), 6.09 (2H, t, Mp C*H* 4 position). ^{31}P{^{1}H} NMR (DMSO-d_6, δ): 52.2 (s, PPh_3).

MpRu(P(OMe)$_3$)(Cl)$_2$ (20). [MpRu(PPh_3)(P(OMe)$_3$)Cl]Cl (0.258 g, 0.334 mmol) was taken up in 50 mL of THF in a thick walled glass reaction vessel and heated in a 130 ^{o}C oil bath for 3 h. The product precipitated during thermolysis and was collected on a fine frit, under N_2, by vacuum filtration. The yellow solid was rinsed with THF and allowed to dry under vacuum overnight. ^{1}H NMR (DMSO-d_6, δ): 9.67 (1H, s, Mp apical C*H*), 8.28 (1H, s, Mp C*H* 3 or 5 position), 8.38 (2H, s, Mp C*H* 3 or 5 position), 8.08 (1H, s, Mp C*H* 3 or 5 position), 7.73 (2H, s, Mp C*H* 3 or 5 position), 6.65 (1H, s, Mp C*H* 4-position), 6.49 (2H, s, Mp C*H* 4 position), 3.45 (9H, d, J_{HP} = 10.4 Hz, P(OMe)$_3$).

MpRu(PMe$_3$)(Cl)$_2$ (21). Method A (Photolysis): [MpRu(PPh_3)(PMe_3)Cl]Cl (0.140 g, 0.180 mmol) was taken up in 90 mL of THF in a thick walled glass reaction vessel and photolyzed for 37 hours with stirring. The product precipitated during photolysis and was collected on a fine frit, under N_2, by vacuum filtration. The yellow solid was rinsed with pentane and allowed to dry under vacuum overnight yielding 0.064 g of product (77.1%). **Method B (Thermolysis):** [MpRu(PPh_3)(PMe_3)Cl]Cl (0.500 g, 0.636 mmol) was taken up in 90 mL of THF in a thick walled glass reaction vessel and heated in a 130 ^{o}C oil bath for 3 days. The product precipitated during thermolysis and was collected on a fine frit, under N_2, by vacuum filtration. The yellow solid was rinsed with NCMe, THF, CH_2Cl_2, hexanes, and Et_2O and then allowed to dry under vacuum overnight yielding 0.180 g of product (61.3%). ^{1}H NMR (DMSO-d_6, δ): 9.63 (1H, s, Mp apical C*H*), 8.41 (1H, d, J_{HH} = 2.7 Hz, Mp C*H* 3 or 5 position), 8.37 (2H, d, J_{HH} = 2.7 Hz, Mp C*H* 3 or 5 position), 8.02 (1H, s, Mp C*H* 3 or 5 position), 7.75 (2H, d, J_{HH} = 2.7 Hz, Mp C*H* 3 or 5 position), 6.61 (1H, t, JHH = 2.7 Hz, Mp C*H* 4-position), 6.47 (2H, d, J_{HH} = 2.7 Hz, Mp C*H* 3 or 5 position), 6.08 (9H, d, J_{HP} = 9.0 Hz, PMe_3). ^{13}C NMR (DMSO-d_6): 148.1 (2C, s, Mp 3 or 5 position), 144.4 (1C, s, Mp 3 or 5 position), 134.3 (2C, s, Mp 3 or 5 position), 132.1

(1C, s, Mp 3 or 5 position), 107.9 (2C, s, Mp 4 position), 107.6 (1C, s, Mp 4 position), 75.6 (1C, s, Mp apical position), 15.3 (3C, d, J_{CP} = 27.5 Hz, PMe_3 CH_3). $^{31}P\{^1H\}$ NMR (DMSO-d_6, δ): 20.73 (s, PMe_3).

$EpRu(PPh_3)(Cl)_2$ (22). $Ru(PPh_3)_3(Cl)_2$ (1.303 g, 1.36 mmol) and Ep (0.310g, 1.36 mmol) were placed in a 100 mL round bottom flask and taken up in 80 mL of toluene. The reaction flask equipped with a Vigreaux column and heated to reflux in a glovebox, under N_2, for 6 h. During reflux the reaction solution turned from a homogeneous brown solution to a heterogeneous yellow solution. After heating, the solution was allowed to cool to room temperature. The mixture was then filtered on a fine frit and rinsed with 50 mL of pentane and then dried overnight in under vacuum leaving a yellow solid (0.710 g, 79%). ^1H NMR (DMSO-d_6, δ): 8.52 (1H, s, Ep C*H* 3 or 5 position), 8.48 (2H, d, J_{HH} = 8.8 Hz, Ep C*H* 3 or 5 position), 8.16 (1H, d, Ep C*H* 3 or 5 position), 7.50 (6H, t, J_{HH} = 8.8 Hz, PPh_3 *ortho*-position), 7.34 (3H, t, J_{HH} = 7.4 Hz, PPh_3 *para*-position), 7.24 (6H, t, J_{HH} = 7.4 Hz, PPh_3 *meta*-position), 6.64 (1H, m, Ep C*H* 4-position), 6.41 (2H, d, J_{HH} = 2.0 Hz, Ep C*H* 3 or 5 position), 6.08 (2H, t, J_{HH} = 3.2 Hz, Ep C*H* 4 position), 3.35 (3H, s, Ep CH_3). ^{13}C NMR (DMSO-d_6): 147.9 (3C, d, J_{CP} = 2.6 Hz, PPh_3 *para*-position), 144.9 (1C, s, Ep 3 or 5 position), 135.2 (3C, d, J_{CP} = 37.3 Hz, PPh_3 *ipso*-position), 134.3 (6C, d, J_{CP} = 9.2 Hz, PPh_3 *ortho*-position), 132.8 (2C, s, Ep 3 or 5 position), 131.0 (1C, s, Ep 3 or 5 position), 128.8 (2C, s, Ep 3 or 5 position), 127.4 (6C, d, J_{CP} = 8.5Hz, PPh_3 meta-position), 107.2 (1C, s, Ep 4 position), 106.9 (2C, s, Ep 4 position), 83.8 (1C, s, Ep apical position), 21.4 (1C, s, Ep CH_3). $^{31}P\{^1H\}$ NMR (DMSO-d_6, δ): 50.75 (s, PPh_3).

$EpRu(PMe_3)(Cl)_2$ (23). $EpRu(Cl)_2(PPh_3)$ (0.572 g, .864 mmol), PMe_3 (0.38 mL, 4.32 mmol) and NCMe (80 mL) were placed in a 100 mL thick walled glass reaction vessel. This heterogeneous solution was heated in an 80 ^oC oil bath for 3 days. With occasional shaking, after 21 hours (of the 3 day period) the reaction mixture became a yellow homogeneous solution. Upon completion of heating, the tube was cooled to room temperature, filtered under N_2 and evacuated of all volatiles. The resulting $[EpRu(Cl)(PPh_3)(PPMe_3)]Cl$ yellow salt was taken up in minimal CH_2Cl_2 (8 mL) and precipitated with excess hexanes (80 mL). The yellow solid was collected on a fine frit by vacuum filtration, rinsed with Et_2O (100 mL) and dried overnight under dynamic vacuum. The yellow solid was then placed in a 50 mL Teflon sealed reaction with 40 mL of THF. This heterogeneous solution was heated in a 120 ^oC oil bath for 3 days. The solution became orange and a darker yellow precipitate was formed ($EpRu(Cl)_2PMe_3$). The yellow solid was cooled to ambient conditions

and collected on a fine frit, under nitrogen, by vacuum filtration. The yellow solid was rinsed with toluene, THF, and Et_2O. This material was taken up in DMSO and purified by both alumina *and* silica column chromatography using DMSO as the mobile phase. The product was then precipitated by addition of Et_2O to the purified DMSO solution and collected by vacuum filtration on a fine frit. This final product was washed with Et_2O (100 mL) and dried under vacuum overnight. ^{13}C NMR (DMSO-d_6): 147.9 (2C, s, Ep 3 or 5 position), 144.5 (1C, s, Ep 3 or 5 position), 132.7 (2C, s, Ep 3 or 5 position), 130.8 (1C, s, Ep 3 or 5 position), 107.4 (2C, s, Ep 4 position), 107.2 (1C, s, Ep 4 position), 83.8 (1C, s, Ep apical position), 21.2 (1C, s, Ep CH_3), 15.2 (3C, d, J_{CP} = 27.5 Hz, $P(CH_3)_3$). $^{31}P\{^1H\}$ NMR (DMSO-d_6, δ): 18.73 (s, PMe_3).

References

1. Oxgaard, J.; Periana, R. A.; Goddard, W. A. *J. Am. Chem. Soc.* **2004,** *126*, 11658-11665.

2. Lail, M.; Bell, C. M.; Conner, D.; Cundari, T. R.; Gunnoe, T. B.; Petersen, J. L. *Organometallics* **2004,** *23*, 5007-5020.

3. Oxgaard, J.; Goddard, W. A. *J. Am. Chem. Soc.* **2004,** *126*, 442-443.

4. Bigmore, H. R.; Lawrence, S. C.; Mountford, P.; Tredget, C. S. *Dalton Transactions* **2005**, 635-651.

5. De Bari, H.; Zimmer, M. *Inorg. Chem.* **2004,** *43*, 3344-3348.

6. Sanchez-Mendez, A.; Silvestri, G. F.; de Jesus, E.; de la Mata, F. J.; Flores, J. C.; Gomez, R.; Gomez-Sal, P. *Eur. J. Inorg. Chem.* **2004**, 3287-3296.

7. Fujisawa, K.; Ono, T.; Ishikawa, Y.; Amir, N.; Miyashita, Y.; Okamoto, K.; Lehnert, N. *Inorg. Chem.* **2006,** *45*, 1698-1713.

8. Gibson, D. H.; Mashuta, M. S.; He, H. Y. *Acta Crystallographica Section C-Crystal Structure Communications* **2001,** *57*, 1135-1137.

9. Lail, M.; Arrowood, B. N.; Gunnoe, T. B. *J. Am. Chem. Soc.* **2003,** *125*, 7506-7507.

10. Yakelis, N. A.; Bergman, R. G. *Organometallics* **2005,** *24*, 3579-3581.

11. Field, L. D.; Messerle, B. A.; Soler, L.; Buys, I. E.; Hambley, T. W. *J. Chem. Soc., Dalton Trans.* **2001**, 1959-1965.

12. Ortiz-Frade, L. A.; Ruiz-Ramirez, L.; Gonzalez, I.; Marin-Becerra, A.; Alcarazo, M.; Alvarado-Rodriguez, J. G.; Moreno-Esparza, R. *Inorg. Chem.* **2003,** *42*, 1825-1834.

13. Reger, D. L.; Grattan, T. C.; Brown, K. J.; Little, C. A.; Lamba, J. J. S.; Rheingold, A. L.; Sommer, R. D. *J. Organomet. Chem.* **2000,** *607*, 120-128.

14. Reger, D. L.; Grattan, T. C. *Synthesis-Stuttgart* **2003**, 350-356.